iScience

CellPress
OPEN ACCESS

Article

Generation of Sulfonylated Tetrazoles through an Iron-Catalyzed Multicomponent Reaction Involving Sulfur Dioxide

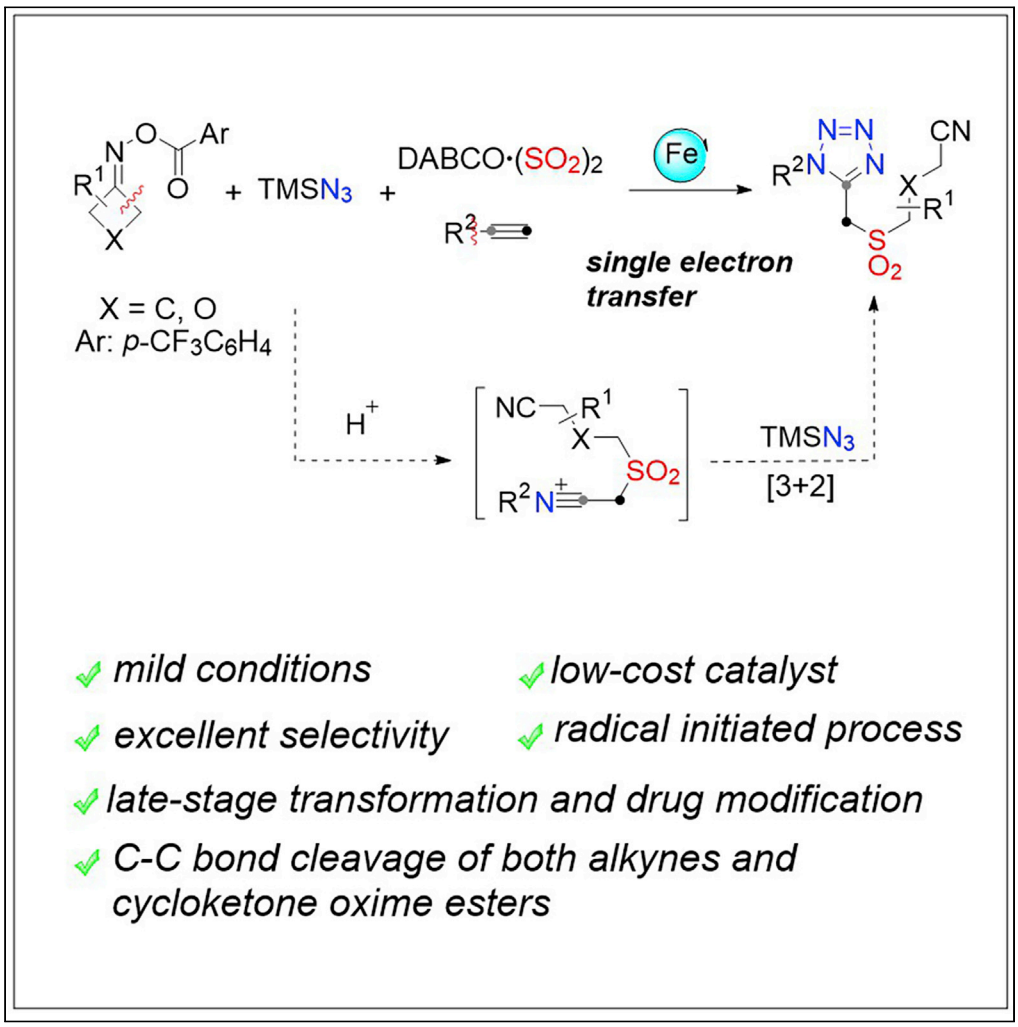

Jun Zhang, Xuefeng Wang, Yunyan Kuang, Jie Wu

yykuang@fudan.edu.cn (Y.K.)
jie_wu@fudan.edu.cn (J.W.)

HIGHLIGHTS

High-value tetrazole motifs were synthesized via a five-component reaction

Fixing sulfur dioxide into tetrazole molecules under mild conditions

Low-cost iron catalyst initiated the transformation

Excellent selectivity with the formation of multiple new chemical bonds

Zhang et al., iScience *23*, 101872
December 18, 2020
https://doi.org/10.1016/j.isci.2020.101872

iScience

CellPress
OPEN ACCESS

Article

Generation of Sulfonylated Tetrazoles through an Iron-Catalyzed Multicomponent Reaction Involving Sulfur Dioxide

Jun Zhang,[1] Xuefeng Wang,[1] Yunyan Kuang,[1,*] and Jie Wu[2,3,4,*]

SUMMARY

As a privileged motif, tetrazoles can be widely found in pharmaceuticals and materials science. Herein, a five-component reaction of cycloketone oxime esters, alkynes, DABCO·$(SO_2)_2$, and two molecules of trimethylsilyl azide under iron catalysis is developed, giving rise to a range of cyano-containing sulfonylated tetrazoles in moderate to good yields. This multicomponent reaction exhibits excellent selectivity and enables the formation of multiple new chemical bonds in one pot. A possible mechanism involving azidosulfonylation of alkynes, C-C bond cleavage of both cycloketone oxime esters and alkynes, and [3 + 2] cycloaddition of trimethylsilyl azide and the nitrilium cation intermediate is proposed. Additionally, the potential of terminal alkynes acting as powerful synthons for the synthesis of tetrazoles in a radical initiated process is demonstrated for the first time.

INTRODUCTION

Since first synthesized and reported by J. A. Bladin in 1885, the unnatural tetrazoles have become prevalent motifs in pharmaceuticals, biochemistry, and materials science due to their unique characteristic structure and biological activities (Benson, 1947; Fischer et al., 2015; Wei et al., 2015). For instance, tetrazoles have emerged as ideal bioisosteres of carboxylic acid and *cis*-amide units because of their more positive pharmacokinetic properties (Juby et al., 1968; Kubo et al., 1993; Peters et al., 2001). Consequently, devising efficient synthetic strategies of various tetrazoles has attracted much attention in organic synthesis. Traditionally, there are two mainstream reaction types for the construction of these valuable compounds: (1) cycloaddition of azides with activated nitriles and (2) cycloaddition of azides with the nitrilium cation intermediates generated *in situ* from isonitriles, amines, and carbonyl compounds via Ugi multicomponent reaction (Neochoritis et al., 2019). Moreover, several innovative synthetic methods for tetrazoles have been reported recently (Chen et al., 2011; Gaydou and Echavarren, 2013; Hu et al., 2015; Li et al., 2018; Nimnual et al., 2019; Qin et al., 2016; Wu et al., 2017; Rokade et al., 2014; Ye et al., 2018). Remarkably, Echavarren's group (Gaydou and Echavarren, 2013) demonstrated that tetrazoles could be prepared from readily available alkynes by C-C single bond cleavage in the presence of Au(I) catalyst (Scheme 1A). Subsequently, Jiao and Shi's groups (Qin et al., 2016) reported that by using Au(I)/Ag(I) as catalysts and TfOH as an additive, amino tetrazoles were obtained from alkynes through both C-C single bond cleavage and C≡C triple bond cleavage (Scheme 1B). To the best of our knowledge, only these two examples demonstrate that alkynes, serving as versatile and easily available building blocks, are powerful synthons for the formation of valuable tetrazole compounds. Mechanistically, we noticed that alkenyl azides generated by nucleophilic attack onto the alkynes were the key intermediates in these transformations, which could go through protonation and rearrangement to provide nitrilium cation intermediates for further transformations, delivering the final tetrazole motifs. Despite these achievements, generation of tetrazoles with novelty, diversity, and complexity under green and mild conditions is still highly desirable, especially in the field of drug discovery.

Sulfones are subjects of great interest in the area of pharmaceuticals and agrochemicals (Drews, 2000; Feng et al., 2016; Patai et al., 1988). In recent years, sulfonylation reaction via a radical process with sulfur dioxide surrogates, DABCO·$(SO_2)_2$ and inorganic sulfites, has proven to be a promising approach for the synthesis of diverse sulfone-containing molecules (Bisseret and Blanchard, 2013;

[1]Department of Chemistry, Fudan University, 2005 Songhu Road, Shanghai 200438, China

[2]School of Pharmaceutical and Materials Engineering, Taizhou University, 1139 Shifu Avenue, Zhejiang 318000, China

[3]State Key Laboratory of Organometallic Chemistry, Shanghai Institute of Organic Chemistry, Chinese Academy of Sciences, 345 Lingling Road, Shanghai 200032, China

[4]Lead Contact

*Correspondence: yykuang@fudan.edu.cn (Y.K.), jie_wu@fudan.edu.cn (J.W.)

https://doi.org/10.1016/j.isci.2020.101872

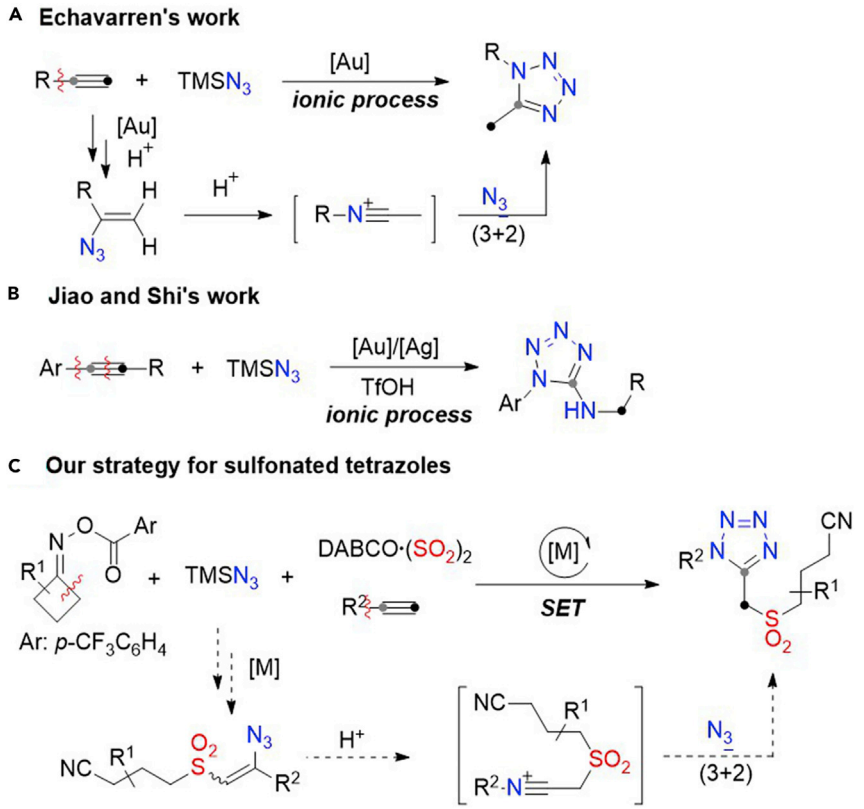

Scheme 1. Synthesis of Tetrazoles from Alkynes and $TMSN_3$

(A) Gold-catalyzed synthesis of tetrazoles from alkynes. (B) Gold/Silver-catalyzed synthesis of amino tetrazoles from alkynes. (C) Iron-catalyzed synthesis of sulfonylated tetrazoles from alkynes.

Chen et al., 2020; Deeming et al., 2014; Emmett and Willis, 2015; Gong et al., 2020; He et al., 2020; Li et al., 2020a, 2020b; Liu et al., 2020; Meng et al., 2020; Nair et al., 2020; Qiu et al., 2018a, 2018b; Wang et al., 2019; Ye et al., 2019, 2020a, 2020b, 2020c; Zheng and Wu, 2017; Zhou et al., 2020). Recently, our group described a copper-catalyzed four-component reaction of terminal alkynes, aryldiazonium tetrafluoroborates, DABCO·$(SO_2)_2$, and potassium halide, giving rising to a range of β-halo alkenylsulfones (Xiang et al., 2017). Inspired by this work and recent advances in the reactions of alkynes with trimethylsilyl azide via a radical process (Liu et al., 2019b; Wang et al., 2015; Wu et al., 2019; Xiong et al., 2019; Ning et al., 2017), we conceived that the sulfone-containing alkenyl azide intermediates might be accessed through the azidosulfonylation of alkynes with the insertion of sulfur dioxide via a radical process. Driven by the importance of tetrazole chemistry and our continuous interest in the insertion of sulfur dioxide, we envisioned that the incorporation of sulfonyl unit into tetrazoles for the construction of valuable sulfonylated tetrazoles might be beneficial for various biological evaluations. Very recently, we reported that the cyanoalkyl radicals generated *in situ* from cycloketone oxime esters (Chen et al., 2019; Dauncey et al., 2018; Deng et al., 2020; Liu et al., 2019a; Wang et al., 2019; Xing et al., 2019; Yin and Wang, 2019; Yin et al., 2018; Yu et al., 2018a, 2018b; Zhang et al., 2019a, 2019b, 2020; Zhao et al., 2018, 2020) through a single electron transfer (SET) reduction with the assistance of copper catalyst or photocatalyst could react with sulfur dioxide to provide sulfonyl radicals for sulfonylation process (Zhang et al., 2019b, 2020). Herein, we report an iron-catalyzed multicomponent reaction of cycloketone oxime esters, alkynes, DABCO·$(SO_2)_2$, and trimethylsilyl azide, affording a range of sulfonylated tetrazoles in moderate to good yields (Scheme 1C). Cycloketone oxime esters are employed as the precursors to provide the cyanoalkyl radicals through a SET reduction in this sulfonylation process. This multicomponent reaction exhibits excellent selectivity and enables the formation of multiple new chemical bonds in one pot. A possible mechanism involving azidosulfonylation of alkynes, C-C bond cleavage of both cycloketone oxime esters and alkynes, and [3 + 2] cycloaddition of trimethylsilyl

azide and the nitrilium cation intermediates is proposed. Additionally, the potential of terminal alkynes acting as powerful synthons for the synthesis of tetrazoles in a radical initiated process is demonstrated for the first time.

RESULTS AND DISCUSSION

Optimization of Reaction Conditions

We commenced this multicomponent reaction of *O*-(4-(trifluoromethyl)benzoyl) oxime **1a**, 1-ethynyl-4-methoxybenzene **2a**, DABCO·$(SO_2)_2$, and trimethylsilyl azide as the model (see Table S1). At the outset, several metal catalysts including $Cu(OAc)_2$, $Co(OAc)_2$, and $Fe(OAc)_2$ were introduced in this transformation to promote the single-electron redox process at 60°C in acetonitrile (Table S1, entries 1–3). Only a trace amount of product was detected when the reaction was treated with copper(II) acetate (Table S1, entry 1). To our delight, the desired sulfonylated tetrazole **3aa** was generated in 15% yield in the presence of $Co(OAc)_2$ (Table S1, entry 2). Further exploration revealed that $Fe(OAc)_2$ was a more efficient catalyst, giving rise to the target tetrazole **3aa** in 54% yield (Table S1, entry 3). Subsequently, other iron catalysts were evaluated. It was found that the choice of iron salt had a slight influence on productivity (Table S1, entries 4–7). In comparison, $Fe(OTf)_2$ led to a higher yield (62%) than others. The yields significantly decreased when we further examined the reaction in different solvents. No desired product was observed when 1,4-dioxane was used as the solvent (Table S1, entry 8). No better results were obtained when the reaction was performed at 40°C and 80°C. The yield reduced to 56% when the catalytic amount of $Fe(OTf)_2$ was changed to 10 mol % (Table S1, entry 13).

Substrate Scope with Alkynes and Cycloketone Oxime Esters

After establishing the aforementioned optimized conditions, the generality of substrate scope in this multicomponent reaction was explored (Scheme 2). At the beginning, a range of alkynes **2** was evaluated in the reaction of *O*-(4-(trifluoromethyl)benzoyl) oxime **1a**, DABCO·$(SO_2)_2$, and trimethylsilyl azide. All reactions worked well, and various sulfonylated tetrazoles were afforded in moderate to good yields. Various substituents on aryl alkynes including alkyl, alkoxyl, halo, ester, and *N*,*N*-dimethyl were suitable in this transformation. Meanwhile, the structure of compound **3ah** was confirmed by X-ray diffraction analysis. Notably, the reaction of 3-ethynylthiophene proceeded smoothly as well leading to the desired product **3at** in 53% yield. The expected tetrazole **3as** was provided in 51% yield when enyne **2s** was used as the substrate. We further extended this approach by using 4-methylumbelliferone derivative, endofolliculina derivative, and erlotinib as the starting material, affording the corresponding tetrazole-modified compounds (**3au-3aw**) in moderate yields, which demonstrated the potential of this methodology for the late-stage modification of more complex molecules. However, the desired product could not be detected when aliphatic alkynes and internal alkynes such as pent-4-yn-1-ylbenzene, ethynylcyclopentane, and prop-1-yn-1-ylbenzene were used in the reaction. Subsequently, the scope of cycloketone oxime esters **1** was examined in the reaction of 1-ethynyl-4-methoxybenzene **2a**, DABCO·$(SO_2)_2$, and trimethylsilyl azide. As expected, various substituents attached on the quaternary ring of cycloketone oxime esters did not influence the reaction efficiency. For instance, reactions of mono-substituted cycloketone oxime esters with ether, ester, and amide groups at the 3-position worked well to furnish the desired products **3ga**-**3ia** in 59%–68% yields. With allyl or benzyl groups at the 2-position, the imine radicals generated from oxime esters underwent selective C-C bond cleavage to provide the more stable secondary alkyl radicals, thus resulting in the products **3ja** and **3ka** in 50% and 64% yields, respectively. Additionally, reaction of oxetan-3-one oxime **1m** gave rise to the corresponding compound **3ma** in 40% yield. In our attempts using five- or six-membered ring substrates, no desired product was observed and the alkyne was recovered.

To evaluate this multicomponent approach on a large scale, 3 mmol 1-ethynyl-4-methoxybenzene **2a** (1.0 equiv) was used to perform the model reaction, giving rise to the product **3aa** in 58% yield (Scheme 3A). As an example of further transformations from product **3aa**, the activated -CH_2- group by the sulfonyl and the tetrazole could undergo nucleophilic substitution and condensation reaction with the assistance of bases (Scheme 3B). The excellent *E*-selectivity of compound **5** was confirmed by X-ray diffraction, which might be attributed to the π-π stacking interaction of aromatic rings.

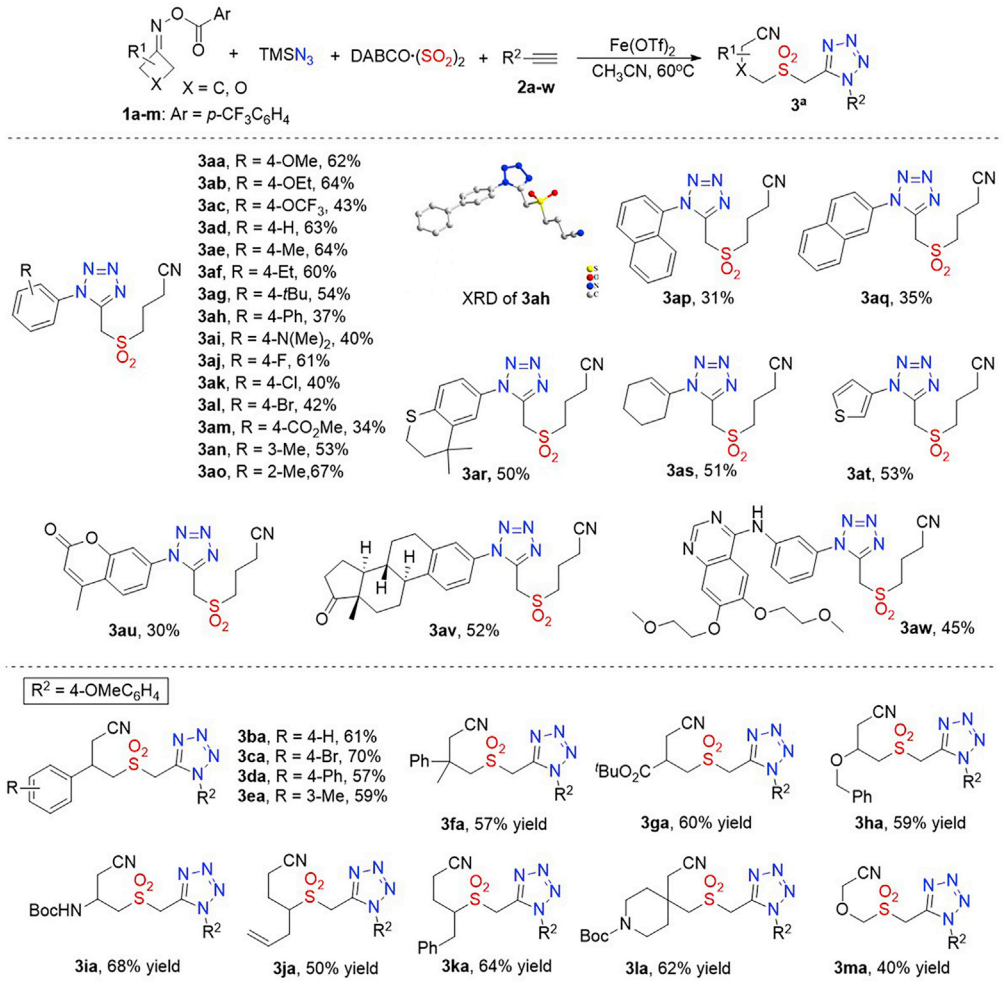

Scheme 2. Scope of Alkynes 2 and Cycloketone Oxime Esters 3

[a] Conditions: **1** (0.3 mmol), DABCO·$(SO_2)_2$ (0.2 mmol), $TMSN_3$ (0.6 mmol), **2** (0.2 mmol), $Fe(OTf)_2$ (20 mol %), CH_3CN (2.0 mL), 60°C, N_2, 12 hr. Isolated yield based on **2**.

Control Experiments and Mechanistic Studies

To confirm the reaction mechanism as described in Scheme 1C, 1.5 equiv 2,2,6,6-tetramethyl-1-piperidinyloxy (TEMPO) was added as a radical scavenger to the reaction of cycloketone oxime esters **1d**, 1-ethynyl-4-methoxybenzene **2a**, DABCO·$(SO_2)_2$, and trimethylsilyl azide under the standard conditions (Scheme 4A). The sulfonylated tetrazole **3da** was isolated in 24% yield, and the radical trapping product **6** was obtained in 15% yield. Additionally, the corresponding product **3da** was not observed when the amount of TEMPO was increased to 3.0 equiv, revealing that a radical process might be involved in this transformation. Interestingly, two tetrazole isomers **3ax** and **3ax′** were isolated in 26% and 12% yield with the utilization of 4-ethynyl benzonitrile as the substrate, which implied a competitive migration in this transformation (Scheme 4B). In comparison, we found that most aryl alkynes bearing electron-withdrawing groups (ester, nitro, carbonyl) showed inferior regioselectivity than that of alkynes with electron-donating group in the reaction, possibly because of difficulty of the rearrangement process.

On the basis of the above observation and previous reports (Gaydou and Echavarren, 2013; Qin et al., 2016; Xiang et al., 2017), a plausible mechanism is depicted in Scheme 5. We reasoned that initially, Fe(II)-mediated single-electron reduction of cycloketone oxime ester **1** would afford iminyl radical intermediate **C** with the generation of Fe(III) species **A**. The iminyl radical intermediate **C** would go

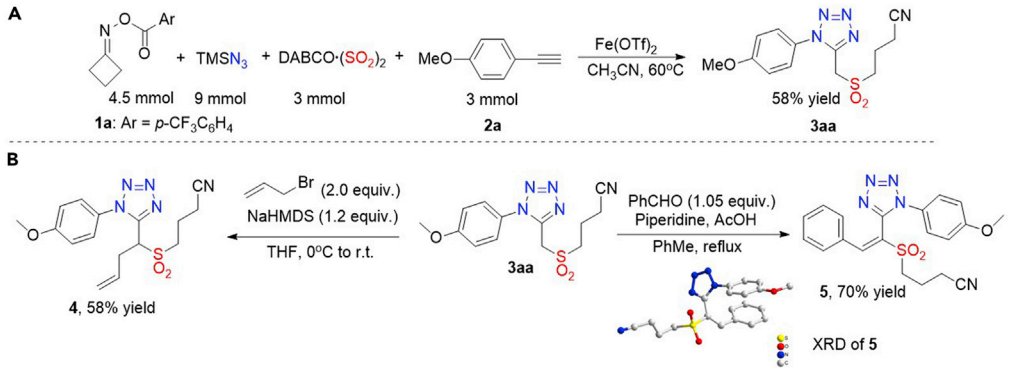

Scheme 3. Scaled-up Version of the Model Reaction and Transformations of the Product

(A) A gram scale reaction. (B) Nucleophilic substitution and condensation reaction of the product **3aa**. NaHMDS, sodium bis(trimethylsilyl)amide.

through intramolecular C-C bond cleavage leading to alkyl radical **D**, which would be trapped by sulfur dioxide to provide the sulfonyl radical **E**. Then, the resulting radical **E** would attack the triple bond of alkyne **2** to afford alkenyl radical **F**. Meanwhile, ligand exchange would occur between Fe (III) species **A** and trimethylsilyl azide providing Fe (III) species **B**, which would undergo azide group transfer with the alkenyl radical **D** to deliver the sulfone-containing alkenyl azide intermediate **G**, with the regeneration of Fe(II) species. Further protonation of intermediate **G** would offer azide cation intermediate **H**, which could convert to nitrilium cation intermediate **I** by migration of R^2 group with the release of nitrogen. Finally, the [3 + 2] cycloaddition reaction of intermediate **I** with trimethylsilyl azide would take place, giving rise to the desired compound **3** (path a). Presumably, if the R^2 group was substituted by electron-withdrawing group, a competitive migration of sulfonyl-substituted methylene (path b) would occur and produce intermediate **J** that is more stable than intermediate **I** (path a), which might explain the formation of isomers **3ax** and **3ax′**.

Conclusion

We have demonstrated an efficient five-component reaction of cycloketone oxime esters, alkynes, DABCO·$(SO_2)_2$, and two molecules of trimethylsilyl azide under iron catalysis, giving rise to a range of sulfonylated tetrazoles in moderate to good yields. This transformation works effectively with a wide range of substrates, and this multicomponent reaction exhibits excellent selectivity and enables the formation of multiple new chemical bonds in one pot. A possible mechanism involving azidosulfonylation of alkynes, C-C bond cleavage of both cycloketone oxime esters and alkynes, and [3 + 2] cycloaddition of trimethylsilyl azide and the nitrilium cation intermediates is proposed. The radical azidosulfonylation of alkynes enables the formation of sulfone-containing alkenyl azide intermediates, which are essential to form tetrazoles. To our knowledge, this is the first example of terminal alkynes acting as powerful synthons for the synthesis of

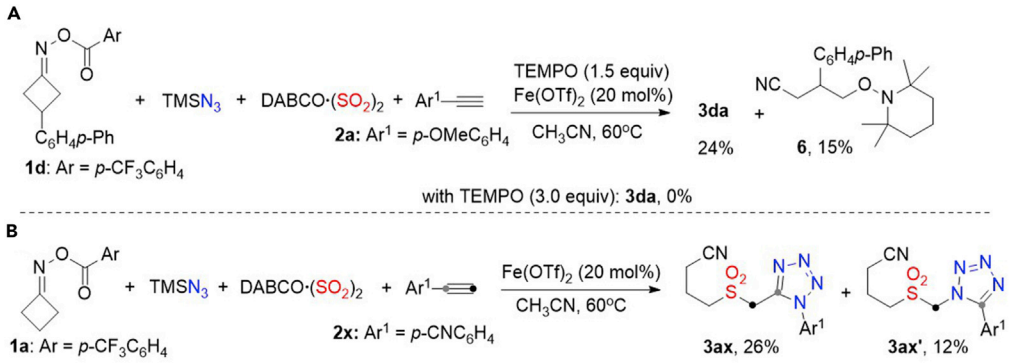

Scheme 4. Control Experiments and Mechanistic Studies

(A) Radical inhibition experiments with Tempo. (B) The isolation of two tetrazole isomers.

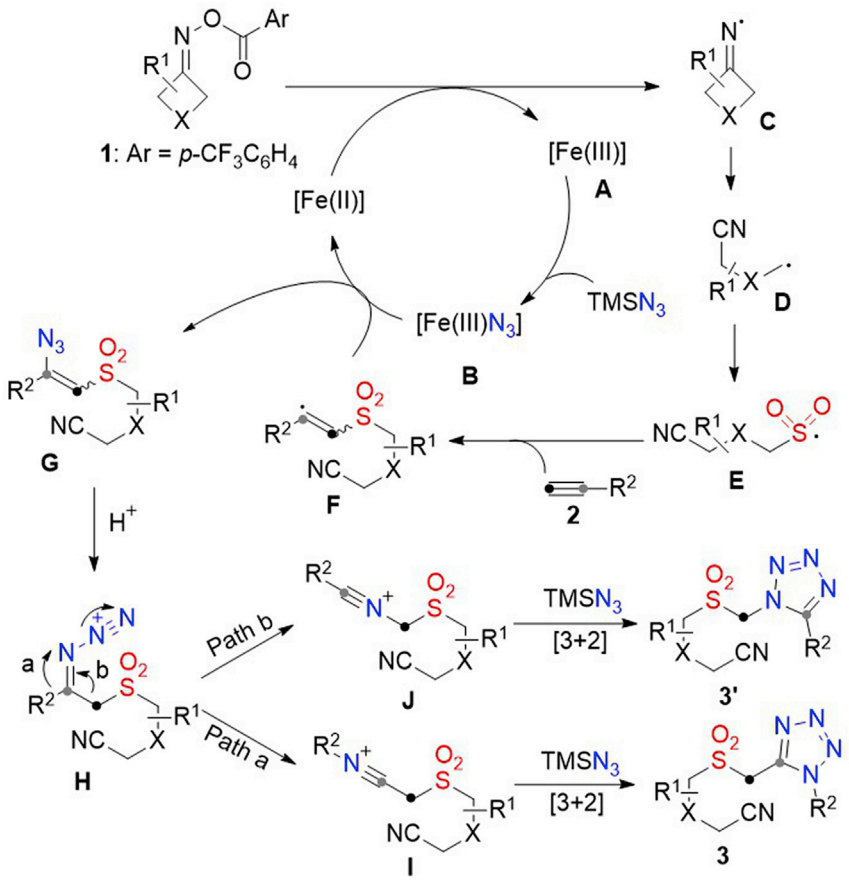

Scheme 5. Proposed Mechanism

tetrazoles in a radical initiated process. From the synthetic point of view, the advantages including mild conditions, low-cost catalyst, and high-value products make this protocol practical and attractive.

Limitations of the Study

In our current work, aliphatic alkynes and internal alkyne were not suitable substrates for this transformation. Specific cycloketone oxime ester substrates limit the wide application of this methodology.

Resource Availability

Lead Contact

Further information and requests for resources should be directed to and will be fulfilled by the Lead Contact, Jie Wu (jie_wu@fudan.edu.cn).

Materials Availability

This study generated new unique reagents, sulfonylated tetrazoles.

Data and Code Availability

The data for the X-ray crystallographic coordinates for structures reported in this paper have been deposited at the Cambridge Crystallographic Data Centre under accession numbers (CCDC for **3ah**: 2005594; CCDC for **5**: 2042215). These data can be obtained free of charge from The Cambridge Crystallographic Data Centre via www.ccdc.cam.ac.uk/data_request/cif.

METHODS

All methods can be found in the accompanying Transparent Methods supplemental file.

SUPPLEMENTAL INFORMATION

Supplemental Information can be found online at https://doi.org/10.1016/j.isci.2020.101872.

ACKNOWLEDGMENTS

We acknowledge the financial support from the National Natural Science Foundation of China (Nos. 21871053 and 21532001) and the Leading Innovative and Entrepreneur Team Introduction Program of Zhejiang (No. 2019R01005).

AUTHOR CONTRIBUTIONS

J.Z. conceived the study. J.Z. and X.W. conducted the experiments and analyzed the data. J.W. and Y.K. directed the project. J.Z. prepared the manuscript and Supplemental Information with input from all authors. All authors discussed the results and commented on the manuscript.

DECLARATION OF INTERESTS

The authors declare no competing interests.

Received: September 25, 2020
Revised: November 5, 2020
Accepted: November 23, 2020
Published: December 18, 2020

REFERENCES

Benson, F.R. (1947). The chemistry of the tetrazoles. Chem. Rev. *41*, 1–61.

Bisseret, P., and Blanchard, N. (2013). Taming sulfur dioxide: a breakthrough for its wide utilization in chemistry and biology. Org. Biomol. Chem. *11*, 5393–5398.

Chen, F., Qin, C., and Cui, Y. (2011). Implanting nitrogen into hydrocarbon molecules through C-H and C-C bond cleavages: a direct approach to tetrazoles. Angew. Chem. Int. Ed. *50*, 11487–11491.

Chen, J., Wang, P.-Z., Lu, B., Liang, D., Yu, X.-Y., Xiao, W.-J., and Chen, J.-R. (2019). Enantioselective radical ring-opening cyanation of oxime esters by dual photoredox and copper catalysis. Org. Lett. *21*, 9763–9768.

Chen, K., Chen, W., Han, B., Chen, W., Liu, M., and Wu, H. (2020). Sequential C–S and S–N coupling approach to sulfonamides. Org. Lett. *22*, 1841–1845.

Dauncey, E.M., Morcillo, S.P., Douglas, J.J., Sheikh, N.S., and Leonori, D. (2018). Photoinduced remote functionalisations by iminyl radical Promoted C−C and C−H bond cleavage cascades. Angew. Chem. Int. Ed. *57*, 744–748.

Deeming, A.S., Emmett, E.J., Richards-Taylor, C.S., and Willis, M.C. (2014). Rediscovering the chemistry of sulfur dioxide:new developments in synthesis and catalysis. Synthesis *46*, 2701–2710.

Deng, Y., Zhao, C., Zhou, Y., Li, X., Cheng, G.-J., and Fu, J. (2020). Directing-group-based strategy enabling intermolecular Heck-Type reaction of cycloketone oxime esters and unactivated alkenes. Org.Lett. *22*, 3524–3530.

Drews, J. (2000). Drug discovery: a historical perspective. Science *287*, 1960–1964.

Emmett, E.J., and Willis, M.C. (2015). The development and application of sulfur dioxide surrogates in synthetic organic chemistry. Asian J. Org. Chem. *4*, 602–611.

Feng, M., Tang, B., Liang, S.H., and Jiang, X. (2016). Sulfur containing scaffolds in drugs: synthesis and application in medicinal chemistry. Curr. Top. Med. Chem. *16*, 1200–1216.

Fischer, D., Klapötke, T.M., and Stierstorfer, J. (2015). 1,5-Di(nitramino)tetrazole: high sensitivity and superior explosive performance. Angew. Chem. Int. Ed. *54*, 10299–10302.

Gaydou, M., and Echavarren, A.M. (2013). Gold-catalyzed synthesis of tetrazoles from alkynes by C-C bond cleavage. Angew. Chem. Int. Ed. *52*, 13468–13471.

Gong, X., Yang, M., Liu, J.-B., He, F.-S., and Wu, J. (2020). Photoinduced synthesis of alkylalkynyl sulfones through a reaction of potassium alkyltrifluoroborates, sulfur dioxide, and alkynyl bromides. Org. Chem. Front. *7*, 938–943.

He, F.-S., Yao, Y., Xie, W., and Wu, J. (2020). Photoredox-catalyzed sulfonylation of difluoroenoxysilanes with the insertion of sulfur dioxide. Chem. Commun. (Camb.) *56*, 9469–9472.

Hu, Y., Yi, R., Yu, X., Xin, X., Wang, C., and Wan, B. (2015). *O*-Transfer-facilitated cyclizations of propargylamides with $TMSN_3$: selective synthesis of tetrazoles and dihydroimidazoles. Chem. Commun. (Camb.) *51*, 15398–15401.

Juby, P.F., Hudyma, T.W., and Brown, M. (1968). Preparation and antiinflammatory properties of some 5-(2-anilinophenyl)tetrazoles. J. Med. Chem. *11*, 111–117.

Kubo, K., Kohara, Y., Imamiya, E., Sugiura, Y., Inada, Y., Furukawa, Y., Nishikawa, K., and Naka, T. (1993). Nonpeptide angiotensin II receptor antagonists. synthesis and biological activity of benzimidazolecarboxylic acids. J. Med. Chem. *36*, 2182–2195.

Li, L.-H., Niu, Z.-J., Li, Y.-X., and Liang, Y.-M. (2018). Transition-metal-free multinitrogenation of amides by C–C bond cleavage: a new approach to tetrazoles. Chem. Commun. (Camb.) *54*, 11148–11151.

Li, Y., Liu, J.-B., He, F.-S., and Wu, J. (2020a). Photoredox-catalyzed functionalization of alkenes with thiourea dioxide: construction of alkyl sulfones or sulfonamides. Chin. J. Chem. *38*, 361–366.

Li, Y., Chen, S., Wang, M., and Jiang, X. (2020b). Sodium dithionite-mediated decarboxylative sulfonylation: facile access to tertiary sulfones. Angew. Chem. Int. Ed. *132*, 8992–8996.

Liu, B., Cheng, Y., Chen, L.-Y., Chen, J.-R., and Xiao, W.-J. (2019a). Photoinduced copper-catalyzed radical aminocarbonylation of cycloketone oxime esters. ACS Catal. *9*, 8159–8164.

Liu, B., Ning, Y., Virelli, M., Zanoni, G., Anderson, E.A., and Bi, X. (2019b). Direct Transformation of terminal alkynes into amidines by a silver-catalyzed four-component reaction. J. Am. Chem. Soc. *141*, 1593–1598.

Liu, Y., Wang, Q.-L., Chen, Z., Li, H., Xiong, B.-Q., Zhang, P.-L., and Tang, K.-W. (2020). Visible-light photoredox-catalyzed dual C–C bond cleavage: synthesis of 2-cyanoalkylsulfonylated 3,4-dihydronaphthalenes through the insertion of sulfur dioxide. Chem. Commun. (Camb.) *156*, 3011–3014.

Meng, Y., Wang, M., and Jiang, X. (2020). Multicomponent reductive cross-coupling of an inorganic sulfur dioxide surrogate: straightforward construction of diversely

functionalized sulfones. Angew. Chem. Int. Ed. *59*, 1346–1353.

Nair, A.M., Halder, I., Khan, S., and Volla, C.M.R. (2020). Metal free sulfonylative spirocyclization of alkenyl and alkynyl amides via insertion of sulfur dioxide. Adv. Synth. Catal. *362*, 224–229.

Neochoritis, C.G., Zhao, T., and Dömling, A. (2019). Tetrazoles via multicomponent reactions. Chem. Rev. *119*, 1970–2042.

Nimnual, P., Tummatorn, J., Boekfa, B., Thongsornkleeb, C., Ruchirawat, S., Piyachat, P., and Punjajom, K. (2019). Construction of 5-aminotetrazoles via in situ generation of carbodiimidium ions from ketones promoted by $TMSN_3$/TfOH. J. Org. Chem. *84*, 5603–5613.

Ning, Y., Ji, Q., Liao, P., Anderson, E.A., and Bi, X. (2017). Silver-catalyzed stereoselective aminosulfonylation of alkynes. Angew. Chem. Int. Ed. *56*, 13805–13808.

Patai, S., Rappoport, Z., and Stirling, C. (1988). The Chemistry of Sulphones and Sulphoxides (Wiley).

Peters, L., FrNhlich, R., Boyd, A.S.F., and Kraft, A. (2001). Noncovalent interactions between tetrazole and an N,N′-diethyl-substituted benzamidine. J. Org. Chem. *66*, 3291–3298.

Qin, C., Su, Y., Shen, T., Shi, X., and Jiao, N. (2016). Splitting a substrate into three parts: gold-catalyzed nitrogenation of alkynes by C-C and C≡C bond cleavage. Angew. Chem. Int. Ed. *55*, 350–354.

Qiu, G., Zhou, K., Gao, L., and Wu, J. (2018a). Insertion of sulfur dioxide via a radical process: an efficient route to sulfonyl compounds. Org. Chem. Front. *5*, 691–705.

Qiu, G., Lai, L., Cheng, J., and Wu, J. (2018b). Recent advances in the sulfonylation of alkenes with the insertion of sulfur dioxide via radical reactions. Chem. Commun. (Camb.) *54*, 10405–10414.

Rokade, B.V., Gadde, K., and Prabhua, K.R. (2014). Copper-catalyzed oxidative transformation of secondary alcohols to 1,5-disubstituted tetrazoles. Adv. Synth. Catal. *356*, 946–950.

Wang, T., Wang, Y.-N., Wang, R., Zhang, B.-C., Yang, C., Li, Y.-L., and Wang, X.-S. (2019). Enantioselective cyanation via radical-mediated C–C single bond cleavage for synthesis of chiral dinitriles. Nat. Commun. *10*, 5373–5381.

Wang, M., Zhao, J., and Wang, X. (2019). Aryl methyl sulfone construction from eco-friendly inorganic sulfur dioxide and methyl reagents. ChemSusChem *12*, 3064–3068.

Wang, F., Zhu, N., Chen, P., Ye, J., and Liu, G. (2015). Copper-catalyzed trifluoromethylazidation of alkynes: efficient access to CF_3-substituted azirines and aziridines. Angew. Chem. Int. Ed. *54*, 9356–9360.

Wei, C.-X., Bian, M., and Gong, G.-H. (2015). Tetrazolium compounds: synthesis and applications in medicine. Molecules *20*, 5528–5553.

Wu, Z., Xu, P., Zhou, N., Duan, Y., Zhang, M., and Zhu, C. (2017). [3+2] Cycloaddition of azide with aldehyde hydrazone through an aminyl radical-polar crossover strategy. Chem. Commun. (Camb.) *53*, 1045–1047.

Wu, J., Dou, Y., Guillot, R., Kouklovsky, C., and Vincent, G. (2019). Electrochemical dearomative 2,3-difunctionalization of indoles. J. Am. Chem. Soc. *141*, 2832–2837.

Xiang, Y., Kuang, Y., and Wu, J. (2017). Generation of β-halo vinylsulfones through a multicomponent reaction with insertion of sulfur dioxide. Chemistry *23*, 6996–6999.

Xing, W.-L., Shang, R., Wang, G.-Z., and Fu, Y. (2019). Visible light-induced palladium-catalyzed ring opening β-H elimination and addition of cyclobutanone oxime esters. Chem. Commun. (Camb.) *55*, 14291–14294.

Xiong, H., Ramkumar, N., Chiou, M.-F., Jian, W., Li, Y., Su, J.-H., Zhang, X., and Bao, H. (2019). Iron-catalyzed carboazidation of alkenes and alkynes. Nat. Commun. *10*, 122–128.

Ye, Z., Wang, F., Li, Y., and Zhang, F. (2018). Electrochemical synthesis of tetrazoles via metal- and oxidant-free [3 + 2] cycloaddition of azides with hydrazones. Green Chem. *20*, 5271–5275.

Ye, S., Qiu, G., and Wu, J. (2019). Photoredox-catalyzed sulfonylation of alkyl iodides, sulfur dioxide, and electron-deficient alkenes. Chem. Commun. (Camb.) *55*, 2214–2217.

Ye, S., Yang, M., and Wu, J. (2020a). Recent advances in sulfonylation reactions using potassium/sodium metabisulfite. Chem. Commun. (Camb.) *56*, 4145–4155.

Ye, S., Li, X., Xie, W., and Wu, J. (2020b). Photoinduced sulfonylation reactions through the insertion of sulfur dioxide. Eur. J. Org. Chem. *10*, 1274–1287.

Ye, S., Zhou, K., Rojsithisak, R., and Wu, J. (2020c). Metal-free insertion of sulfur dioxide with aryl iodides under ultraviolet irradiation: direct access to sulfonated cyclic compounds. Org. Chem. Front. *7*, 14–18.

Yin, W., and Wang, X. (2019). Recent advances in iminyl radical-mediated catalytic cyclizations and ring-opening reactions. New J. Chem. *43*, 3254–3264.

Yin, Z., Rabeah, J., Brückner, A., and Wu, X.-F. (2018). Gallic acid-promoted SET process for cyclobutanone oximes activation and (carbonylative-)alkylation of olefins. ACS Catal. *8*, 10926–10930.

Yu, X.-Y., Chen, J.-R., Wang, P.-Z., Yang, M.-N., Liang, D., and Xiao, W.-J. (2018a). A visible-light-driven iminyl radical-mediated C−C single bond cleavage/radical addition cascade of oxime esters. Angew. Chem. Int. Ed. *57*, 738–743.

Yu, X.-Y., Zhao, Q.-Q., Chen, J., Chen, J.-R., and Xiao, W.-J. (2018b). Copper-catalyzed radical cross-coupling of redox-active oxime esters, styrenes, and boronic acids. Angew. Chem. Int. Ed. *57*, 15505–15509.

Zhang, J.-J., Duan, X.-H., Wu, Y., Yang, J.-C., and Guo, L.-N. (2019a). Transition-metal free C–C bond cleavage/borylation of cycloketone oxime esters. Chem. Sci. *10*, 161–166.

Zhang, J., Li, X., Xie, W., Ye, S., and Wu, J. (2019b). Photoredox-catalyzed sulfonylation of O-acyl oximes via iminyl radicals with the insertion of sulfur dioxide. Org. Lett. *21*, 4950–4954.

Zhang, J., Yang, M., Liu, J.-B., He, F.-S., and Wu, J. (2020). A copper-catalyzed insertion of sulfur dioxide via radical coupling. Chem. Commun. (Camb.) *56*, 3225–3228.

Zhao, B., Wu, Y., Yuan, Y., and Shi, Z. (2020). Copper-catalysed Csp^3–Csp cross-couplings between cyclobutanone oxime esters and terminal alkynes induced by visible light. Chem. Commun. (Camb.) *56*, 4676–4679.

Zhao, J.-F., Duan, X.-H., Gu, Y.-R., Gao, P., and Guo, L.-N. (2018). Iron-catalyzed decarboxylative olefination of cycloketone oxime esters with α,β-unsaturated carboxylic acids via C–C bond cleavage. Org. Lett. *20*, 4614–4617.

Zheng, D., and Wu, J. (2017). Sulfur Dioxide Insertion Reactions for Organic Synthesis (Springer).

Zhou, K., Liu, J.-B., Xie, W., Ye, S., and Wu, J. (2020). Photoinduced synthesis of 2-sulfonylacetonitriles with the insertion of sulfur dioxide under ultraviolet irradiation. Chem. Commun. (Camb.) *56*, 2554–2557.

iScience, Volume *23*

Supplemental Information

Generation of Sulfonylated Tetrazoles through an Iron-Catalyzed Multicomponent Reaction Involving Sulfur Dioxide

Jun Zhang, Xuefeng Wang, Yunyan Kuang, and Jie Wu

Supplemental Information

1. Supplemental table

Table S1. Optimization of Conditions, Related to Scheme 2.

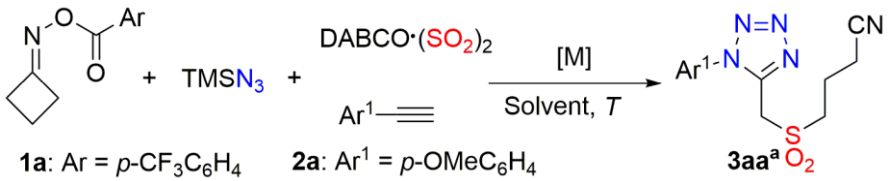

1a: Ar = *p*-$CF_3C_6H_4$ **2a**: Ar^1 = *p*-$OMeC_6H_4$ **3aa**[a]

Entry	[M]	Solvent	T	Yield(%)[b]
1	$Cu(OAc)_2$	CH_3CN	60°C	trace
2	$Co(OAc)_2$	CH_3CN	60°C	15
3	$Fe(OAc)_2$	CH_3CN	60°C	54
4	$FeBr_2$	CH_3CN	60°C	56
5	$FeCl_2$	CH_3CN	60°C	58
6	$FeCl_3$	CH_3CN	60°C	56
7	$Fe(OTf)_2$	CH_3CN	60°C	62
8	$Fe(OTf)_2$	1,4-dioxane	60°C	n.r.
9	$Fe(OTf)_2$	DCE	60°C	21
10	$Fe(OTf)_2$	DMF	60°C	30
11	$Fe(OTf)_2$	CH_3CN	40°C	53
12	$Fe(OTf)_2$	CH_3CN	80°C	59
13[c]	$Fe(OTf)_2$	CH_3CN	60°C	56

[a]Conditons: cyclobutanone *O*-(4-(trifluoromethyl)benzoyl) oxime **1a** (0.3 mmol), $DABCO·(SO_2)_2$ (0.2 mmol), $TMSN_3$ (0.6 mmol), 1-ethynyl-4-methoxybenzene **2a** (0.2 mmol), [M] (20 mol %), CH_3CN (2.0 mL), 60°C, N_2, 12 h.[b] Isolated yield based on 1-ethynyl-4-methoxybenzene **2a**.[c] In the presence of 10 mol % of $Fe(OTf)_2$.

2. Transparent method

2.1 General information:

Unless otherwise stated, all commercial reagents were used as received. All solvents were dried and distilled according to standard procedures. Flash column chromatography was performed using silica gel (60-Å pore size, 32–63μm, standard grade). Analytical thin–layer chromatography was performed using glass plates pre-coated with 0.25 mm 230–400 mesh silica gel impregnated with a fluorescent indicator (254 nm). Thin layer chromatography plates were visualized by exposure to ultraviolet light. Organic solutions were concentrated on rotary evaporators at ~20 Torr at 25–35°C. Nuclear magnetic resonance (NMR) spectra are recorded in parts per million from internal tetramethylsilane on the δ scale. ^1H,^{13}C and ^{19}F NMR spectra were recorded in DMSO-d^6, $CDCl_3$ or Acetone-d^6 on a Bruker DRX-400 spectrometer operating at 400 MHz, 100 MHz and 376 MHz, respectively. Melting points are tested automatically on a Melting Point Apparatus produced by *Shanghai JINGMI Scientific Instruments Co., Ltd*. All chemical shift values are quoted in ppm and coupling constants quoted in Hz. High resolution mass spectrometry (HRMS) spectra were obtained on a micrOTOF II Instrument.

2.2 Experimental procedures

Experimental procedure for the synthesis of cycloketone oxime esters **1**

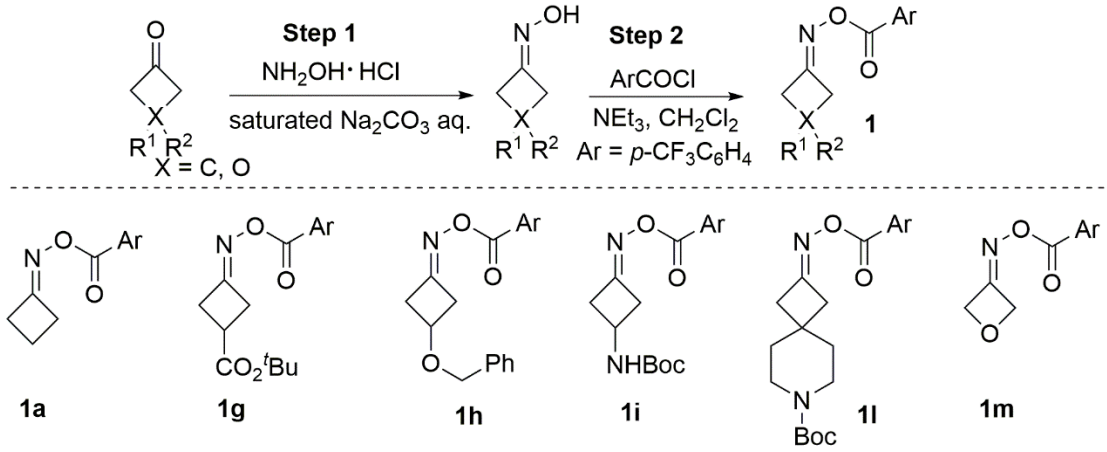

Step 1：To a mixture of ketone (10 mmol, 1.0 equiv.) and hydroxylamine hydrochloride (11 mmol, 1.1 equiv.) were added sat. Na_2CO_3 (20 mL). The resulting mixture was stirred at 40 °C overnight. After extraction with ethyl acetate, the solution dried over Na_2SO_4, and evaporated to provide crude products which were used in the next step without further purification.

Step 2：*p*-CF_3 Benzoyl chloride (1.5 equiv.) was added to a mixture of cyclobutanone oxime (1.0 equiv.), triethylamine (2.0 equiv.) and DCM (0.5 M) in a 50 mL round-bottom flask at 0 °C. After stirring for 6 h, water was added and the mixture was stirred for a few more minutes. Then the mixture was diluted with DCM. The organic layer was washed with brine and dried over Na_2SO_4. The solvent was removed under reduced pressure and the residue was purified directly by column chromatography with *n*-hexane/EtOAc as an eluent to give cycloketone oxime ester. The products **1a**, **1g**, **1h**, **1i, 1l** and **1m** (Yu et al., 2018a) are known compounds.

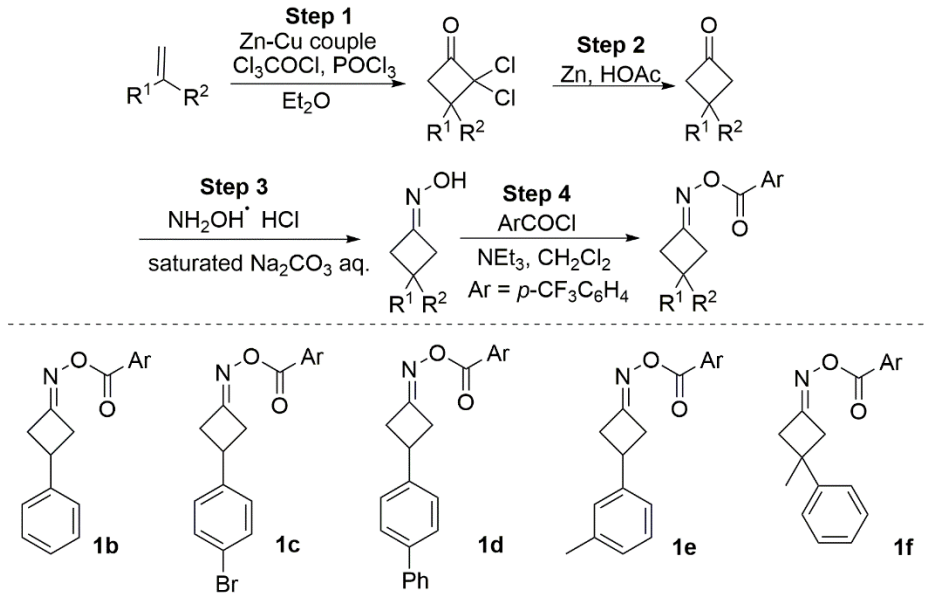

Step 1: Alkene (10.0 mmol, 1.0 equiv.), zinc-copper couple (30 mmol, 3.0 equiv.), and anhydrous ether (0.5 M) were added to a round-bottom flask (50 mL). Then a mixed solution of phosphorus oxychloride (11 mmol, 1.1 equiv.) and trichloroacetyl chloride (20 mmol, 2.0 equiv.) in ether (0.5 M) was added dropwise through an addition funnel in 1h. The resulting solution was refluxed overnight. After completion of the starting material as indicated by TLC, the mixture was filtered through a pad of celite and the celite pad was washed with ether (40 mL). The organic solution was successively washed with water (2 x 30 mL), sat. $NaHCO_3$ (2 x 30

mL) and brine (2 x 30 mL), and dried over Na_2SO_4. Then the solution was filtered, concentrated and used in the next step without further purification.

Step 2: A mixture of the corresponding 2,2-dichloro-3-substituted cyclobutanone (1.0 equiv.) and zinc powder (4.0 equiv.) in acetic acid (20 mL) was stirred at room temperature for 2 h, which was followed by heating to 80 °C for 5 h. After the scheduled time, the suspension was cooled to room temperature, then water and ether was added to the above solution for extraction. The organic layer was washed successively with sat. $NaHCO_3$, water and brine, and dried over Na_2SO_4. The solvent was concentrated under reduced pressure. The crude material was then purified by flash chromatography (*n*-hexane/ethyl acetate) to afford the corresponding 3-substituted cyclobutanone.

Step 3: A mixture of 3-substituted cyclobutanone (1.0 equiv.) and hydroxylamine hydrochloride (2.0 equiv.) in pyridine (0.5 M) was stirred at room temperature for 2 hours. Then pyridine was removed under reduced pressure, and the residue was diluted with water and extracted with ethyl acetate. The combined organic phase was washed with brine and dried over Na_2SO_4. The solvent was concentrated under reduced pressure to provide crude product, which was used in the next step without further purification.

Step 4: *p*-CF_3 Benzoyl chloride (1.5 equiv.) was added to a mixture of cyclobutanone oxime (1.0 equiv.), triethylamine (2.0 equiv.) and DCM (0.5 M) in a round-bottom flask at 0 °C. After stirring for 6 h, water was added and the mixture was stirred for a few more minutes. Then the resulting mixture was diluted with DCM. The organic layer was separated, washed with brine and dried over Na_2SO_4. The solvent was removed under reduced pressure, and the residue was purified directly by column chromatography with *n*-hexane/EtOAc as eluent to give the 3-substituted cycloketone oxime ester as white solid. The products **1b, 1c, 1d, 1e and 1f** (Yu et al., 2018a) are known compounds.

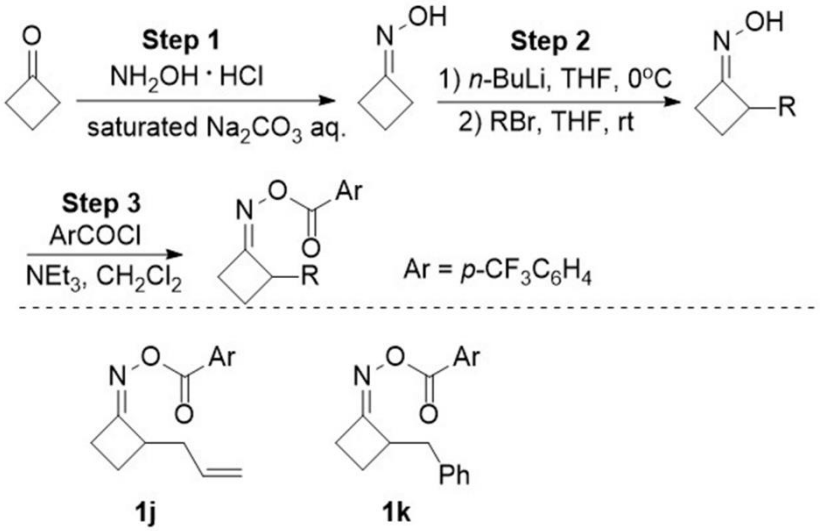

Step 1: To a flask (100 mL) equipped with a stirrer, cyclobutanone (10 mmol, 1.0 equiv.) and hydroxylamine hydrochloride (11 mmol, 1.1 equiv.) were added. Then sat. Na_2CO_3 (20 mL) was added and the resulting mixture was stirred at 40 °C overnight. After extraction with ether, the combined organic phase was dried over Na_2SO_4, and concentrated to provide crude product which was used in the next step without further purification.

Step 2: *n*-BuLi (2.0 equiv.) was added slowly to the solution of cyclobutanone oxime (1.0 equiv.) in THF (0.5 M) at 0 °C. Then the mixture was continued to stir for another 15 min at this temperature. After that, RBr (1.0 equiv.) was added dropwise, then the mixture was warmed to room temperature and stirred for another 2 h. Subsequently, cold water and ethyl acetate were successively added to the above solution. The organic layer was separated, washed with water, and dried over Na_2SO_4. The solvent was concentrated under reduced pressure, and the residue was purified by column chromatography (*n*-hexane/EtOAc) to give 2-substituted cyclobutanone oxime.

Step 3: To a mixture of 2-substituted cyclobutanone oxime (1.0 equiv.), triethylamine (1.5 equiv.) and DCM (0.5 M) in a round-bottom flask (50 mL) was added *p*-CF_3 benzoyl chloride (1.1 equiv.) dropwise at 0 °C. After 3 h, sat. $NaHCO_3$ was added to the mixture, and the mixture was diluted with DCM. The organic layer was washed with brine, dried over Na_2SO_4 and concentrated under reduced pressure. The residue was purified by column chromatography (*n*-hexane/EtOAc) to give 2-substituted cycloketone oxime ester. The products **1j and 1k** (Ai et al., 2018) are known compounds.

Experimental procedure for the synthesis of alkynes **2u** and **2v**.

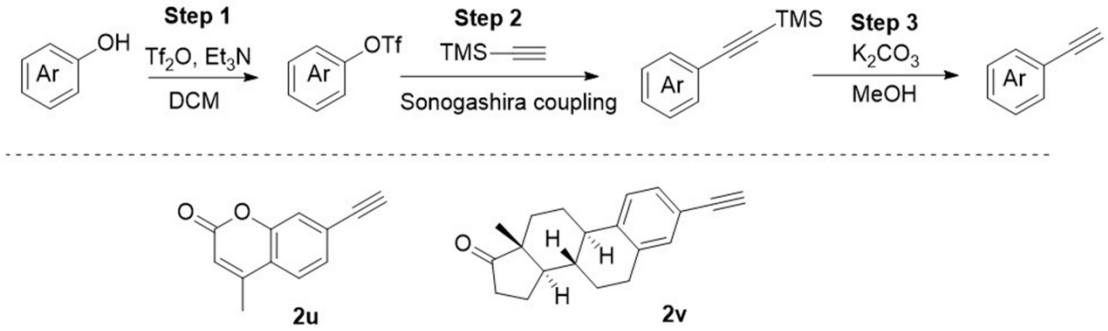

Step 1: Triethylamine (12 mmol, 2 equiv.) and trifluoromethanesulfonic anhydride (13.2 mmol, 2.2 equiv.) were added to the solution of phenol (6 mmol, 1.0 equiv.) in CH_2Cl_2 (50 ml) at 0°C. The mixture was continued to stir for 30 min at this temperature. Subsequently, water (50 ml) were added to the above solution and do an extraction. The aqueous phase was extracted with CH_2Cl_2 (3 x 30 ml). The combined organic phase was successively washed with brine, dried over Na_2SO_4, and concentrated to provide crude product, which was purified by column chromatography to give aryl trifluoromethanesulfonate.

Step 2: To a mixture of aryl trifluoromethanesulfonate (1.0 equiv.), $Pd(PPh_3)Cl_2$ (10 mol%), CuI (10 mol%), triethylamine (3 equiv.) and DMF (0.1 M) in a round-bottom flask was added TMSA (5.0 equiv.) slowly. Then the flask was backfilled with nitrogen three times and stirred at 80 °C for 4 h. After completion as monitored by TLC, water and ethyl acetate were successively added to the above solution and do an extraction. The organic layer was separated, washed with brine, and dried over Na_2SO_4. The filtrate was concentrated under reduced pressure, and the residue was purified by column chromatography (*n*-hexane/EtOAc) to afford trimethyl(arylethynyl)silane.

Step 3: K_2CO_3 (2.0 equiv.) was added to the mixture of trimethyl(arylethynyl)silane (1.0 equiv.) in MeOH (0.1M). The mixture was stirred at room temperature for 4 h. After that, the mixture was quenched with water and extracted with EtOAc. The organic layer was washed with brine, dried over Na_2SO_4 and concentrated under reduced pressure. The residue was purified by column chromatography (*n*-hexane/EtOAc) to arylalkynes. The products **2u** (Zhang et al., 2014) **and 2v** (Breed et al., 2009) are known compounds.

General experimental procedure for the reaction of cycloketone oxime esters **1**, alkynes **2**, DABCO·$(SO_2)_2$, and $TMSN_3$, Related to Scheme 2 and Scheme 4.

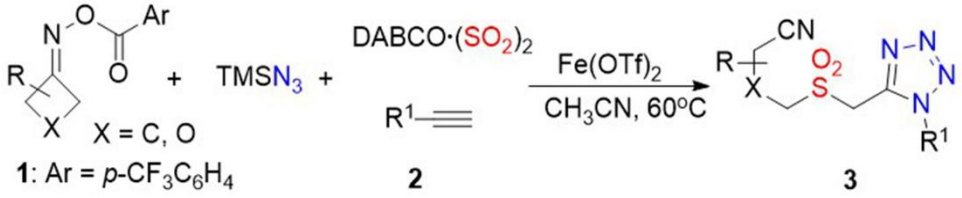

$TMSN_3$ (0.6 mmol) was added to a mixture of cycloketone oxime ester **1** (0.3 mmol), DABCO·$(SO_2)_2$ (0.2 mmol), alkyne **2** (0.2 mmol) and $Fe(OTf)_2$ (0.04 mmol, 20 mol %) in CH_3CN under N_2 atmosphere. The resulting mixture was stirred at 60 °C for 12 hours. After completion of reaction as indicated by TLC, sat. $NaHCO_3$ (20 ml) and ethyl acetate (15 mL) was added for extraction. Subsequently, the combined organic layers were washed with brine, dried over anhydrous Na_2SO_4, filtered and concentrated under reduced pressure. The aqueous waste was

treated with aqueous NaClO to decompose the N_3^- specie. The crude product was purified directly by flash column chromatography to give the corresponding product **3**.

Scaled-up version of the model reaction and transformations of the product, Related to Scheme 3.

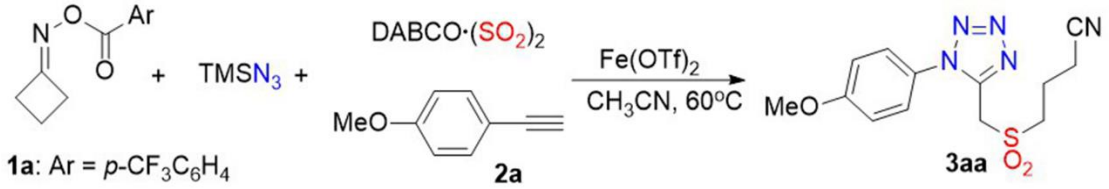

To a 100 mL round-bottom flask, cycloketone oxime ester **1a** (4.5 mmol, 1.16 g), $DABCO^{\cdot}(SO_2)_2$ (3 mmol, 732 mg) and $Fe(OTf)_2$ (0.6 mmol, 300 mg) were added. Then the flask was sealed with a rubber stopper and backfilled with nitrogen three times. The solvent MeCN (30 ml), 1-ethynyl-4-methoxybenzene (3 mmol, 396.5 mg) and $TMSN_3$ (9 mmol, 1.04 g) were injected sequentially. The mixture was stirred at 60°C for 12 h. Upon completion, sat. $NaHCO_3$ (30 ml) was added. Next, the most organic solvent was evaporated and ethyl acetate (30 mL) were added for extraction. The organic layer was successively washed with sat. $NaHCO_3$ (30 mL) and brine (30 mL), and dried over Na_2SO_4. The solution was filtered, concentrated and the residue was purified directly by flash column chromatography (*n*-hexane/ethyl acetate = 3:1-1:1) to give the corresponding product **3aa** (561.4 mg, 58% yield), and the aqueous waste was treated with aqueous NaClO to decompose the N_3^- specie.

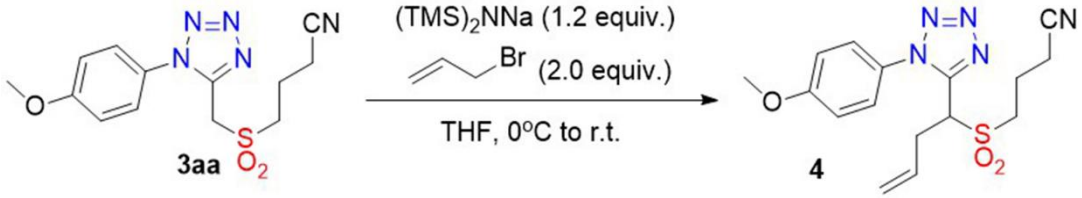

To a solution of **3aa** (64.3 mg, 0.2 mmol) in dried THF (2.0 mL, 0.1 M) was added a solution of NaHMDS in THF (2M, 0.12 mL) dropwise at 0°C. After stirring for 10 minutes, the allyl bromide (48.4 mg, 0.4 mmol) was added. The resulting mixture was stirred at room temperature for 6 h and then quenched with H_2O, extracted with ethyl acetate. The combined organic layers were washed with brine, dried over Na_2SO_4, filtered and concentrated under reduced pressure. The crude product was purified by flash column chromatography on silica gel (*n*-hexane/ethyl acetate = 3/1) to give compound **4** (colorless oil, 42.0 mg, 58%).

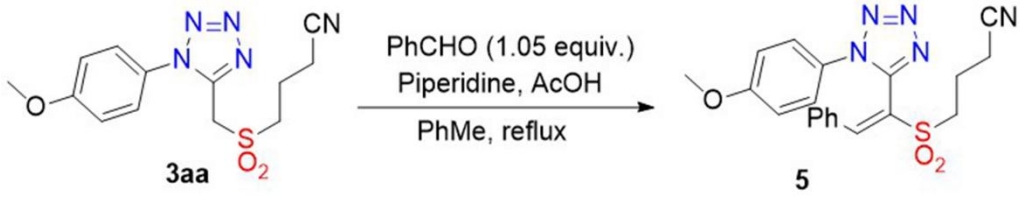

A sealed tube was charged with **3aa** (48.2 mg, 0.15 mmol), followed by benzene (1 mL), benzaldehyde (17.0 mg, 0.16 mmol), piperidine (about 10 mol%), and acetic acid (about 10 mol%). The resulting solution heated to reflux. After stirred for 4h, the mixture was purified by silica gel column chromatography directly (*n*-hexane/ethyl acetate = 3/1) to give compound **5** (white solid, 57.2 mg, 70%).

3. Data S1. The characterization of 3, 4, 5 and 6, Related to Scheme 2, Scheme 3 and Scheme 4.

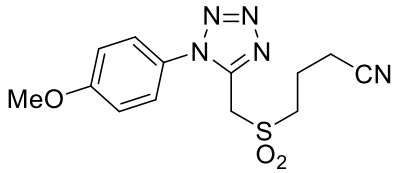

4-(((1-(4-Methoxyphenyl)-1*H*-tetrazol-5-yl)methyl)sulfonyl)butanenitrile (**3aa**); yield: 39.6 mg (62%); white solid; m.p.: 93.3-95.0 °C. ^{1}H NMR (400 MHz, $CDCl_3$) δ (ppm) 7.50 (d, *J* = 8.9 Hz, 2H), 7.09 (d, *J* = 8.9 Hz, 2H), 4.61 (s, 2H), 3.90 (s, 3H), 3.66 – 3.51 (m, 2H), 2.66 (t, *J* = 7.1 Hz, 2H), 2.38 – 2.23 (m, 2H). ^{13}C NMR (100 MHz, $CDCl_3$) δ (ppm) 161.6, 146.2, 127.2, 124.9, 118.1, 115.2, 55.7, 50.6, 47.4, 18.1, 16.1. HRMS (ESI) calcd for $C_{13}H_{15}N_5NaO_3S^+$: 344.0788 ($M+Na^+$), found: 344.0791.

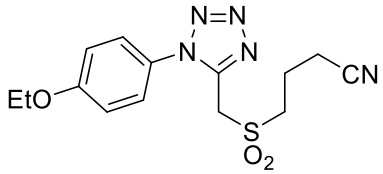

4-(((1-(4-Ethoxyphenyl)-1*H*-tetrazol-5-yl)methyl)sulfonyl)butanenitrile (**3ab**); yield: 43.0 mg (64%); white solid; m.p.: 128.8-130.2 °C. ^{1}H NMR (400 MHz, Acetone-*d*^{6}) δ (ppm) 7.62 (d, *J* = 8.3 Hz, 2H), 7.20 (d, *J* = 8.3 Hz, 2H), 4.96 (s, 2H), 4.20 (q, *J* = 6.8 Hz, 2H), 3.60 (t, *J* = 7.6 Hz, 2H), 2.78 (t, *J* = 7.1 Hz, 2H), 2.31 - 2.24 (m, 2H), 1.44 (t, *J* = 6.8 Hz, 3H). ^{13}C NMR (100 MHz, Acetone-*d*^{6}) δ (ppm) 160.9, 147.0, 127.5, 125.7, 118.7, 115.4, 63.9, 51.1, 47.2, 18.4, 15.4, 14.1. HRMS (ESI) calcd for $C_{14}H_{18}N_5O_3S^+$: 336.1125 ($M+H^+$), found: 336.1127.

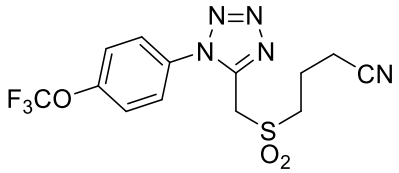

4-(((1-(4-(Trifluoromethoxy)phenyl)-1*H*-tetrazol-5-yl)methyl)sulfonyl)butanenitrile (**3ac**); yield: 32.2 mg (43%); white solid; m.p.: 87.1-88.3 °C. ^{1}H NMR (400 MHz, $CDCl_3$) δ (ppm) 7.80 – 7.58 (m, 2H), 7.48 (d, *J* = 8.5 Hz, 2H), 4.64 (s, 2H), 3.70 – 3.48 (m, 2H), 2.67 (t, *J* = 7.1 Hz, 2H), 2.41 – 2.21 (m, 2H). ^{19}F NMR (376 MHz, $CDCl_3$) δ (ppm) -57.83 (s). ^{13}C NMR (100 MHz, $CDCl_3$) δ (ppm) 151.1, 146.2, 130.7, 127.6, 122.4, 120.2 (d, $^{1}J_{CF}$ = 259.4 Hz), 118.0, 50.6, 47.5, 18.2, 16.2. HRMS (ESI) calcd for $C_{13}H_{13}F_3N_5O_3S^+$: 376.0686 ($M+H^+$), found: 376.0672.

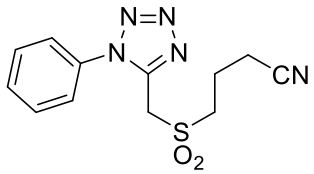

4-(((1-Phenyl-1*H*-tetrazol-5-yl)methyl)sulfonyl)butanenitrile (**3ad**); yield: 36.5 mg (63%); white solid; m.p.: 117.1-118.2 °C. ^{1}H NMR (400 MHz, DMSO-*d*^{6}) δ (ppm) 7.74 – 7.54 (m, 5H), 5.13 (s, 2H), 3.60 – 3.38 (m, 2H), 2.66 (t, *J* = 7.2 Hz, 2H), 2.14 – 1.88 (m, 2H). ^{13}C NMR (100 MHz, DMSO-*d*^{6}) δ (ppm) 146.9, 133.3, 131.3, 130.3, 126.0, 120.0, 51.3, 47.2, 18.0, 15.5. HRMS (ESI) calcd for $C_{12}H_{14}N_5O_2S^+$: 292.0863 ($M+H^+$), found: 292.0861.

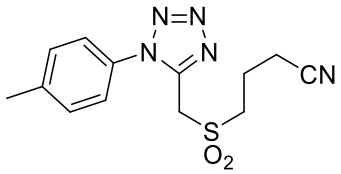

4-(((1-(*p*-Tolyl)-1*H*-tetrazol-5-yl)methyl)sulfonyl)butanenitrile (**3ae**); yield: 39.2 mg (64%); white solid; m.p.: 116.4-116.6 °C. ^{1}H NMR (400 MHz, DMSO-*d*^{6}) δ (ppm) 7.57 (d, *J* = 8.0 Hz, 2H), 7.48 (d, *J* = 7.8 Hz, 2H), 5.11 (s, 2H), 3.49 (t, *J* = 7.7 Hz, 2H), 2.68 (t, *J* = 7.1 Hz, 2H), 2.44 (s, 3H), 2.16 – 1.93 (m, 2H). ^{13}C NMR (100 MHz, DMSO-*d*^{6}) δ (ppm) 147.0, 141.4, 130.9, 130.8, 125.9, 120.1, 51.5, 47.3, 21.3, 18.2, 15.7. HRMS (ESI) calcd for $C_{13}H_{16}N_5O_2S^+$: 306.1019 (M+H$^+$), found: 306.1027.

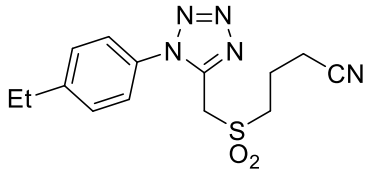

4-(((1-(4-Ethylphenyl)-1*H*-tetrazol-5-yl)methyl)sulfonyl)butanenitrile (**3af**); yield: 38.3 mg (60%); white solid; m.p.: 53.3-54.8 °C. ^{1}H NMR (400 MHz, $CDCl_3$) δ (ppm) 7.51 (d, *J* = 8.0 Hz, 2H), 7.45 (d, *J* = 8.0 Hz, 2H), 4.60 (s, 2H), 3.61 (t, *J* = 7.3 Hz, 2H), 2.79 (q, *J* = 7.5 Hz, 2H), 2.68 (t, *J* = 7.1 Hz, 2H), 2.38 - 2.30 (m, 2H), 1.32 (t, *J* = 7.5 Hz, 3H). ^{13}C NMR (100 MHz, $CDCl_3$) δ (ppm) 148.2, 146.0, 130.1, 129.7, 125.6, 118.0, 50.7, 47.6, 28.7, 18.3, 16.3, 15.2. HRMS (ESI) calcd for $C_{14}H_{18}N_5O_2S^+$: 320.1176 (M+H$^+$), found: 320.1181.

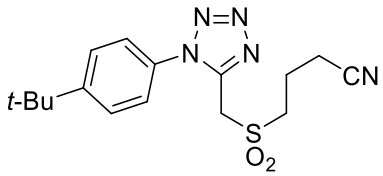

4-(((1-(4-(*tert*-Butyl)phenyl)-1*H*-tetrazol-5-yl)methyl)sulfonyl)butanenitrile (**3ag**); yield: 37.4 mg (54%); white solid; m.p.: 100.5-102.5 °C. ^{1}H NMR (400 MHz, $CDCl_3$) δ (ppm) 7.63 (d, *J* = 8.1 Hz, 2H), 7.51 (d, *J* = 8.0 Hz, 2H), 4.62 (s, 2H), 3.61 (t, *J* = 7.3 Hz, 2H), 2.67 (t, *J* = 7.0 Hz, 2H), 2.39 – 2.28 (m, 2H), 1.39 (s, 9H). ^{13}C NMR (100 MHz, $CDCl_3$) δ (ppm) 155.0, 146.0, 129.8, 127.2, 125.2, 118.0, 50.6, 47.5, 35.0, 31.1, 18.2, 16.2. HRMS (ESI) calcd for $C_{16}H_{22}N_5O_2S^+$: 348.1489 (M+H$^+$), found: 348.1492.

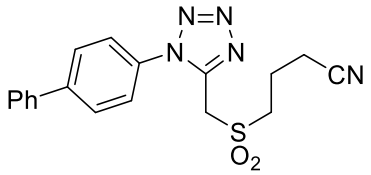

4-(((1-([1,1'-Biphenyl]-4-yl)-1*H*-tetrazol-5-yl)methyl)sulfonyl)butanenitrile (**3ah**); yield: 27.0 mg (37%); pale yellow solid; m.p.: 168.5-169.7 °C. ^{1}H NMR (400 MHz, DMSO-*d*^{6}) δ (ppm) 7.98 (d, *J* = 8.2 Hz, 2H), 7.80 (d, *J* = 7.8 Hz, 4H), 7.54 (t, *J* = 7.5 Hz, 2H), 7.46 (t, *J* = 7.2 Hz, 1H), 5.20 (s, 2H), 3.59 – 3.44 (m, 2H), 2.70 (t, *J* = 7.1 Hz, 2H), 2.21 – 1.97 (m, 2H). ^{13}C NMR (100 MHz, DMSO-*d*^{6}) δ (ppm) 147.1, 143.0, 139.0, 132.6, 129.6, 128.8, 128.6, 127.5, 126.6, 120.1, 51.5, 47.4, 18.2, 15.7. HRMS (ESI) calcd for $C_{18}H_{18}N_5O_2S^+$: 368.1176 (M+H$^+$), found: 368.1179.

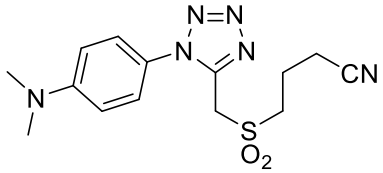

4-(((1-(4-(Dimethylamino)phenyl)-1*H*-tetrazol-5-yl)methyl)sulfonyl)butanenitrile (**3ai**); yield: 26.5 mg (40%); pale yellow solid; m.p.: 121.8-123.1 °C. ^{1}H NMR (400 MHz, Acetone-*d*^{6}) δ (ppm) 7.47 (d, *J* = 8.3 Hz, 2H), 6.92 (d, *J* = 8.3 Hz, 2H), 4.91 (s, 2H), 3.59 (t, *J* = 7.6 Hz, 2H), 3.09 (s, 6H), 2.78 (t, *J* = 7.5 Hz, 2H), 2.32 – 2.23 (m, 2H). ^{13}C NMR (100 MHz, Acetone-*d*^{6}) δ (ppm) 151.9, 146.9, 126.6, 121.1, 118.7, 111.9, 51.0, 47.1, 39.4, 18.3, 15.3. HRMS (ESI) calcd for $C_{14}H_{18}N_6NaO_2S^+$: 357.1104 (M+Na$^+$), found: 357.1113.

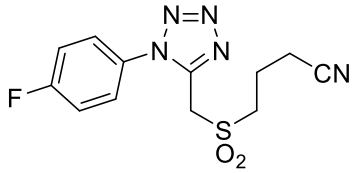

4-(((1-(4-Fluorophenyl)-1*H*-tetrazol-5-yl)methyl)sulfonyl)butanenitrile (**3aj**); yield: 37.9 mg (61%); white solid; m.p.: 88.2-89.6 °C. ^{1}H NMR (400 MHz, DMSO-*d*^{6}) δ (ppm 7.82 – 7.69 (m, 2H), 7.52 (t, *J* = 8.6 Hz, 2H), 5.13 (s, 2H), 3.49 – 3.44 (m, 2H), 2.66 (t, *J* = 7.1 Hz, 2H), 2.07 - 1.98 (m, 2H). ^{19}F NMR (376 MHz, DMSO-*d*^{6}) δ (ppm) -109.65 – -109.85 (m). ^{13}C NMR (100 MHz, DMSO-*d*^{6}) δ (ppm) 163.4 (d, $^{1}J_{CF}$ = 248.6 Hz), 147.2, 129.6, 128.8 (d, $^{3}J_{CF}$ = 9.4 Hz), 120.0, 117.3 (d, $^{2}J_{CF}$ = 23.5 Hz), 51.3, 47.0, 18.0, 15.5. HRMS (ESI) calcd for $C_{12}H_{13}FN_5O_2S^+$: 310.0768 ($M+H^+$), found: 310.0769.

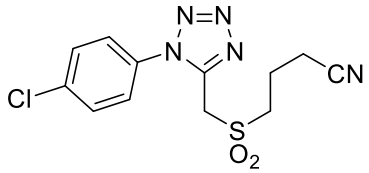

4-(((1-(4-Chlorophenyl)-1*H*-tetrazol-5-yl)methyl)sulfonyl)butanenitrile (**3ak**); yield: 26.7 mg (40%); white solid; m.p.: 124.5-125.6 °C. ^{1}H NMR (400 MHz, DMSO-*d*^{6}) δ (ppm) 7.83 – 7.69 (m, 4H), 5.18 (s, 2H), 3.49 (t, *J* = 7.7 Hz, 2H), 2.69 (t, *J* = 7.1 Hz, 2H), 2.15 – 1.96 (m, 2H). ^{13}C NMR (100 MHz, DMSO-*d*^{6}) δ (ppm) 147.2, 136.1, 132.3, 130.5, 128.1, 120.1, 51.5, 47.2, 18.1, 15.7. HRMS (ESI) calcd for $C_{12}H_{13}ClN_5O_2S^+$: 326.0473 ($M+H^+$), found: 326.0480.

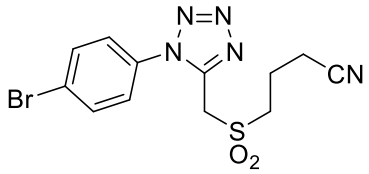

4-(((1-(4-Bromophenyl)-1*H*-tetrazol-5-yl)methyl)sulfonyl)butanenitrile (**3al**); yield: 31.0 mg (42%); white solid; m.p.: 143.8-145.2 °C. ^{1}H NMR (400 MHz, DMSO-*d*^{6}) δ (ppm) 7.90 (d, *J* = 8.1 Hz, 2H), 7.67 (d, *J* = 8.1 Hz, 2H), 5.18 (s, 2H), 3.49 (t, *J* = 7.5 Hz, 2H), 2.69 (t, *J* = 7.0 Hz, 2H), 2.16 – 1.98 (m, 2H). ^{13}C NMR (100 MHz, DMSO-*d*^{6}) δ (ppm) 147.2, 133.42, 132.7, 128.3, 124.8, 120.1, 51.5, 47.17, 18.1, 15.7. HRMS (ESI) calcd for $C_{12}H_{13}BrN_5O_2S^+$: 369.9968 ($M+H^+$), found: 369.9979.

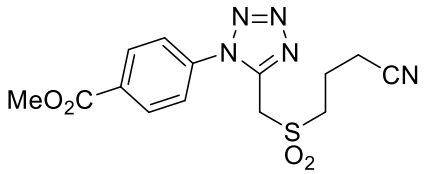

Methyl 4-(5-(((3-cyanopropyl)sulfonyl)methyl)-1*H*-tetrazol-1-yl)benzoate (**3am**); yield: 23.7 mg (34%); white solid; m.p.: 152.4-154.2 °C. ^{1}H NMR (400 MHz, Acetone-*d*^{6}) δ (ppm) 8.31 (d, *J* = 8.3 Hz, 2H), 7.92 (d, *J* = 8.3 Hz, 2H), 5.11 (s, 2H), 3.98 (s, 3H), 3.60 (t, *J* = 7.6 Hz, 2H), 2.78 (t, *J* = 7.2 Hz, 2H), 2.33 – 2.22 (m, 2H). ^{13}C NMR (100 MHz, Acetone-*d*^{6}) δ (ppm) 165.2, 146.9, 137.0, 132.44, 131.0, 126.0, 118.6, 52.0, 51.2, 47.2, 18.3, 15.4. HRMS (ESI) calcd for $C_{14}H_{16}N_5O_4S^+$: 350.0918 ($M+H^+$), found: 350.0912.

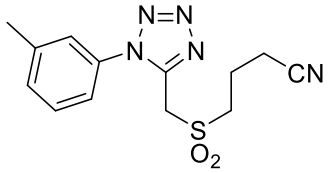

4-(((1-(*m*-Tolyl)-1*H*-tetrazol-5-yl)methyl)sulfonyl)butanenitrile (**3an**); yield: 32.5 mg (53%); white solid; m.p.: 62.2-64.2 °C. ^{1}H NMR (400 MHz, $CDCl_3$) δ (ppm) 7.54 – 7.43 (m, 2H), 7.41-7.35 (m, 2H), 4.62 (s, 2H), 3.60 (t, *J* = 7.4 Hz, 2H), 2.67 (t, *J* = 7.1 Hz, 2H), 2.47 (s, 3H), 2.37 - 2.27 (m, 2H). ^{13}C NMR (100 MHz, $CDCl_3$) δ (ppm) 145.9, 140.7, 132.4, 132.1, 129.9, 126.1, 122.6, 118.0, 50.6, 47.5, 21.2, 18.2, 16.2. HRMS (ESI) calcd for $C_{13}H_{16}N_5O_2S^+$: 306.1019 ($M+H^+$), found: 306.1029.

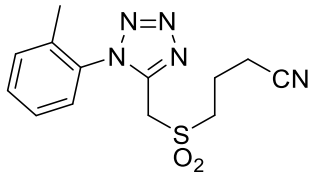

4-(((1-(*o*-Tolyl)-1*H*-tetrazol-5-yl)methyl)sulfonyl)butanenitrile (**3ao**); yield: 40.7 mg (67%); pale yellow oil. ^{1}H NMR (400 MHz, $CDCl_3$) δ (ppm) 7.55 (td, *J* = 7.6, 1.3 Hz, 1H), 7.48 – 7.40 (m, 2H), 7.35 (dd, *J* = 7.8, 1.2 Hz, 1H), 4.52 (s, 2H), 3.72 – 3.49 (m, 2H), 2.65 (t, *J* = 7.1 Hz, 2H), 2.43 – 2.18 (m, 2H), 2.08 (s, 3H). ^{13}C NMR (100 MHz, $CDCl_3$) δ (ppm) 146.7, 135.8, 131.9, 131.7, 131.3, 127.4, 127.2, 118.0, 50.6, 47.2, 18.2, 17.2, 16.1. HRMS (ESI) calcd for $C_{13}H_{16}N_5O_2S^+$: 306.1019 ($M+H^+$), found: 306.1000.

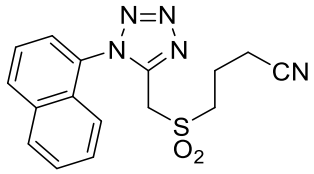

4-(((1-(Naphthalen-1-yl)-1*H*-tetrazol-5-yl)methyl)sulfonyl)butanenitrile (**3ap**); yield: 21.3 mg (31%); pale yellow oil. ^{1}H NMR (400 MHz, $CDCl_3$) δ (ppm) 8.16 (d, *J* = 8.0 Hz, 1H), 8.03 (d, *J* = 8.1 Hz, 1H), 7.76 – 7.53 (m, 4H), 7.10 (d, *J* = 8.5 Hz, 1H), 4.45 (s, 2H), 3.61 (dd, *J* = 14.6, 7.1 Hz, 2H), 2.72 – 2.56 (m, 2H), 2.38 – 2.21 (m, 2H). ^{13}C NMR (100 MHz, $CDCl_3$) δ (ppm) 147.6, 134.1, 132.4, 128.8, 128.8, 128.7, 128.1, 127.7, 126.2, 125.2, 121.1, 117.9, 50.7, 47.4, 18.2, 16.2. HRMS (ESI) calcd for $C_{16}H_{16}N_5O_2S^+$: 342.1019 ($M+H^+$), found: 342.1027.

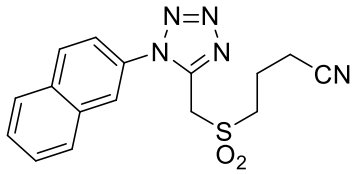

4-(((1-(Naphthalen-2-yl)-1*H*-tetrazol-5-yl)methyl)sulfonyl)butanenitrile (**3aq**); yield: 23.7 mg (35%); white solid; m.p.: 128.4-129.2 °C. ^{1}H NMR (400 MHz, Acetone-*d*^{6}) δ (ppm) 8.34 (d, *J* = 1.9 Hz, 1H), 8.23 (d, *J* = 8.8 Hz, 1H), 8.15 – 8.05 (m, 2H), 7.81 – 7.67 (m, 3H), 5.13 (s, 2H), 3.66 – 3.58 (m, 2H), 2.77 (t, *J* = 7.2 Hz, 2H), 2.31 - 2.24 (m, 2H). ^{13}C NMR (100 MHz, Acetone-*d*^{6}) δ (ppm) 147.1, 133.9, 133.0, 130.8, 130.2, 128.7, 128.2, 128.1, 127.7, 125.2, 122.9, 118.6, 51.2, 47.3, 18.4, 15.4. HRMS (ESI) calcd for $C_{16}H_{16}N_5O_2S^+$: 342.1019 ($M+H^+$), found: 342.1012.

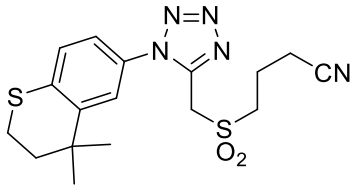

4-(((1-(4,4-Dimethylthiochroman-6-yl)-1*H*-tetrazol-5-yl)methyl)sulfonyl)butanenitrile (**3ar**); yield: 39.0 mg (50%); yellow oil. ^{1}H NMR (400 MHz, $CDCl_3$) δ (ppm) 7.62 (d, *J* = 2.3 Hz, 1H), 7.30 – 7.20 (m, 2H), 4.57 (s, 2H), 3.71 – 3.50 (m, 2H), 3.13 – 3.05 (m, 2H), 2.68 (t, *J* = 7.2 Hz, 2H), 2.38 – 2.31 (m, 2H), 2.02 – 1.96 (m, 2H), 1.36 (s, 6H). ^{13}C NMR (100 MHz, $CDCl_3$) δ (ppm) 145.9, 144.1, 137.3, 128.1, 127.9, 123.9, 122.8, 117.9, 50.6, 47.6, 36.4, 33.4, 29.8, 23.1, 18.2, 16.2. HRMS (ESI) calcd for $C_{17}H_{22}N_5O_2S_2^+$: 392.1209 (M+H$^+$), found: 392.1219.

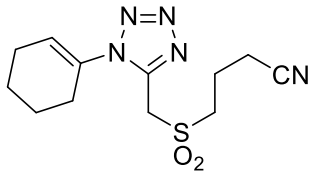

4-(((1-(Cyclohex-1-en-1-yl)-1*H*-tetrazol-5-yl)methyl)sulfonyl)butanenitrile (**3as**); yield: 30.0 mg (51%); yellow oil. ^{1}H NMR (400 MHz, $CDCl_3$) δ (ppm) 6.30 – 6.10 (m, 1H), 4.66 (s, 2H), 3.58 – 3.48 (m, 2H), 2.66 (t, *J* = 7.1 Hz, 2H), 2.54 – 2.45 (m, 2H), 2.38 – 2.24 (m, 4H), 1.95 – 1.84 (m, 2H), 1.78 – 1.72 (m, 2H). ^{13}C NMR (100 MHz, $CDCl_3$) δ (ppm) 145.1, 132.5, 129.6, 118.0, 50.5, 47.6, 28.5, 24.5, 22.0, 20.8, 18.2, 16.1. HRMS (ESI) calcd for $C_{12}H_{18}N_5O_2S^+$: 296.1176 (M+H$^+$), found: 296.1177.

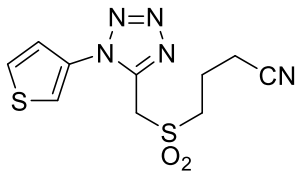

4-(((1-(Thiophen-3-yl)-1*H*-tetrazol-5-yl)methyl)sulfonyl)butanenitrile (**3at**); yield: 31.5 mg (53%); white solid; m.p.: 195.2-196.7 ^{o}C. ^{1}H NMR (400 MHz, Acetone-*d*^{6}) δ (ppm) 8.11 (s, 1H), 7.88 – 7.82 (m, 1H), 7.49 (d, *J* = 5.1 Hz, 1H), 5.06 (s, 2H), 3.60 (t, *J* = 7.6 Hz, 2H), 2.79 (t, *J* = 7.1 Hz, 2H), 2.35 - 2.24 (m, 2H). ^{13}C NMR (100 MHz, Acetone-*d*^{6}) δ (ppm) 146.9, 130.8, 128.2, 124.4, 122.8, 118.7, 51.1, 47.2, 18.4, 15.4. HRMS (ESI) calcd for $C_{10}H_{12}N_5O_2S_2^+$: 298.0427 (M+H$^+$), found: 298.0428.

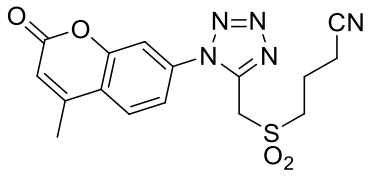

4-(((1-(4-Methyl-2-oxo-2*H*-chromen-7-yl)-1*H*-tetrazol-5-yl)methyl)sulfonyl)butanenitrile (**3au**); yield: 22.7 mg (30%); pale-yellow solid; m.p.: 185.1-187.0 ^{o}C. ^{1}H NMR (400 MHz, DMSO-*d*^{6}) δ (ppm) 8.06 (d, *J* = 8.4 Hz, 1H), 7.87 (s, 1H), 7.69 (d, *J* = 8.3 Hz, 1H), 6.58 (s, 1H), 5.27 (s, 2H), 3.50 – 3.45 (m, 2H), 2.67 (t, *J* = 6.9 Hz, 2H), 2.07 – 1.99 (m, 2H). ^{13}C NMR (100 MHz, DMSO-*d*^{6}) δ(ppm) 159.6, 153.5, 153.0, 147.2, 135.4, 127.5, 122.0, 121.8, 120.1, 116.3, 114.4, 51.4, 47.15, 18.6, 18.0, 15.6. HRMS (ESI) calcd for $C_{16}H_{16}N_5O_4S^+$: 374.0918 (M+H$^+$), found: 374.0915.

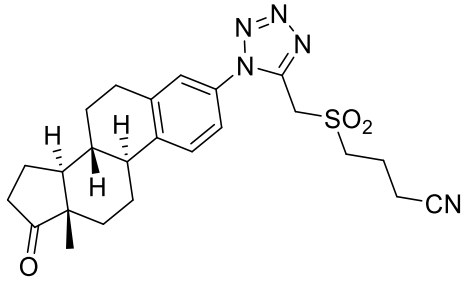

4-(((1-((8*R*,9*S*,13*S*,14*S*)-13-Methyl-17-oxo-7,8,9,11,12,13,14,15,16,17-decahydro-6*H*-cyclopenta[*a*]phenanthren-3-yl)-1*H*-tetrazol-5-yl)methyl)sulfonyl)butanenitrile (**3av**); yield: 48.5 mg (52%); white solid; m.p.: 78.2-80.0 °C. ^{1}H NMR (400 MHz, Acetone-*d*^{6}) δ (ppm) 7.63 (d, *J* = 8.1 Hz, 1H), 7.51 – 7.41 (m, 2H), 5.00 (s, 2H), 3.59 (t, *J* = 7.3 Hz, 2H), 3.04 (d, *J* = 4.3 Hz, 2H), 2.78 (t, *J* = 7.0 Hz, 2H), 2.50 (dd, *J* = 24.5, 14.6 Hz, 3H), 2.32 – 2.22 (m, 2H), 2.19 – 2.04 (m, 3H), 1.92 (d, *J* = 12.6 Hz, 1H), 1.81 – 1.46 (m, 6H), 0.95 (s, 3H). ^{13}C NMR (100 MHz, Acetone-*d*^{6}) δ (ppm) 218.4, 146.7, 143.2, 139.0, 130.9, 127.0, 125.8, 122.8, 118.7, 51.0, 50.2, 47.4, 47.2, 44.3, 37.7, 35.1, 31.6, 25.9, 25.4, 21.2, 18.3, 15.3, 13.2. HRMS (ESI) calcd for $C_{24}H_{30}N_5O_3S^+$: 468.2064 (M+H$^+$), found: 468.2057.

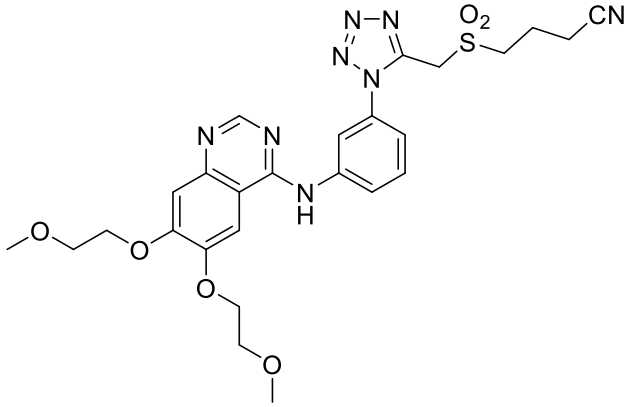

4-(((1-(3-((6,7-Bis(2-methoxyethoxy)quinazolin-4-yl)amino)phenyl)-1*H*-tetrazol-5-yl)methyl)sulfonyl)butanenitrile (**3aw**); yield: 52.4 mg (45%); white solid; m.p.: 104.6-105.8. ^{1}H NMR (400 MHz, DMSO-*d*^{6}) δ (ppm) 9.81 (s, 1H), 8.55 (s, 1H), 8.29 (s, 1H), 8.05 (d, *J* = 8.1 Hz, 1H), 7.90 (s, 1H), 7.70 (t, *J* = 8.0 Hz, 1H), 7.44 (d, *J* = 7.8 Hz, 1H), 7.26 (s, 1H), 5.25 (s, 2H), 4.31 (s, 4H), 3.79 (s, 2H), 3.76 (s, 2H), 3.59 – 3.48 (m, 2H), 3.38 (s, 3H), 3.36 (s, 3H), 2.69 (t, *J* = 7.0 Hz, 2H), 2.14 – 2.02 (m, 2H). ^{1}H NMR (100 MHz, DMSO-*d*^{6}) δ (ppm) 156.5, 154.3, 153.0, 148.7, 147.2, 147.2, 141.2, 133.3, 130.5, 124.0, 120.1,120.0, 119.1, 109.3, 108.4, 103.6, 70.5, 70.5, 68.8, 68.5, 58.8, 58.8, 51.4, 47.4, 18.1, 15.6. HRMS (ESI) calcd for $C_{26}H_{31}N_8O_6S^+$: 583.2082 (M+H$^+$), found: 583.2075.

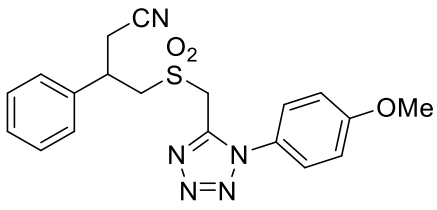

4-(((1-(4-Methoxyphenyl)-1H-tetrazol-5-yl)methyl)sulfonyl)-3-phenylbutanenitrile (**3ba**); yield: 48.1 mg (61%); pale yellow oil. ^{1}H NMR (400 MHz, $CDCl_3$) δ (ppm) 7.46 – 7.32 (m, 7H), 7.05 (d, *J* = 7.6 Hz, 2H), 4.26 (d, *J* = 15.3 Hz, 1H), 4.16 (dd, *J* = 13.8, 6.2 Hz, 1H), 4.02 (d, *J* = 15.2 Hz, 1H), 3.88 (s, 3H), 3.82 – 3.66 (m, 2H), 2.96 – 2.92 (m, 2H). ^{13}C NMR (100 MHz, $CDCl_3$) δ (ppm) 161.6, 146.1, 137.7, 129.46, 128.8, 127.6, 127.2, 124.9, 117.0, 115.2, 55.7, 48.1, 36.7, 24.4. HRMS (ESI) calcd for $C_{19}H_{20}N_5O_3S^+$: 398.1281 (M+H$^+$), found: 398.1295.

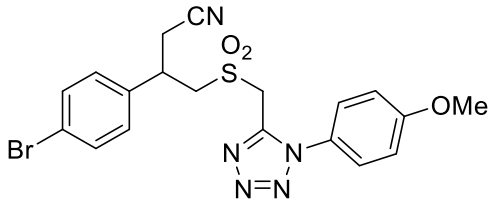

3-(4-Bromophenyl)-4-(((1-(4-methoxyphenyl)-1*H*-tetrazol-5-yl)methyl)sulfonyl)butanenitrile (**3ca**); yield: 66.4 mg (70%); pale yellow solid; m.p.: 61.8-62.7 °C. ^{1}H NMR (400 MHz, $CDCl_3$) δ (ppm) 7.54 (d, *J* = 8.0 Hz, 2H), 7.44 (d, *J* = 8.3 Hz, 2H), 7.30 (d, *J* = 7.9 Hz, 2H), 7.06 (d, *J* = 8.2 Hz, 2H), 4.34 (d, *J* = 15.2 Hz, 1H), 4.20 – 4.04 (m, 2H), 3.89 (s, 3H), 3.76 – 3.62 (m, 2H), 3.04 – 2.80 (m, 2H). ^{13}C NMR (100 MHz, $CDCl_3$) δ (ppm) 161.6, 146.0, 136.8, 132.5, 129.3, 127.2, 124.8, 122.8, 116.8, 115.2, 55.71, 55.5, 48.3, 36.1, 24.3. HRMS (ESI) calcd for $C_{19}H_{19}BrN_5O_3S^+$: 476.0386 (M+H$^+$), found: 476.0388.

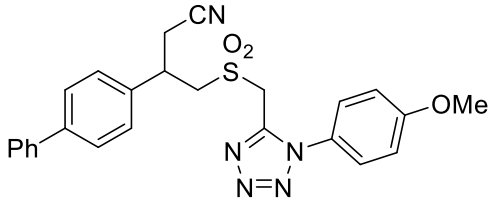

3-([1,1'-Biphenyl]-4-yl)-4-(((1-(4-methoxyphenyl)-1*H*-tetrazol-5-yl)methyl)sulfonyl)butanenitrile (**3da**); yield: 54.2 mg (57%); pale yellow solid; m.p.: 139.1-141.0 °C. ^{1}H NMR (400 MHz, $CDCl_3$) δ (ppm) 7.64 – 7.54 (m, 4H), 7.51 – 7.32 (m, 7H), 7.02 (d, *J* = 7.6 Hz, 2H), 4.29 (d, *J* = 15.3 Hz, 1H), 4.19 (dd, *J* = 13.9, 6.4 Hz, 1H), 4.09 (d, *J* = 15.2 Hz, 1H), 3.88 – 3.69 (m, 5H), 3.05 – 2.85 (m, 2H). ^{13}C NMR (100 MHz, $CDCl_3$) δ (ppm) 161.5, 146.1, 141.5, 139.8, 136.6, 128.8, 128.0, 128.0, 127.7, 127.2, 126.9, 124.8, 117.0, 115.2, 55.7, 48.2, 36.4, 24.4. HRMS (ESI) calcd for $C_{25}H_{24}N_5O_3S^+$: 474.1594 (M+H$^+$), found: 474.1590.

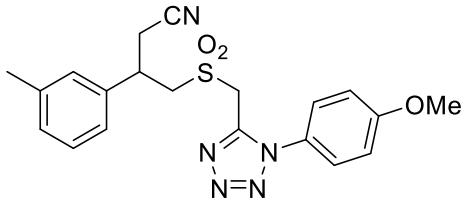

4-(((1-(4-Methoxyphenyl)-1*H*-tetrazol-5-yl)methyl)sulfonyl)-3-(*m*-tolyl)butanenitrile (**3ea**); yield: 48.6 mg (59%); pale yellow oil. ^{1}H NMR (400 MHz, $CDCl_3$) δ (ppm) 7.44 (d, *J* = 7.9 Hz, 2H), 7.32 – 7.13 (m, 4H), 7.05 (d, *J* = 8.0 Hz, 2H), 4.28 – 4.10 (m, 2H), 3.98 (d, *J* = 15.2 Hz, 1H), 3.88 (s, 3H), 3.76-3.62 (m, 2H), 3.00 – 2.84 (m, 2H), 2.36 (s, 3H). ^{13}C NMR (100 MHz, $CDCl_3$) δ (ppm) 161.6, 146.1, 139.4, 137.5, 129.6, 129.3, 128.3, 127.2, 124.9, 124.6, 117.0, 115.2, 55.8, 55.7, 48.1, 36.8, 24.4, 21.4. HRMS (ESI) calcd for $C_{20}H_{22}N_5O_3S^+$: 412.1438 (M+H$^+$), found: 412.1442.

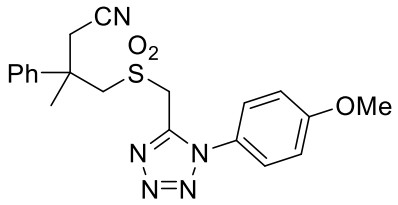

4-(((1-(4-Methoxyphenyl)-1*H*-tetrazol-5-yl)methyl)sulfonyl)-3-methyl-3-phenylbutanenitrile (**3fa**); yield: 46.7 mg (57%); pale yellow solid; m.p.: 48.6-51.3 °C. ^{1}H NMR (400 MHz, $CDCl_3$) δ (ppm) 7.54 (d, *J* = 7.5 Hz, 2H), 7.45 - 7.35 (m, 4H), 7.32 (t, *J* = 7.2 Hz, 1H), 7.02 (d, *J* = 8.0 Hz, 2H), 4.08 (d, *J* = 15.2 Hz, 1H), 3.93 – 3.77 (m, 5H), 3.71 (d, *J* = 15.3 Hz, 1H), 3.27 – 3.14 (m, 2H), 1.85 (s, 3H). ^{13}C NMR (100 MHz, $CDCl_3$) 161.5, 146.2, 139.9, 129.1, 128.3, 127.2, 126.3,

124.9, 117.0, 115.1, 61.0, 55.7, 48.5, 40.0, 29.1, 26.3. HRMS (ESI) calcd for $C_{20}H_{22}N_5O_3S^+$: 412.1438 ($M+H^+$), found: 412.1449.

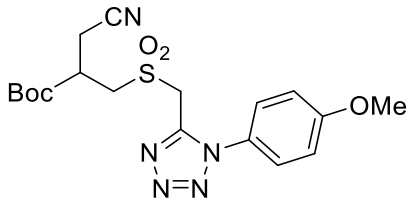

tert-Butyl 3-cyano-2-((((1-(4-methoxyphenyl)-1*H*-tetrazol-5-yl)methyl)sulfonyl)methyl)propanoate (**3ga**); yield: 50.6 mg (60%); pale yellow oil. ^{1}H NMR (400 MHz, $CDCl_3$) δ (ppm) 7.49 (d, *J* = 8.1 Hz, 2H), 7.09 (d, *J* = 8.1 Hz, 2H), 4.68 (q, *J* = 15.2 Hz, 2H), 4.12 (dd, *J* = 14.5, 5.9 Hz, 1H), 3.90 (s, 3H), 3.67 (dd, *J* = 14.5, 6.7 Hz, 1H), 3.42 – 3.25 (m, 1H), 3.02 – 2.81 (m, 2H), 1.50 (s, 9H). ^{13}C NMR (100 MHz, $CDCl_3$) δ (ppm) 168.2, 161.6, 146.1, 127.2, 125.0, 116.4, 115.2, 84.2, 55.7, 52.4, 48.5, 36.9, 27.7, 19.6. HRMS (ESI) calcd for $C_{18}H_{24}N_5O_5S^+$: 422.1493 ($M+H^+$), found: 422.1489.

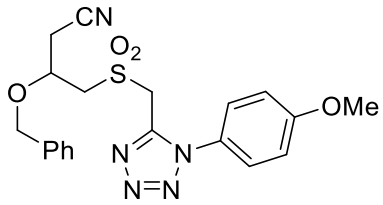

3-(Benzyloxy)-4-(((1-(4-methoxyphenyl)-1*H*-tetrazol-5-yl)methyl)sulfonyl)butanenitrile (**3ha**); yield: 50.7 mg (59%); pale yellow oil. ^{1}H NMR (400 MHz, $CDCl_3$) δ (ppm) 7.46 – 7.28 (m, 7H), 7.05 (d, *J* = 8.3 Hz, 2H), 4.82 – 4.60 (m, 3H), 4.53 – 4.33 (m, 2H), 4.13 – 3.97 (m, 1H), 3.88 (s, 3H), 3.54 (d, *J* = 15.0 Hz, 1H), 2.81 (d, *J* = 5.3 Hz, 2H). ^{13}C NMR (100 MHz, $CDCl_3$) δ (ppm) 161.5, 146.2, 135.9, 128.7, 128.5, 128.2, 127.2, 125.0, 116.1, 115.2, 73.0, 70.4, 55.7, 55.2, 49.1, 22.6. HRMS (ESI) calcd for $C_{20}H_{22}N_5O_4S^+$: 428.1387 ($M+H^+$), found: 428.1384.

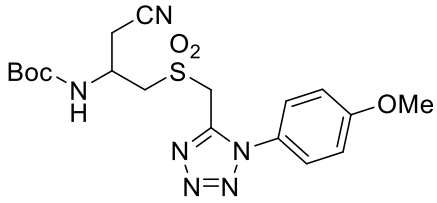

tert-Butyl (1-cyano-3-(((1-(4-methoxyphenyl)-1*H*-tetrazol-5-yl)methyl)sulfonyl)propan-2-yl)carbamate (**3ia**); yield: 59.5 mg (68%); pale yellow oil. ^{1}H NMR (400 MHz, $CDCl_3$) δ (ppm) 7.51 – 7.46 (m, 2H), 7.09 -7.04 (m, 2H), 5.76 (s, 1H), 4.77 – 4.65 (m, 3H), 3.91 – 3.84 (m, 4H), 3.70 – 3.62 (m, 1H), 2.92 (d, *J* = 5.4 Hz, 2H), 1.42 (s, 9H). ^{13}C NMR (100 MHz, $CDCl_3$) δ (ppm) 161.6, 154.9, 146.3, 127.3, 124.9, 116.5, 115.3, 81.1, 55.8, 54.4, 48.1, 43.4, 28.2, 23.8. HRMS (ESI) calcd for $C_{18}H_{24}N_6NaO_5S^+$: 459.1421 ($M+Na^+$), found: 459.1417.

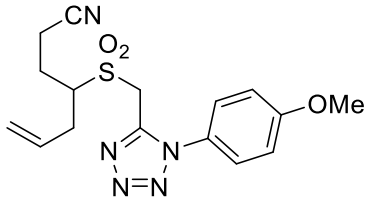

4-(((1-(4-Methoxyphenyl)-1*H*-tetrazol-5-yl)methyl)sulfonyl)hept-6-enenitrile (**3ja**); yield: 36.1 mg (50%); pale yellow oil. ^{1}H NMR (400 MHz, $CDCl_3$) δ (ppm) 7.50 (d, *J* = 7.8 Hz, 2H), 7.09 (d, *J* = 7.8 Hz, 2H), 6.01 – 5.80 (m, 1H), 5.37 – 5.26 (m, 2H), 4.69 (d, *J* = 15.3 Hz, 1H), 4.49 (d, *J* = 15.2 Hz, 1H), 3.90 (s, 3H), 3.85 – 3.74 (m, 1H), 2.92 – 2.80 (m, 1H), 2.68 – 2.51 (m, 3H), 2.41 – 2.28 (m, 1H), 2.26 – 2.14 (m, 1H). ^{13}C NMR (100 MHz, $CDCl_3$) δ (ppm) 161.6, 146.1, 131.7,

127.2, 125.0, 120.6, 118.4, 115.2, 58.8, 55.7, 46.1, 32.4, 22.9, 14.8. HRMS (ESI) calcd for $C_{16}H_{20}N_5O_3S^+$: 362.1281 (M+H$^+$), found: 362.1292.

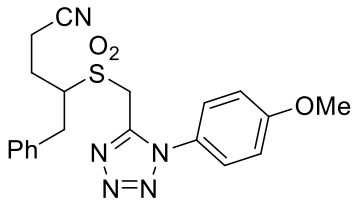

4-(((1-(4-Methoxyphenyl)-1*H*-tetrazol-5-yl)methyl)sulfonyl)-5-phenylpentanenitrile (**3ka**); yield: 52.7 mg (64%); pale yellow oil. ^{1}H NMR (400 MHz, $CDCl_3$) δ (ppm) 7.47 (d, *J* = 7.8 Hz, 2H), 7.43 – 7.35 (m, 4H), 7.34 7.28 (m, 1H), 7.07 (d, *J* = 7.8 Hz, 2H), 4.42- 4.29 (m, 2H), 4.15 – 4.04 (m, 1H), 3.89 (s, 3H), 3.51 (dd, *J* = 13.8, 4.8 Hz, 1H), 3.01 – 2.87 (m, 1H), 2.60 – 2.21 (m, 3H), 2.17 – 2.04 (m, 1H). ^{13}C NMR (100 MHz, $CDCl_3$) δ (ppm) 161.6, 146.1, 134.9, 129.3, 129.2, 127.8, 127.2, 124.9, 118.2, 115.2, 60.6, 55.7, 46.1, 34.7, 22.9, 15.0. HRMS (ESI) calcd for $C_{20}H_{22}N_5O_3S^+$: 412.1438 (M+H$^+$), found: 412.1445.

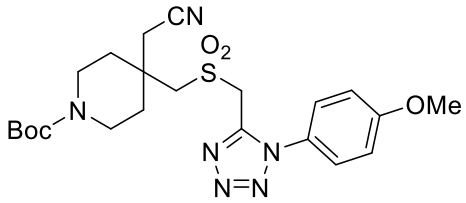

tert-Butyl 4-(cyanomethyl)-4-((((1-(4-methoxyphenyl)-1*H*-tetrazol-5-yl)methyl)sulfonyl)methyl)piperidine-1-carboxylate (**3la**); yield: 61.1 mg (62%); white solid; m.p.: 83.6-85.1 ^{o}C. ^{1}H NMR (400 MHz, $CDCl_3$) δ (ppm) 7.49 (d, *J* = 7.9 Hz, 2H), 7.09 (d, *J* = 7.9 Hz, 2H), 4.57 (s, 2H), 3.90 (s, 3H), 3.77 (s, 2H), 3.68 - 3.56 (m, 2H), 3.38 – 3.25 (m, 2H), 2.86 (s, 2H), 1.97 – 1.86 (m, 2H), 1.72 – 1.64 (m, 2H), 1.46 (s, 9H). ^{13}C NMR (100 MHz, $CDCl_3$) δ (ppm) 161.6, 154.4, 146.2, 127.2, 124.9, 116.6, 115.2, 80.1, 55.7, 55.4, 50.2, 36.0, 34.3, 28.3, 26.8. HRMS (ESI) calcd for $C_{22}H_{31}N_6O_5S^+$: 491.2071 (M+H$^+$), found: 491.2062.

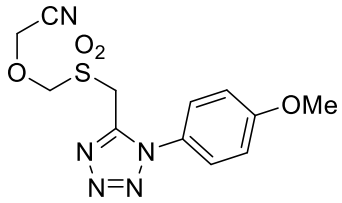

2-((((1-(4-Methoxyphenyl)-1*H*-tetrazol-5-yl)methyl)sulfonyl)methoxy)acetonitrile (**3ma**); yield: 25.7 mg (40%); white solid; m.p.: 122.7-123.7 ^{o}C. ^{1}H NMR (400 MHz, Acetone-*d*^{6}) δ (ppm) 7.63 (d, *J* = 7.6 Hz, 2H), 7.23 (d, *J* = 7.6 Hz, 2H), 5.08 (s, 2H), 4.96 (s, 2H), 4.89 (s, 2H), 3.95 (s, 3H). ^{13}C NMR (100 MHz, Acetone-*d*^{6}) δ (ppm) 161.6, 146.5, 127.4, 125.8, 115.3, 115.0, 82.0, 57.6, 55.3, 44.5. HRMS (ESI) calcd for $C_{12}H_{14}N_5O_4S^+$: 324.0761 (M+H$^+$), found: 324.0769.

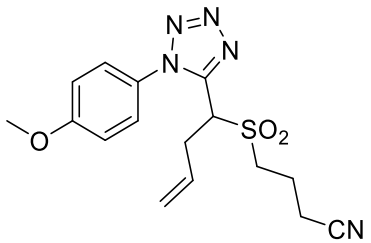

4-((1-(1-(4-Methoxyphenyl)-1*H*-tetrazol-5-yl)but-3-en-1-yl)sulfonyl)butanenitrile (**4**); yield: 42.0 mg (58%); colorless oil. ^{1}H NMR (400 MHz, $CDCl_3$) δ (ppm) 7.41 (d, *J* = 8.8 Hz, 2H), 7.08 (d, *J* = 8.8 Hz, 2H), 5.59 – 5.38 (m, 1H), 5.12 – 5.00 (m, 2H), 4.36 – 4.25 (m, 1H), 3.90 (s, 3H), 3.78 – 3.65 (m, 1H), 3.47 – 3.35 (m, 1H), 3.23 – 3.02 (m, 2H), 2.76 – 2.53 (m, 2H), 2.35 - 2.18 (m,

2H). ^{13}C NMR (100 MHz, $CDCl_3$) δ (ppm) 161.6, 149.8, 130.1, 127.7, 124.8, 121.0, 118.0, 115.2, 59.65, 55.8, 46.8, 33.9, 17.4, 16.4. HRMS (ESI) calcd for $C_{16}H_{20}N_5O_3S^+$: 362.1281 ($M+H^+$), found: 362.1298.

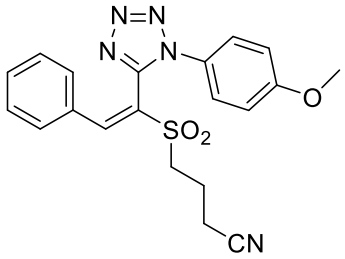

(*E*)-4-((1-(1-(4-methoxyphenyl)-1*H*-tetrazol-5-yl)-2-phenylvinyl)sulfonyl)butanenitrile (**5**); yield: 57.2 mg (70%); white solid; m.p.:130.8-131.1 °C. ^{1}H NMR (400 MHz, $CDCl_3$) δ (ppm) 8.00 (s, 1H), 7.39 (t, *J* = 7.3 Hz, 1H), 7.29 - 7.19 (m, 2H), 7.01 (d, *J* = 8.1 Hz, 2H), 6.83 - 6.65 (m, 4H), 3.80 – 3.63 (m, 5H), 2.84 - 2.54 (m, 2H), 2.45 - 2.25 (m, 2H). ^{13}C NMR (100 MHz, $CDCl_3$) δ (ppm) 160.8, 149.6, 147.7, 132.1, 130.5, 129.4, 129.2, 125.8, 125.3, 123.4, 118.1, 114.4, 55.6, 51.5, 19.1, 16.2. HRMS (ESI) calcd for $C_{20}H_{20}N_5O_3S^+$: 410.1281 ($M+H^+$), found: 410.1275.

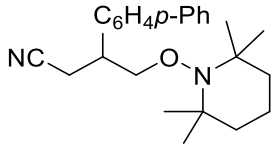

3-([1,1'-Biphenyl]-4-yl)-4-((2,2,6,6-tetramethylpiperidin-1-yl)oxy)butanenitrile (**6**) (Zhang et al., 2020); yield: 11.4 mg (15%); colorless oil. ^{1}H NMR (400 MHz, $CDCl_3$) δ (ppm) 7.60 – 7.55 (m, 4H), 7.47 – 4.41 (m, 2H), 7.37 – 7.31 (m, 3H), 4.02 (d, *J* = 6.4 Hz, 2H), 3.27 (dt, *J* = 12.5, 6.3 Hz, 1H), 2.95 (dd, *J* = 16.7, 5.8 Hz, 1H), 2.78 (dd, *J* = 16.7, 8.0 Hz, 1H), 1.55 – 1.27 (m, 6H), 1.16 – 1.06 (m, 12H). ^{13}C NMR (100 MHz, $CDCl_3$) δ (ppm) 140.6, 140.6, 138.3, 128.8, 128.0, 127.4, 127.4, 127.1, 118.7, 78.2, 60.1, 41.7, 39.7, 39.7, 33.1, 21.2, 20.3, 20.2, 17.0 .

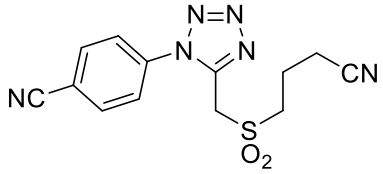

4-(5-(((3-Cyanopropyl)sulfonyl)methyl)-1*H*-tetrazol-1-yl)benzonitrile (**3ax**); yield: 16.7 mg (26%); pale yellow solid; m.p.: 138.0-139.6 °C. ^{1}H NMR (400 MHz, Acetone-*d*^{6}) δ (ppm) 8.19 – 8.13 (m, 2H), 8.04 – 7.98 (m, 2H), 5.13 (s, 2H), 3.66 – 3.52 (m, 2H), 2.76 (t, *J* = 7.2 Hz, 2H), 2.32 – 2.22 (m, 2H). ^{13}C NMR (100 MHz, Acetone-*d*^{6}) δ (ppm) 147.0, 137.0, 134.1, 126.8, 118.6, 117.3, 114.7, 51.1, 47.1, 18.3, 15.36. HRMS (ESI) calcd for $C_{13}H_{13}N_6O_2S^+$: 317.0815 ($M+H^+$), found: 317.0810.

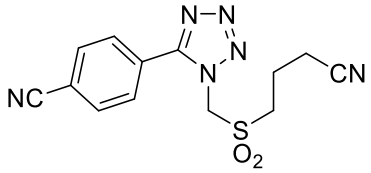

4-(1-(((3-Cyanopropyl)sulfonyl)methyl)-1*H*-tetrazol-5-yl)benzonitrile (**3ax'**); yield: 7.3 mg (12%); white solid; m.p.: 151.4-152.6 °C. ^{1}H NMR (400 MHz, DMSO-*d*^{6}) δ (ppm) 8.15 – 8.11 (m, 2H), 8.08 – 8.04 (m, 2H), 6.38 (s, 2H), 3.53 – 3.40 (m, 2H), 2.68 (t, *J* = 7.2 Hz, 2H), 2.10 – 1.96 (m, 2H). ^{13}C NMR (100 MHz, DMSO-*d*^{6}) δ (ppm) 155.1, 133.6, 130.6, 127.8, 120.0, 118.5, 114.7, 63.4, 50.5, 17.8, 15.7. HRMS (ESI) calcd for $C_{13}H_{13}N_6O_2S^+$: 317.0815 ($M+H^+$), found: 317.0806.

4. Data S2. The copies of NMR spectra, Related to Scheme 2, Scheme 3 and Scheme 4.

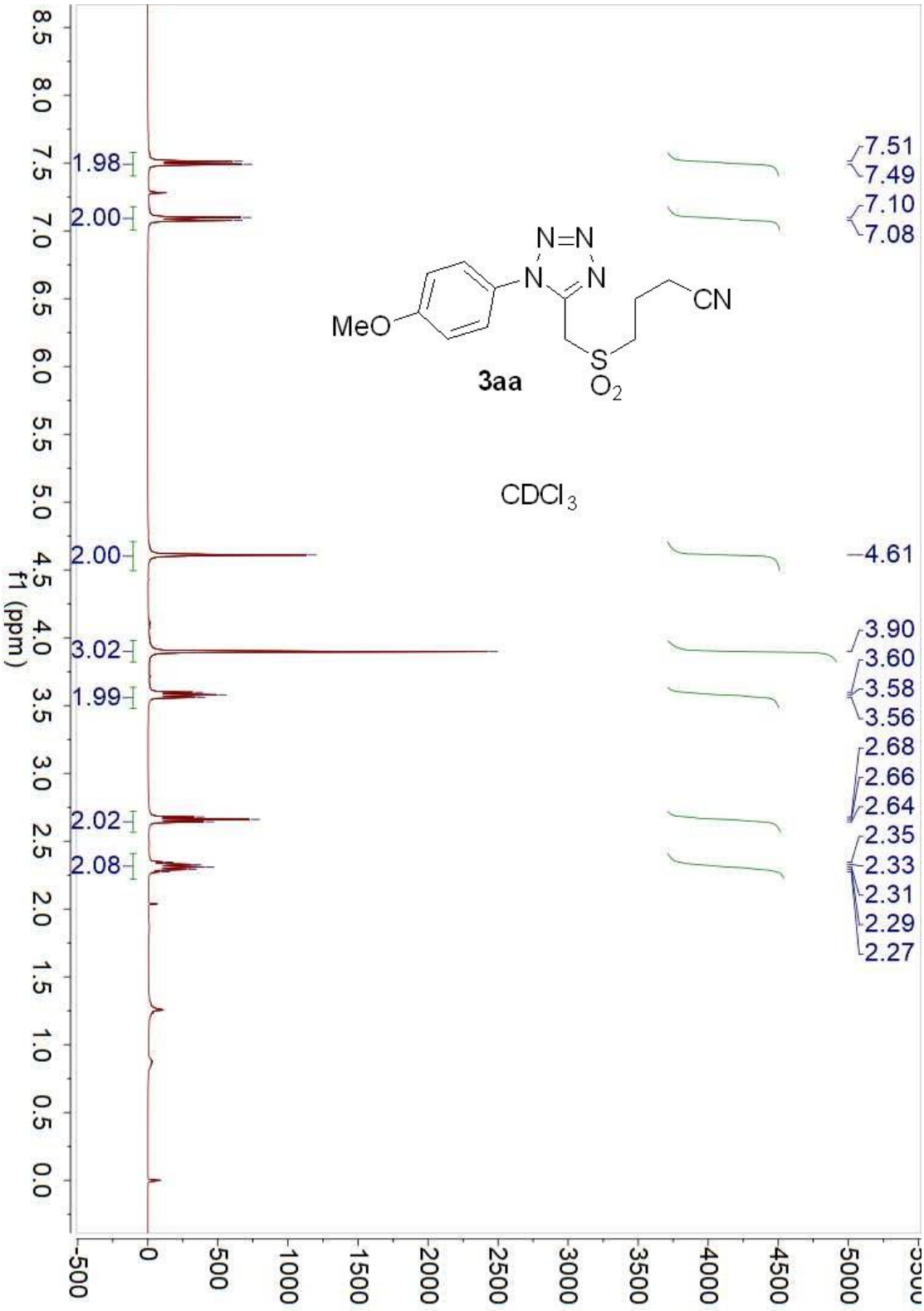

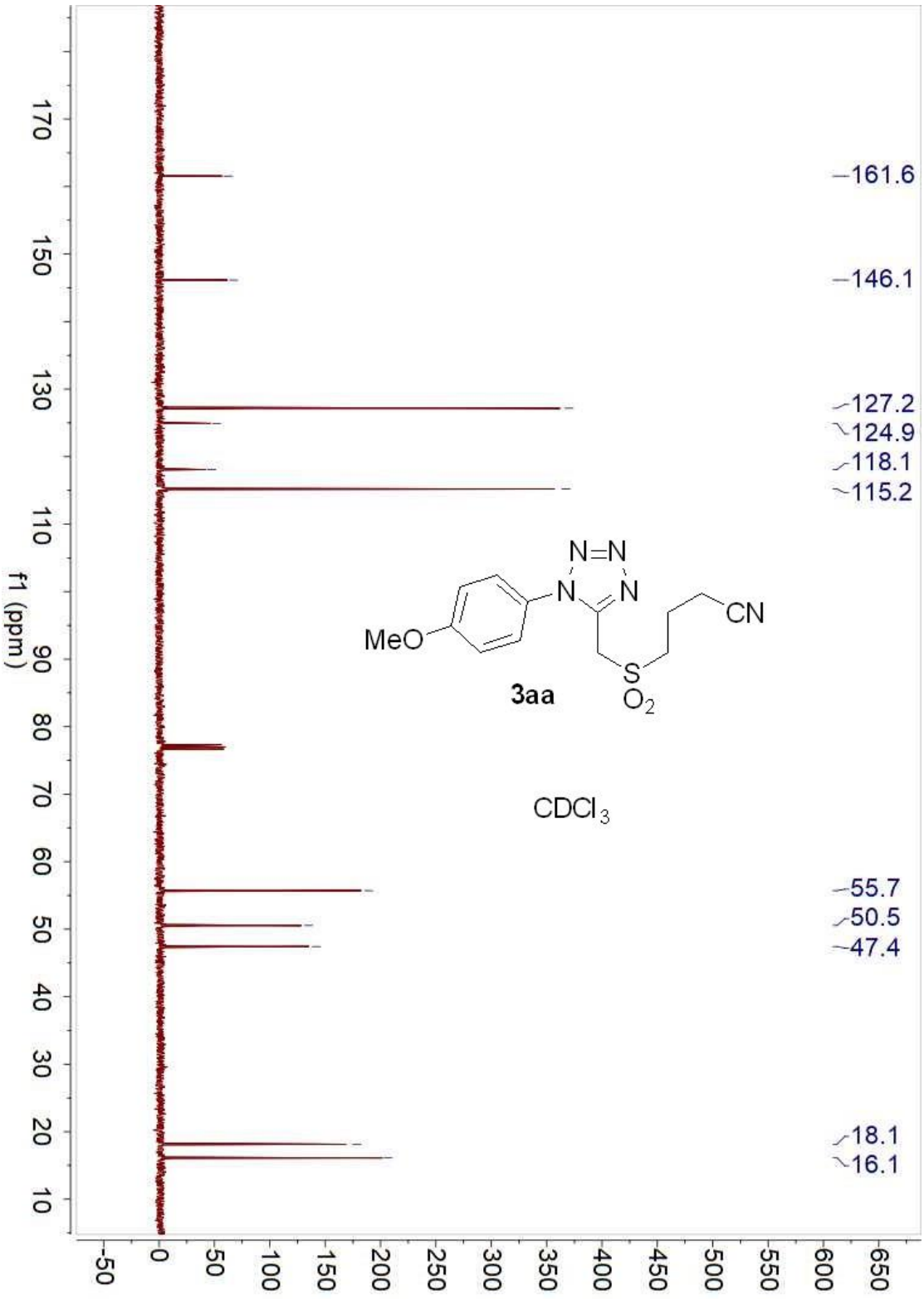
161.6
146.1
127.2
124.9
118.1
115.2
55.7
50.5
47.4
18.1
16.1
f1 (ppm)
MeO
N=N
N
N
CN
S
O2
3aa
CDCl3

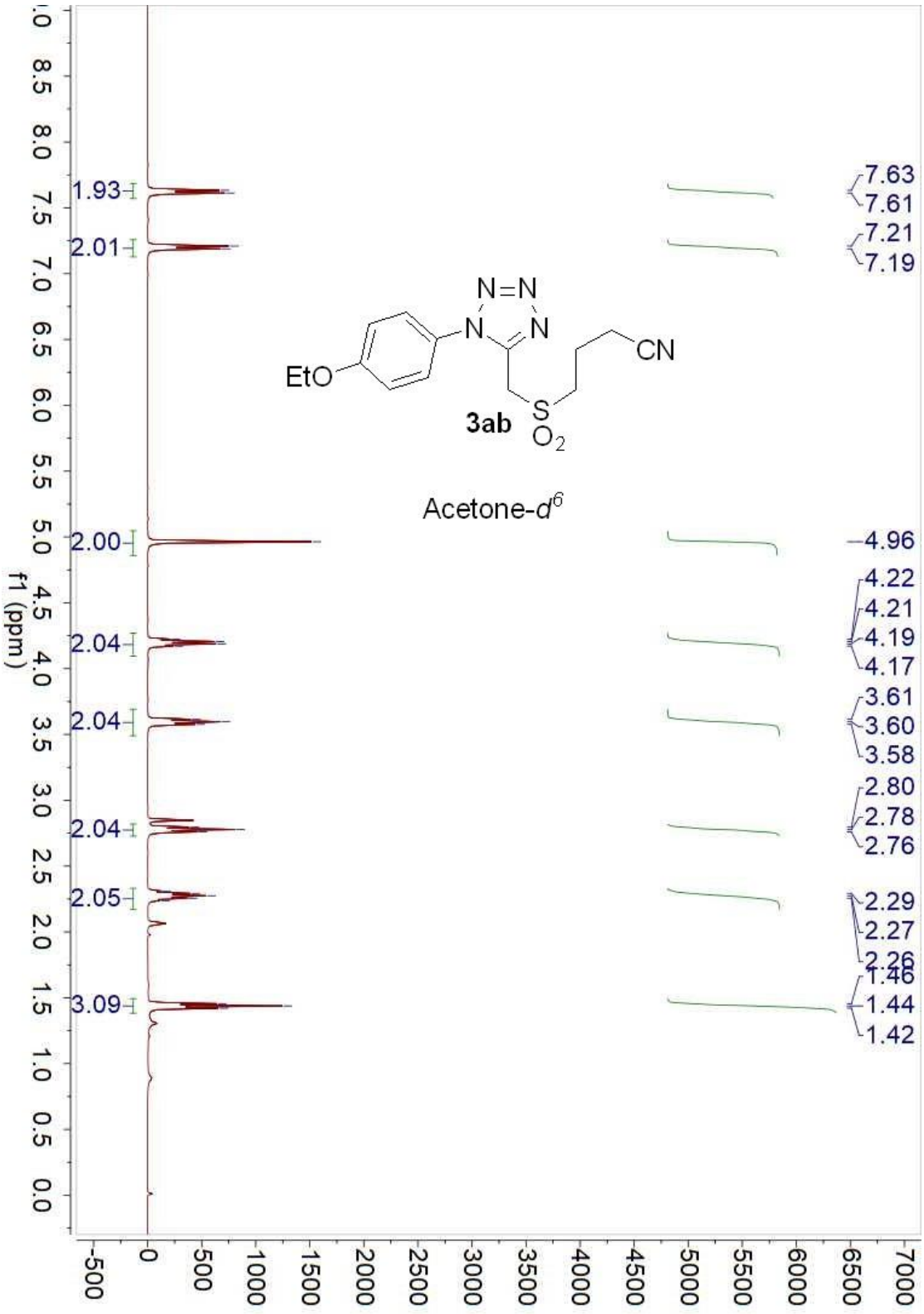
1.93
2.01
2.00
2.04
2.04
2.04
2.05
3.09
7.63
7.61
7.21
7.19
4.96
4.22
4.21
4.19
4.17
3.61
3.60
3.58
2.80
2.78
2.76
2.29
2.27
2.26
1.46
1.44
1.42
N=N
N
N
EtO
CN
S
O2
3ab
Acetone-d6
f1 (ppm)

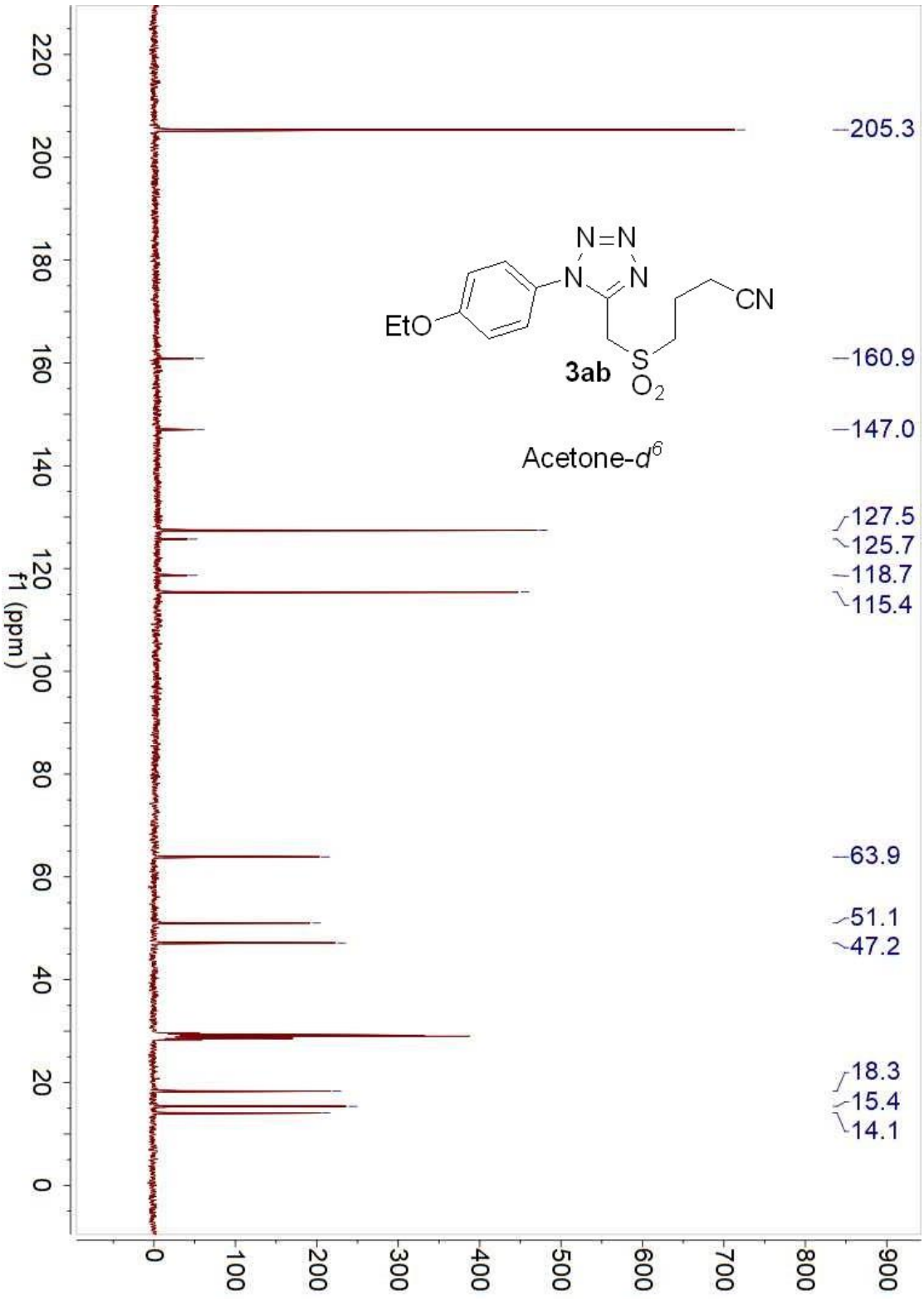
205.3
160.9
147.0
127.5
125.7
118.7
115.4
63.9
51.1
47.2
18.3
15.4
14.1
EtO
N=N
N
N
CN
S
O2
3ab
Acetone-d6
f1 (ppm)
0
20
40
60
80
100
120
140
160
180
200
220
0
100
200
300
400
500
600
700
800
900

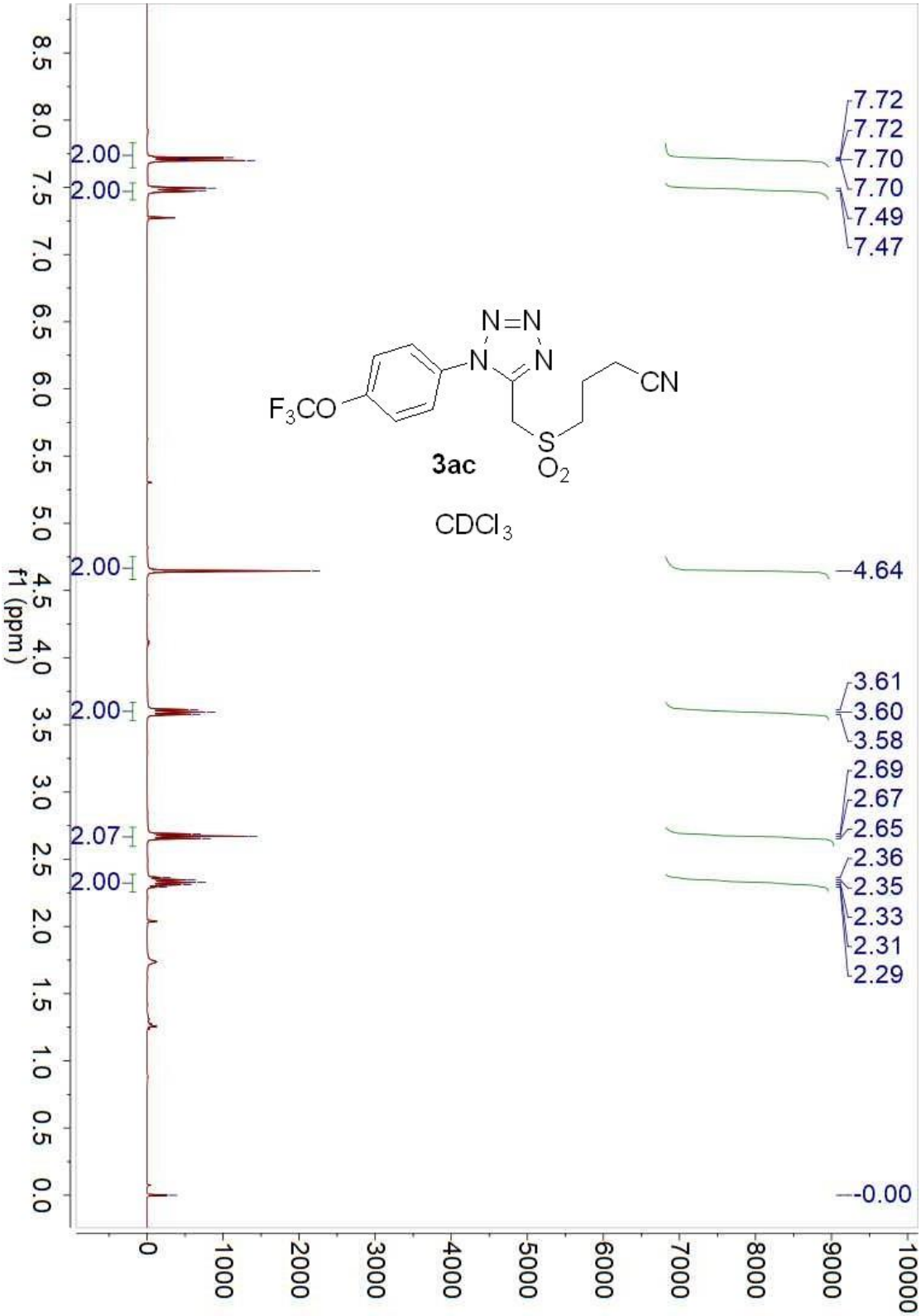
7.72
7.72
7.70
7.70
7.49
7.47
2.00
2.00
N=N
N
N
N
F3CO
CN
S
O2
3ac
CDCl3
2.00
4.64
3.61
3.60
3.58
2.00
2.69
2.67
2.65
2.07
2.36
2.35
2.33
2.31
2.29
2.00
-0.00
f1 (ppm)
8.5
8.0
7.5
7.0
6.5
6.0
5.5
5.0
4.5
4.0
3.5
3.0
2.5
2.0
1.5
1.0
0.5
0.0
0
1000
2000
3000
4000
5000
6000
7000
8000
9000
10000

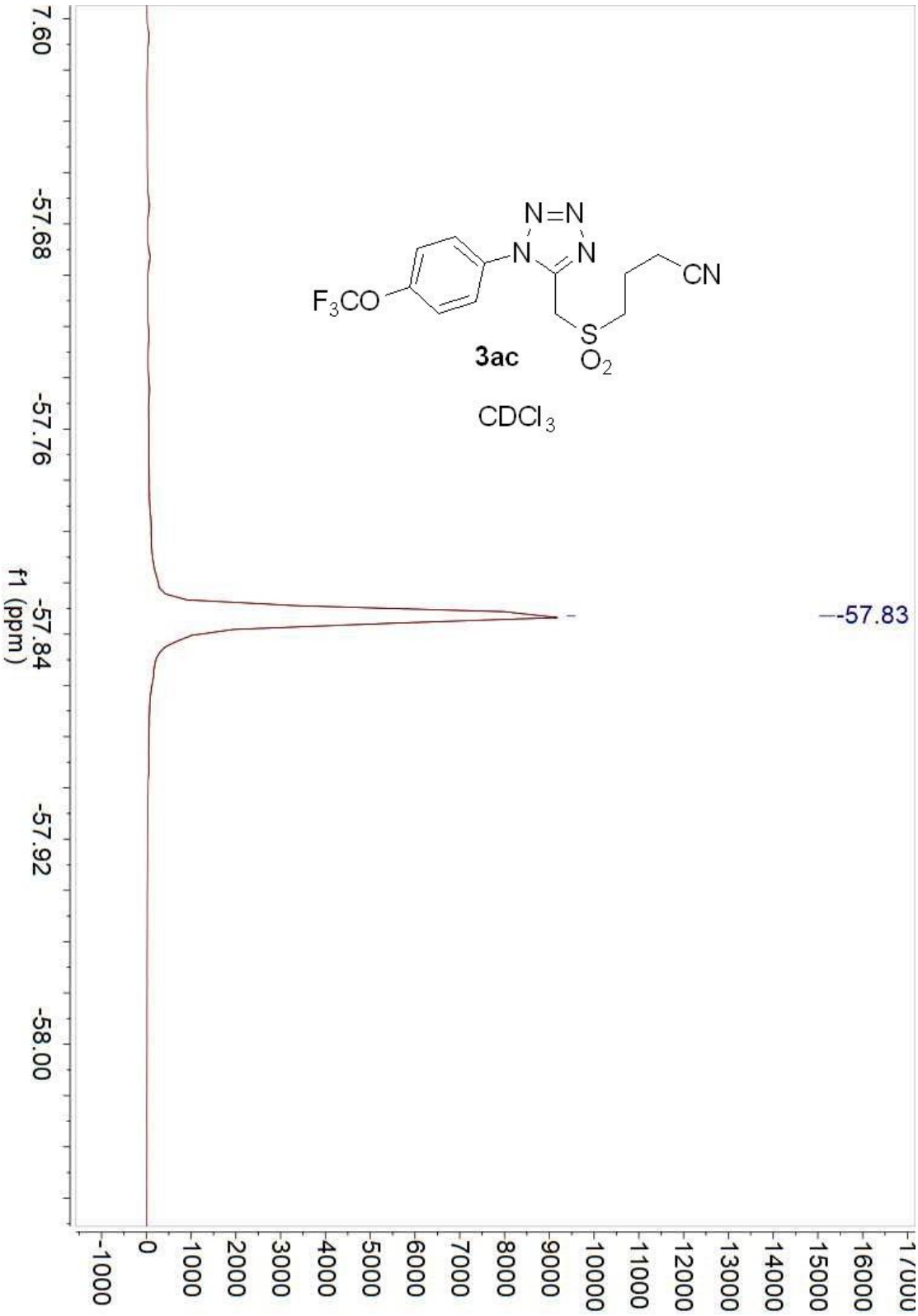
N=N
N
N
F3CO
CN
S
O2
3ac
CDCl3
-57.83
7.60
-57.68
-57.76
-57.84
-57.92
-58.00
f1 (ppm)
-1000
0
1000
2000
3000
4000
5000
6000
7000
8000
9000
10000
11000
12000
13000
14000
15000
16000

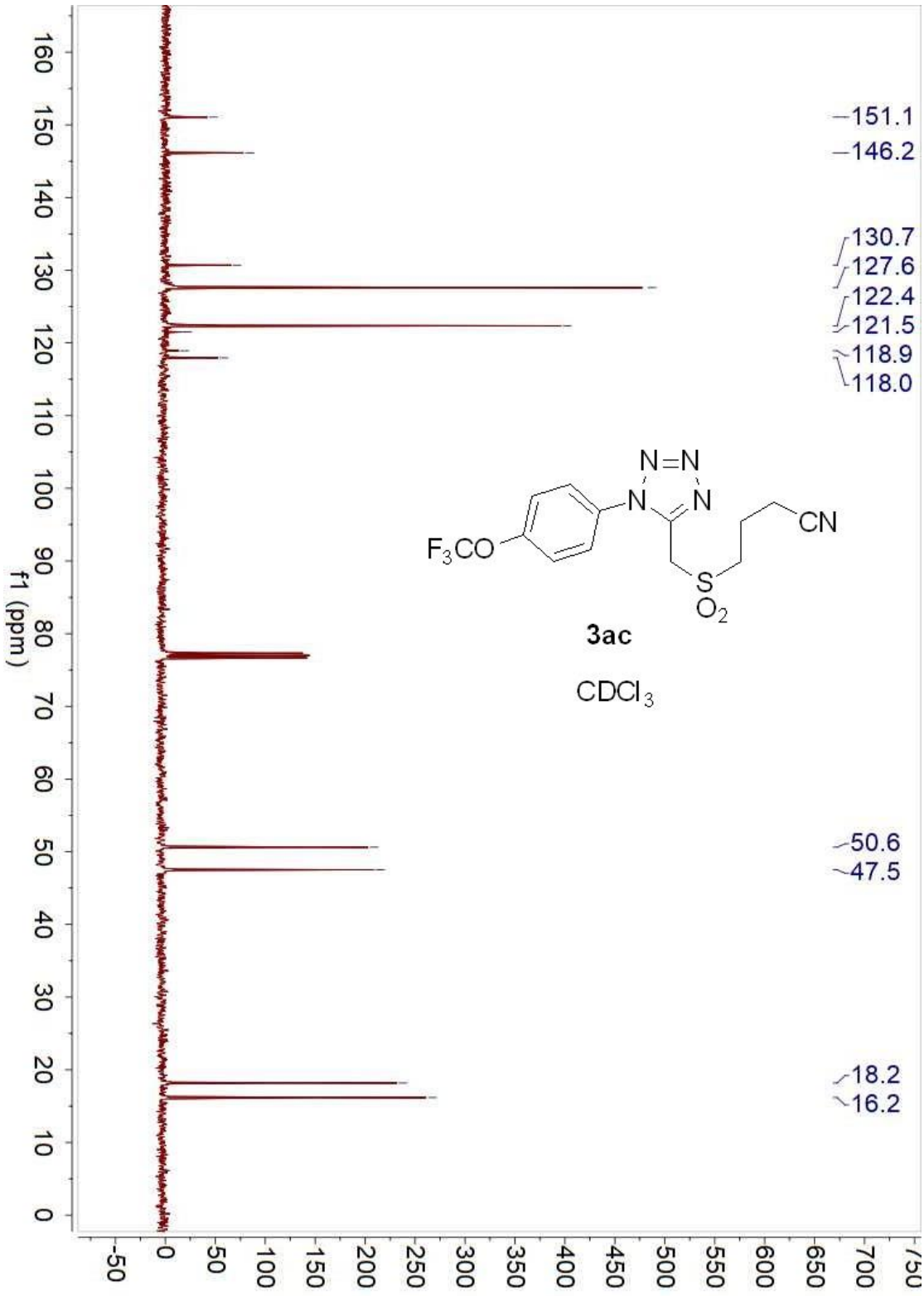
151.1
146.2
130.7
127.6
122.4
121.5
118.9
118.0
50.6
47.5
18.2
16.2
N=N
N
N
CN
F3CO
S
O2
3ac
CDCl3
f1 (ppm)

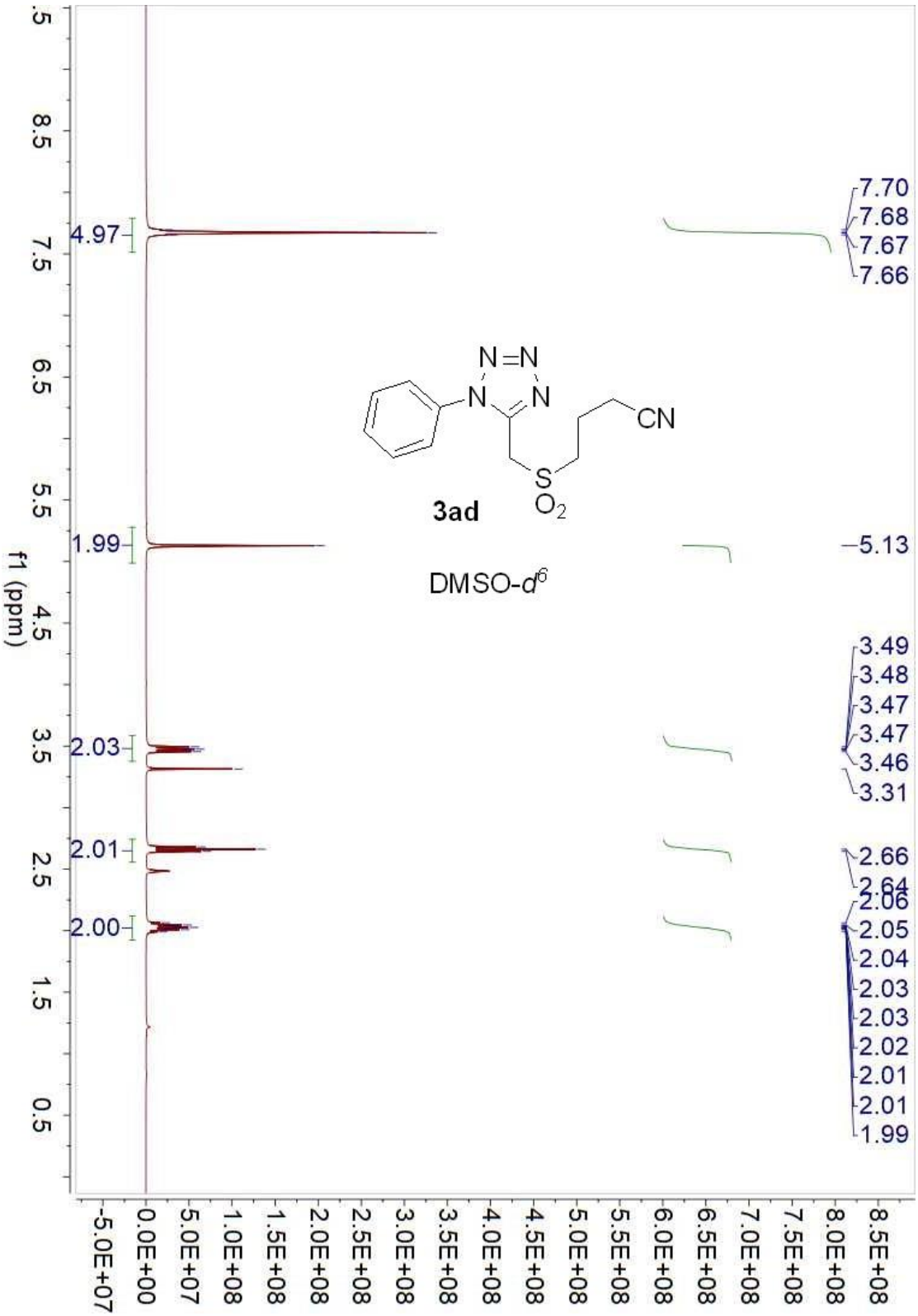
7.70
7.68
7.67
7.66
5.13
3.49
3.48
3.47
3.47
3.46
3.31
2.66
2.64
2.06
2.05
2.04
2.03
2.03
2.02
2.01
2.01
1.99
4.97
1.99
2.03
2.01
2.00
N=N
N
N
CN
S
O2
3ad
DMSO-d6
f1 (ppm)

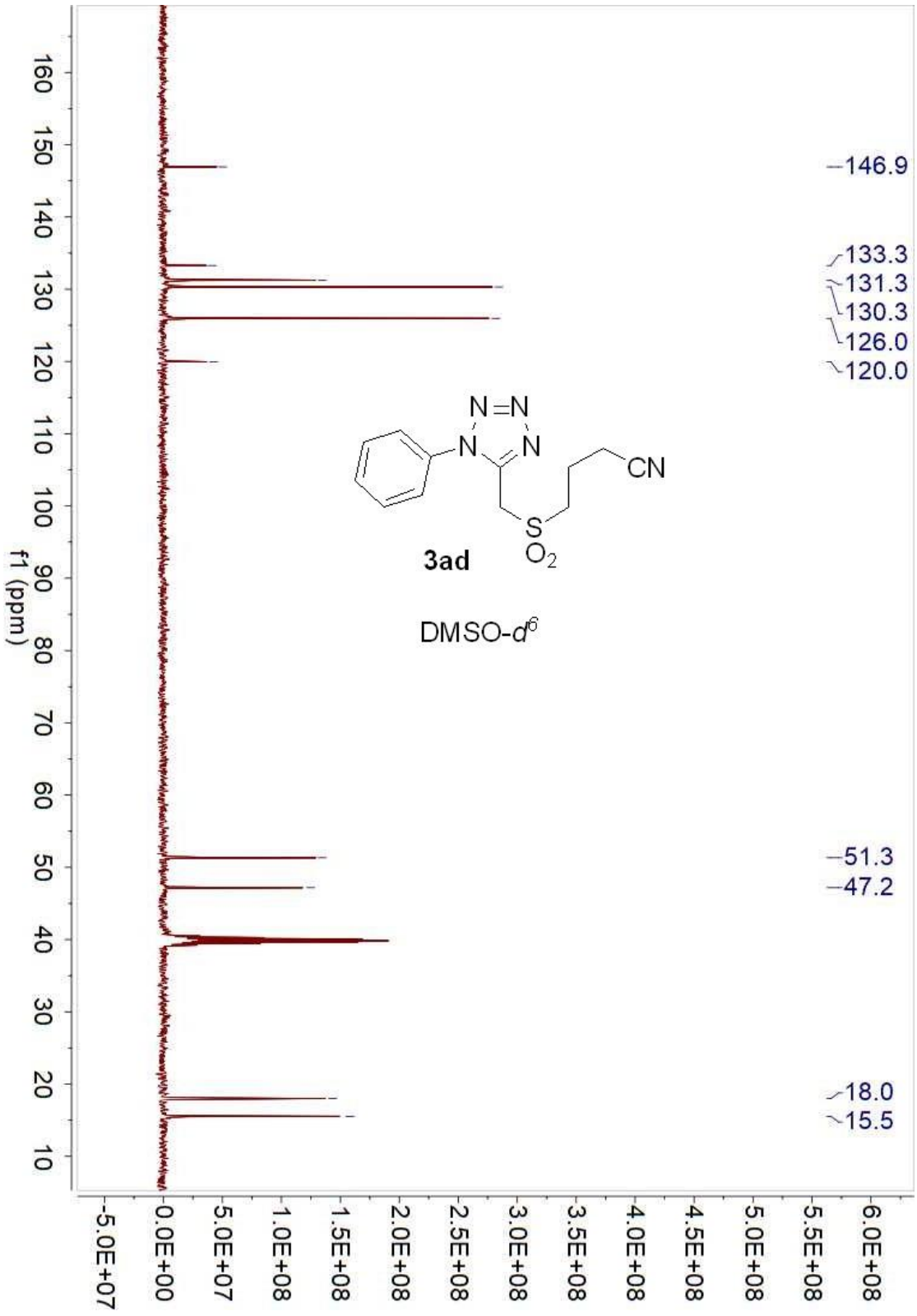
146.9
133.3
131.3
130.3
126.0
120.0
51.3
47.2
18.0
15.5
N=N
N
N
CN
S
O2
3ad
DMSO-d6
f1 (ppm)

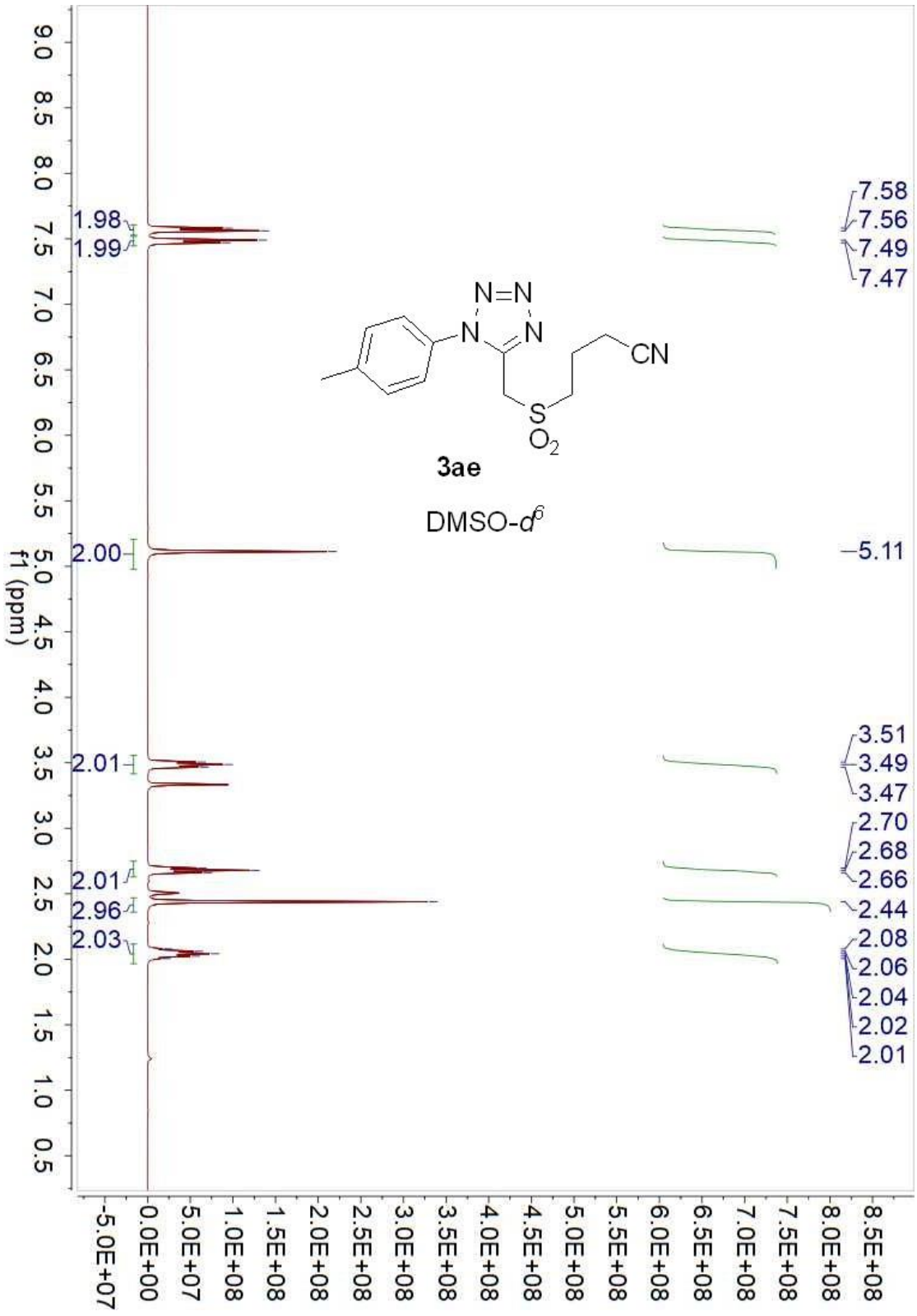
7.58
7.56
7.49
7.47
1.98
1.99
N=N
N
N
CN
S
O2
3ae
DMSO-d6
2.00
5.11
3.51
3.49
3.47
2.70
2.68
2.66
2.01
2.01
2.96
2.44
2.03
2.08
2.06
2.04
2.02
2.01
f1 (ppm)

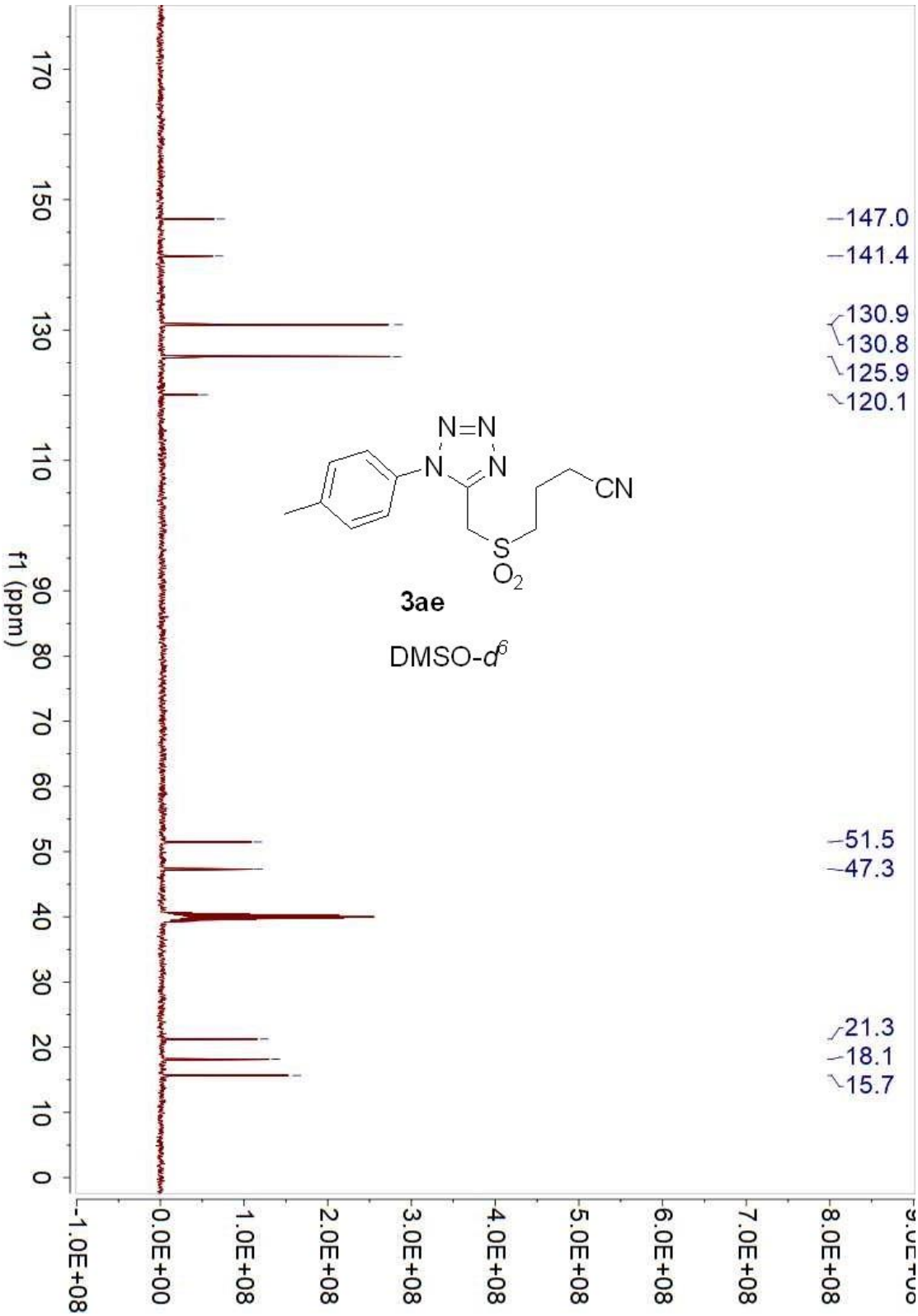
147.0
141.4
130.9
130.8
125.9
120.1
51.5
47.3
21.3
18.1
15.7
N=N
N
N
CN
S
O2
3ae
DMSO-d6
f1 (ppm)
170
150
130
110
90
80
70
60
50
40
30
20
10
0
-1.0E+08
0.0E+00
1.0E+08
2.0E+08
3.0E+08
4.0E+08
5.0E+08
6.0E+08
7.0E+08
8.0E+08

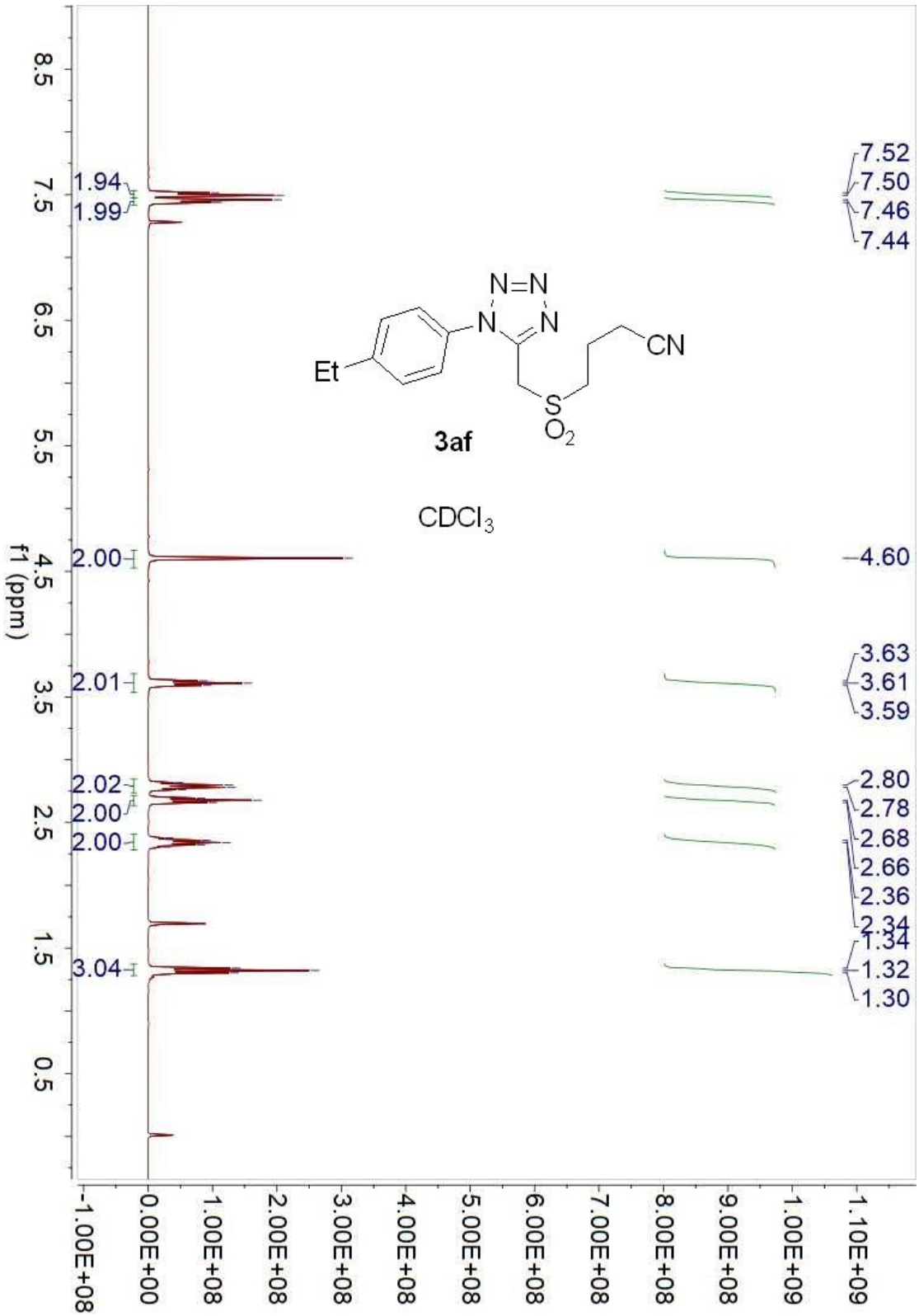
7.52
7.50
7.46
7.44
1.94
1.99
N=N
N
N
CN
Et
S
O2
3af
CDCl3
2.00
4.60
3.63
3.61
3.59
2.01
2.80
2.78
2.68
2.66
2.36
2.34
2.02
2.00
2.00
1.34
1.32
1.30
3.04
f1 (ppm)
8.5
7.5
6.5
5.5
4.5
3.5
2.5
1.5
0.5
-1.00E+08
0.00E+00
1.00E+08
2.00E+08
3.00E+08
4.00E+08
5.00E+08
6.00E+08
7.00E+08
8.00E+08
9.00E+08
1.00E+09
1.10E+09

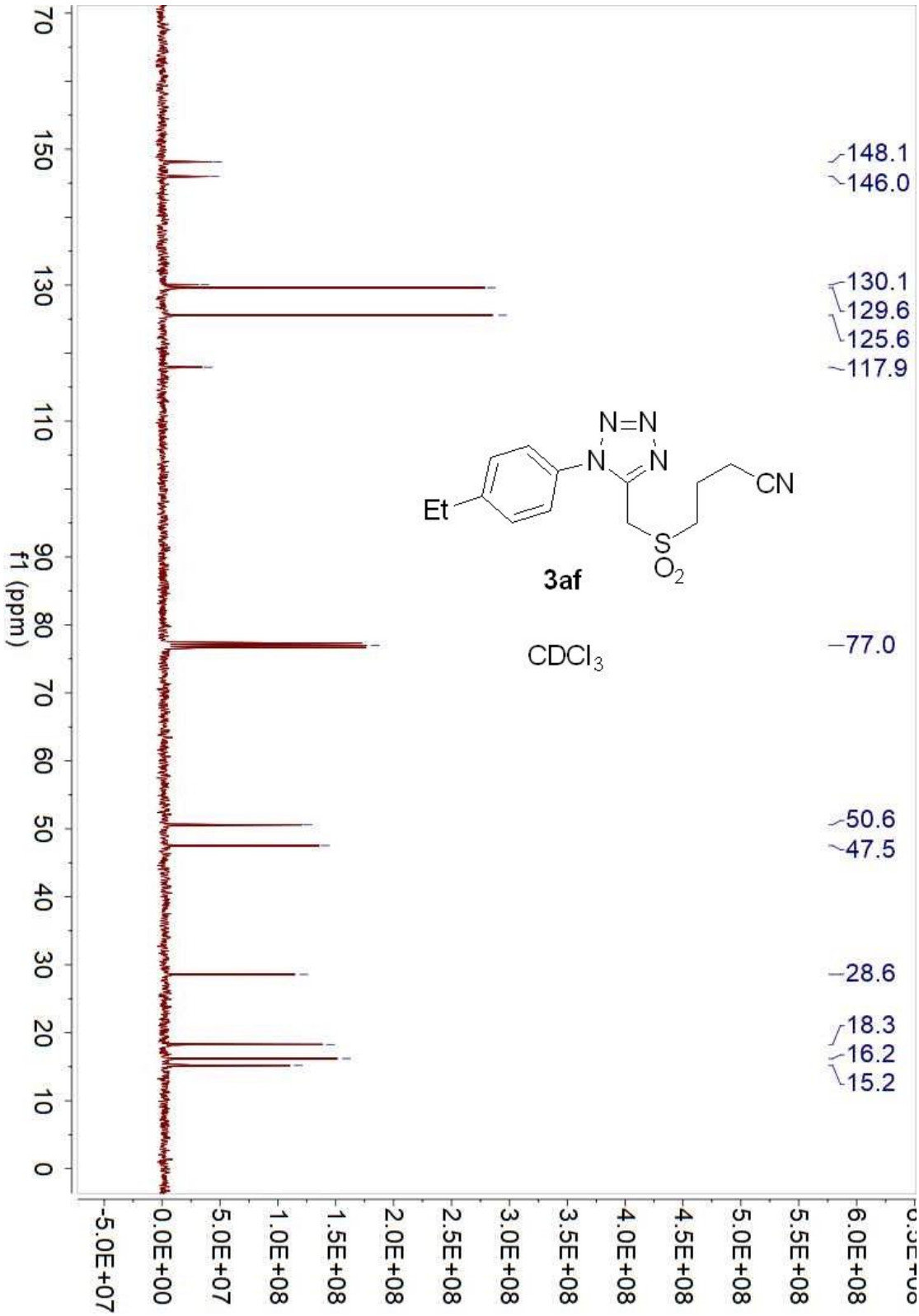
148.1
146.0
130.1
129.6
125.6
117.9
77.0
50.6
47.5
28.6
18.3
16.2
15.2
N=N
N
N
Et
CN
S
O2
3af
CDCl3
f1 (ppm)

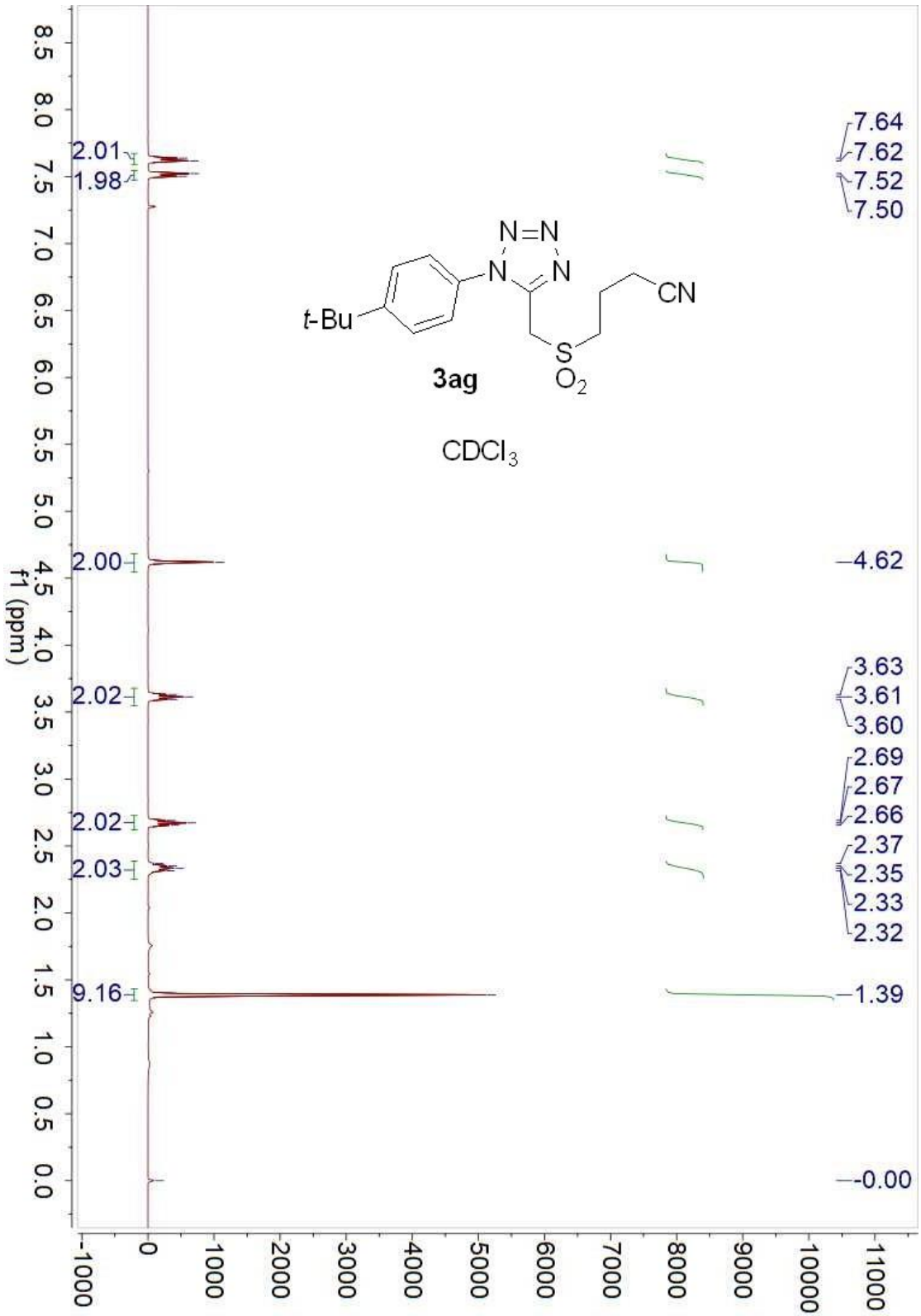
7.64
7.62
7.52
7.50
2.01
1.98
N=N
N
N
t-Bu
CN
S
O2
3ag
CDCl3
2.00
4.62
3.63
3.61
3.60
2.02
2.69
2.67
2.66
2.02
2.37
2.35
2.33
2.32
2.03
9.16
1.39
0.00
f1 (ppm)

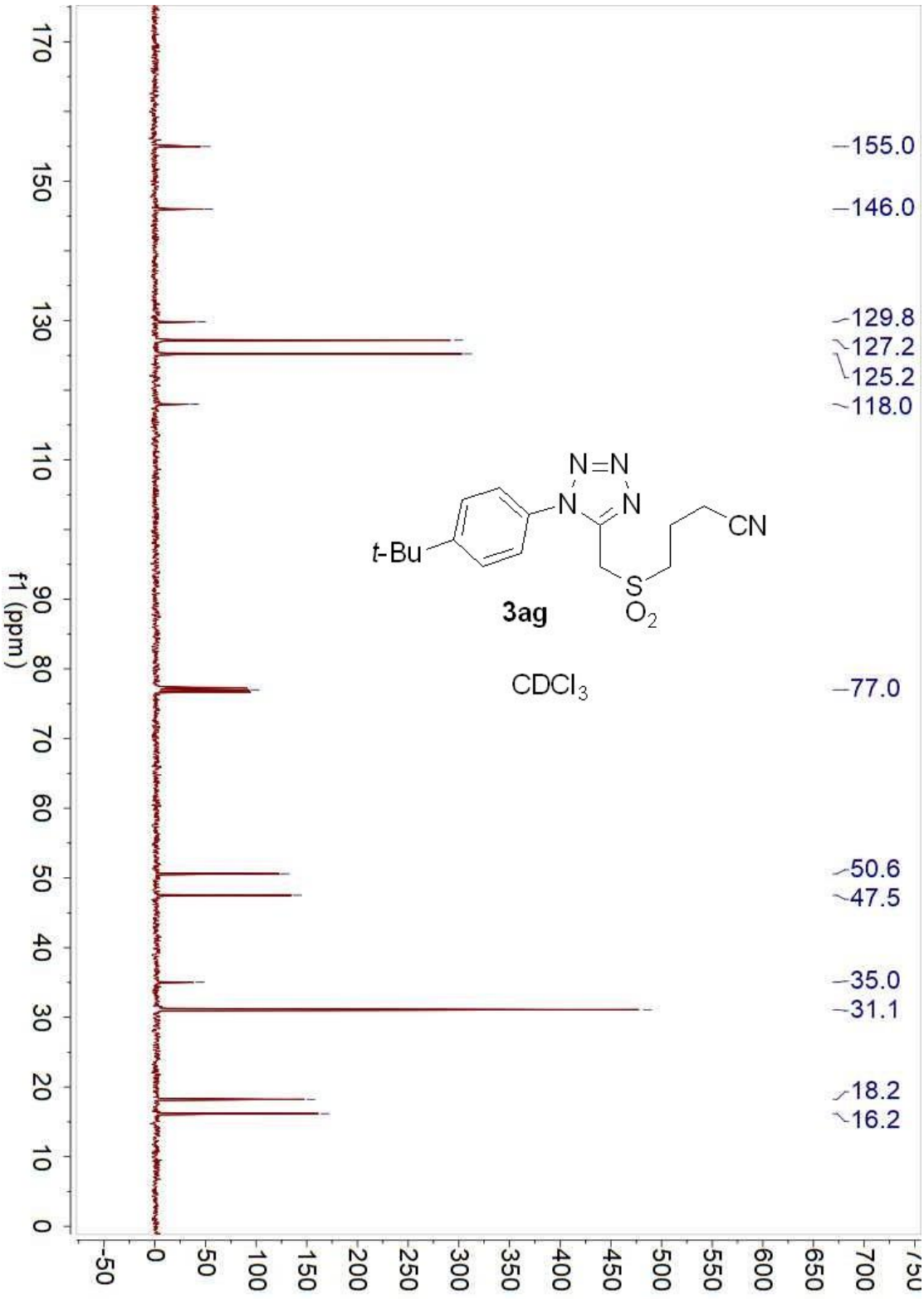
155.0
146.0
129.8
127.2
125.2
118.0
77.0
50.6
47.5
35.0
31.1
18.2
16.2
N=N
N
N
t-Bu
CN
S
O2
3ag
CDCl3
f1 (ppm)

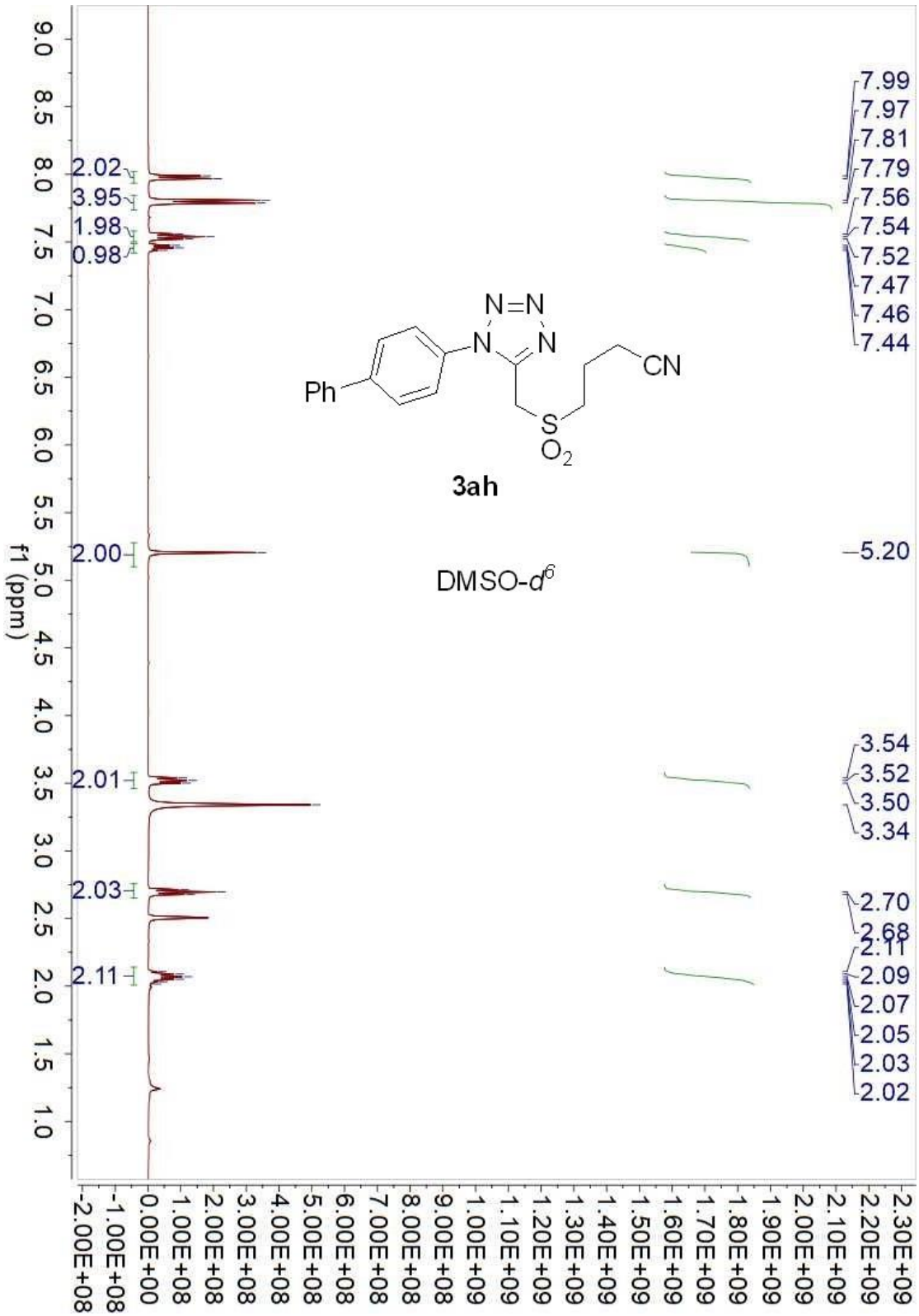
7.99
7.97
7.81
7.79
7.56
7.54
7.52
7.47
7.46
7.44
5.20
3.54
3.52
3.50
3.34
2.70
2.68
2.11
2.09
2.07
2.05
2.03
2.02
2.02
3.95
1.98
0.98
2.00
2.01
2.03
2.11
N=N
N
N
Ph
CN
S
O2
3ah
DMSO-d6
f1 (ppm)

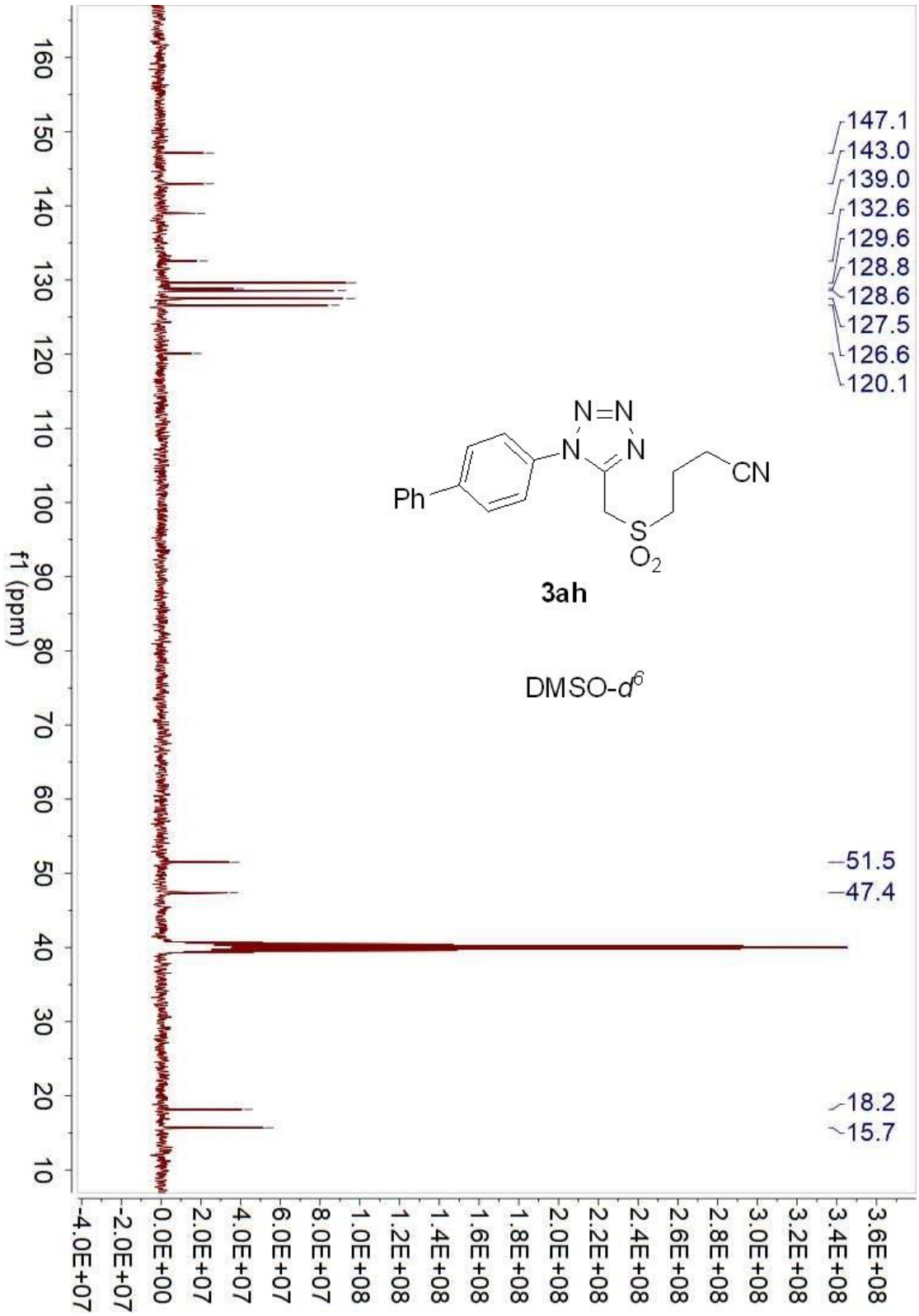
147.1
143.0
139.0
132.6
129.6
128.8
128.6
127.5
126.6
120.1
51.5
47.4
18.2
15.7
N=N
N
N
Ph
CN
S
O2
3ah
DMSO-d6
f1 (ppm)

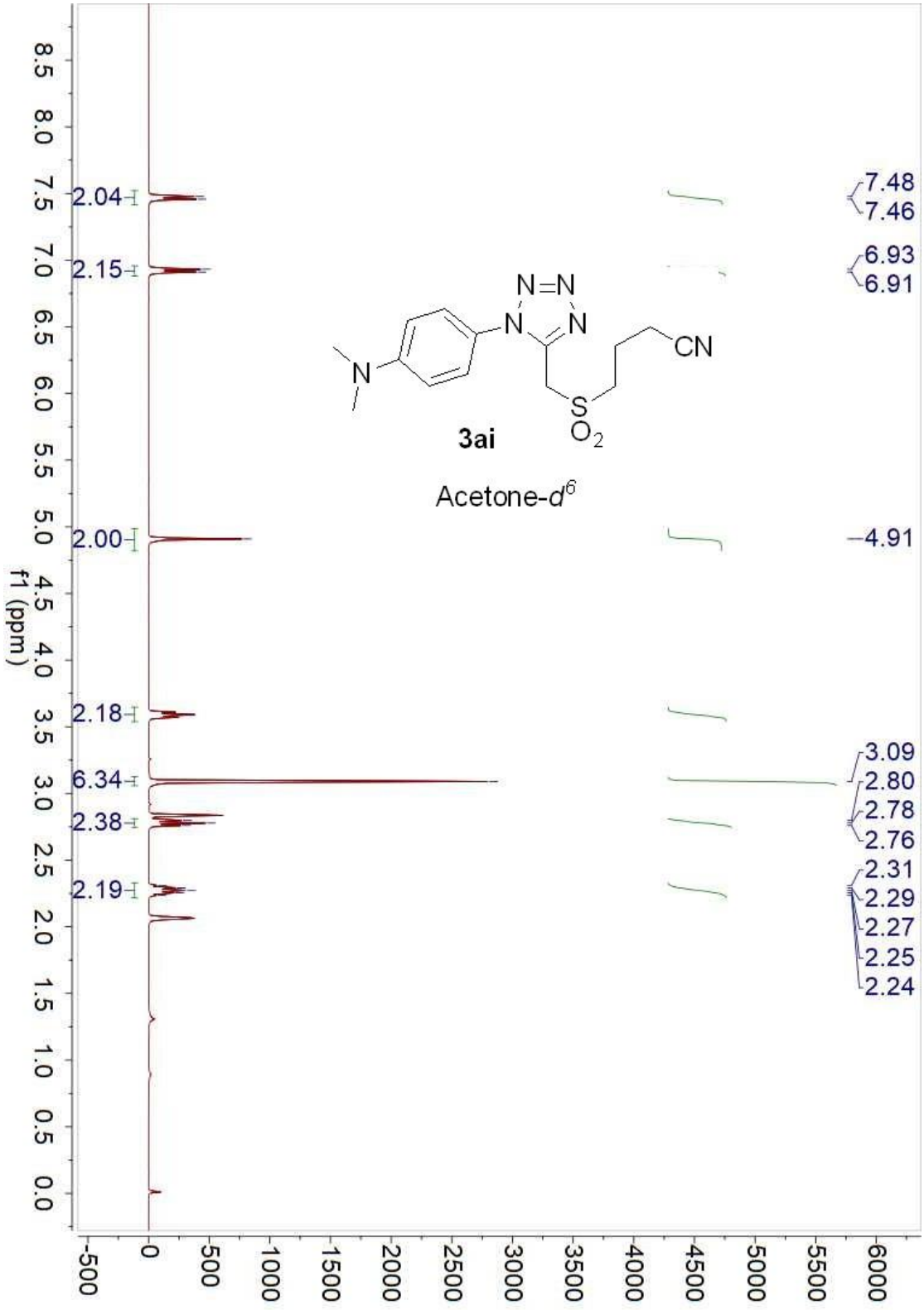
2.04
2.15
2.00
2.18
6.34
2.38
2.19
7.48
7.46
6.93
6.91
4.91
3.09
2.80
2.78
2.76
2.31
2.29
2.27
2.25
2.24
N=N
N
N
N
CN
S
O2
3ai
Acetone-d6
f1 (ppm)

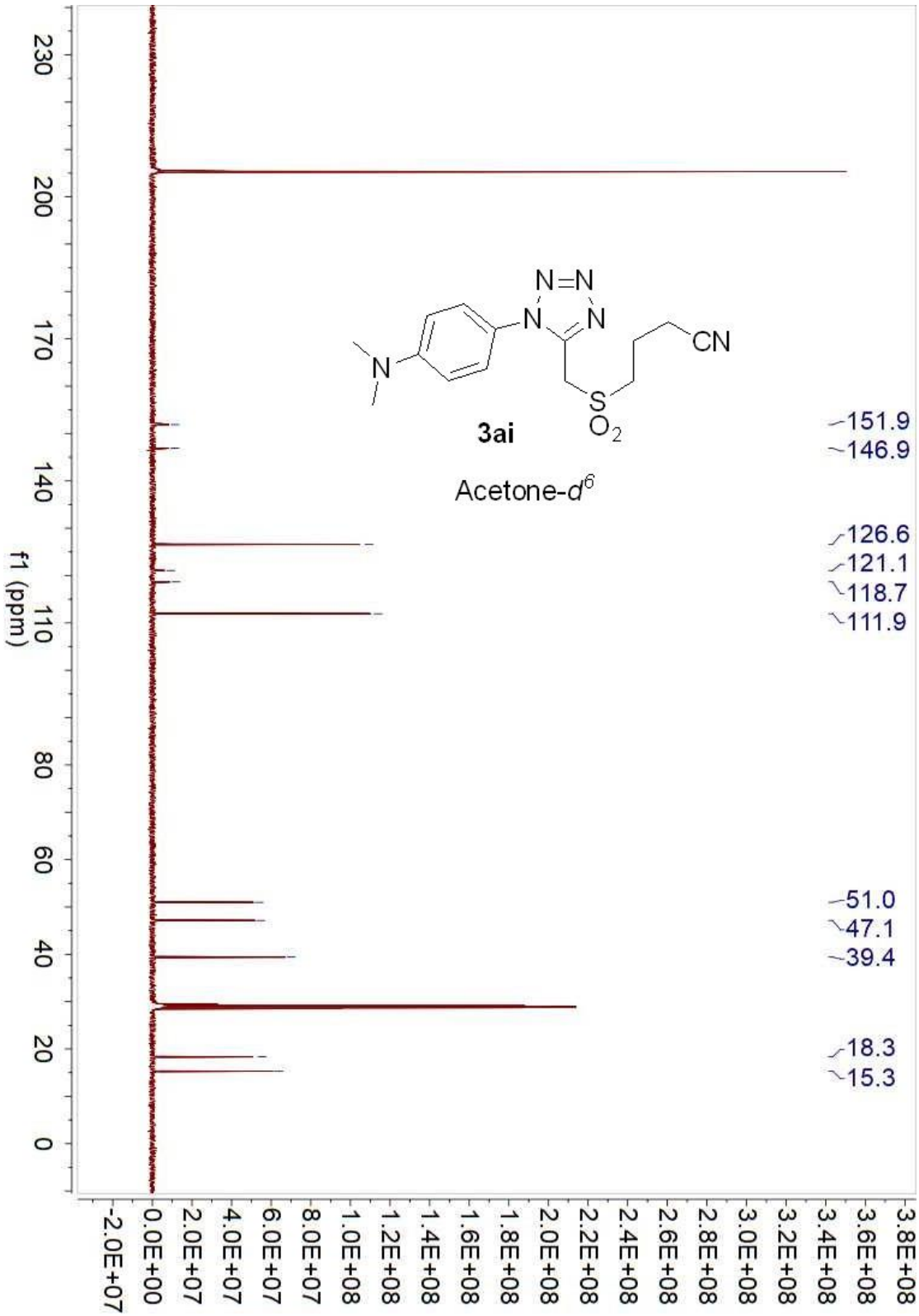
N=N
N
N
N
CN
S
O2
3ai
Acetone-d6
151.9
146.9
126.6
121.1
118.7
111.9
51.0
47.1
39.4
18.3
15.3
f1 (ppm)

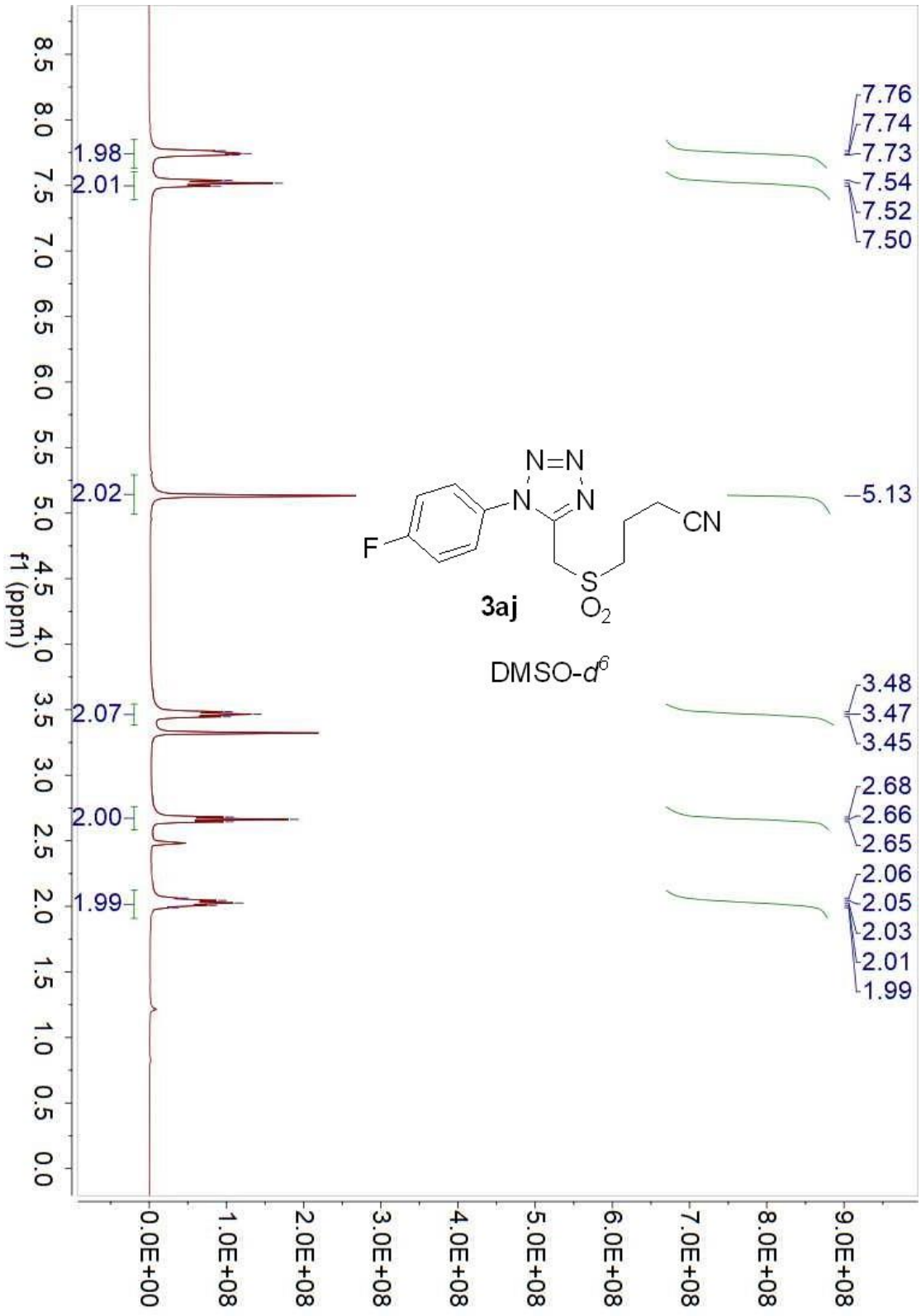
7.76
7.74
7.73
7.54
7.52
7.50
5.13
3.48
3.47
3.45
2.68
2.66
2.65
2.06
2.05
2.03
2.01
1.99
1.98
2.01
2.02
2.07
2.00
1.99
N=N
N
N
F
CN
S
O2
3aj
DMSO-d6
f1 (ppm)
8.5 8.0 7.5 7.0 6.5 6.0 5.5 5.0 4.5 4.0 3.5 3.0 2.5 2.0 1.5 1.0 0.5 0.0
0.0E+00 1.0E+08 2.0E+08 3.0E+08 4.0E+08 5.0E+08 6.0E+08 7.0E+08 8.0E+08 9.0E+08

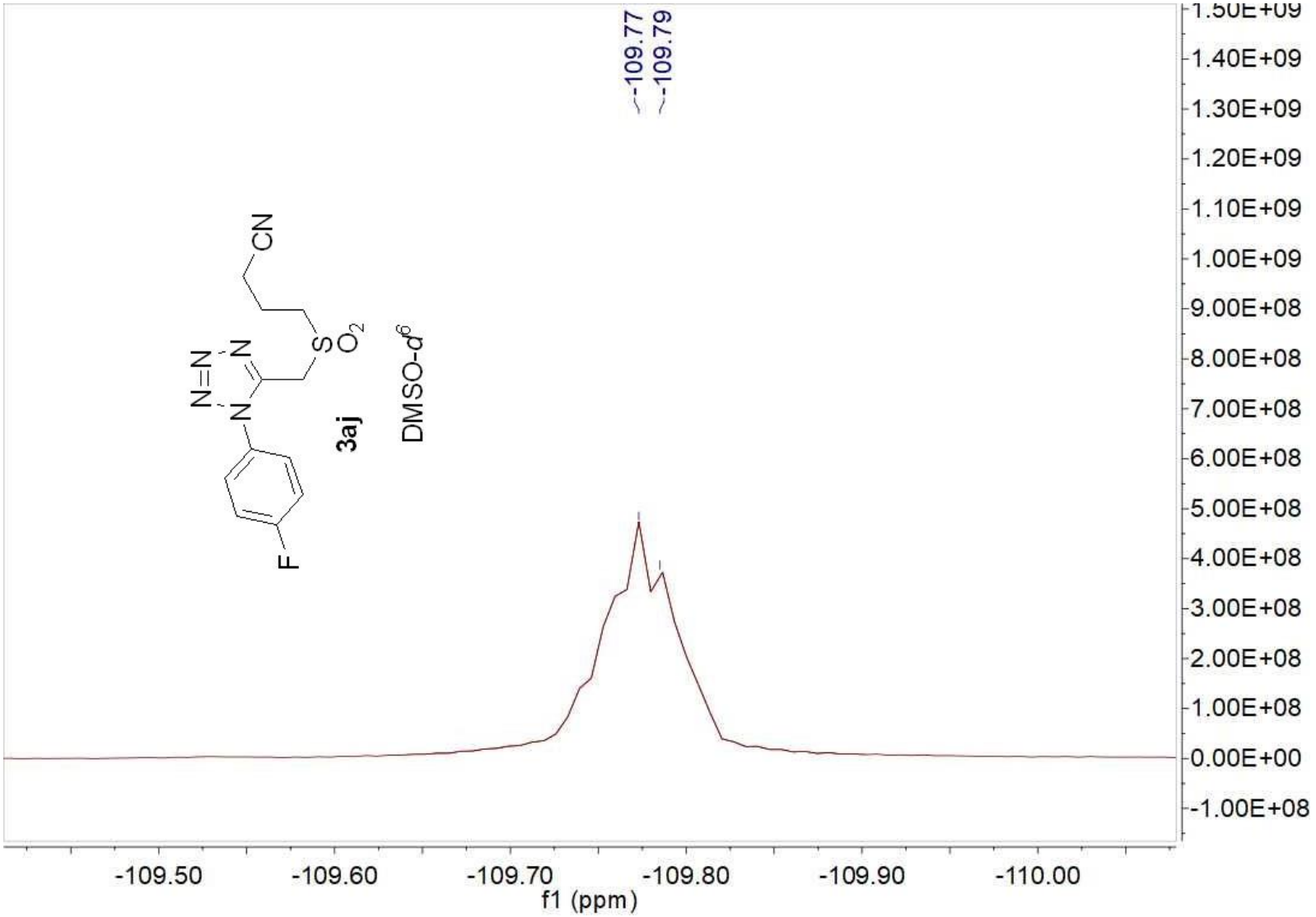
-109.77
-109.79
CN
S
O2
N=N
N
N
F
3aj
DMSO-d6
1.50E+09
1.40E+09
1.30E+09
1.20E+09
1.10E+09
1.00E+09
9.00E+08
8.00E+08
7.00E+08
6.00E+08
5.00E+08
4.00E+08
3.00E+08
2.00E+08
1.00E+08
0.00E+00
-1.00E+08
-109.50
-109.60
-109.70
-109.80
-109.90
-110.00
f1 (ppm)

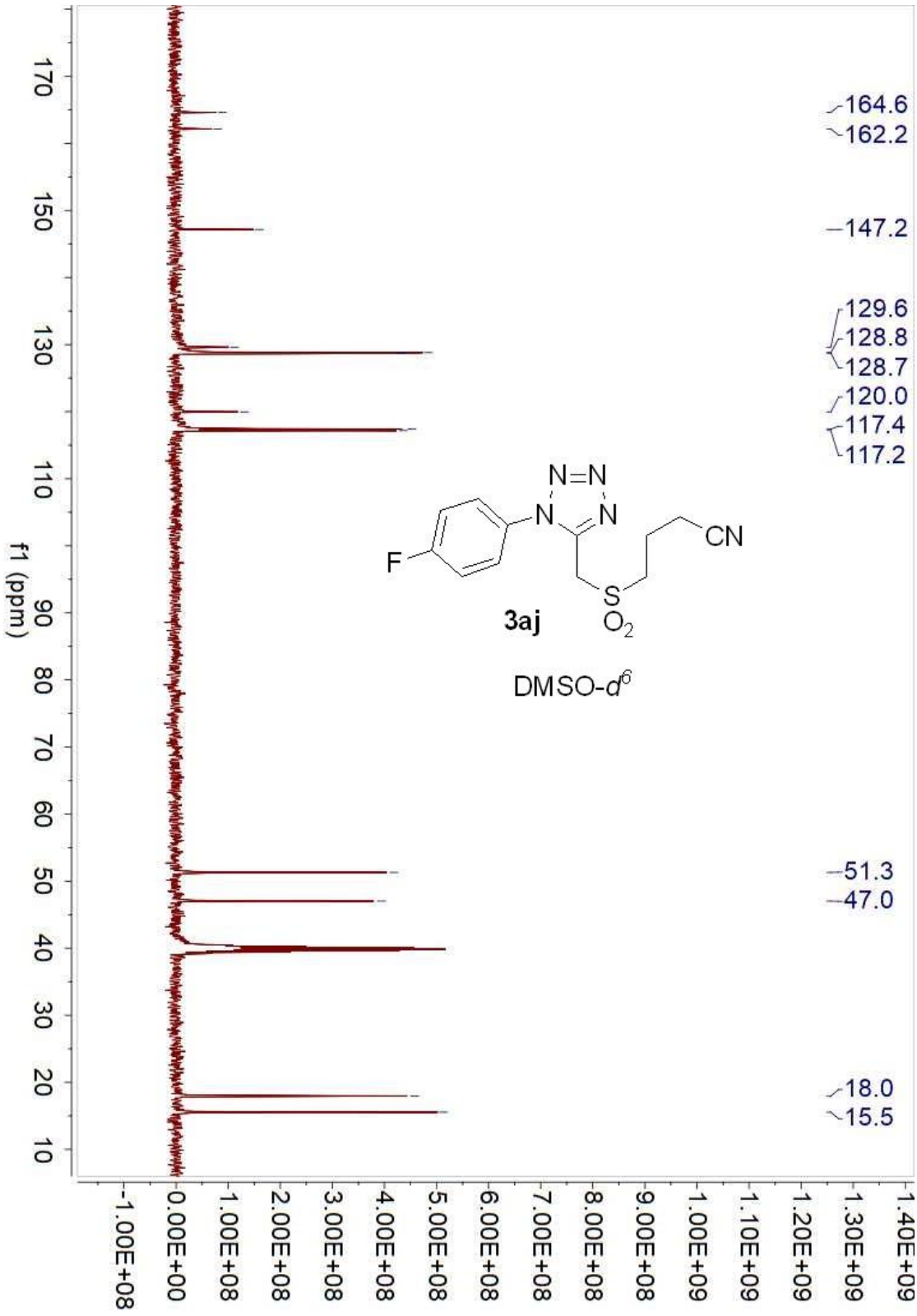
164.6
162.2
147.2
129.6
128.8
128.7
120.0
117.4
117.2
51.3
47.0
18.0
15.5
N=N
N
N
F
CN
S
O2
3aj
DMSO-d6
f1 (ppm)
170
150
130
110
90
80
70
60
50
40
30
20
10
-1.00E+08
0.00E+00
1.00E+08
2.00E+08
3.00E+08
4.00E+08
5.00E+08
6.00E+08
7.00E+08
8.00E+08
9.00E+08
1.00E+09
1.10E+09
1.20E+09
1.30E+09
1.40E+09

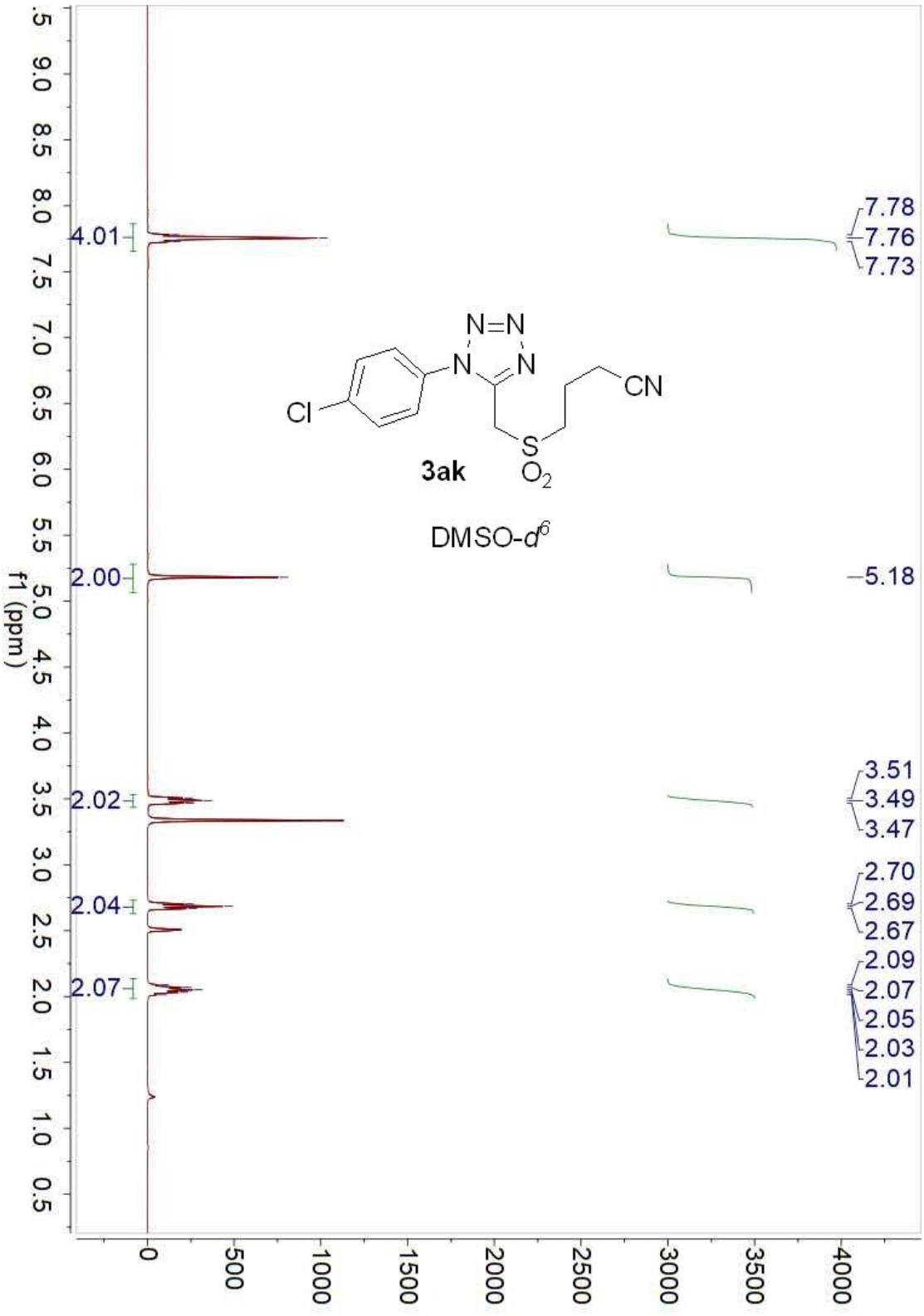
7.78
7.76
7.73
5.18
3.51
3.49
3.47
2.70
2.69
2.67
2.09
2.07
2.05
2.03
2.01
4.01
2.00
2.02
2.04
2.07
N=N
N
N
Cl
CN
S
O2
3ak
DMSO-d6
f1 (ppm)

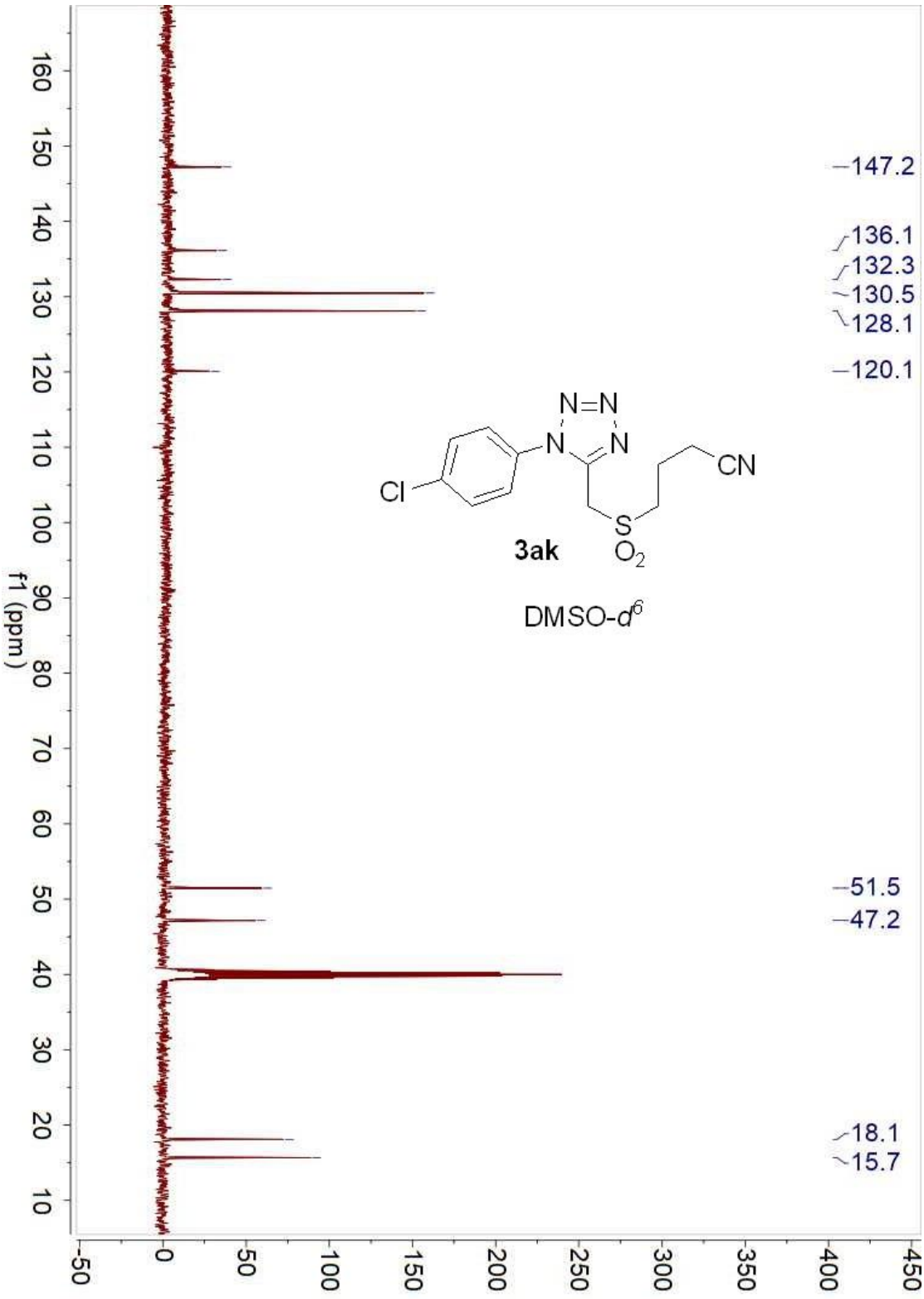
147.2
136.1
132.3
130.5
128.1
120.1
51.5
47.2
18.1
15.7
N=N
N
N
Cl
CN
S
O2
3ak
DMSO-d6
f1 (ppm)
160
150
140
130
120
110
100
90
80
70
60
50
40
30
20
10
-50
0
50
100
150
200
250
300
350
400
450

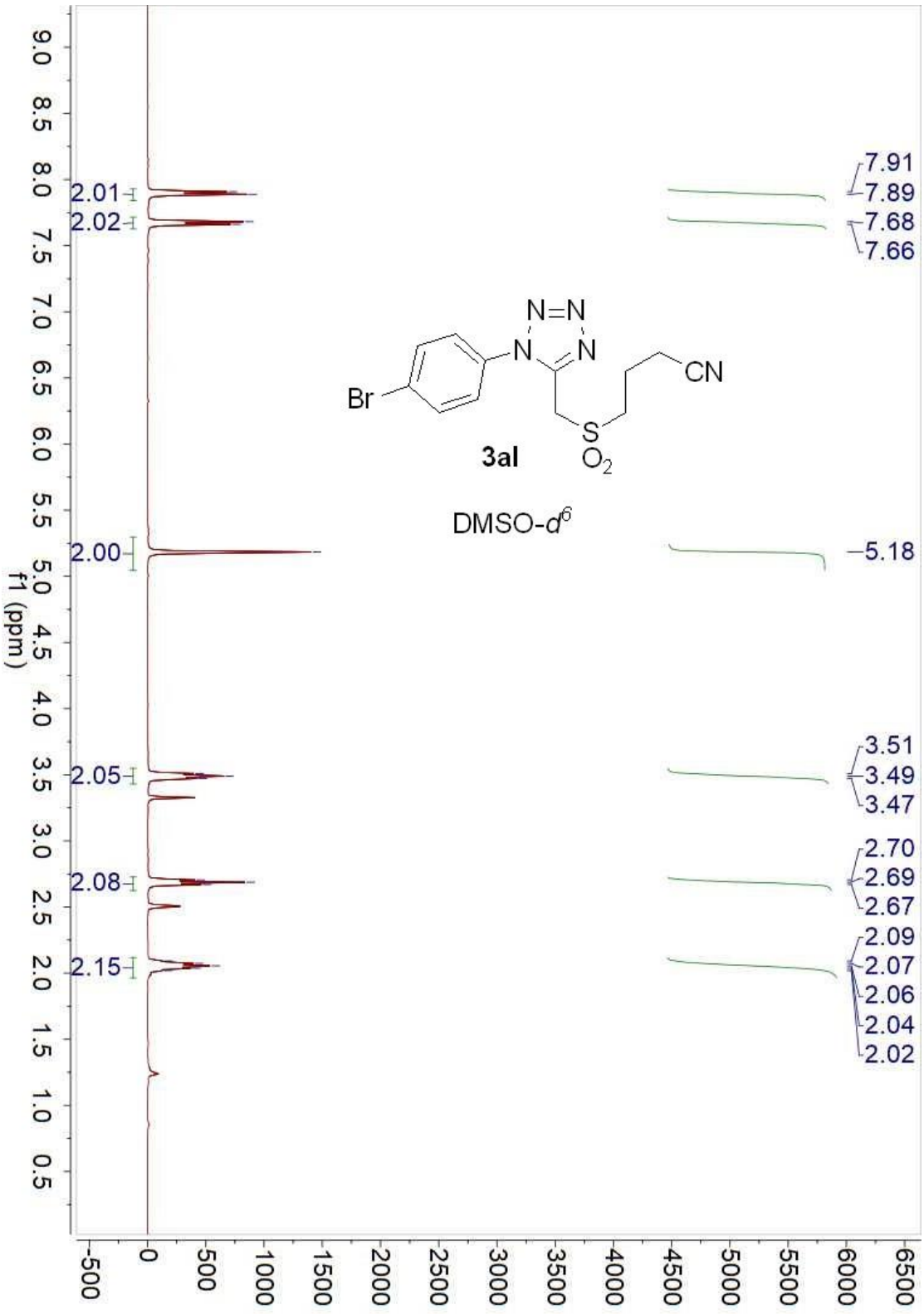
7.91
7.89
7.68
7.66
5.18
3.51
3.49
3.47
2.70
2.69
2.67
2.09
2.07
2.06
2.04
2.02
2.01
2.02
2.00
2.05
2.08
2.15
N=N
N
N
Br
CN
S
O2
3al
DMSO-d6
f1 (ppm)

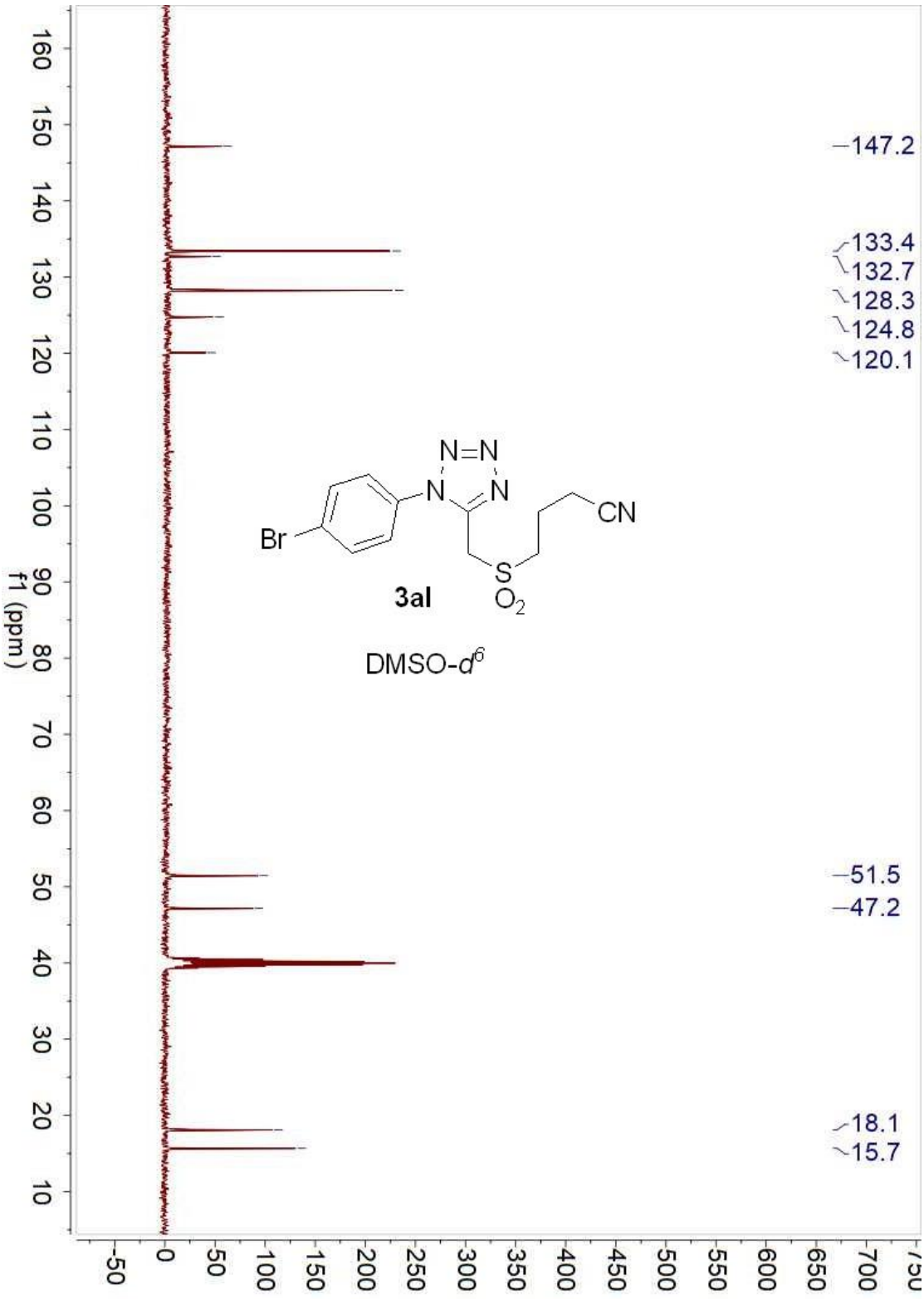
147.2
133.4
132.7
128.3
124.8
120.1
51.5
47.2
18.1
15.7
N=N
N
N
Br
CN
S
O2
3aI
DMSO-d6
f1 (ppm)

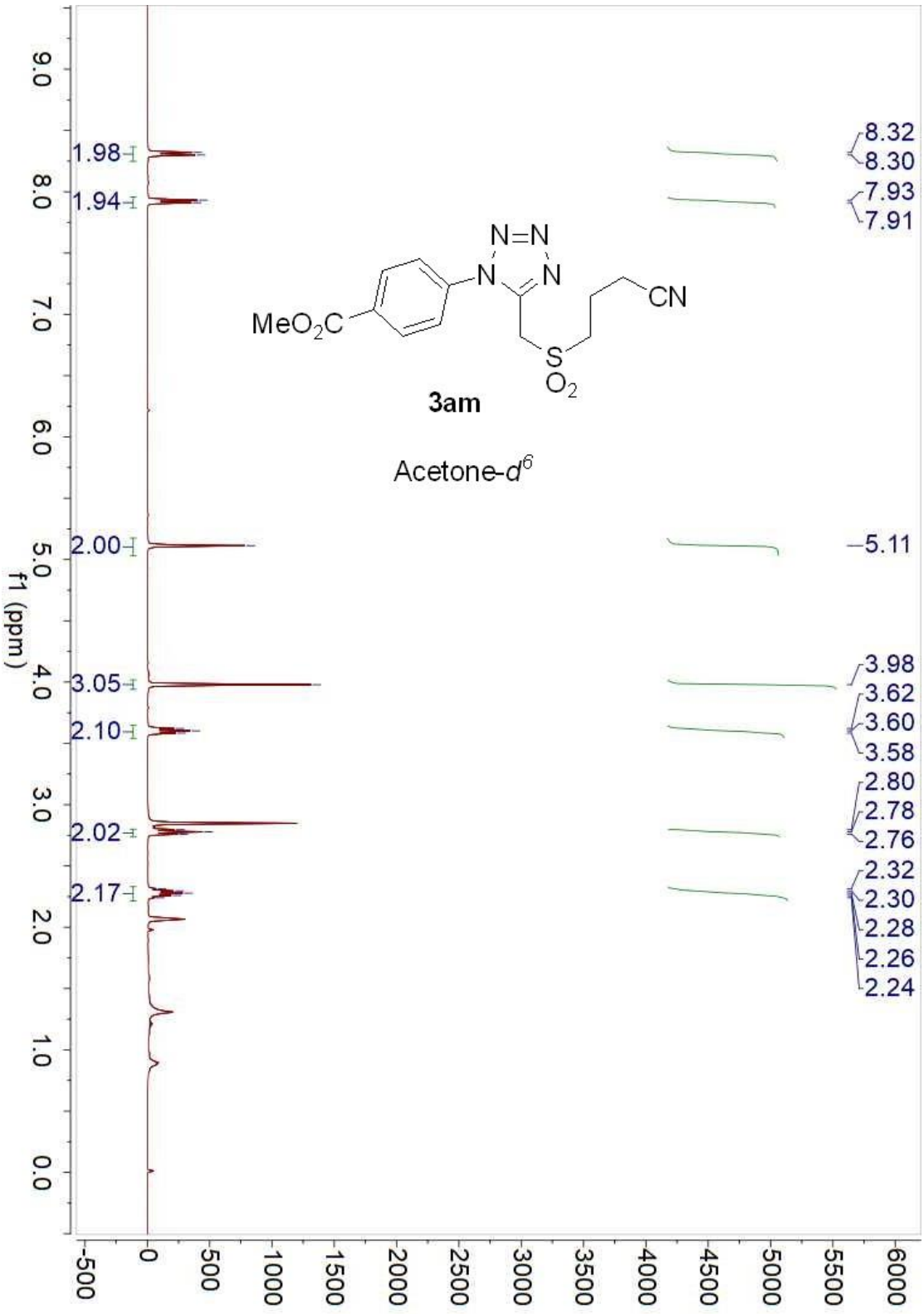
1.98
1.94
2.00
3.05
2.10
2.02
2.17
8.32
8.30
7.93
7.91
5.11
3.98
3.62
3.60
3.58
2.80
2.78
2.76
2.32
2.30
2.28
2.26
2.24
N=N
N
N
MeO2C
CN
S
O2
3am
Acetone-d6
f1 (ppm)
9.0
8.0
7.0
6.0
5.0
4.0
3.0
2.0
1.0
0.0
-500
0
500
1000
1500
2000
2500
3000
3500
4000
4500
5000
5500
6000

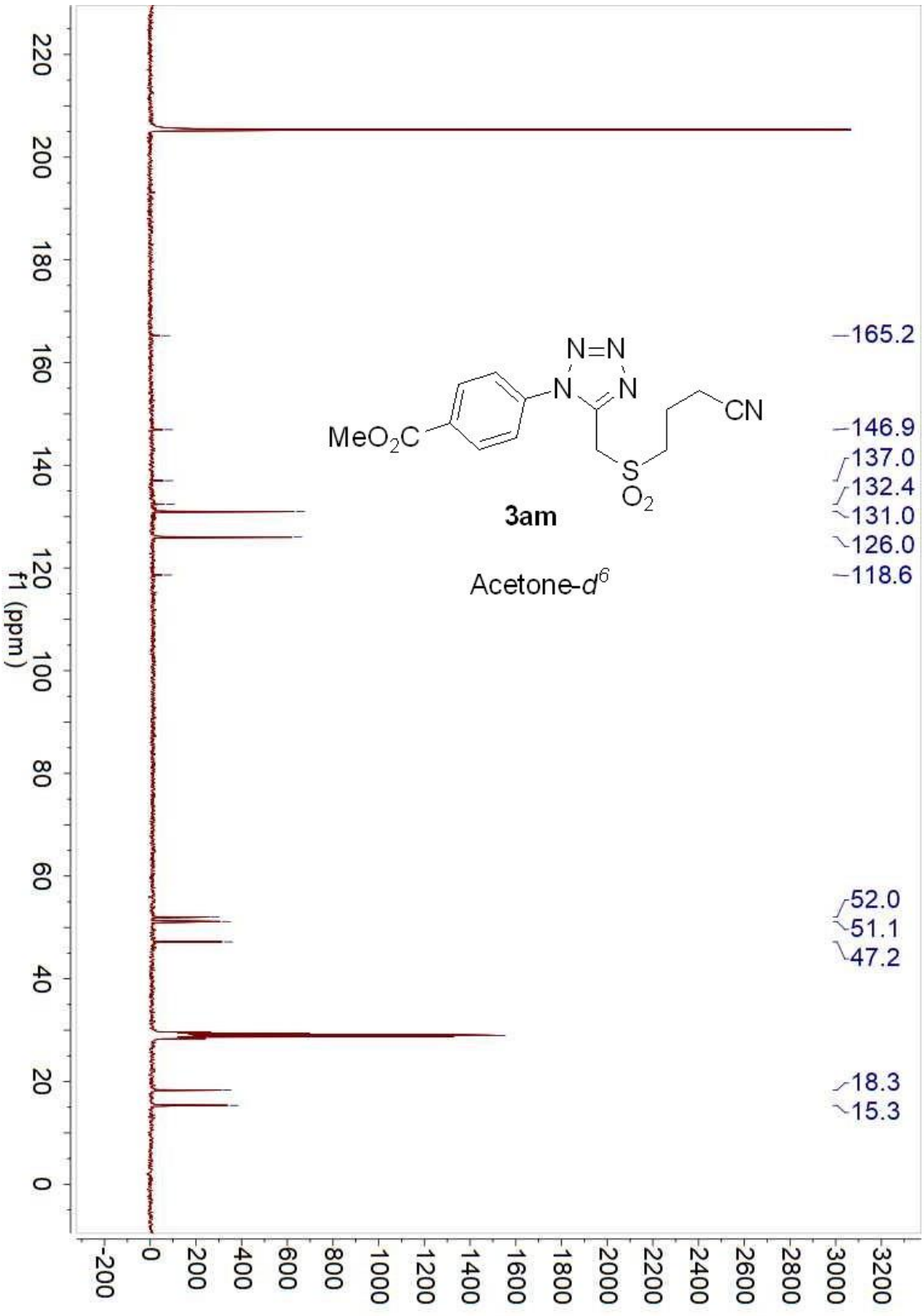
165.2
146.9
137.0
132.4
131.0
126.0
118.6
52.0
51.1
47.2
18.3
15.3
MeO2C
N=N
N
N
CN
S
O2
3am
Acetone-d6
f1 (ppm)

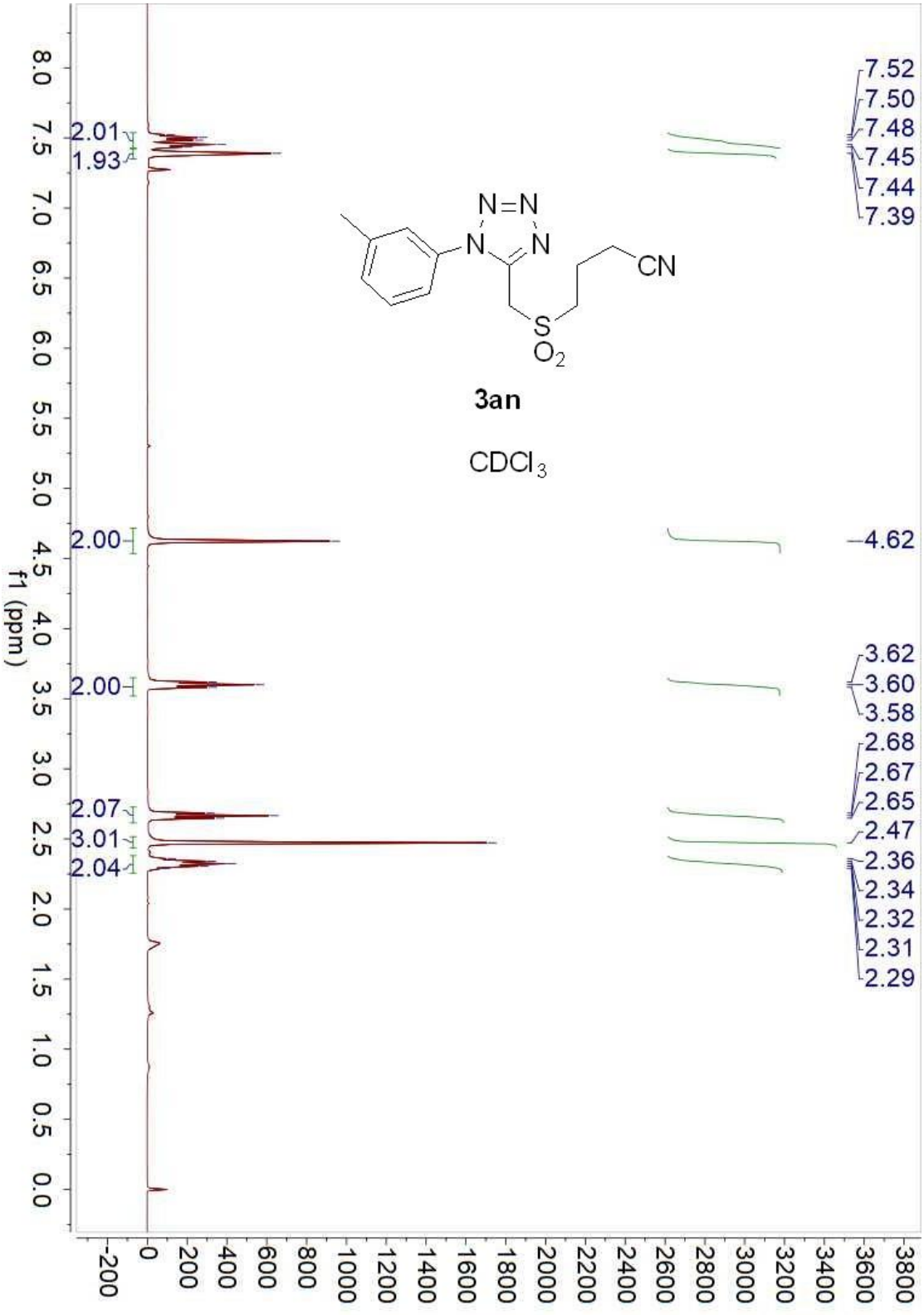
7.52
7.50
7.48
7.45
7.44
7.39
2.01
1.93
N=N
N
N
CN
S
O2
3an
CDCl3
2.00
4.62
3.62
3.60
3.58
2.00
2.68
2.67
2.65
2.07
2.47
3.01
2.36
2.04
2.34
2.32
2.31
2.29
f1 (ppm)

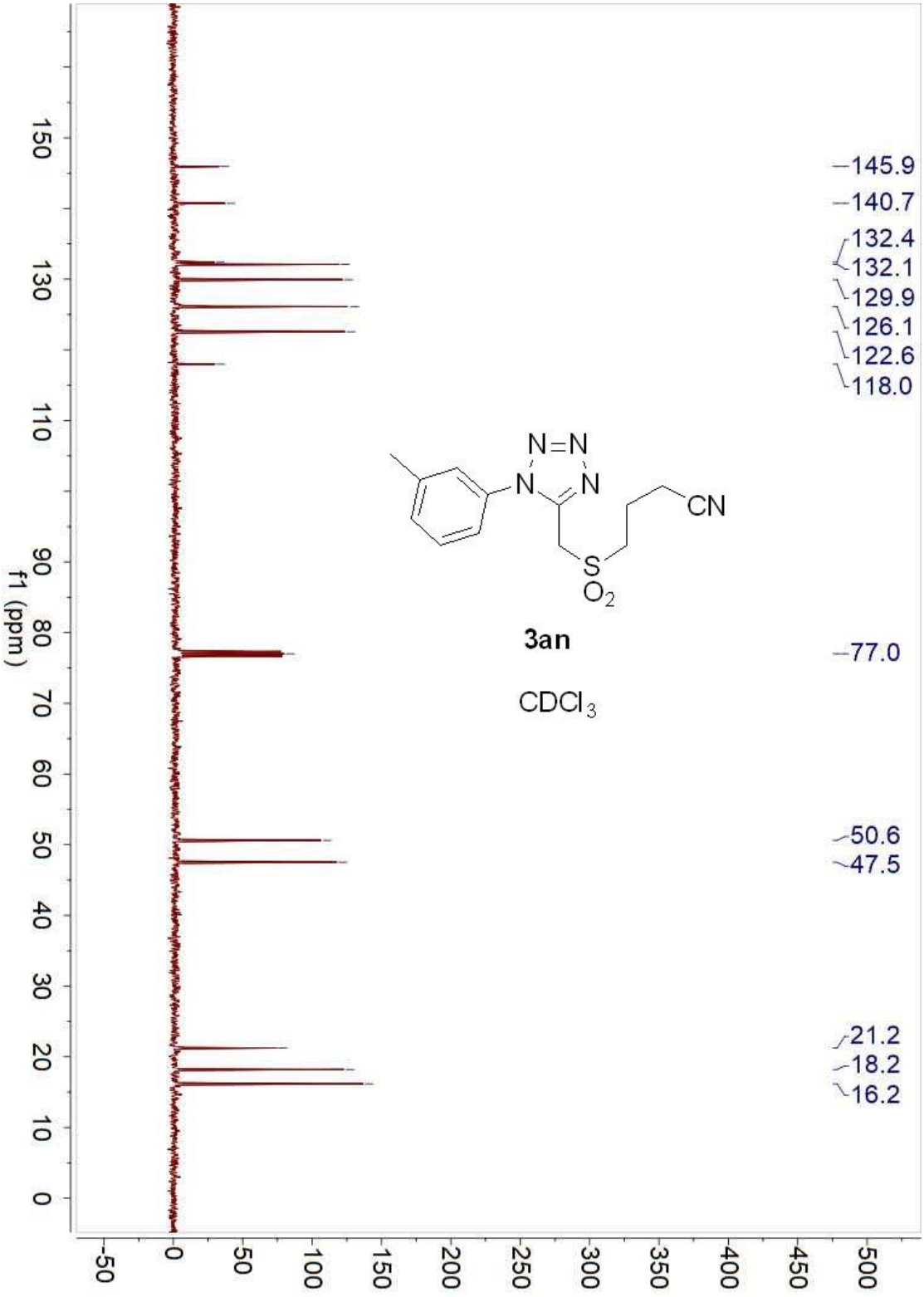
145.9
140.7
132.4
132.1
129.9
126.1
122.6
118.0
77.0
50.6
47.5
21.2
18.2
16.2
N=N
N
N
CN
S
O2
3an
CDCl3
f1 (ppm)
150
130
110
90
80
70
60
50
40
30
20
10
0
-50
0
50
100
150
200
250
300
350
400
450
500

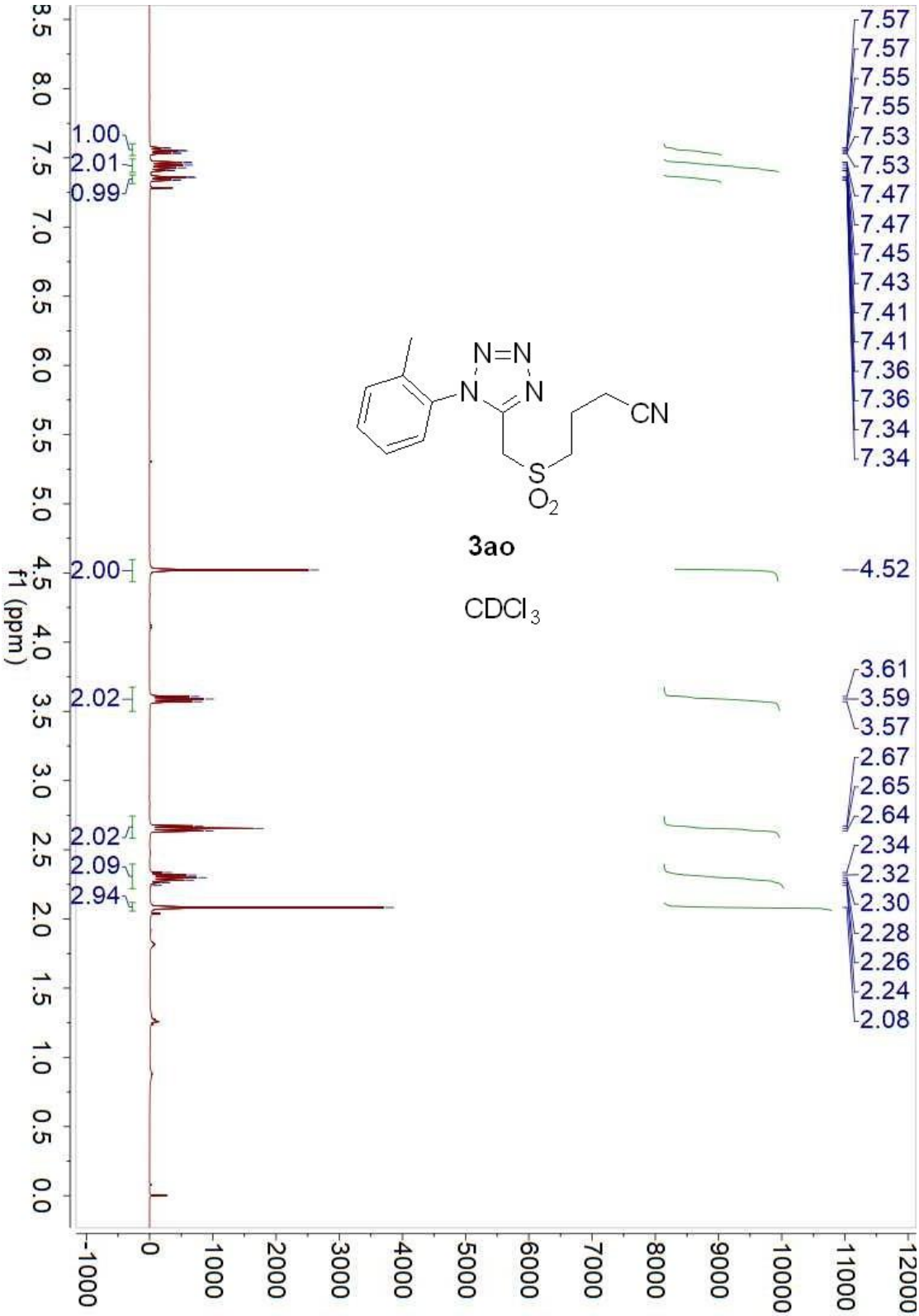
7.57
7.57
7.55
7.55
7.53
7.53
7.47
7.47
7.45
7.43
7.41
7.41
7.36
7.36
7.34
7.34
1.00
2.01
0.99
N=N
N
N
CN
S
O2
3ao
CDCl3
2.00
4.52
3.61
3.59
3.57
2.02
2.67
2.65
2.64
2.02
2.34
2.09
2.32
2.94
2.30
2.28
2.26
2.24
2.08
f1 (ppm)
8.5
8.0
7.5
7.0
6.5
6.0
5.5
5.0
4.5
4.0
3.5
3.0
2.5
2.0
1.5
1.0
0.5
0.0
-1000
0
1000
2000
3000
4000
5000
6000
7000
8000
9000
10000
11000
12000

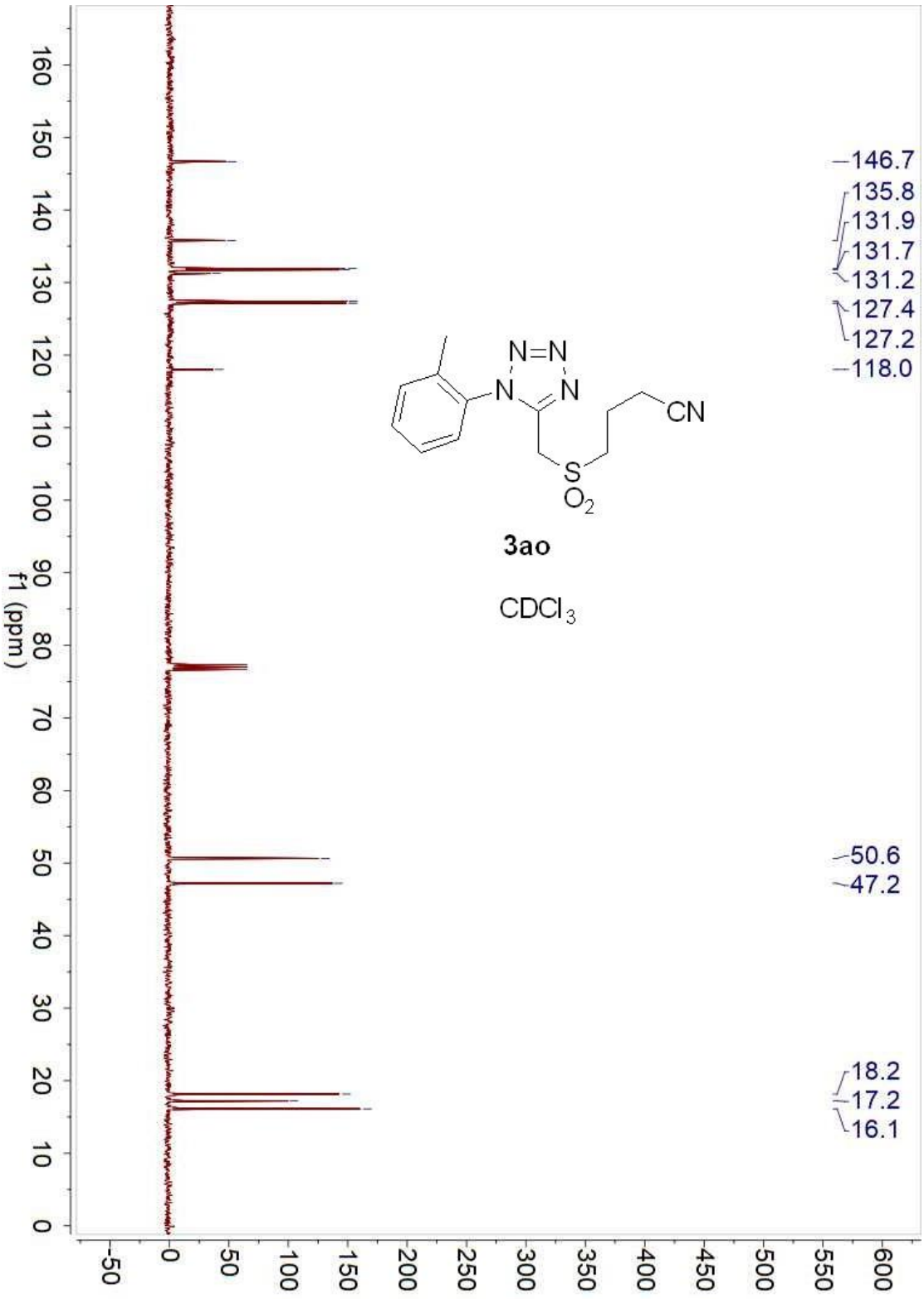
146.7
135.8
131.9
131.7
131.2
127.4
127.2
118.0
50.6
47.2
18.2
17.2
16.1
N=N
N
N
CN
S
O2
3ao
CDCl3
f1 (ppm)

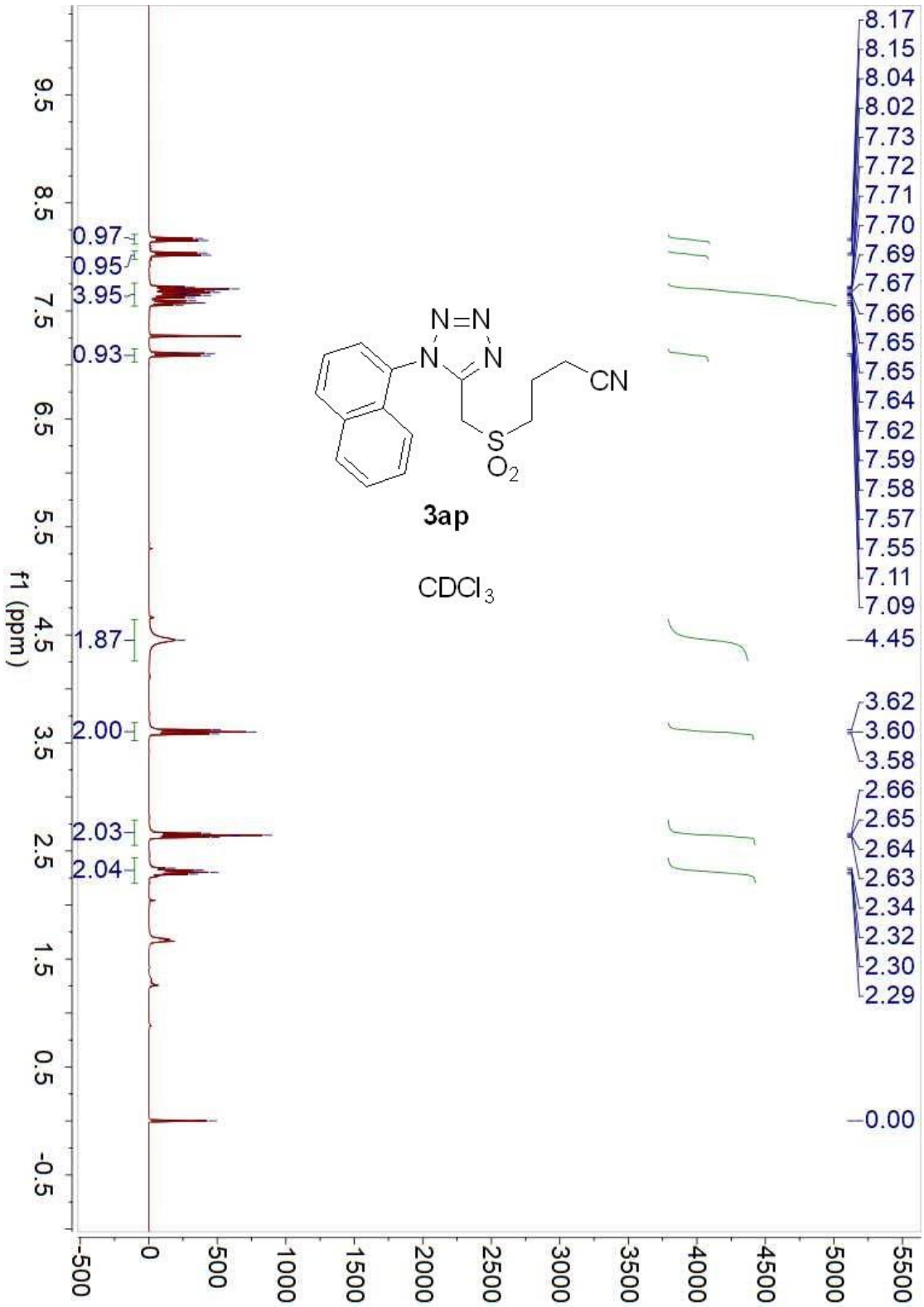
8.17
8.15
8.04
8.02
7.73
7.72
7.71
7.70
7.69
7.67
7.66
7.65
7.65
7.64
7.62
7.59
7.58
7.57
7.55
7.11
7.09
4.45
3.62
3.60
3.58
2.66
2.65
2.64
2.63
2.34
2.32
2.30
2.29
0.00
0.97
0.95
3.95
0.93
1.87
2.00
2.03
2.04
N=N
N
N
CN
S
O2
3ap
CDCl3
f1 (ppm)
9.5
8.5
7.5
6.5
5.5
4.5
3.5
2.5
1.5
0.5
-0.5
-500
0
500
1000
1500
2000
2500
3000
3500
4000
4500
5000
5500

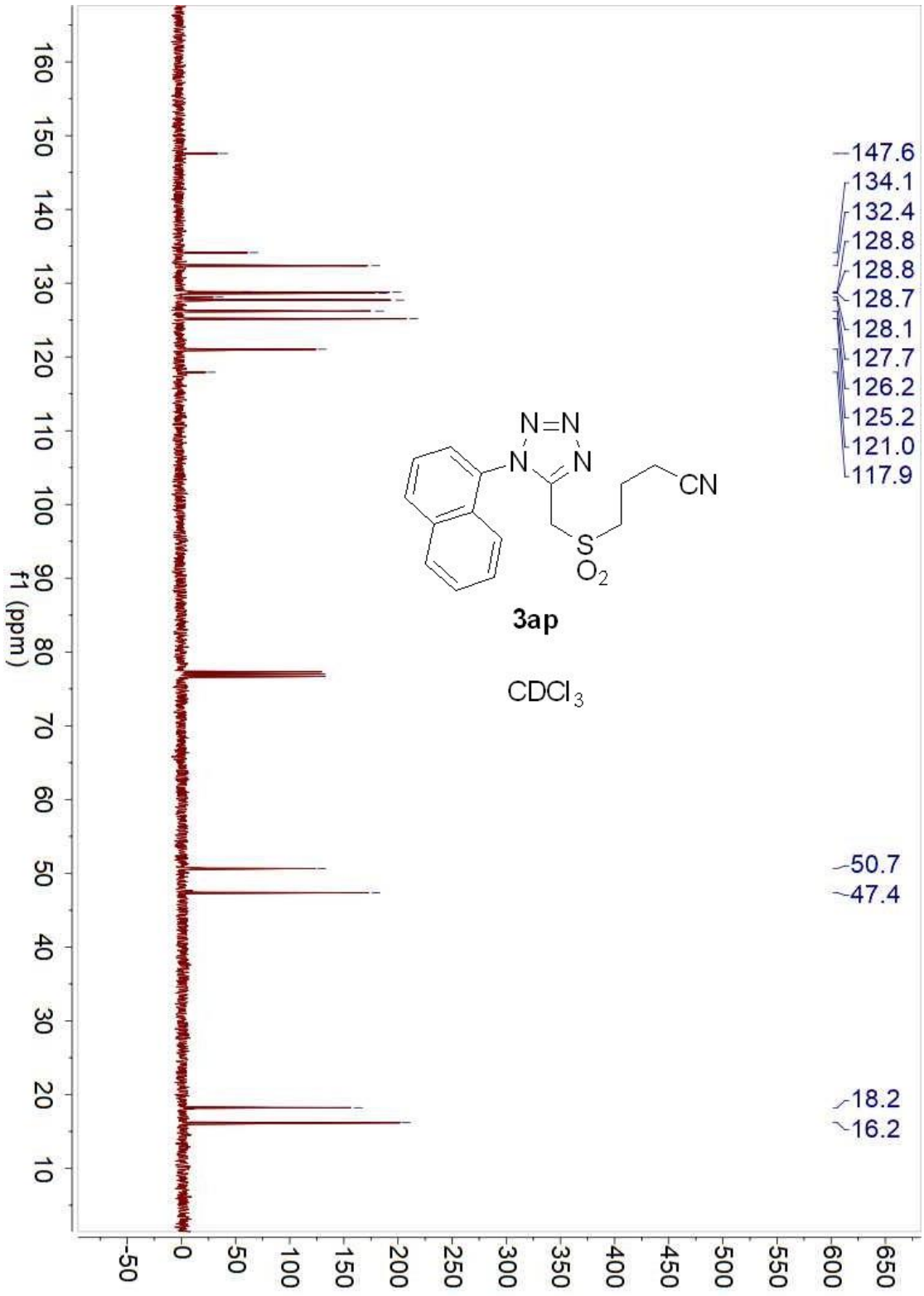
147.6
134.1
132.4
128.8
128.8
128.7
128.1
127.7
126.2
125.2
121.0
117.9
50.7
47.4
18.2
16.2
N=N
N
N
CN
S
O2
3ap
CDCl3
f1 (ppm)

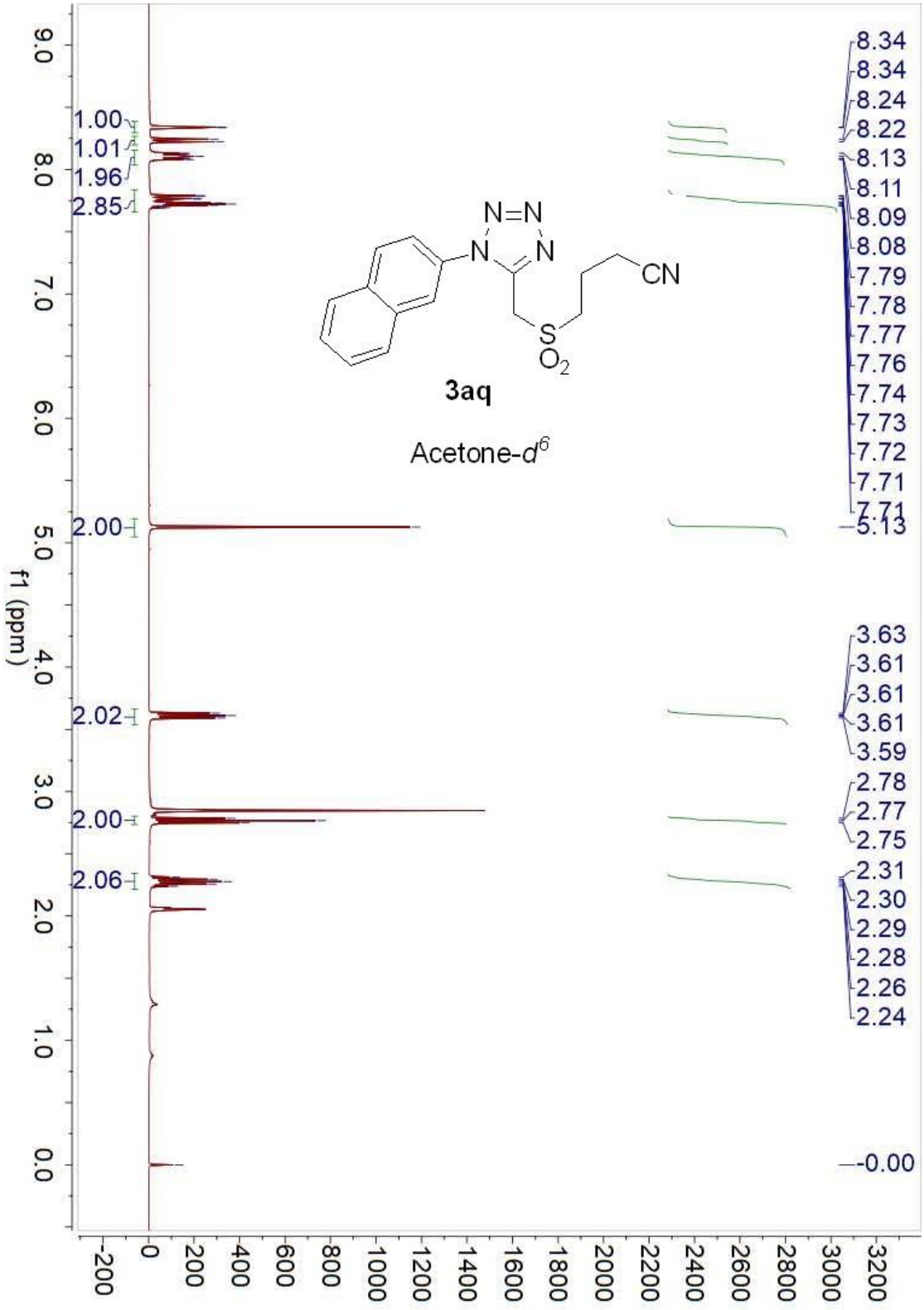
8.34
8.34
8.24
8.22
8.13
8.11
8.09
8.08
7.79
7.78
7.77
7.76
7.74
7.73
7.72
7.71
7.71
5.13
3.63
3.61
3.61
3.61
3.59
2.78
2.77
2.75
2.31
2.30
2.29
2.28
2.26
2.24
-0.00
1.00
1.01
1.96
2.85
2.00
2.02
2.00
2.06
N=N
N
N
CN
S
O2
3aq
Acetone-d6
f1 (ppm)
9.0
8.0
7.0
6.0
5.0
4.0
3.0
2.0
1.0
0.0
-200
0
200
400
600
800
1000
1200
1400
1600
1800
2000
2200
2400
2600
2800
3000
3200

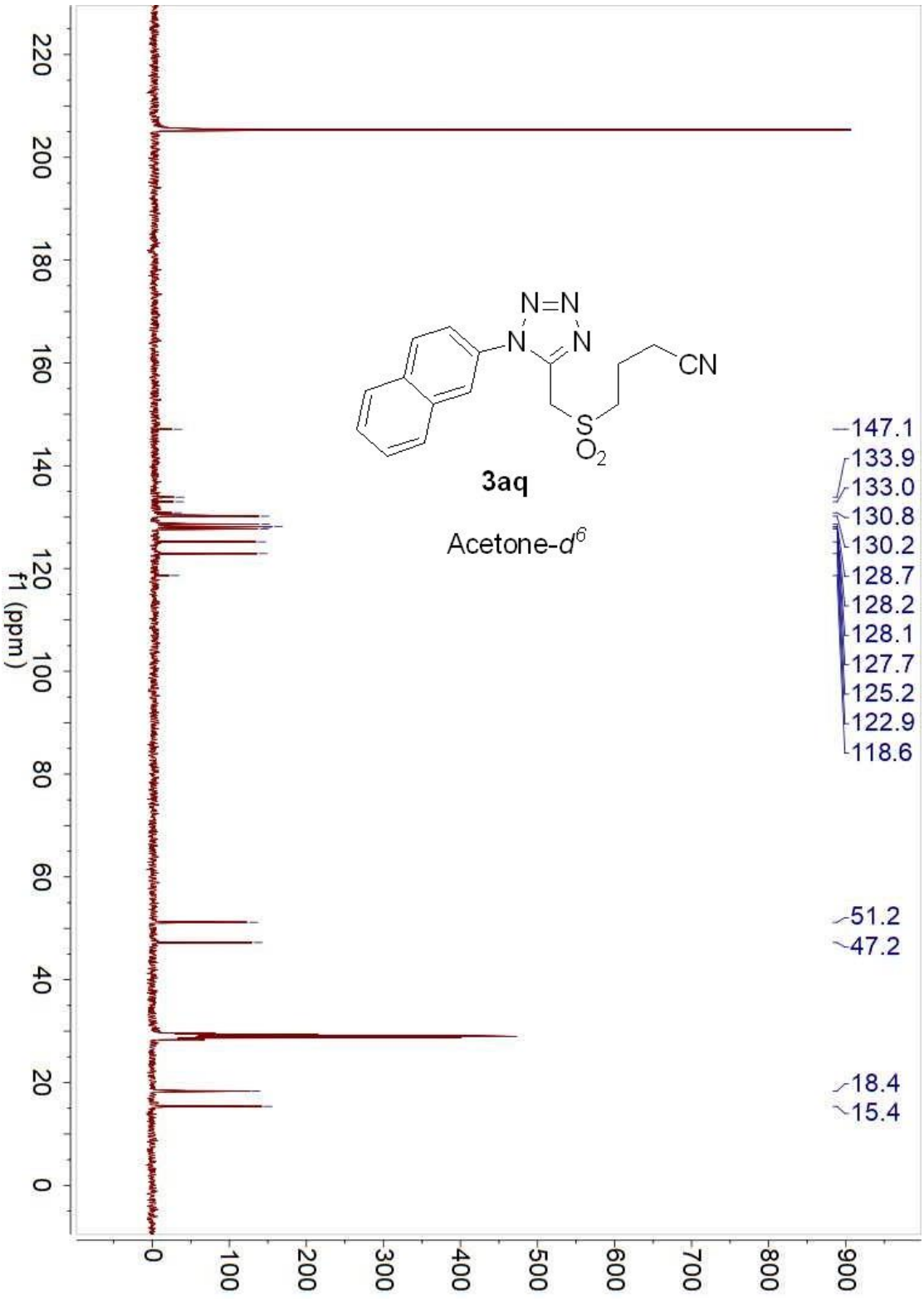
N=N
N
N
CN
S
O2
3aq
Acetone-d6
f1 (ppm)
147.1
133.9
133.0
130.8
130.2
128.7
128.2
128.1
127.7
125.2
122.9
118.6
51.2
47.2
18.4
15.4
0
20
40
60
80
100
120
140
160
180
200
220
0
100
200
300
400
500
600
700
800
900

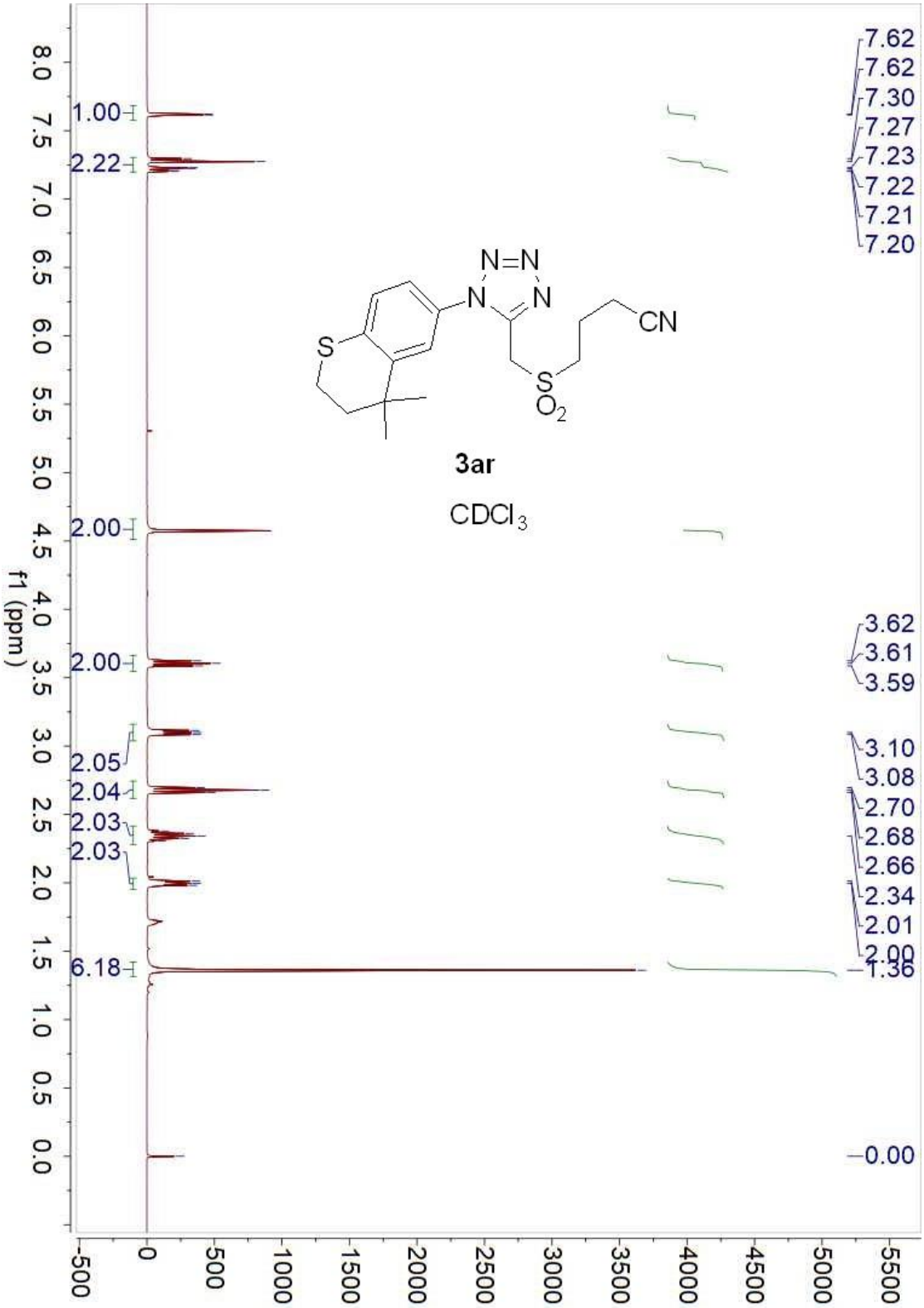
7.62
7.62
7.30
7.27
7.23
7.22
7.21
7.20
3.62
3.61
3.59
3.10
3.08
2.70
2.68
2.66
2.34
2.01
2.00
1.36
0.00
1.00
2.22
2.00
2.00
2.05
2.04
2.03
2.03
6.18
N=N
N
N
S
CN
S
O2
3ar
CDCl3
f1 (ppm)

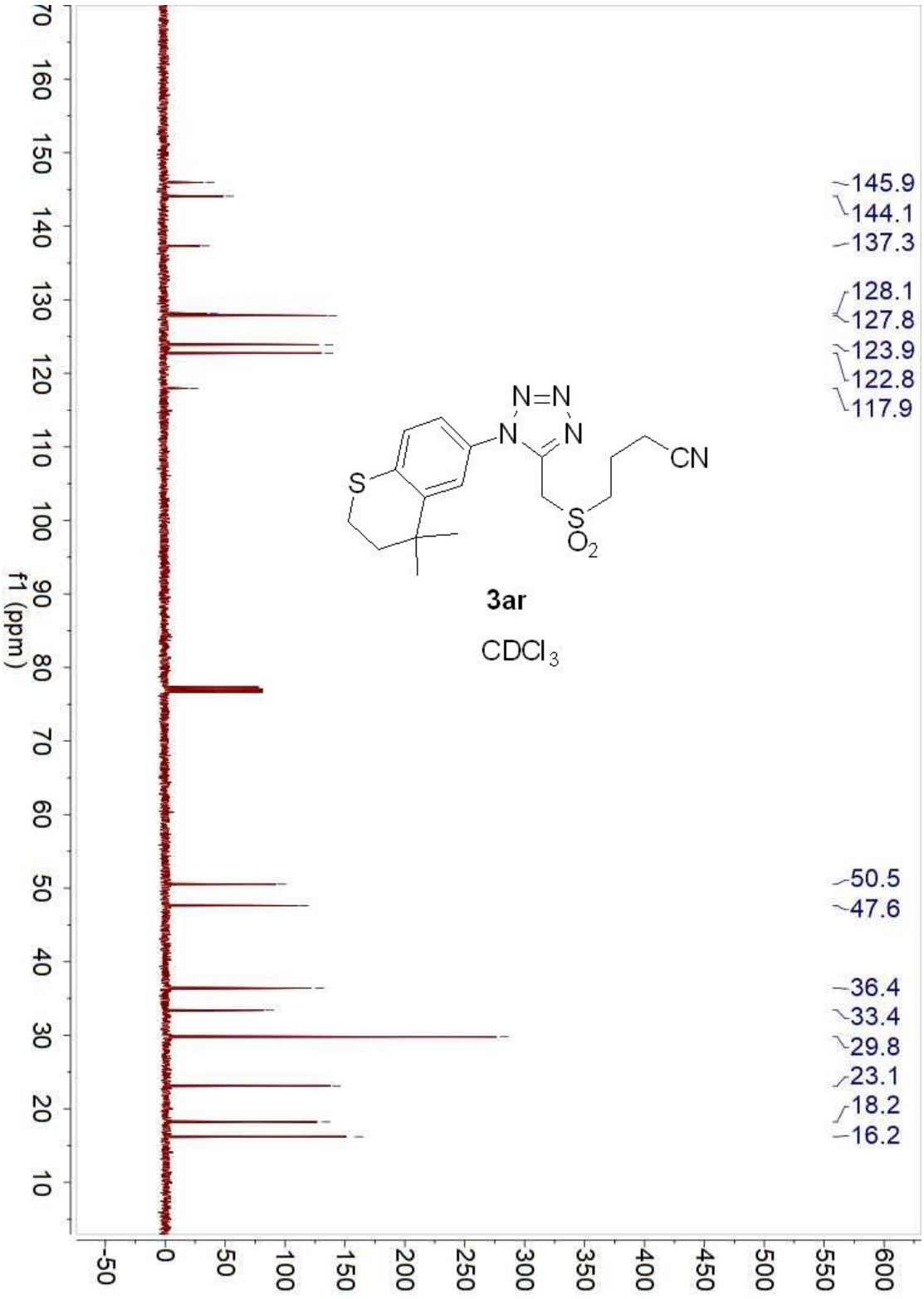
145.9
144.1
137.3
128.1
127.8
123.9
122.8
117.9
50.5
47.6
36.4
33.4
29.8
23.1
18.2
16.2
N=N
N
N
S
CN
S
O2
3ar
CDCl3
f1 (ppm)

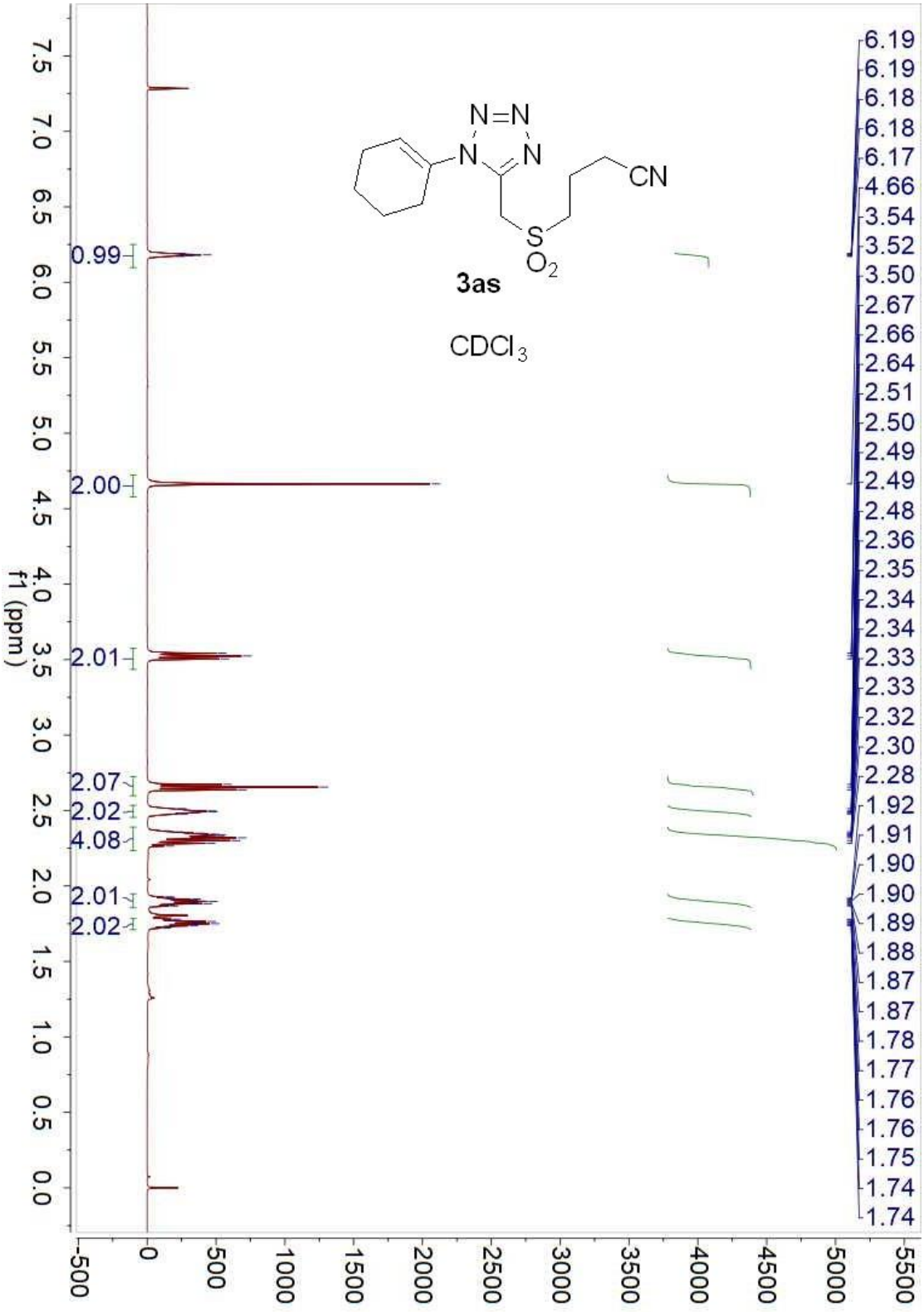
N=N
N
N
CN
S
O2
3as
CDCl3
0.99
2.00
2.01
2.07
2.02
4.08
2.01
2.02
f1 (ppm)
6.19
6.19
6.18
6.18
6.17
4.66
3.54
3.52
3.50
2.67
2.66
2.64
2.51
2.50
2.49
2.49
2.48
2.36
2.35
2.34
2.34
2.33
2.33
2.32
2.30
2.28
1.92
1.91
1.90
1.90
1.89
1.88
1.87
1.87
1.78
1.77
1.76
1.76
1.75
1.74
1.74

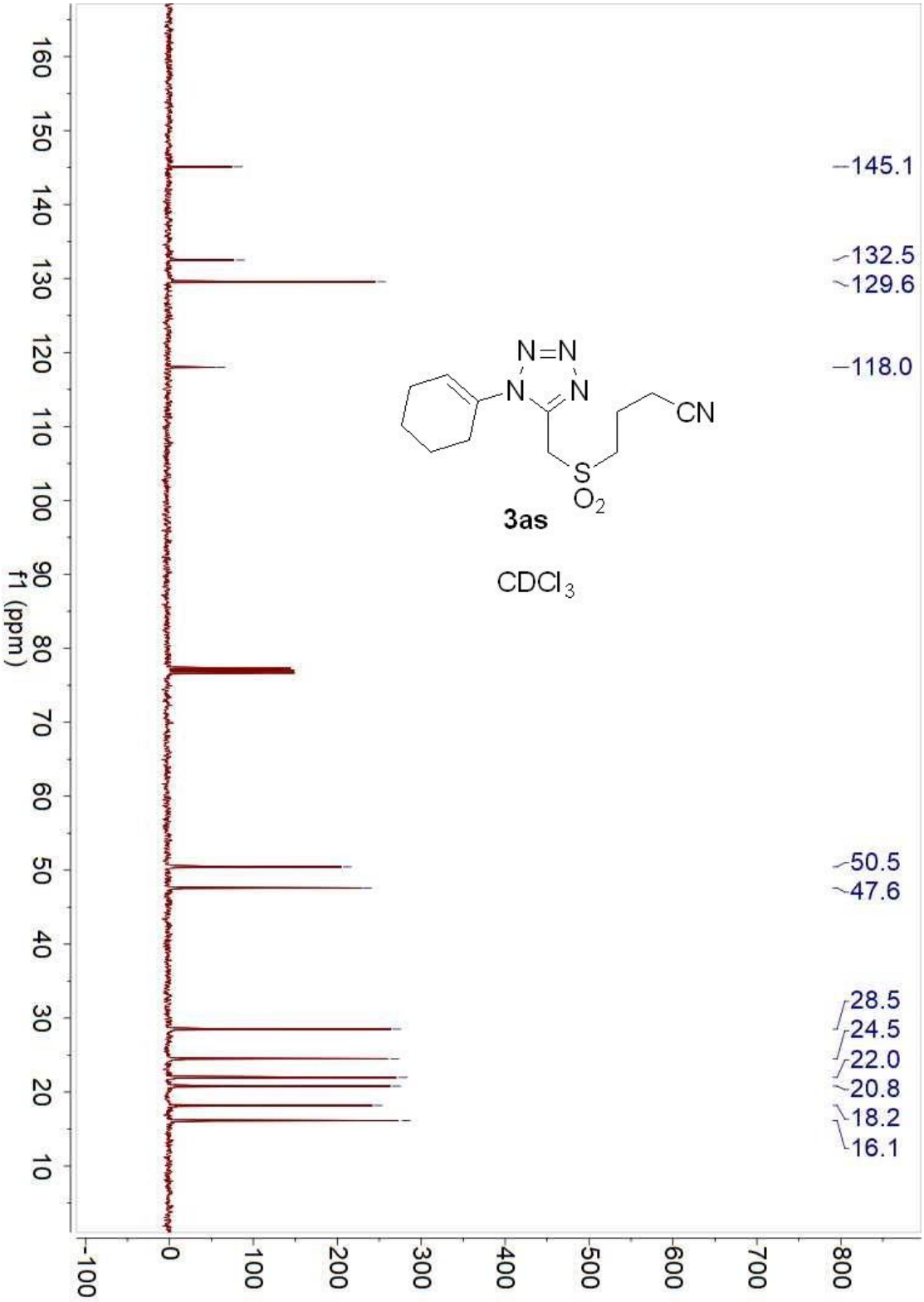
145.1
132.5
129.6
118.0
50.5
47.6
28.5
24.5
22.0
20.8
18.2
16.1
N=N
N
N
CN
S
O2
3as
CDCl3
f1 (ppm)

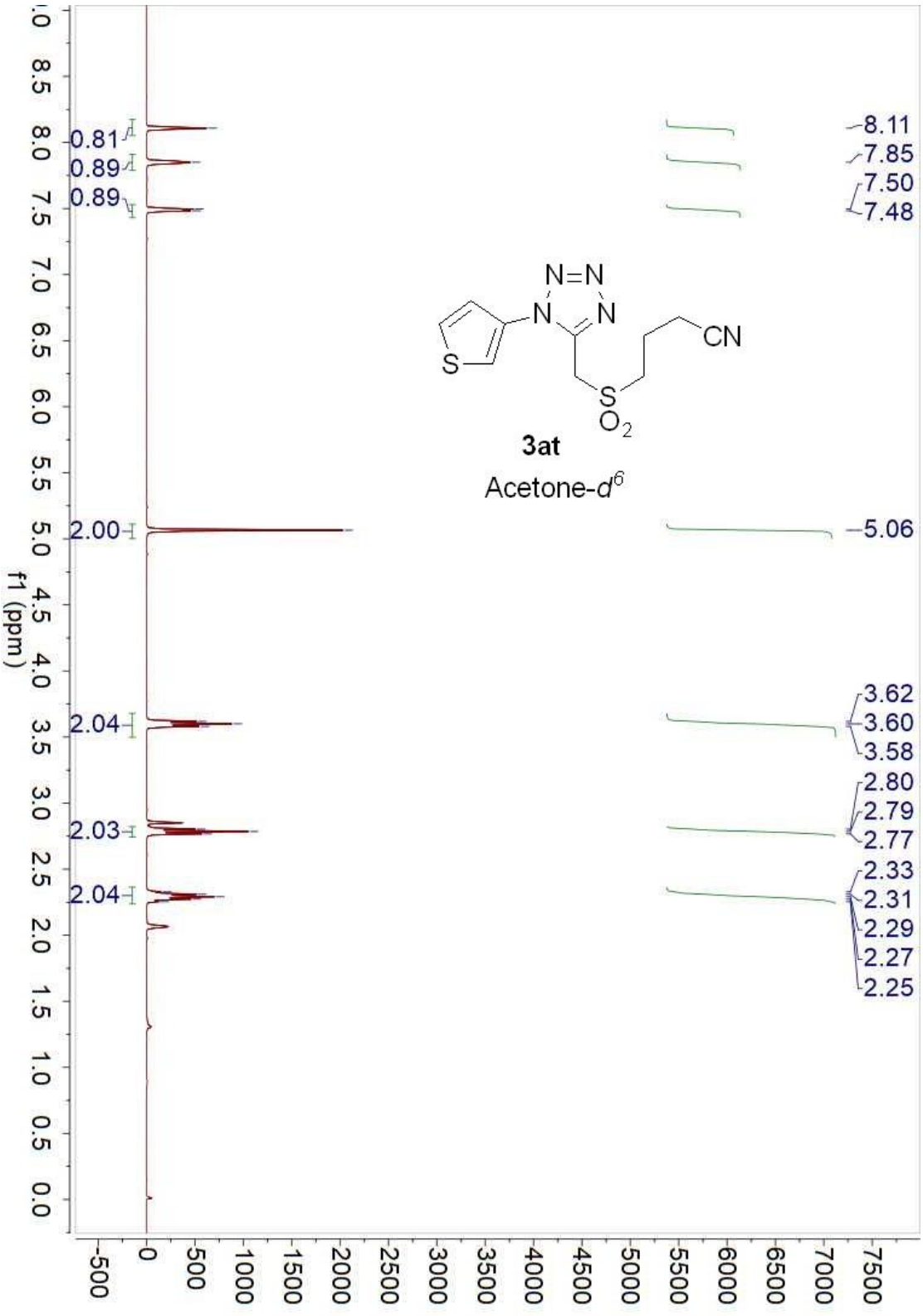
8.11
7.85
7.50
7.48
5.06
3.62
3.60
3.58
2.80
2.79
2.77
2.33
2.31
2.29
2.27
2.25
0.81
0.89
0.89
2.00
2.04
2.03
2.04
N=N
N
N
S
CN
SO2
3at
Acetone-d6
f1 (ppm)

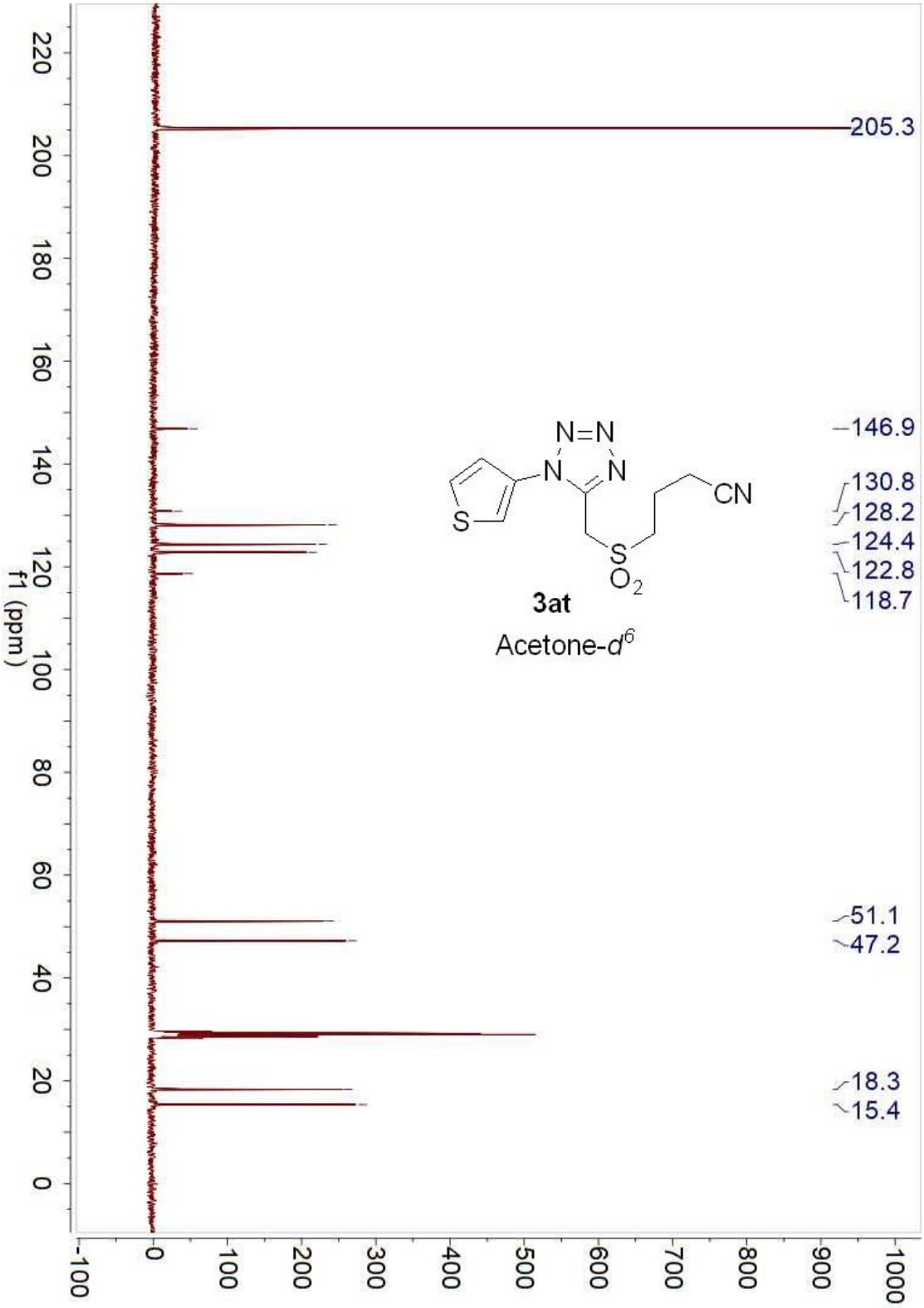
205.3
146.9
130.8
128.2
124.4
122.8
118.7
51.1
47.2
18.3
15.4
N=N
N
N
S
CN
S
O2
3at
Acetone-d6
f1 (ppm)
220
200
180
160
140
120
100
80
60
40
20
0
-100
0
100
200
300
400
500
600
700
800
900
1000

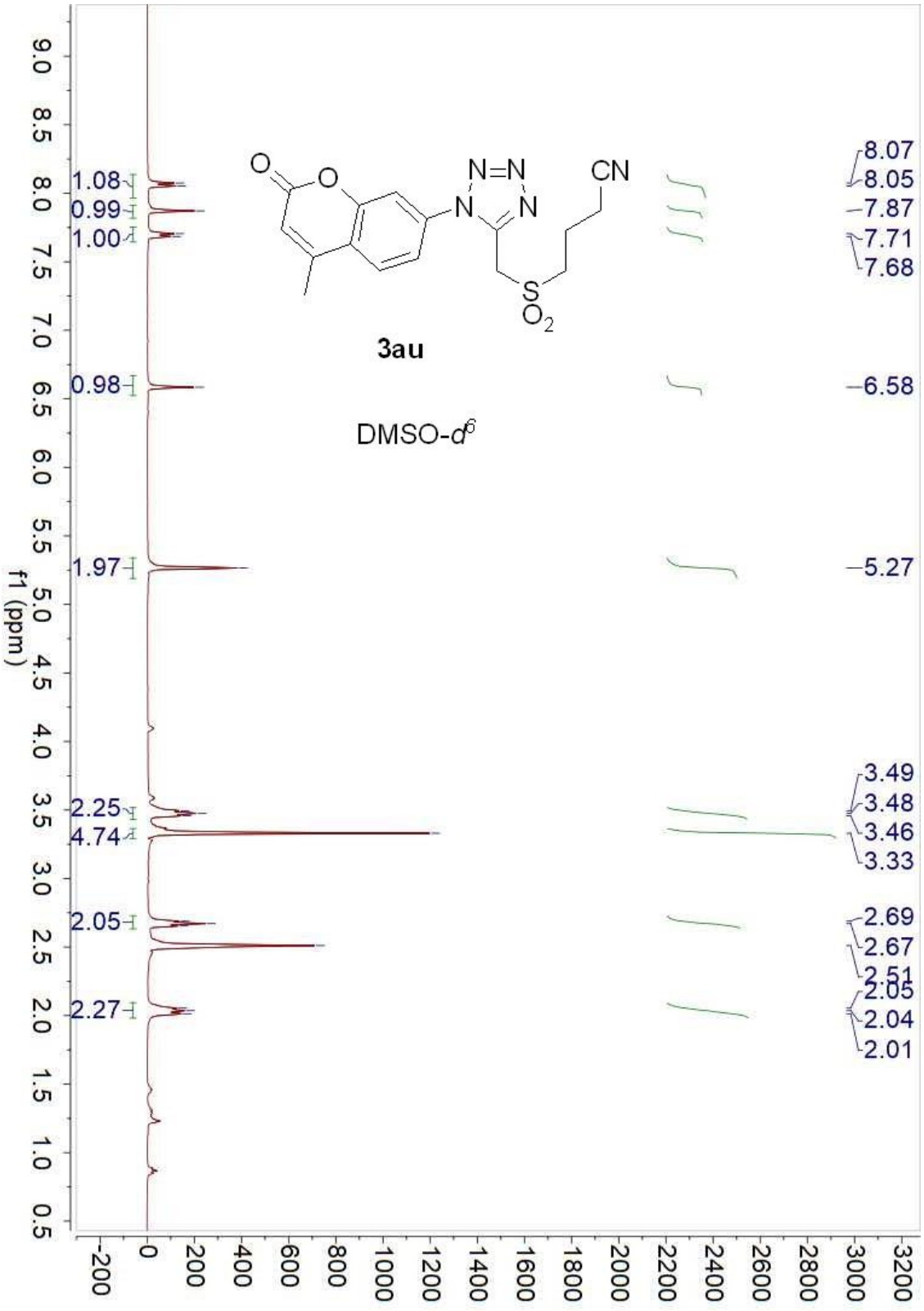
3au
DMSO-d6
f1 (ppm)
1.08
0.99
1.00
0.98
1.97
2.25
4.74
2.05
2.27
8.07
8.05
7.87
7.71
7.68
6.58
5.27
3.49
3.48
3.46
3.33
2.69
2.67
2.51
2.05
2.04
2.01

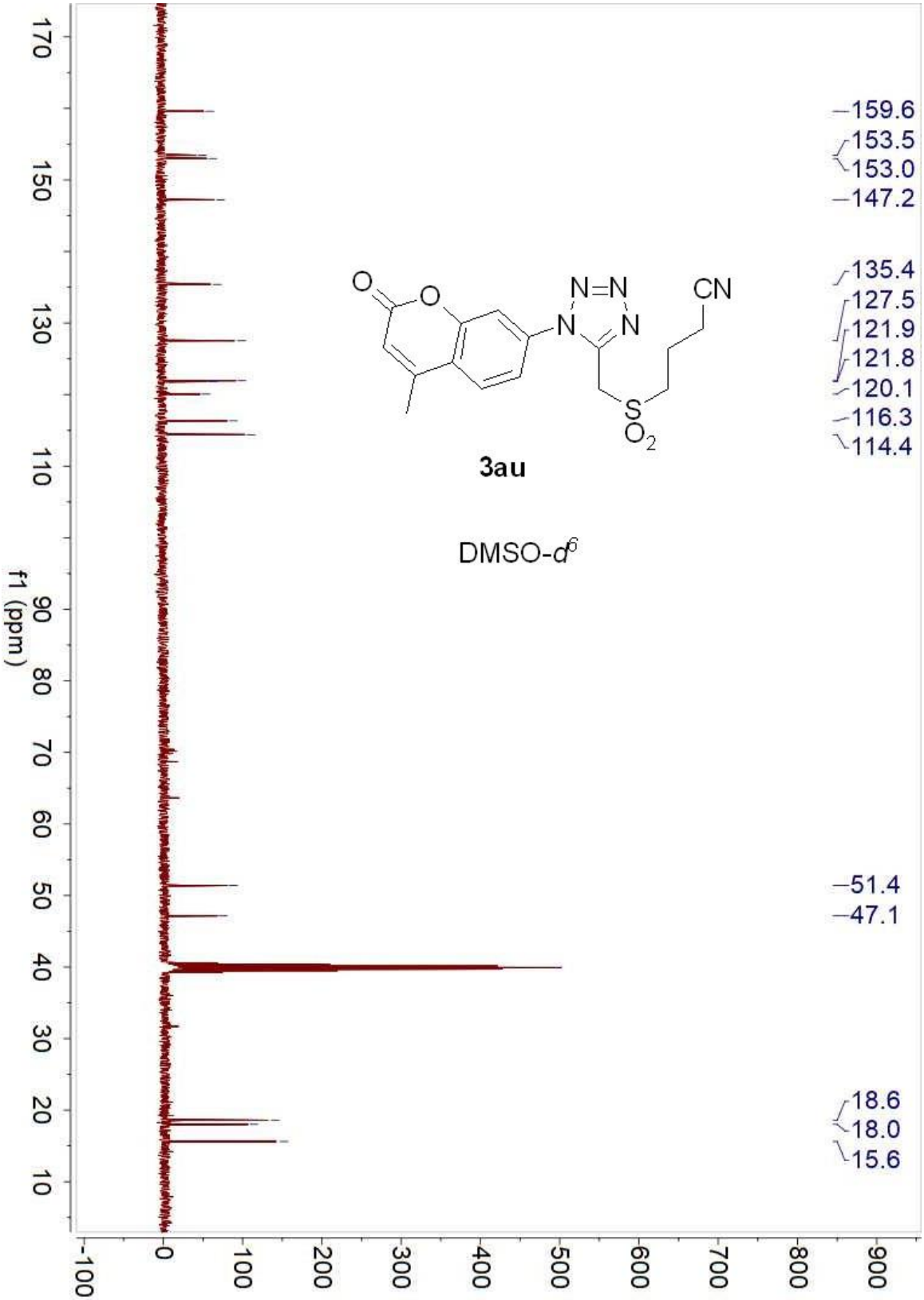
159.6
153.5
153.0
147.2
135.4
127.5
121.9
121.8
120.1
116.3
114.4
51.4
47.1
18.6
18.0
15.6
O
O
N=N
N
N
CN
S
O2
3au
DMSO-d6
f1 (ppm)
170
150
130
110
90
80
70
60
50
40
30
20
10
-100
0
100
200
300
400
500
600
700
800
900

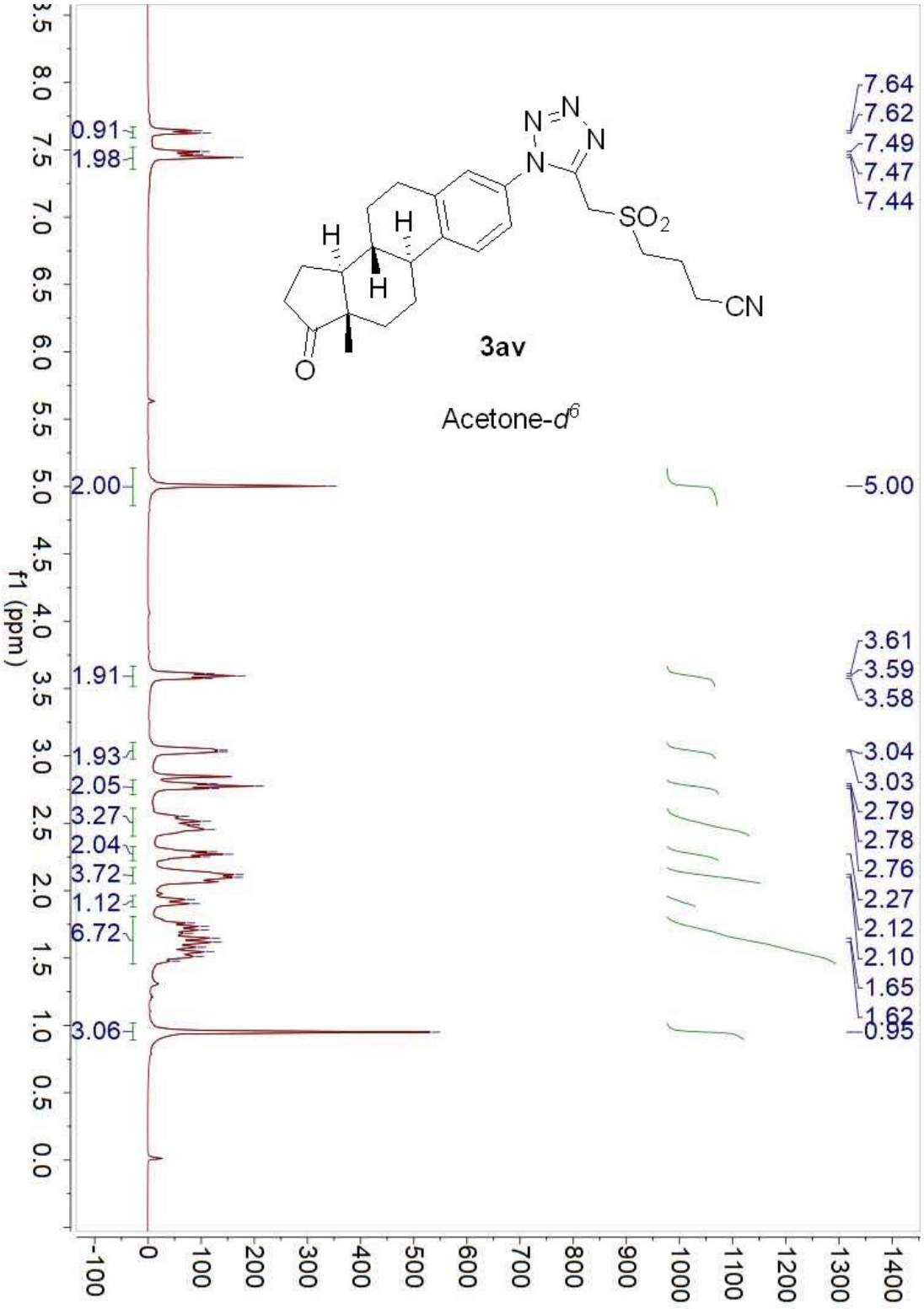
7.64
7.62
7.49
7.47
7.44
0.91
1.98
2.00
5.00
1.91
3.61
3.59
3.58
1.93
2.05
3.27
2.04
3.72
1.12
6.72
3.06
3.04
3.03
2.79
2.78
2.76
2.27
2.12
2.10
1.65
1.62
0.95
f1 (ppm)
3av
Acetone-d6

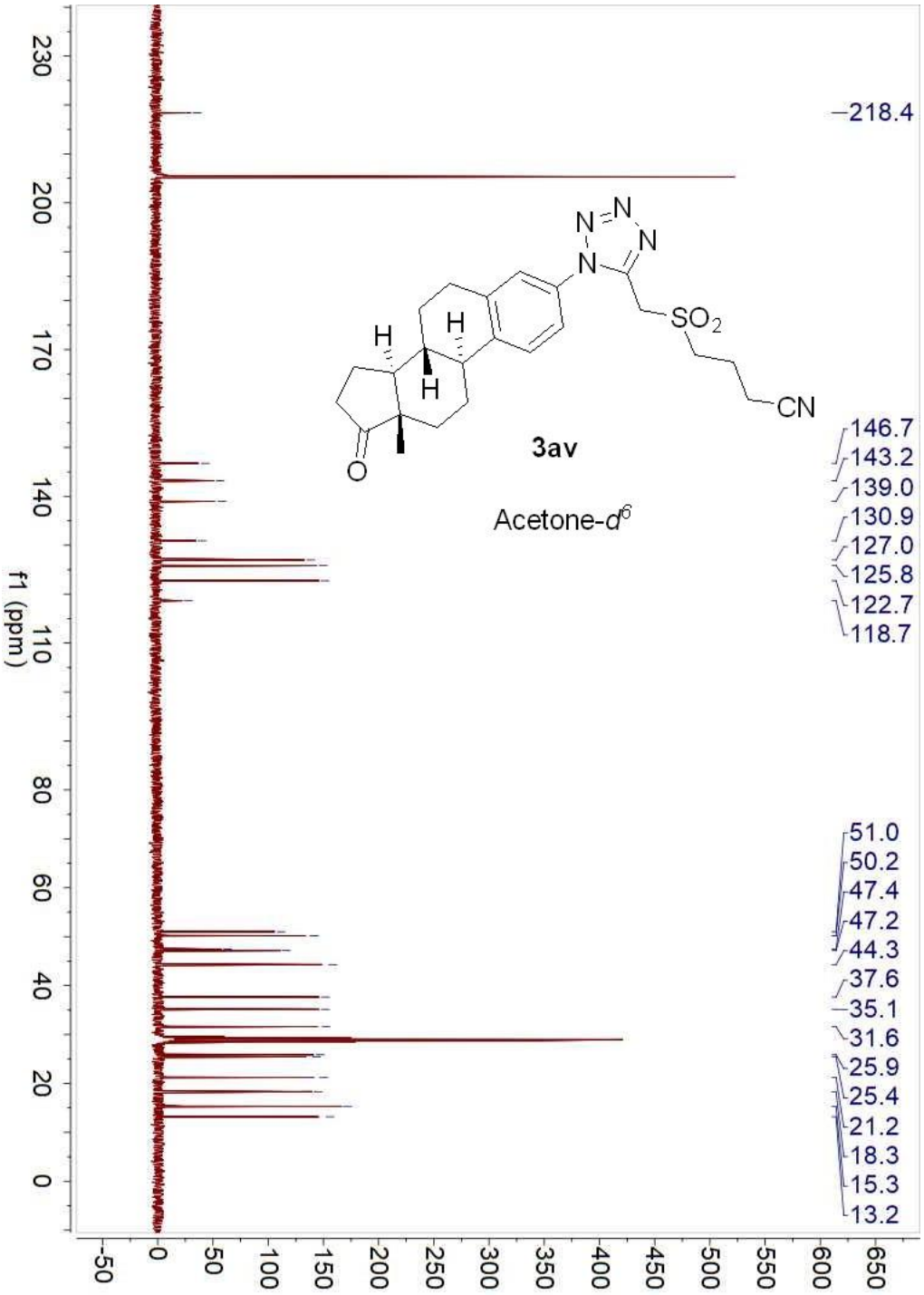
218.4
146.7
143.2
139.0
130.9
127.0
125.8
122.7
118.7
51.0
50.2
47.4
47.2
44.3
37.6
35.1
31.6
25.9
25.4
21.2
18.3
15.3
13.2
3av
Acetone-d6
f1 (ppm)

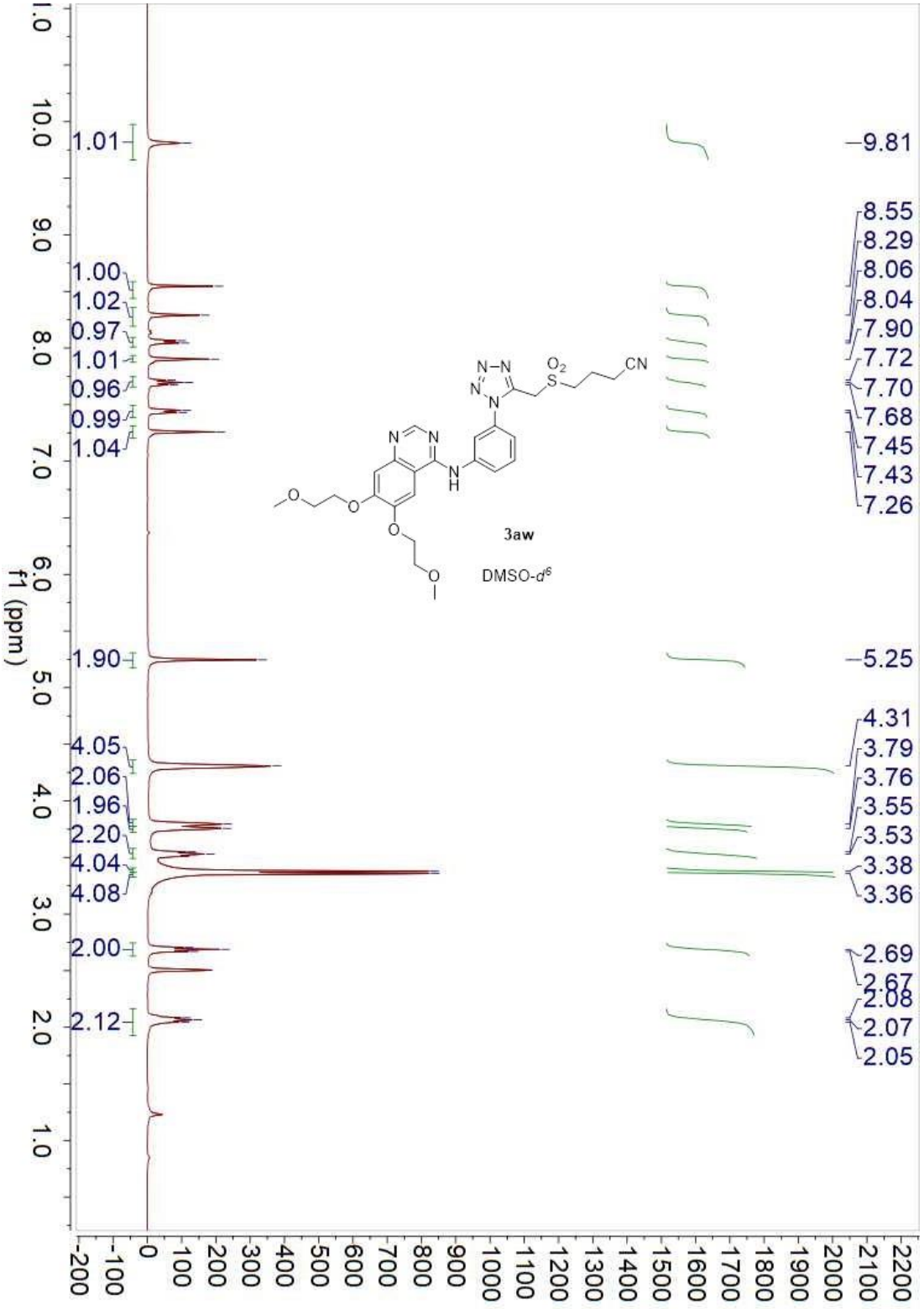
3aw
DMSO-d^6
f1 (ppm)
1.01
1.00
1.02
0.97
1.01
0.96
0.99
1.04
1.90
4.05
2.06
1.96
2.20
4.04
4.08
2.00
2.12
9.81
8.55
8.29
8.06
8.04
7.90
7.72
7.70
7.68
7.45
7.43
7.26
5.25
4.31
3.79
3.76
3.55
3.53
3.38
3.36
2.69
2.67
2.08
2.07
2.05

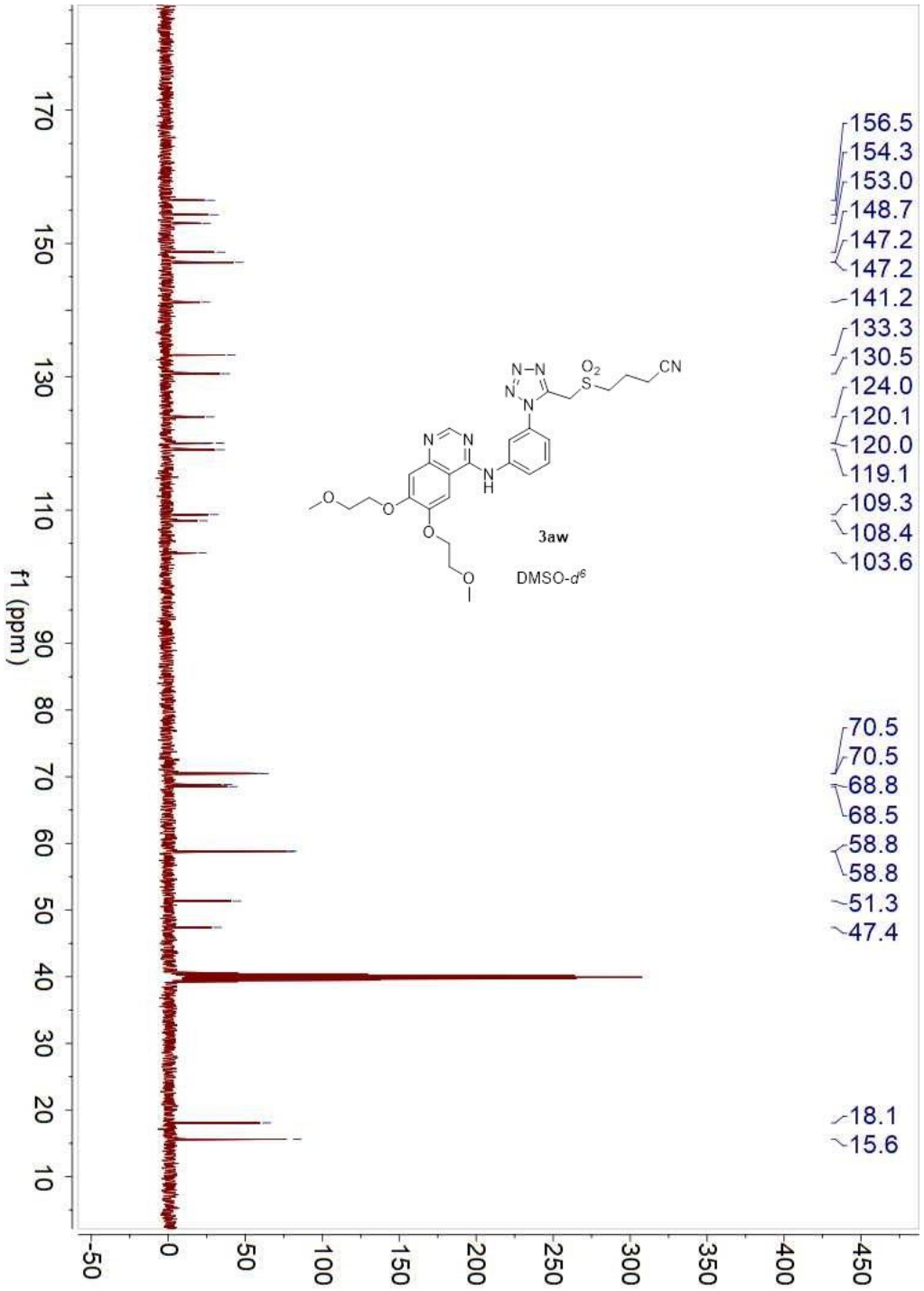
156.5
154.3
153.0
148.7
147.2
147.2
141.2
133.3
130.5
124.0
120.1
120.0
119.1
109.3
108.4
103.6
70.5
70.5
68.8
68.5
58.8
58.8
51.3
47.4
18.1
15.6
3aw
DMSO-d6
f1 (ppm)

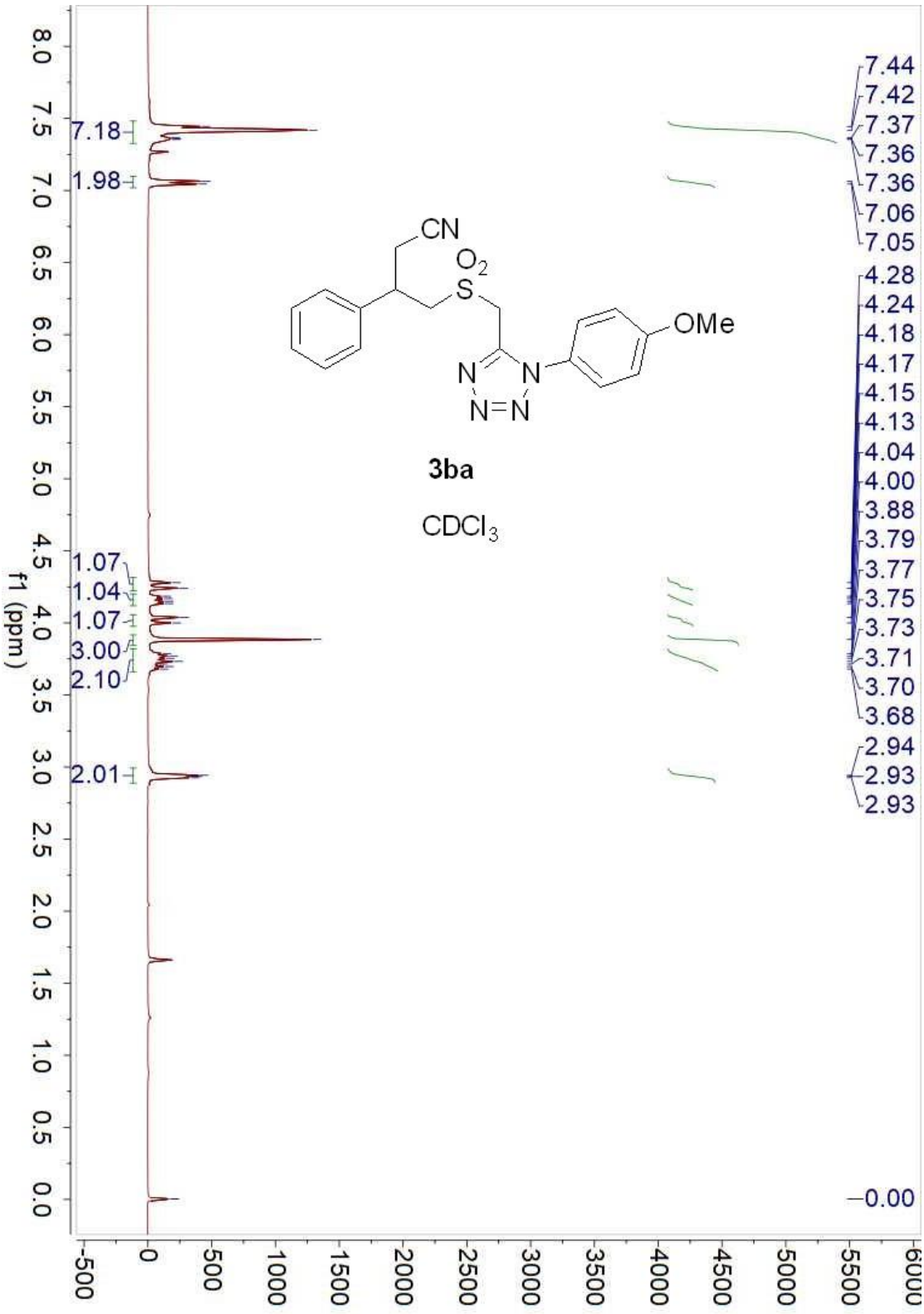
CN
O2
S
OMe
N
N
N=N
3ba
CDCl3
7.18
1.98
1.07
1.04
1.07
3.00
2.10
2.01
7.44
7.42
7.37
7.36
7.36
7.06
7.05
4.28
4.24
4.18
4.17
4.15
4.13
4.04
4.00
3.88
3.79
3.77
3.75
3.73
3.71
3.70
3.68
2.94
2.93
2.93
0.00
f1 (ppm)

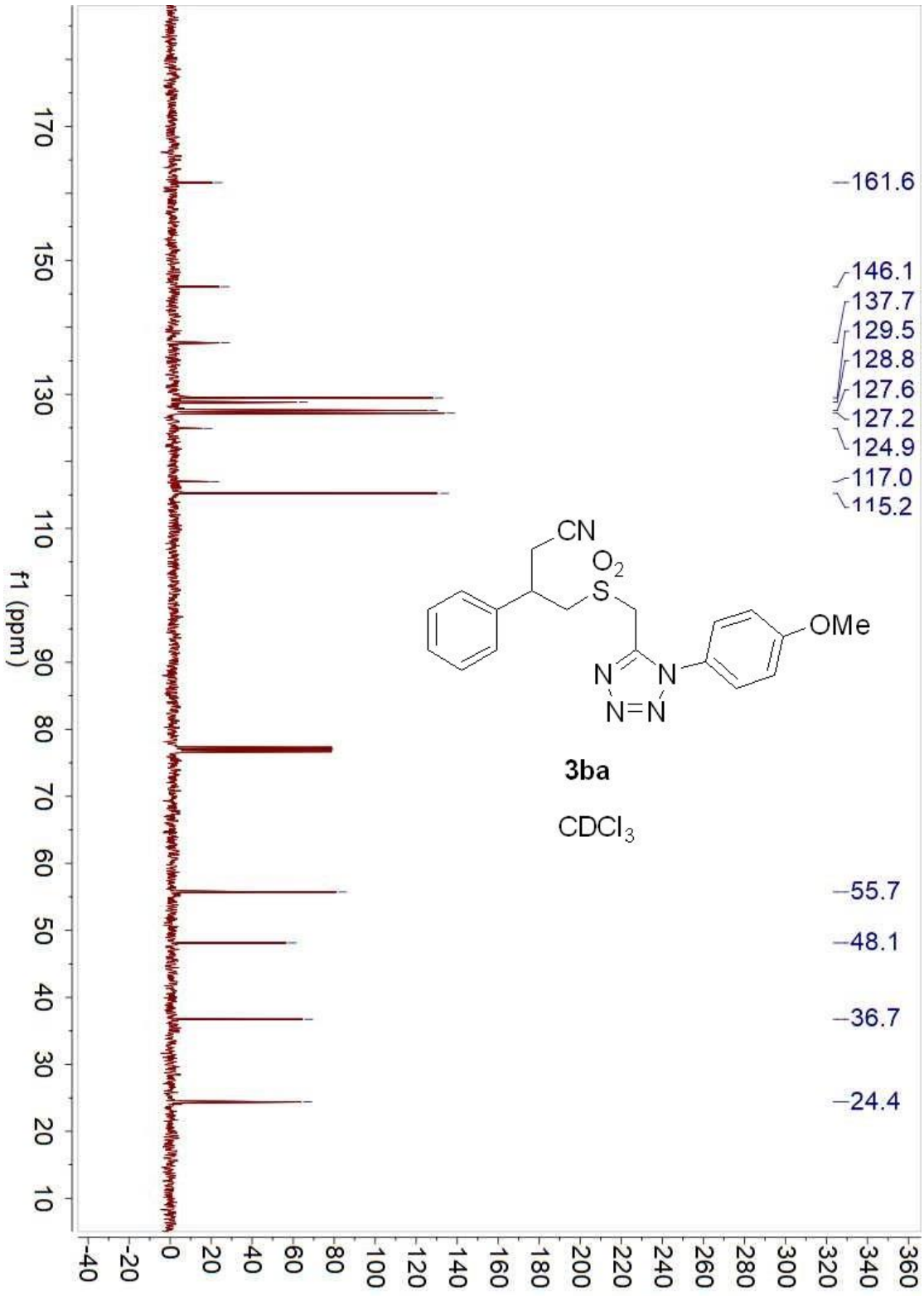
161.6
146.1
137.7
129.5
128.8
127.6
127.2
124.9
117.0
115.2
55.7
48.1
36.7
24.4
CN
O2
S
N
N
N=N
OMe
3ba
CDCl3
f1 (ppm)

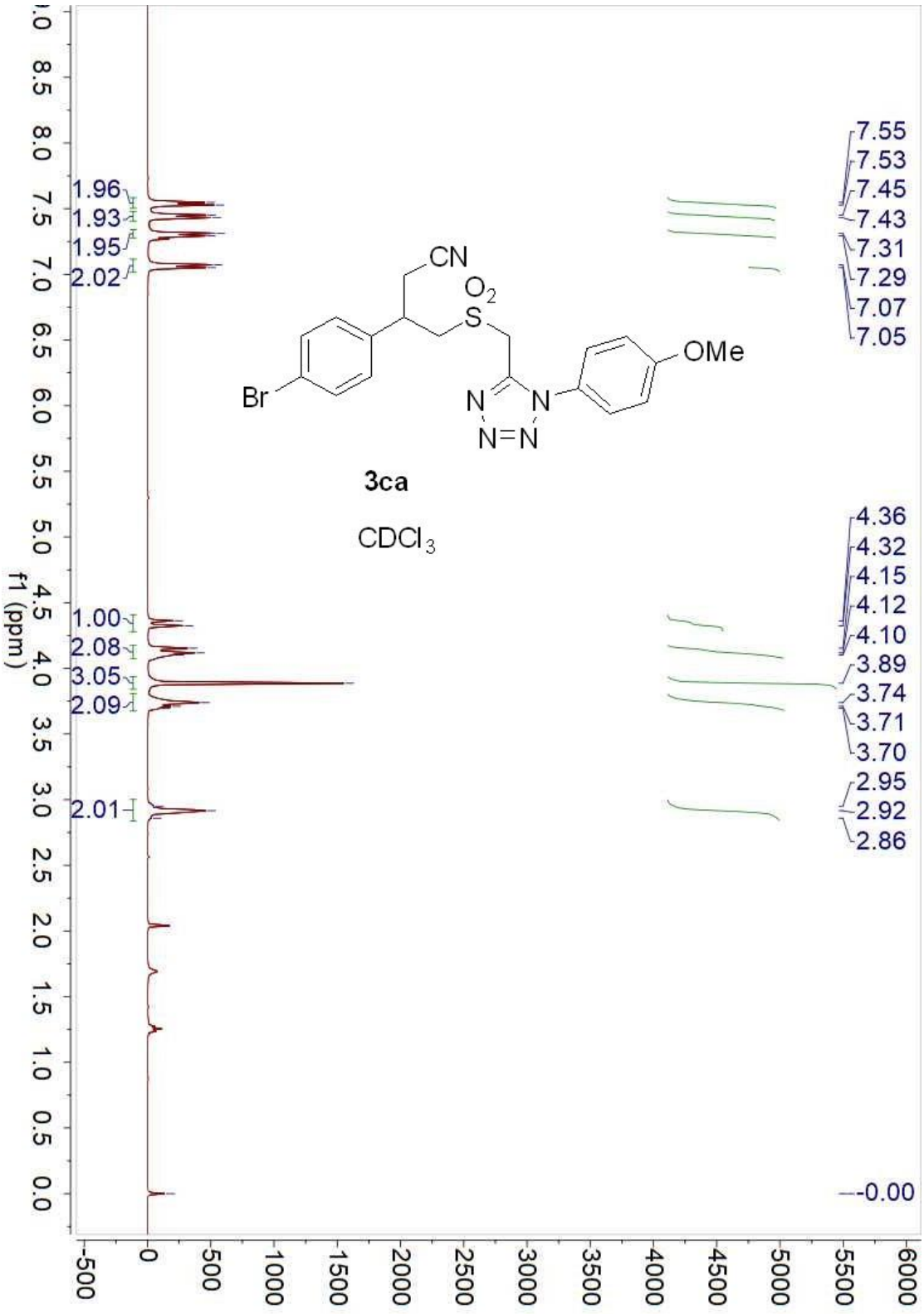
7.55
7.53
7.45
7.43
7.31
7.29
7.07
7.05
4.36
4.32
4.15
4.12
4.10
3.89
3.74
3.71
3.70
2.95
2.92
2.86
-0.00
1.96
1.93
1.95
2.02
1.00
2.08
3.05
2.09
2.01
CN
O2
S
Br
OMe
N
N
N=N
3ca
CDCl3
f1 (ppm)

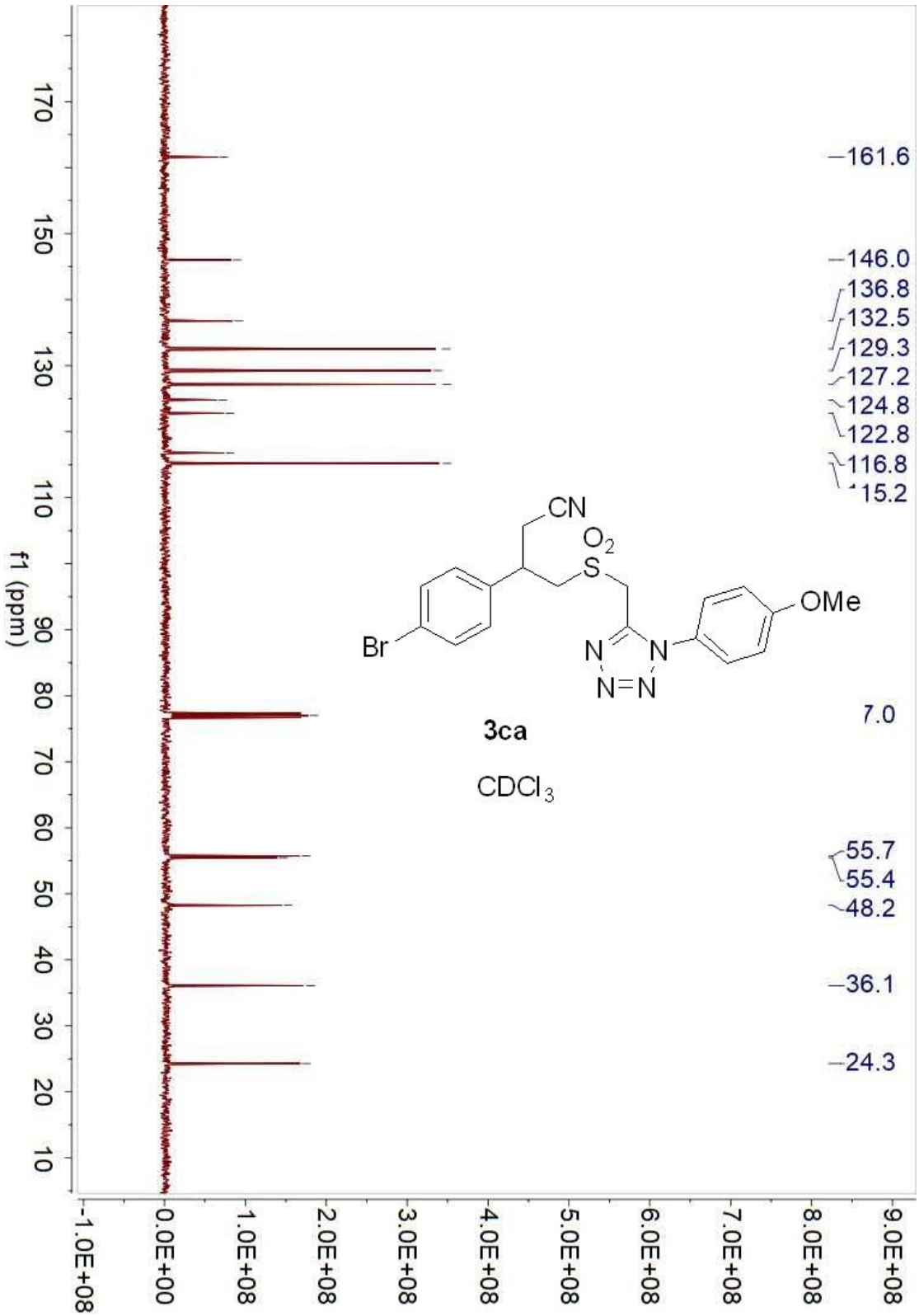
161.6
146.0
136.8
132.5
129.3
127.2
124.8
122.8
116.8
115.2
7.0
55.7
55.4
48.2
36.1
24.3
CN
O2
S
Br
OMe
N
N
N=N
3ca
CDCl3
f1 (ppm)
170
150
130
110
90
80
70
60
50
40
30
20
10
-1.0E+08
0.0E+00
1.0E+08
2.0E+08
3.0E+08
4.0E+08
5.0E+08
6.0E+08
7.0E+08
8.0E+08
9.0E+08

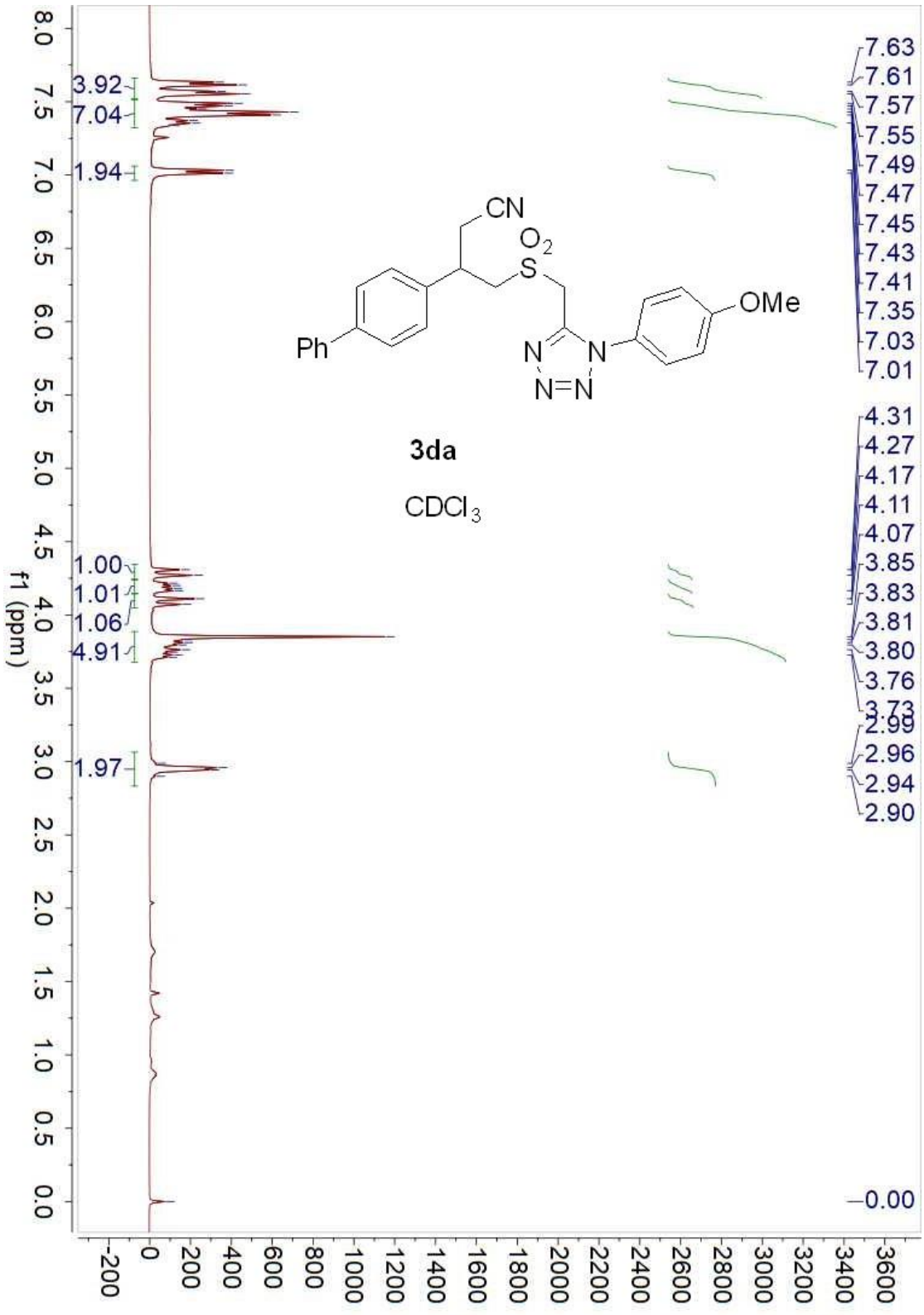
CN
O2
S
Ph
N
N
N=N
OMe
3da
CDCl3
3.92
7.04
1.94
1.00
1.01
1.06
4.91
1.97
7.63
7.61
7.57
7.55
7.49
7.47
7.45
7.43
7.41
7.35
7.03
7.01
4.31
4.27
4.17
4.11
4.07
3.85
3.83
3.81
3.80
3.76
3.73
2.99
2.96
2.94
2.90
0.00
f1 (ppm)

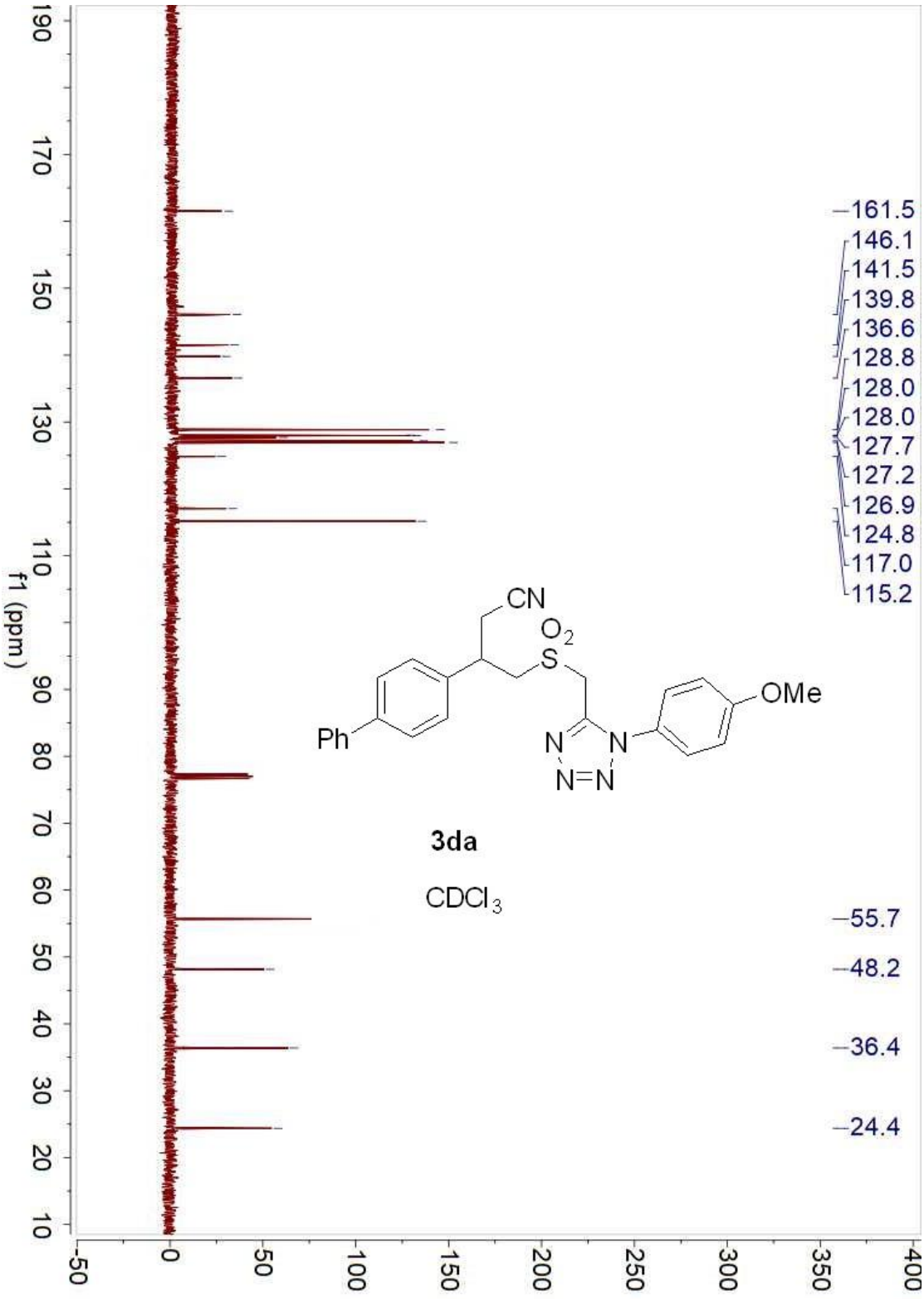
161.5
146.1
141.5
139.8
136.6
128.8
128.0
128.0
127.7
127.2
126.9
124.8
117.0
115.2
55.7
48.2
36.4
24.4
CN
O2
S
OMe
Ph
N
N
N=N
3da
CDCl3
f1 (ppm)

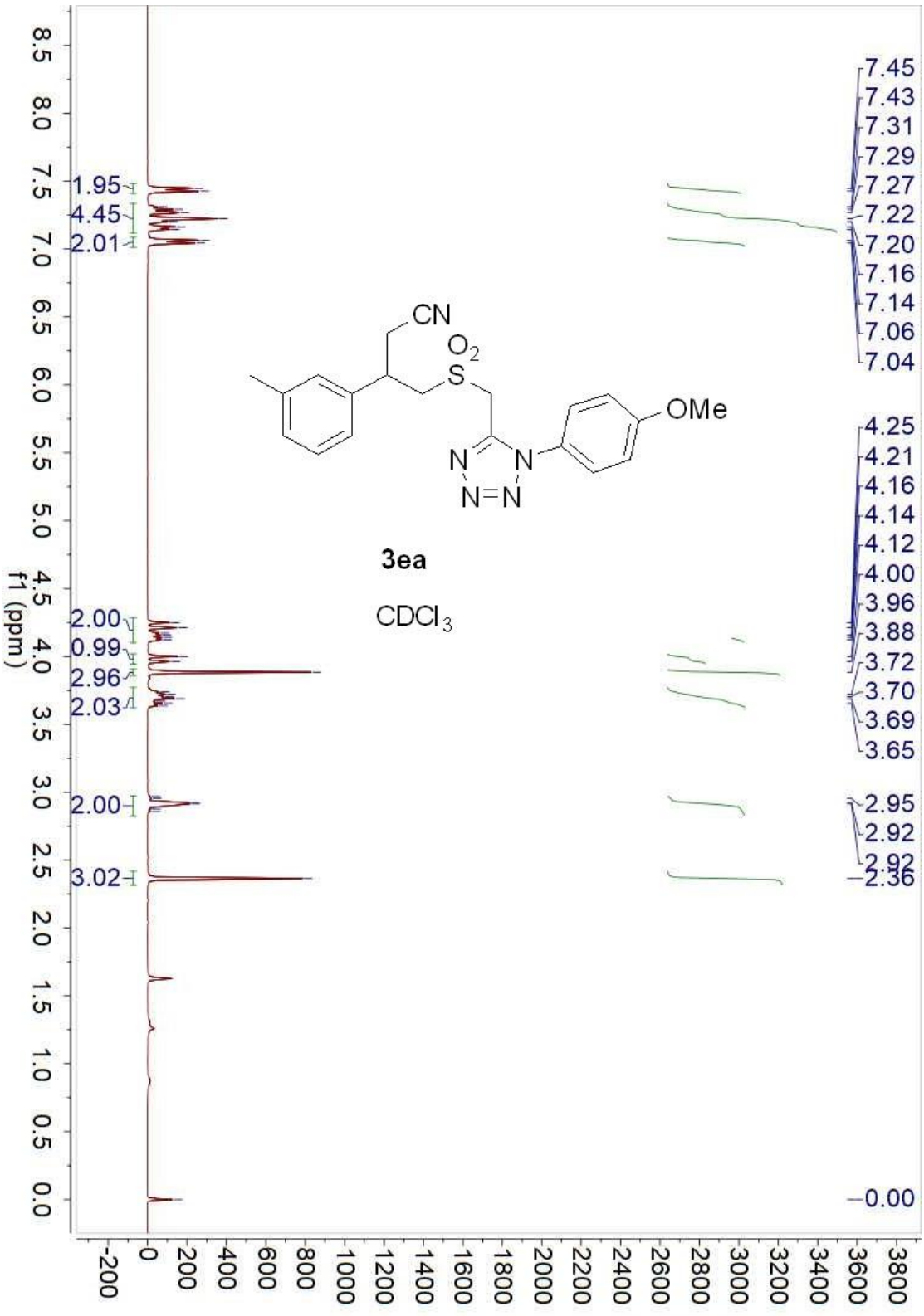
7.45
7.43
7.31
7.29
7.27
7.22
7.20
7.16
7.14
7.06
7.04
4.25
4.21
4.16
4.14
4.12
4.00
3.96
3.88
3.72
3.70
3.69
3.65
2.95
2.92
2.92
2.36
0.00
1.95
4.45
2.01
2.00
0.99
2.96
2.03
2.00
3.02
CN
O2
S
OMe
N
N
N=N
3ea
CDCl3
f1 (ppm)

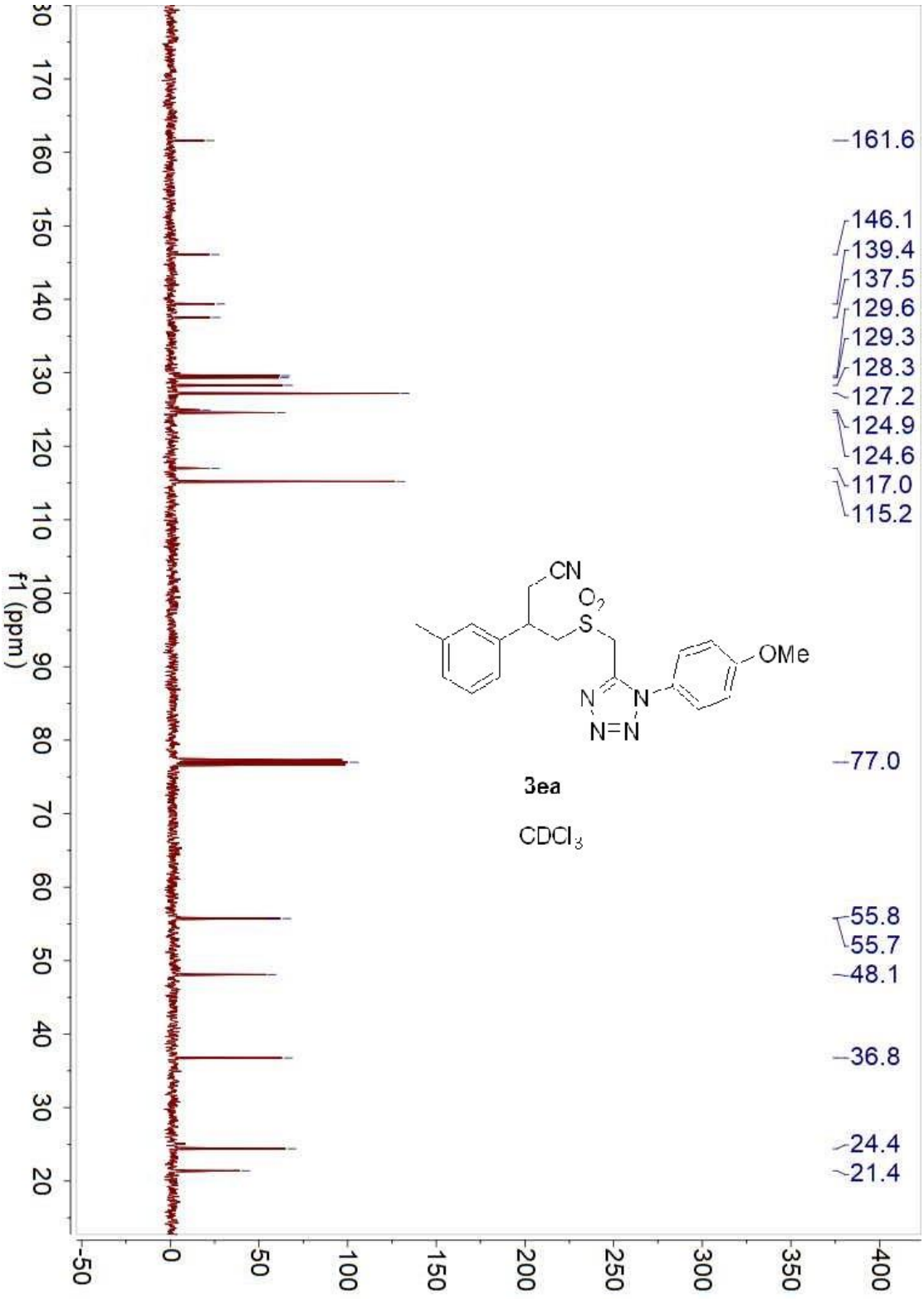
161.6
146.1
139.4
137.5
129.6
129.3
128.3
127.2
124.9
124.6
117.0
115.2
77.0
55.8
55.7
48.1
36.8
24.4
21.4
CN
O
O
S
N
N
N=N
OMe
3ea
CDCl3
f1 (ppm)

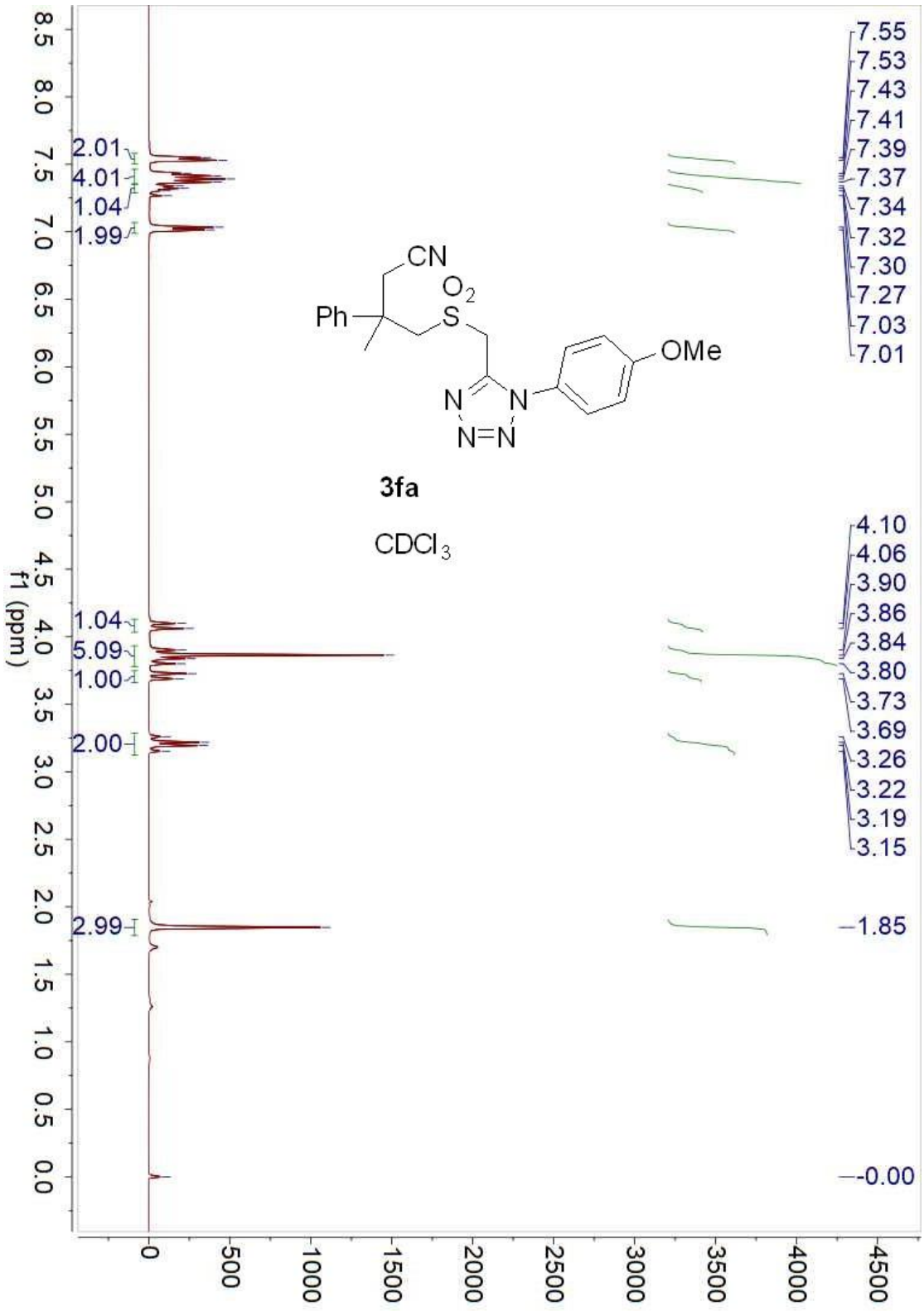
7.55
7.53
7.43
7.41
7.39
7.37
7.34
7.32
7.30
7.27
7.03
7.01
2.01
4.01
1.04
1.99
CN
O2
S
Ph
OMe
N
N
N=N
3fa
CDCl3
4.10
4.06
3.90
3.86
3.84
3.80
3.73
3.69
3.26
3.22
3.19
3.15
1.04
5.09
1.00
2.00
2.99
1.85
0.00
f1 (ppm)

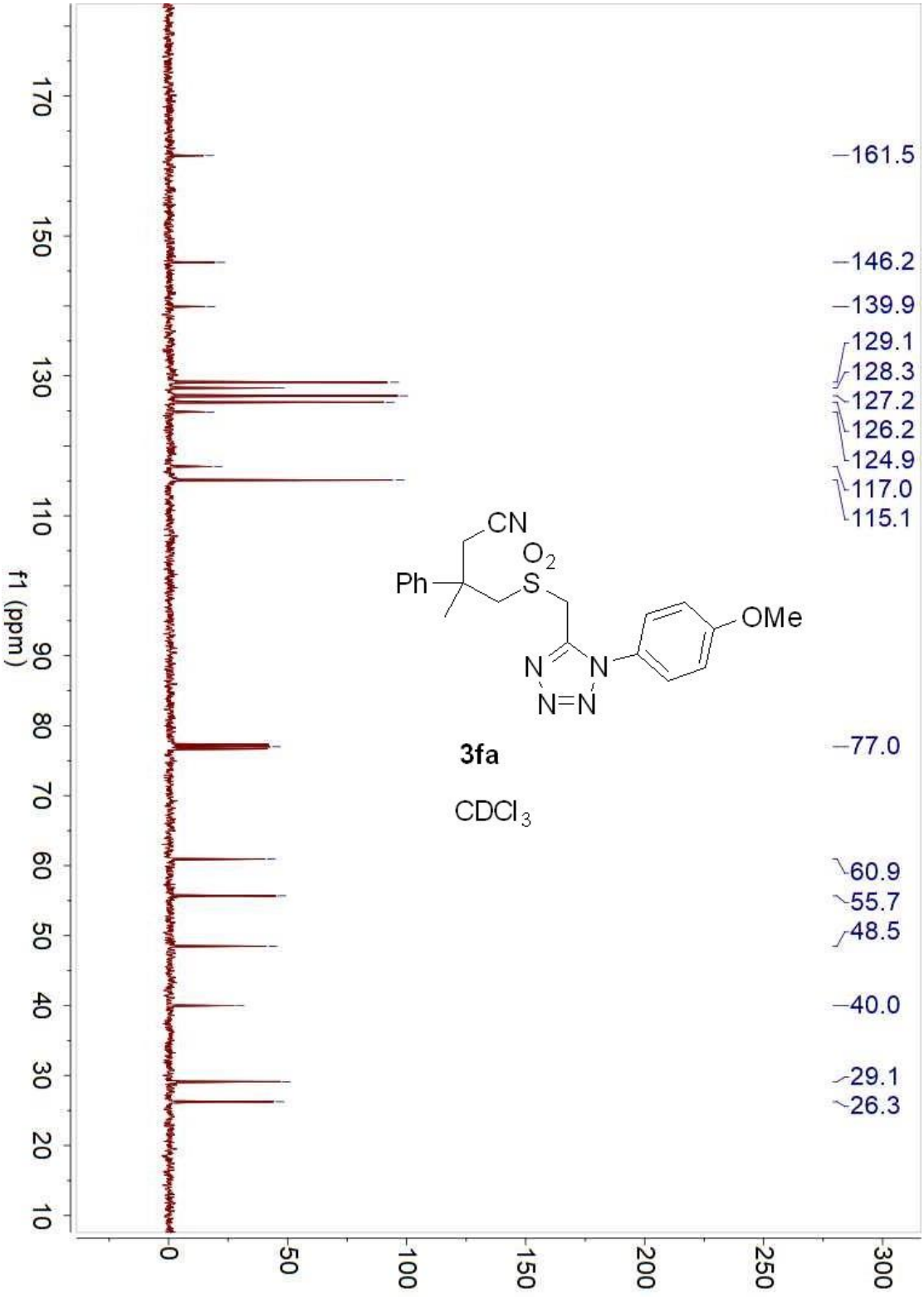
161.5
146.2
139.9
129.1
128.3
127.2
126.2
124.9
117.0
115.1
77.0
60.9
55.7
48.5
40.0
29.1
26.3
CN
O2
S
Ph
OMe
N
N
N=N
3fa
CDCl3
f1 (ppm)
170
150
130
110
90
80
70
60
50
40
30
20
10
0
50
100
150
200
250
300

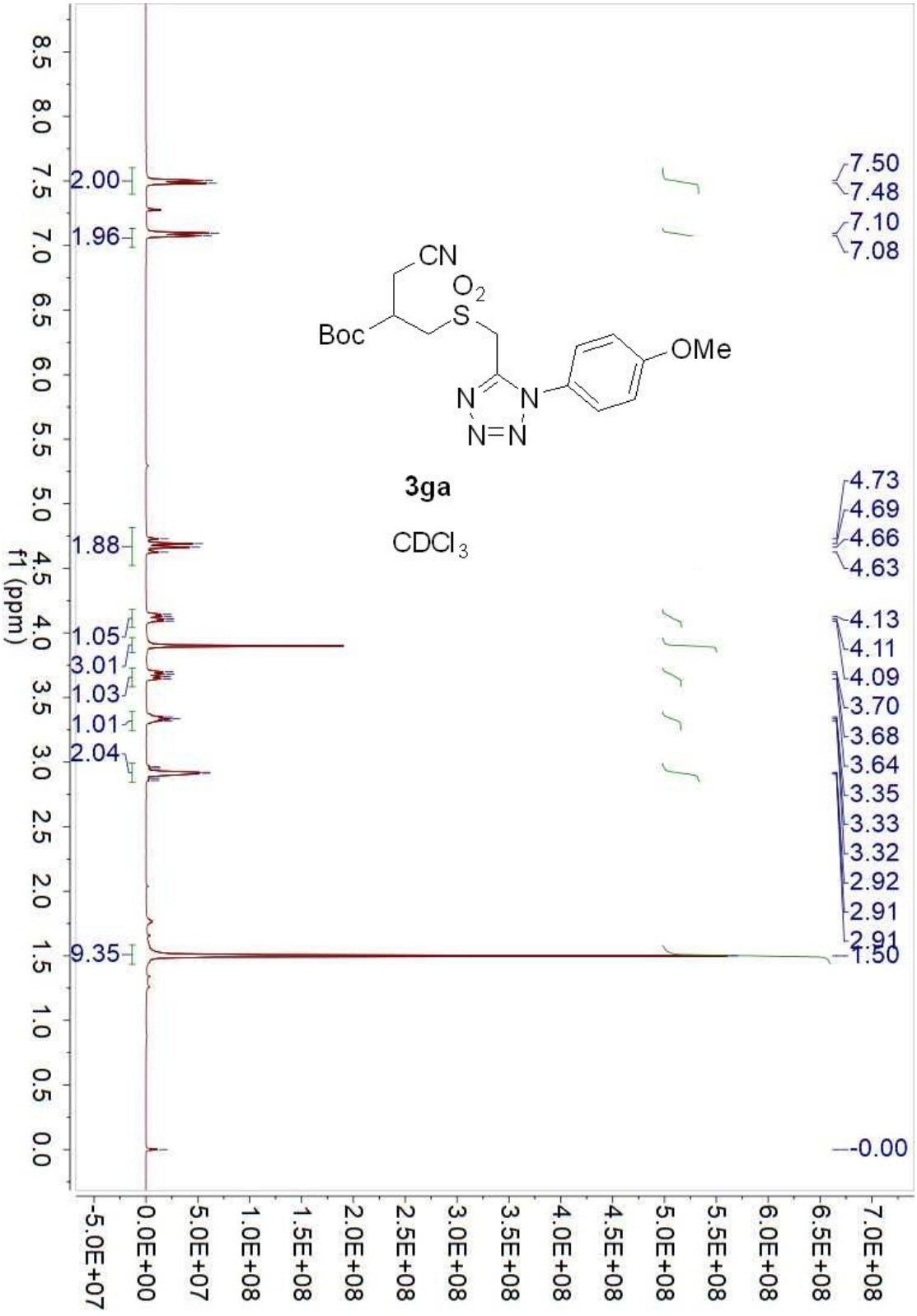
CN
O2
S
Boc
OMe
N
N
N=N
3ga
CDCl3
f1 (ppm)
2.00
1.96
1.88
1.05
3.01
1.03
1.01
2.04
9.35
7.50
7.48
7.10
7.08
4.73
4.69
4.66
4.63
4.13
4.11
4.09
3.70
3.68
3.64
3.35
3.33
3.32
2.92
2.91
2.91
1.50
-0.00

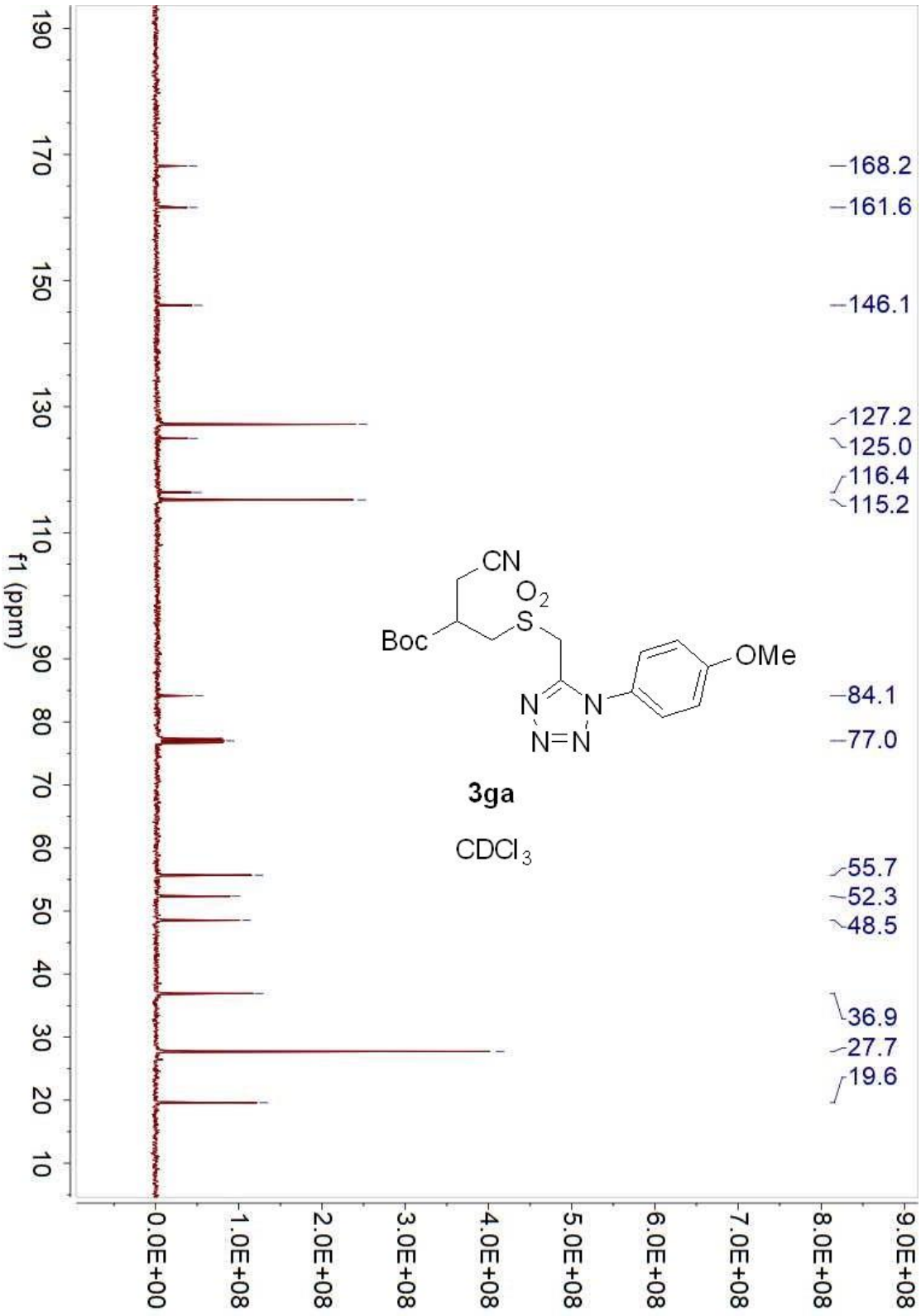
168.2
161.6
146.1
127.2
125.0
116.4
115.2
84.1
77.0
55.7
52.3
48.5
36.9
27.7
19.6
CN
O2
S
Boc
OMe
N
N
N=N
3ga
CDCl3
f1 (ppm)
190
170
150
130
110
90
80
70
60
50
40
30
20
10
0.0E+00
1.0E+08
2.0E+08
3.0E+08
4.0E+08
5.0E+08
6.0E+08
7.0E+08
8.0E+08
9.0E+08

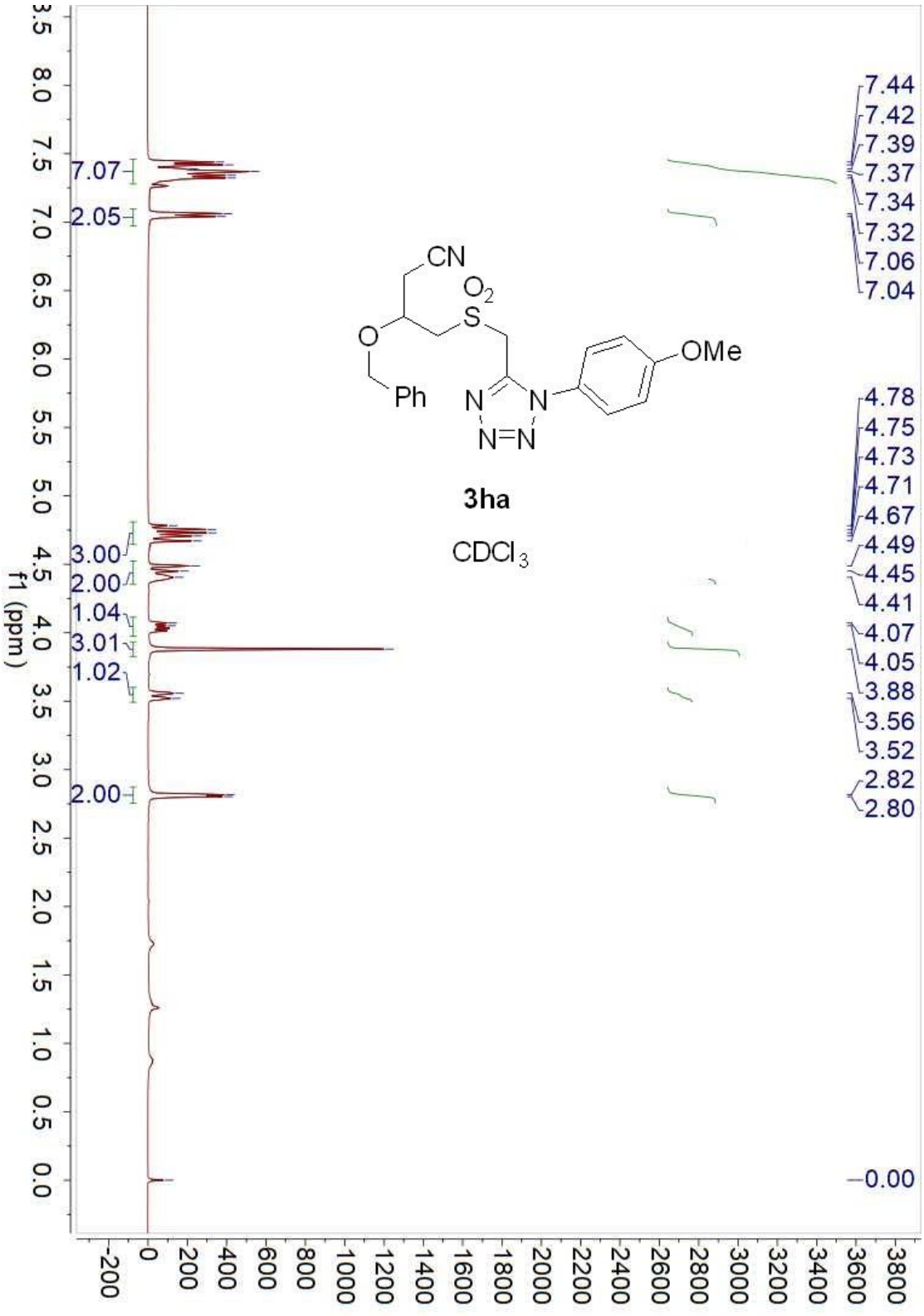
7.44
7.42
7.39
7.37
7.34
7.32
7.06
7.04
4.78
4.75
4.73
4.71
4.67
4.49
4.45
4.41
4.07
4.05
3.88
3.56
3.52
2.82
2.80
0.00
7.07
2.05
3.00
2.00
1.04
3.01
1.02
2.00
CN
O2
S
O
Ph
N
N
N=N
OMe
3ha
CDCl3
f1 (ppm)

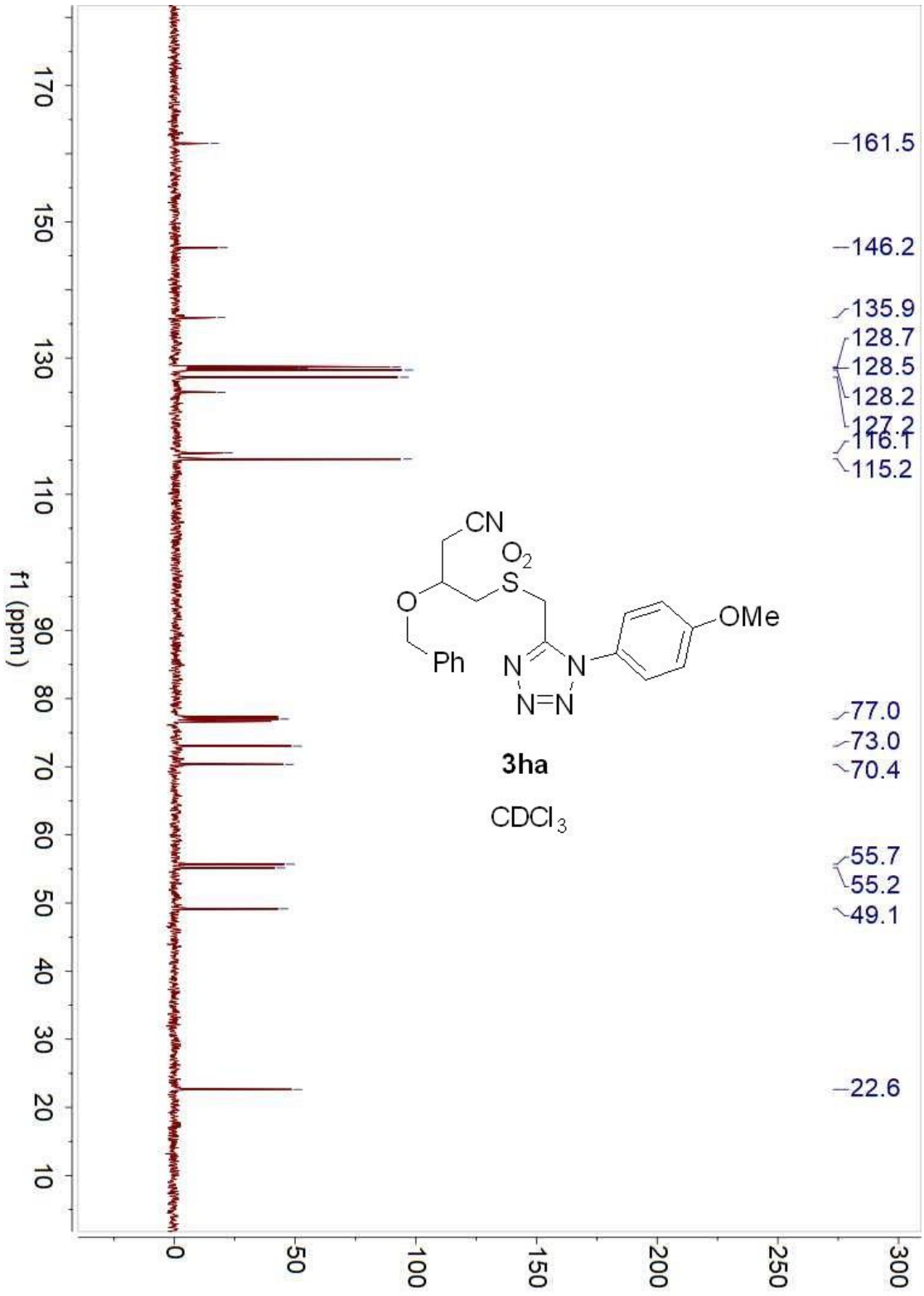
161.5
146.2
135.9
128.7
128.5
128.2
127.2
116.1
115.2
77.0
73.0
70.4
55.7
55.2
49.1
22.6
CN
O2
S
O
Ph
N
N
N=N
OMe
3ha
CDCl3
f1 (ppm)
170
150
130
110
90
80
70
60
50
40
30
20
10
0
50
100
150
200
250
300

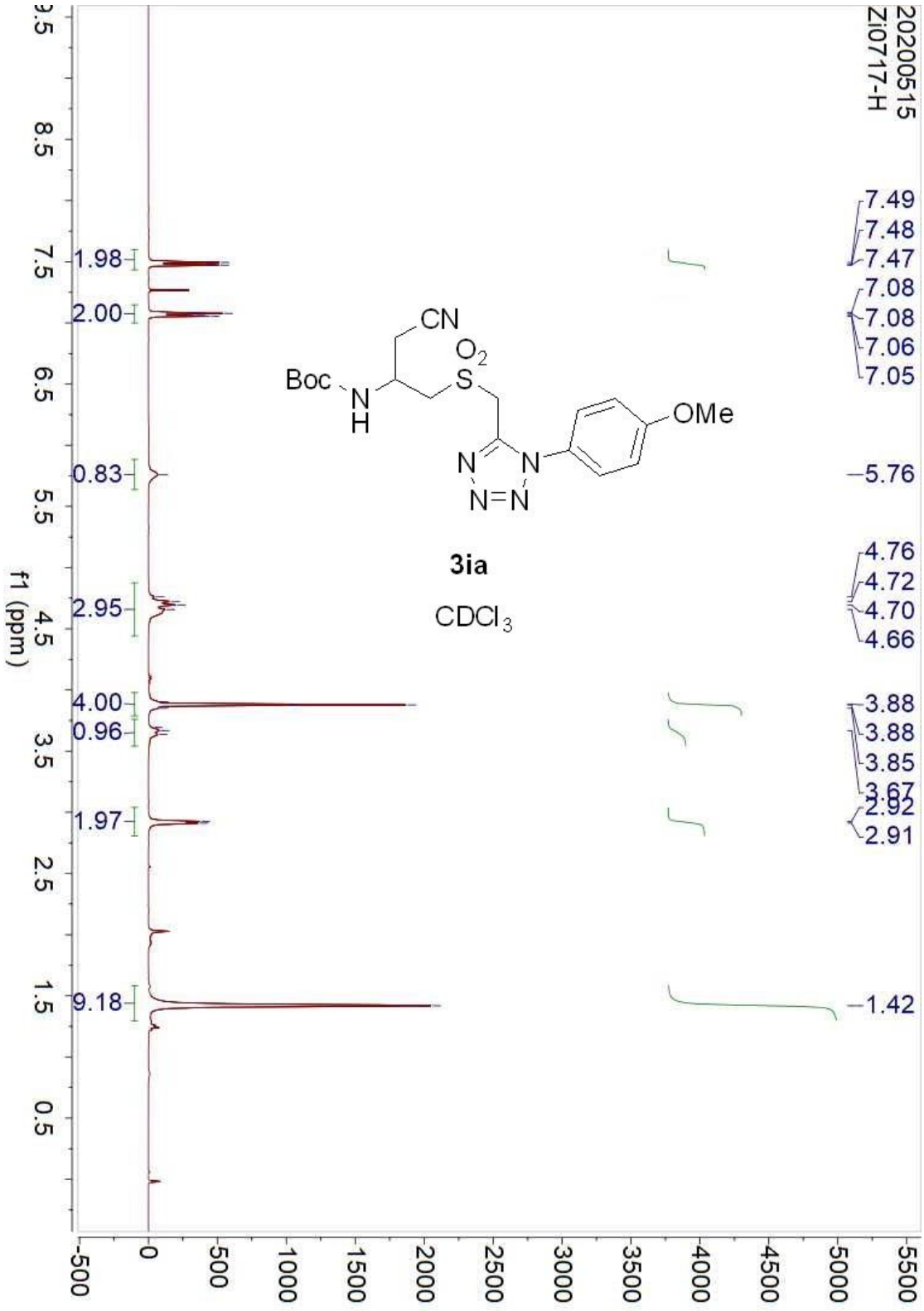
20200515
Zi0717-H
7.49
7.48
7.47
7.08
7.08
7.06
7.05
5.76
4.76
4.72
4.70
4.66
3.88
3.88
3.85
3.67
2.92
2.91
1.42
1.98
2.00
0.83
2.95
4.00
0.96
1.97
9.18
CN
O2
S
Boc
NH
N
N
N=N
OMe
3ia
CDCl3
f1 (ppm)

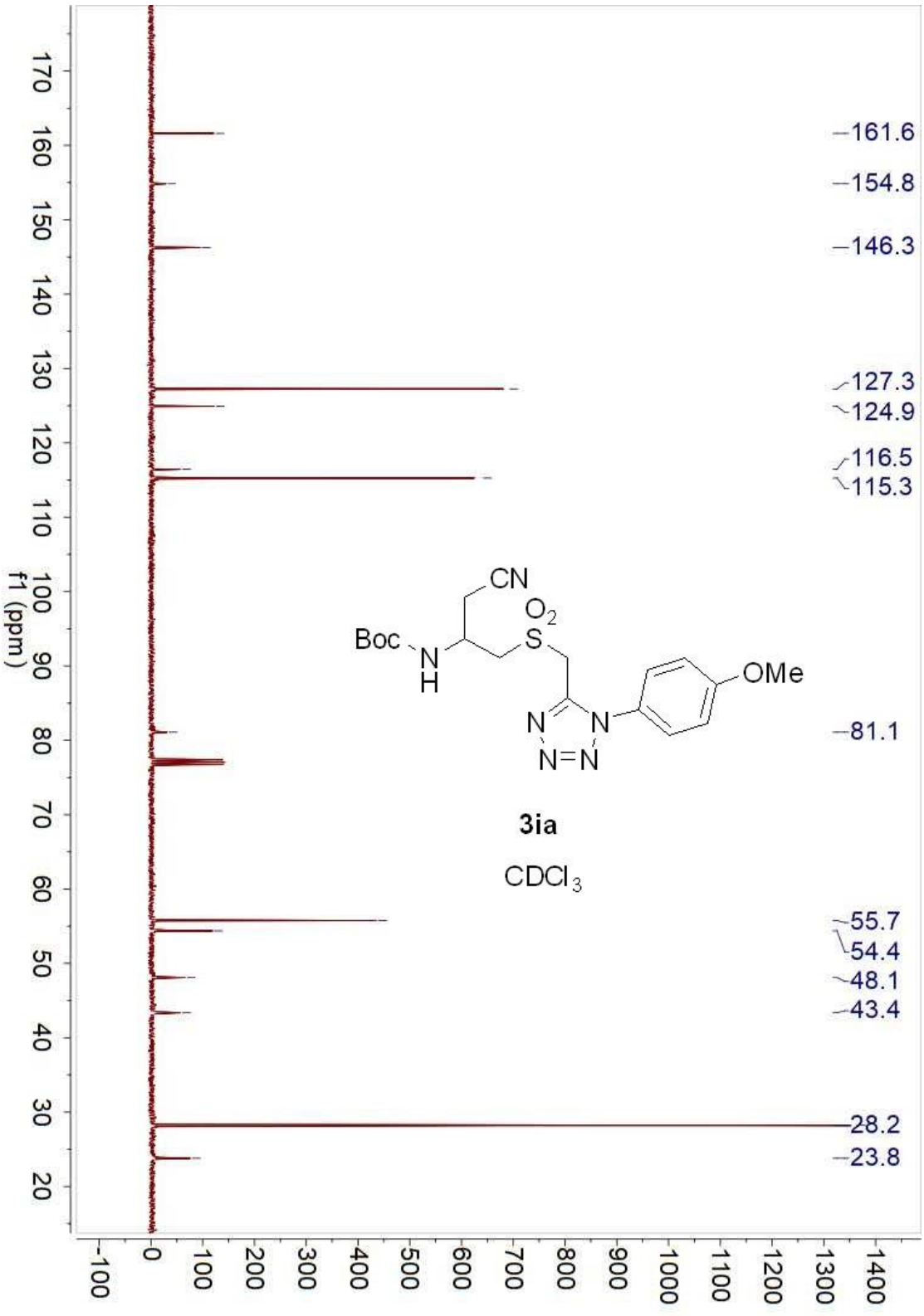
161.6
154.8
146.3
127.3
124.9
116.5
115.3
81.1
55.7
54.4
48.1
43.4
28.2
23.8
CN
O2
S
Boc
N
H
N
N
N=N
OMe
3ia
CDCl3
f1 (ppm)

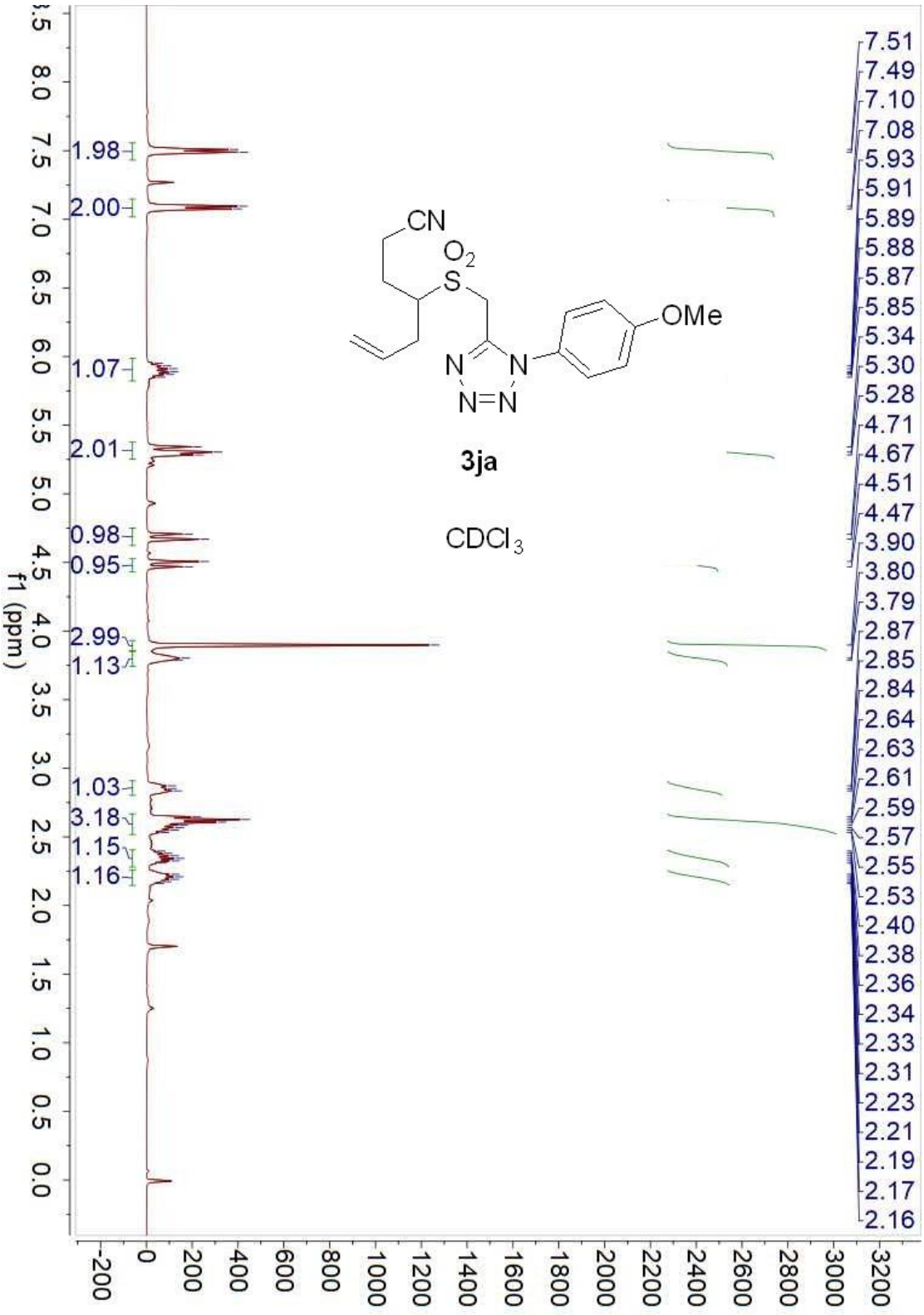
CN
O2
S
OMe
N
N
N=N
3ja
CDCl3
1.98
2.00
1.07
2.01
0.98
0.95
2.99
1.13
1.03
3.18
1.15
1.16
7.51
7.49
7.10
7.08
5.93
5.91
5.89
5.88
5.87
5.85
5.34
5.30
5.28
4.71
4.67
4.51
4.47
3.90
3.80
3.79
2.87
2.85
2.84
2.64
2.63
2.61
2.59
2.57
2.55
2.53
2.40
2.38
2.36
2.34
2.33
2.31
2.23
2.21
2.19
2.17
2.16
f1 (ppm)

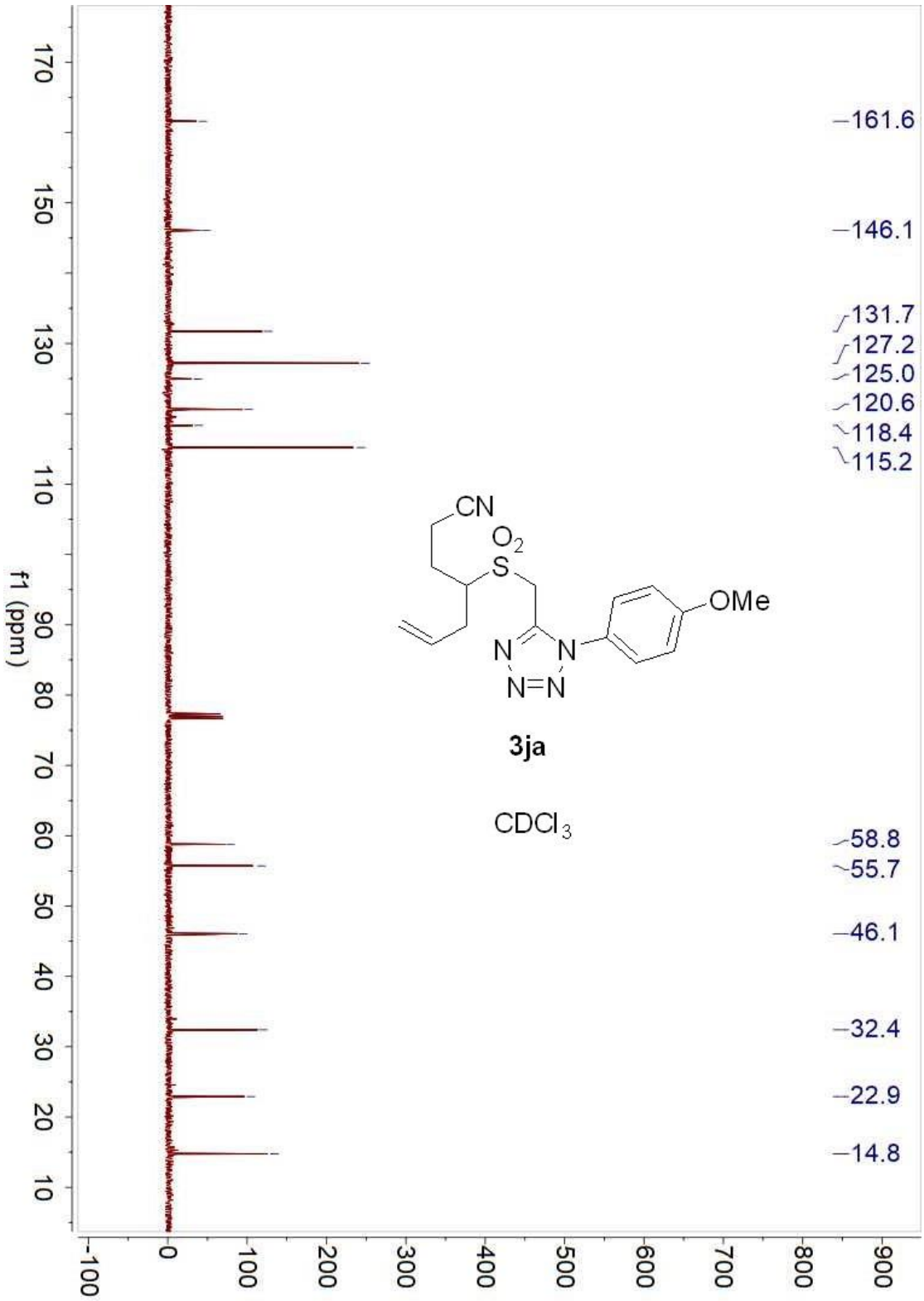
161.6
146.1
131.7
127.2
125.0
120.6
118.4
115.2
58.8
55.7
46.1
32.4
22.9
14.8
CN
O2
S
OMe
N
N
N=N
3ja
CDCl3
f1 (ppm)
170
150
130
110
90
80
70
60
50
40
30
20
10
-100
0
100
200
300
400
500
600
700
800
900

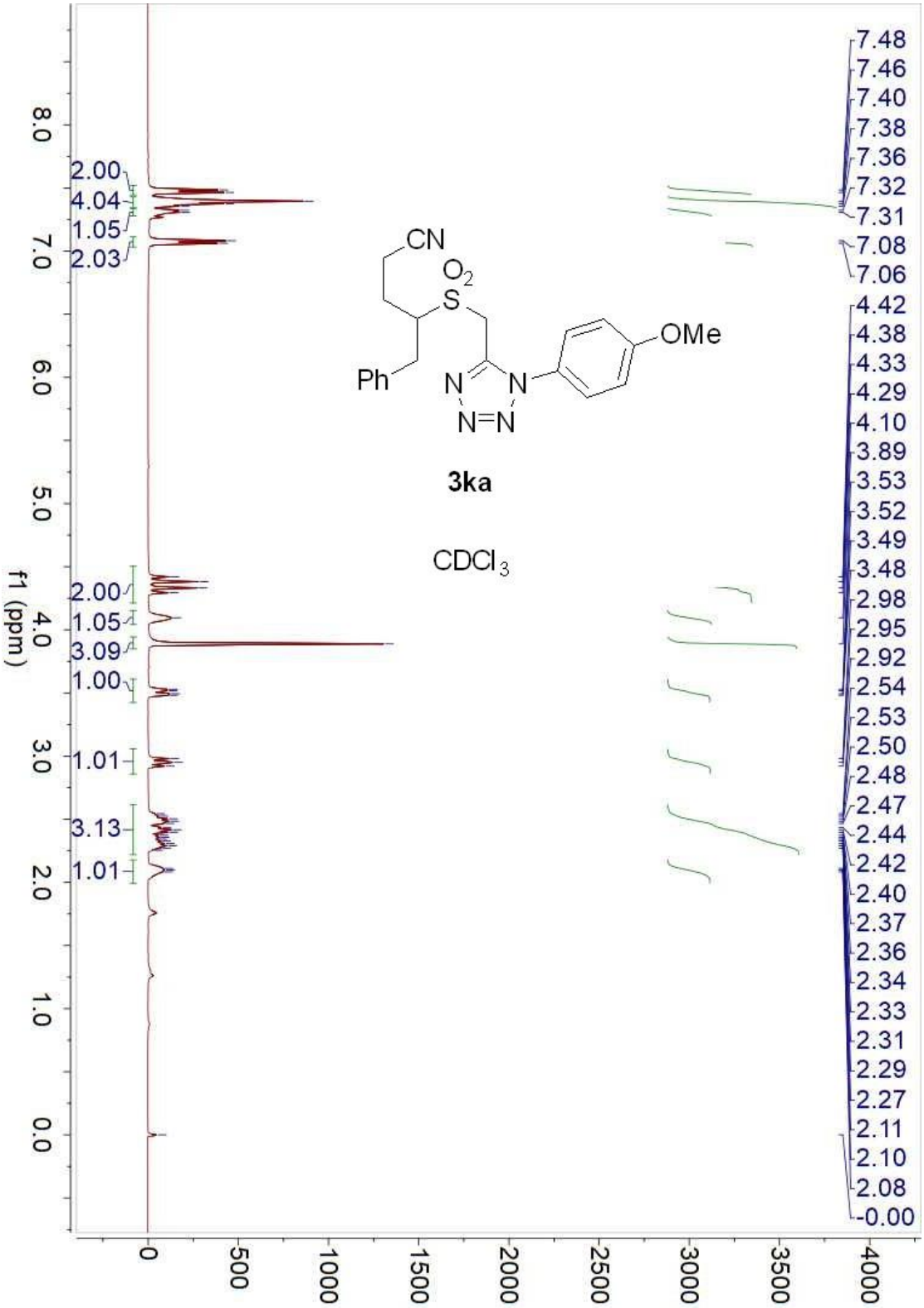
CN
O2
S
Ph
N
N
N=N
OMe
3ka
CDCl3
f1 (ppm)
8.0
7.0
6.0
5.0
4.0
3.0
2.0
1.0
0.0
2.00
4.04
1.05
2.03
2.00
1.05
3.09
1.00
1.01
3.13
1.01
7.48
7.46
7.40
7.38
7.36
7.32
7.31
7.08
7.06
4.42
4.38
4.33
4.29
4.10
3.89
3.53
3.52
3.49
3.48
2.98
2.95
2.92
2.54
2.53
2.50
2.48
2.47
2.44
2.42
2.40
2.37
2.36
2.34
2.33
2.31
2.29
2.27
2.11
2.10
2.08
-0.00
0
500
1000
1500
2000
2500
3000
3500
4000

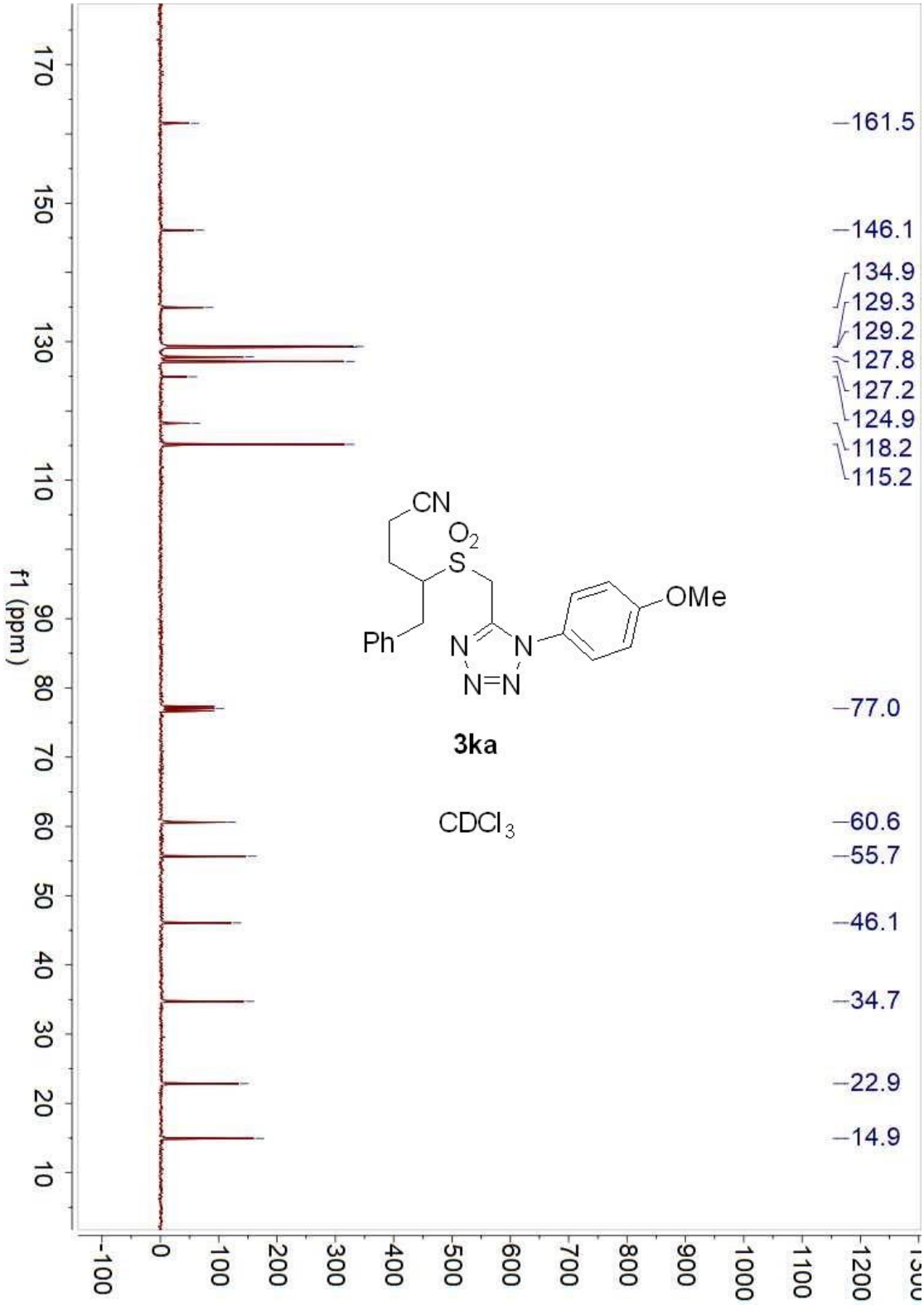
161.5
146.1
134.9
129.3
129.2
127.8
127.2
124.9
118.2
115.2
77.0
60.6
55.7
46.1
34.7
22.9
14.9
CN
O2
S
Ph
N
N
N=N
OMe
3ka
CDCl3
f1 (ppm)

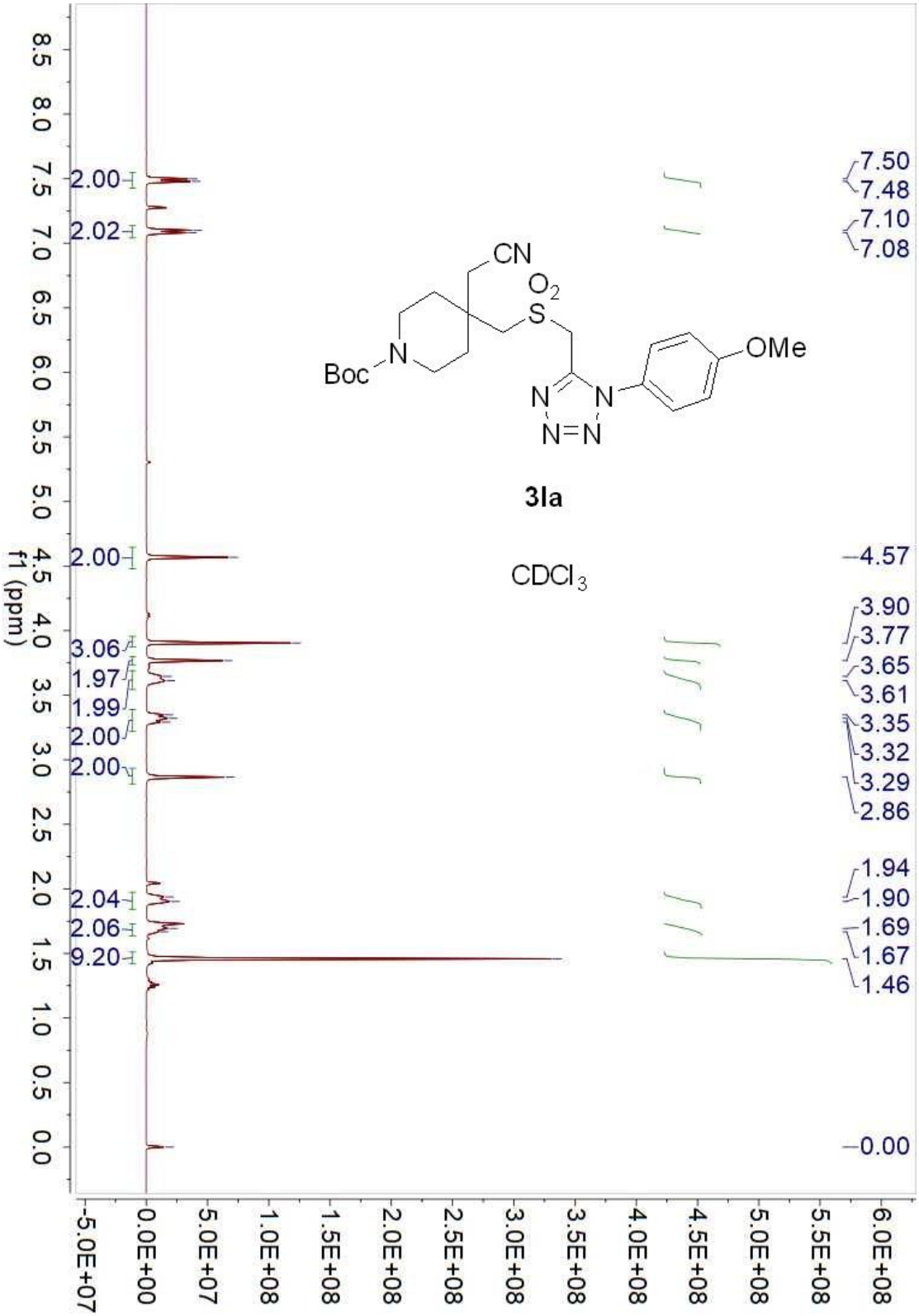
CN
O2
S
N
Boc
N
N
N=N
OMe
3la
CDCl3
f1 (ppm)
2.00
2.02
2.00
3.06
1.97
1.99
2.00
2.00
2.04
2.06
9.20
7.50
7.48
7.10
7.08
4.57
3.90
3.77
3.65
3.61
3.35
3.32
3.29
2.86
1.94
1.90
1.69
1.67
1.46
0.00

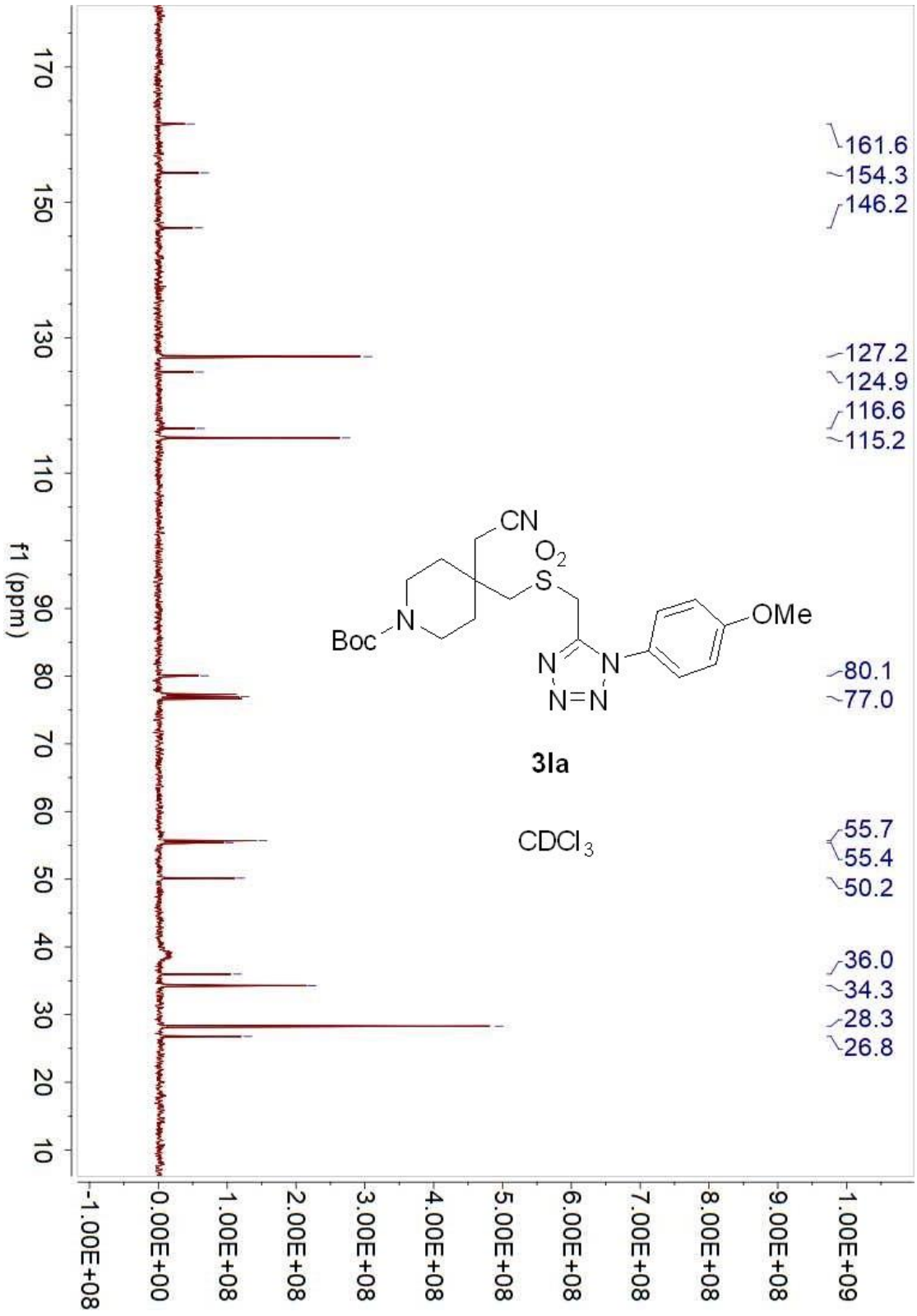
161.6
154.3
146.2
127.2
124.9
116.6
115.2
80.1
77.0
55.7
55.4
50.2
36.0
34.3
28.3
26.8
CN
O2
S
Boc
N
N
N
N=N
OMe
3la
CDCl3
f1 (ppm)
170
150
130
110
90
80
70
60
50
40
30
20
10
-1.00E+08
0.00E+00
1.00E+08
2.00E+08
3.00E+08
4.00E+08
5.00E+08
6.00E+08
7.00E+08
8.00E+08
9.00E+08
1.00E+09

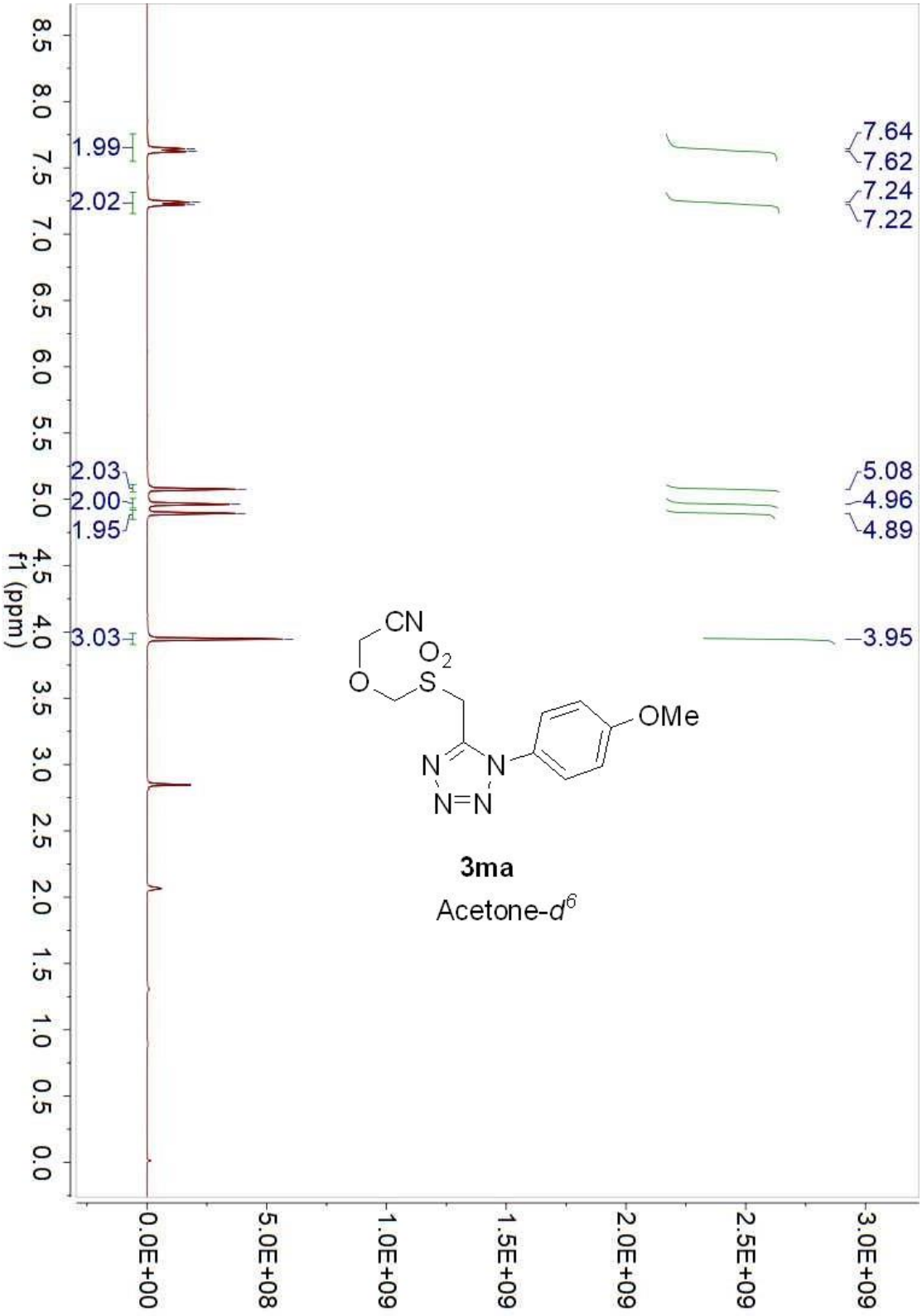
1.99
2.02
2.03
2.00
1.95
3.03
7.64
7.62
7.24
7.22
5.08
4.96
4.89
3.95
f1 (ppm)
CN
O2
S
O
OMe
N
N
N=N
3ma
Acetone-d6

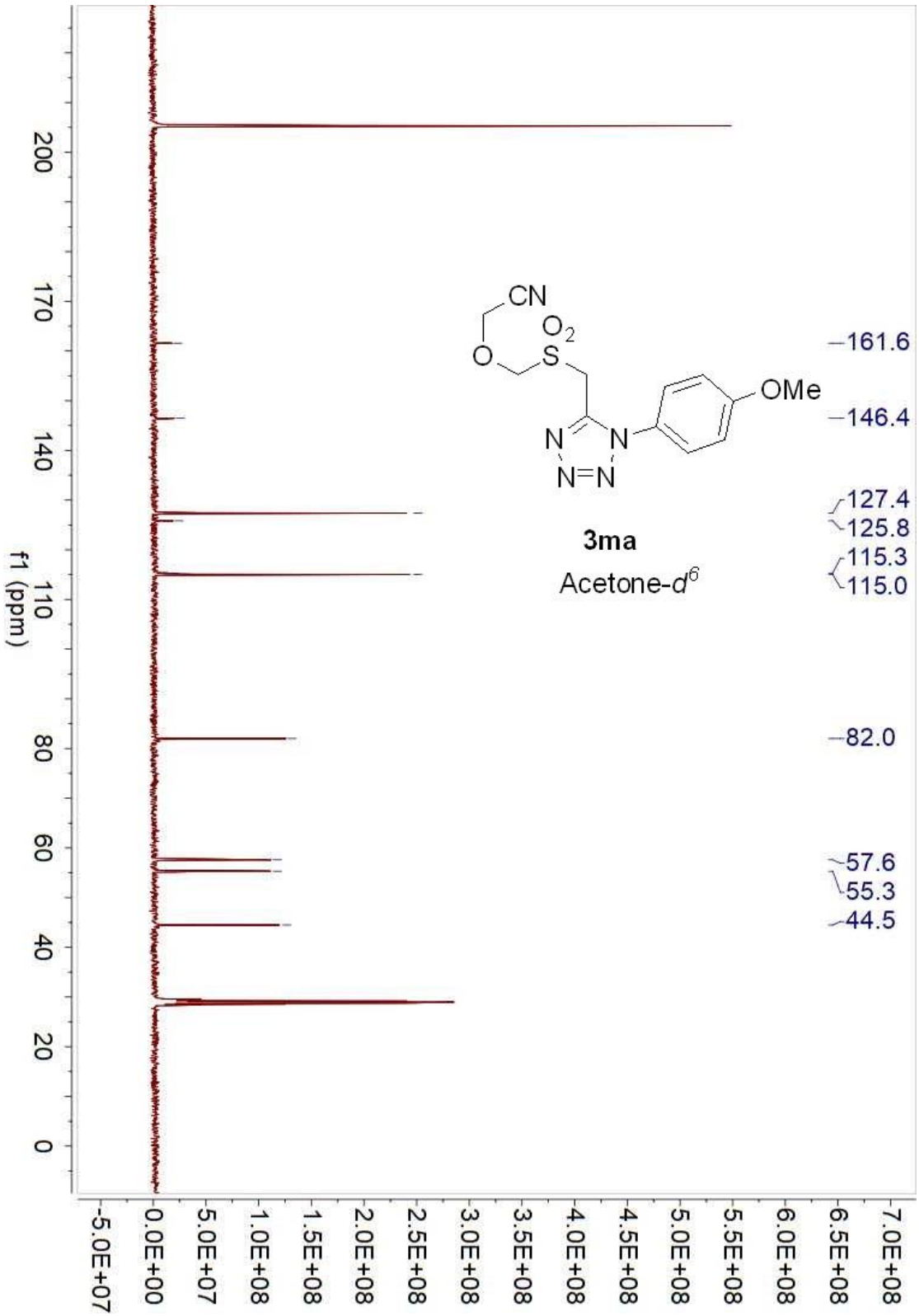
CN
O2
O
S
OMe
N
N
N=N
3ma
Acetone-d6
161.6
146.4
127.4
125.8
115.3
115.0
82.0
57.6
55.3
44.5
f1 (ppm)
200
170
140
110
80
60
40
20
0
-5.0E+07
0.0E+00
5.0E+07
1.0E+08
1.5E+08
2.0E+08
2.5E+08
3.0E+08
3.5E+08
4.0E+08
4.5E+08
5.0E+08
5.5E+08
6.0E+08
6.5E+08
7.0E+08

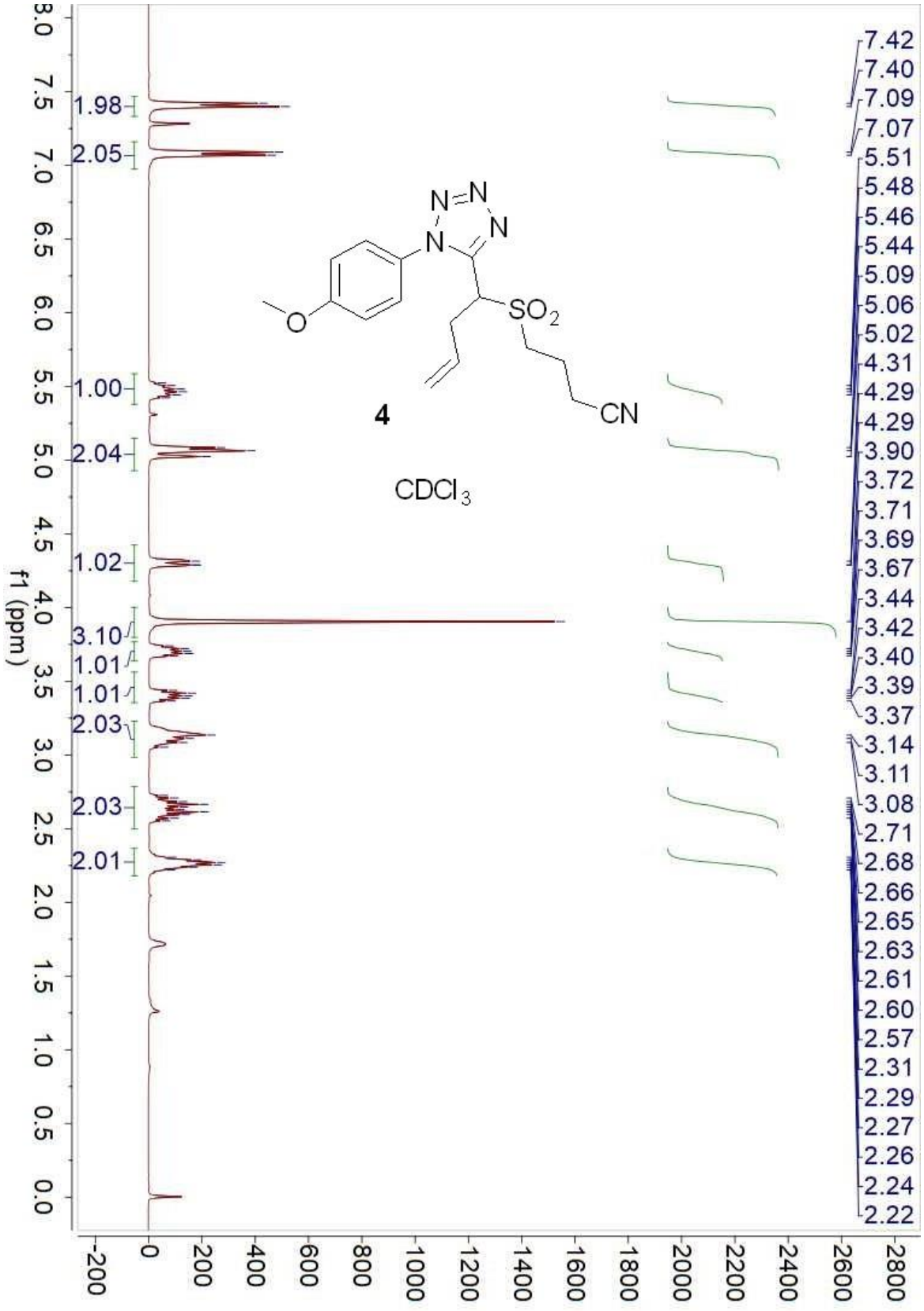
7.42
7.40
7.09
7.07
5.51
5.48
5.46
5.44
5.09
5.06
5.02
4.31
4.29
4.29
3.90
3.72
3.71
3.69
3.67
3.44
3.42
3.40
3.39
3.37
3.14
3.11
3.08
2.71
2.68
2.66
2.65
2.63
2.61
2.60
2.57
2.31
2.29
2.27
2.26
2.24
2.22
1.98
2.05
1.00
2.04
1.02
3.10
1.01
1.01
2.03
2.03
2.01
N
N
N
N
O
SO2
CN
4
CDCl3
f1 (ppm)

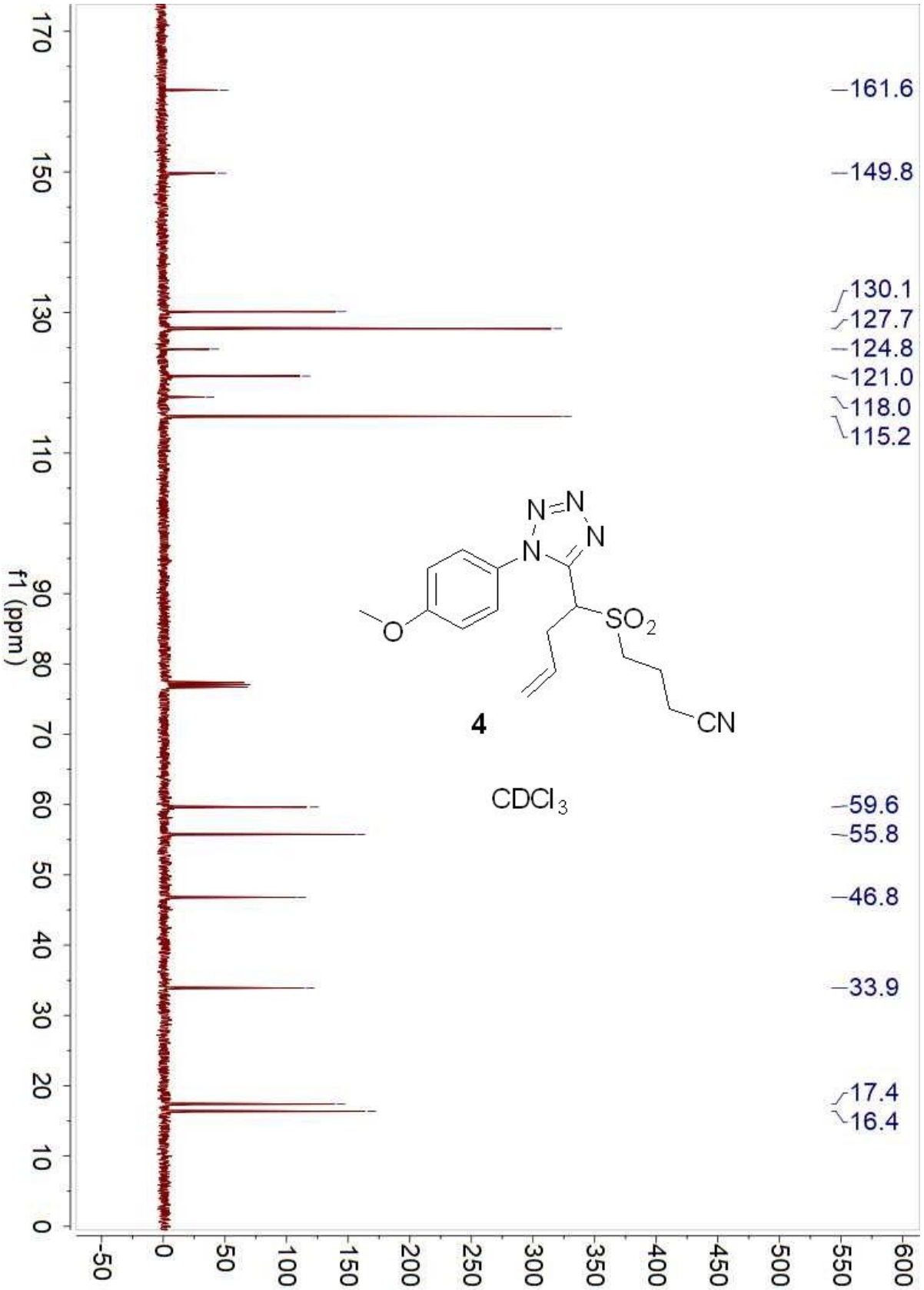
161.6
149.8
130.1
127.7
124.8
121.0
118.0
115.2
59.6
55.8
46.8
33.9
17.4
16.4
f1 (ppm)
N
N
N
N
O
SO2
CN
4
CDCl3

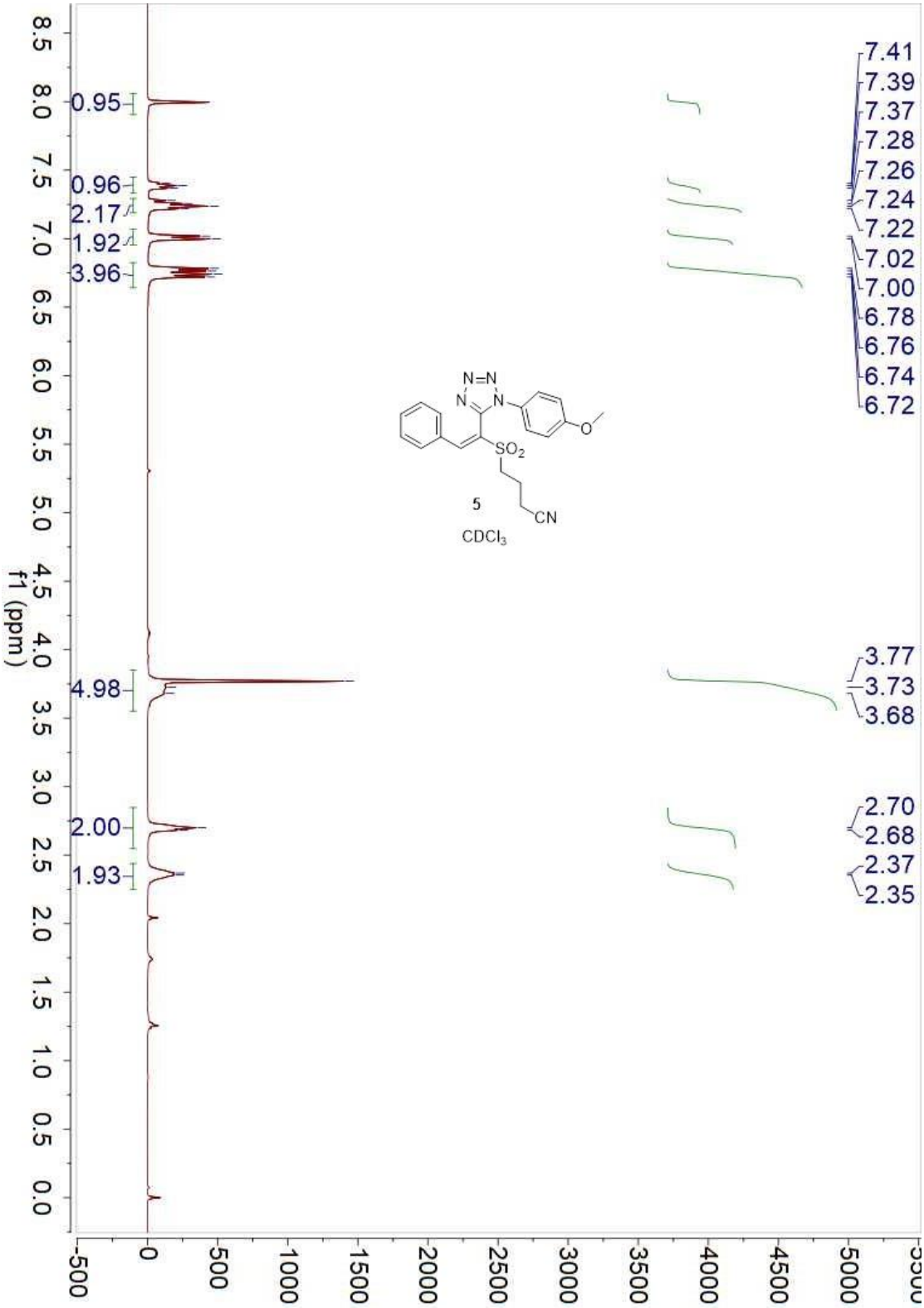
7.41
7.39
7.37
7.28
7.26
7.24
7.22
7.02
7.00
6.78
6.76
6.74
6.72
3.77
3.73
3.68
2.70
2.68
2.37
2.35
0.95
0.96
2.17
1.92
3.96
4.98
2.00
1.93
N=N
N
N
O
SO2
CN
5
CDCl3
f1 (ppm)

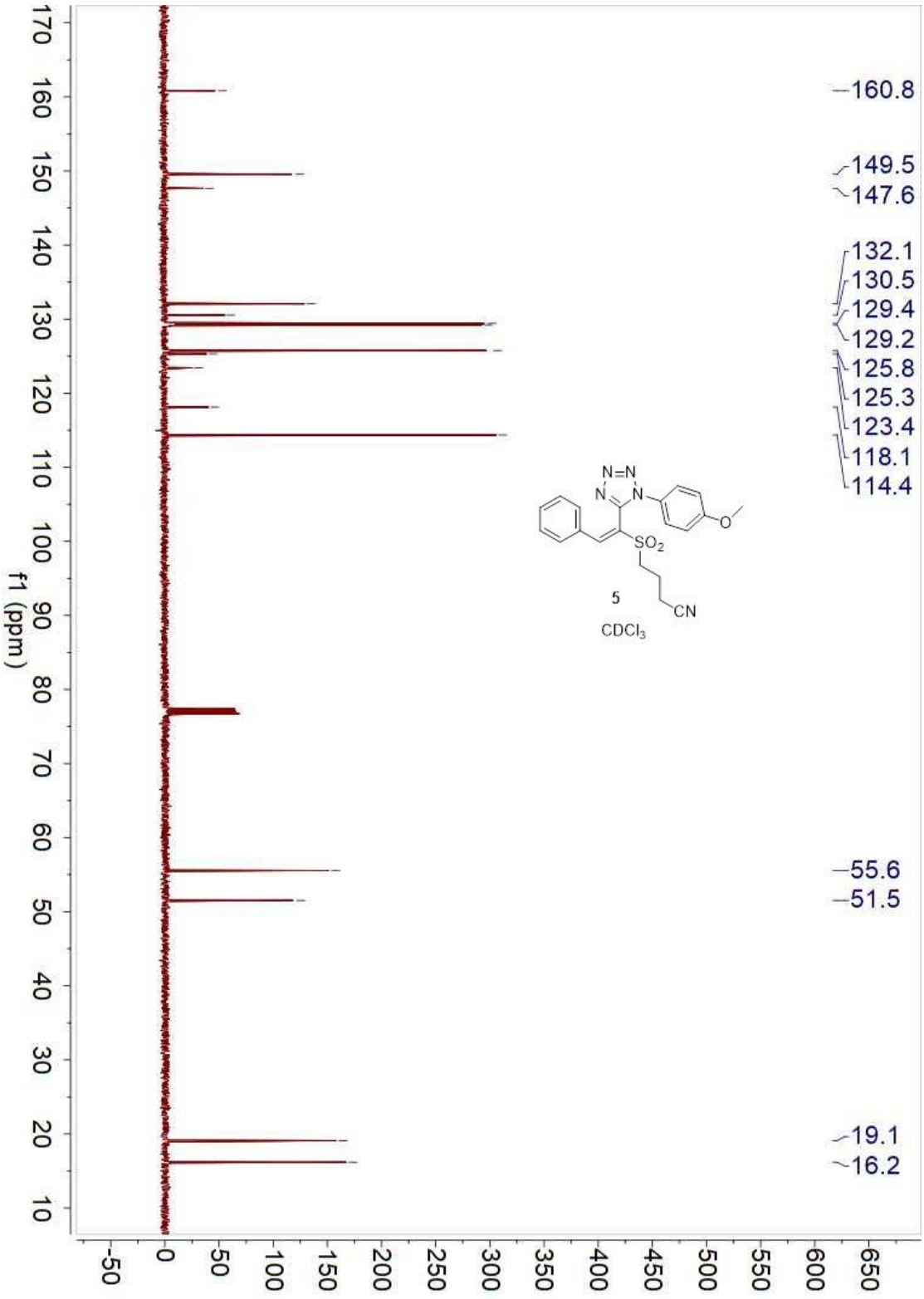
160.8
149.5
147.6
132.1
130.5
129.4
129.2
125.8
125.3
123.4
118.1
114.4
55.6
51.5
19.1
16.2
f1 (ppm)
5
CDCl3

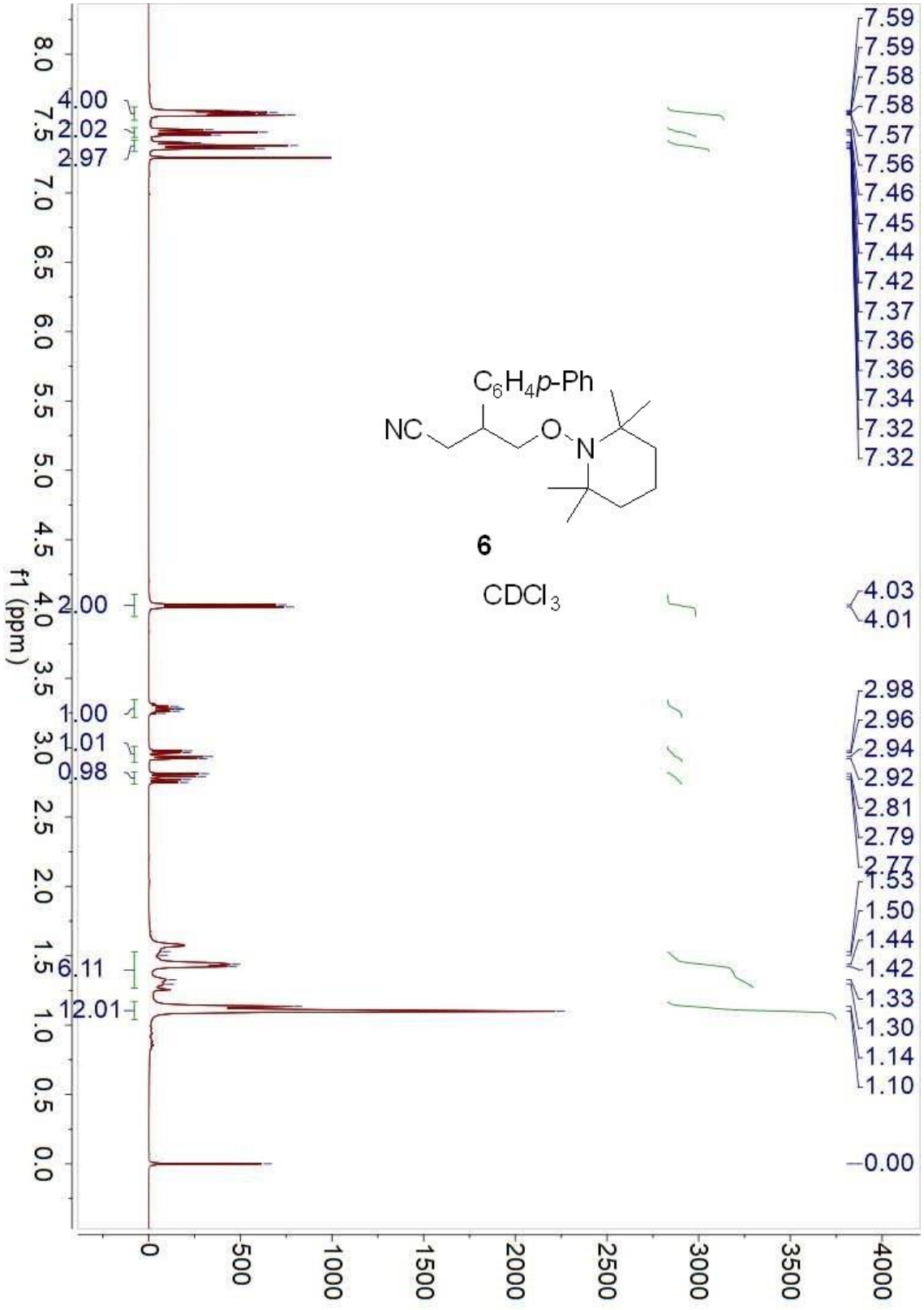
7.59
7.59
7.58
7.58
7.57
7.56
7.46
7.45
7.44
7.42
7.37
7.36
7.36
7.34
7.32
7.32
4.03
4.01
2.98
2.96
2.94
2.92
2.81
2.79
2.77
1.53
1.50
1.44
1.42
1.33
1.30
1.14
1.10
0.00
4.00
2.02
2.97
2.00
1.00
1.01
0.98
6.11
12.01
C6H4p-Ph
NC
O
N
6
CDCl3
f1 (ppm)
8.0
7.5
7.0
6.5
6.0
5.5
5.0
4.5
4.0
3.5
3.0
2.5
2.0
1.5
1.0
0.5
0.0
0
500
1000
1500
2000
2500
3000
3500
4000

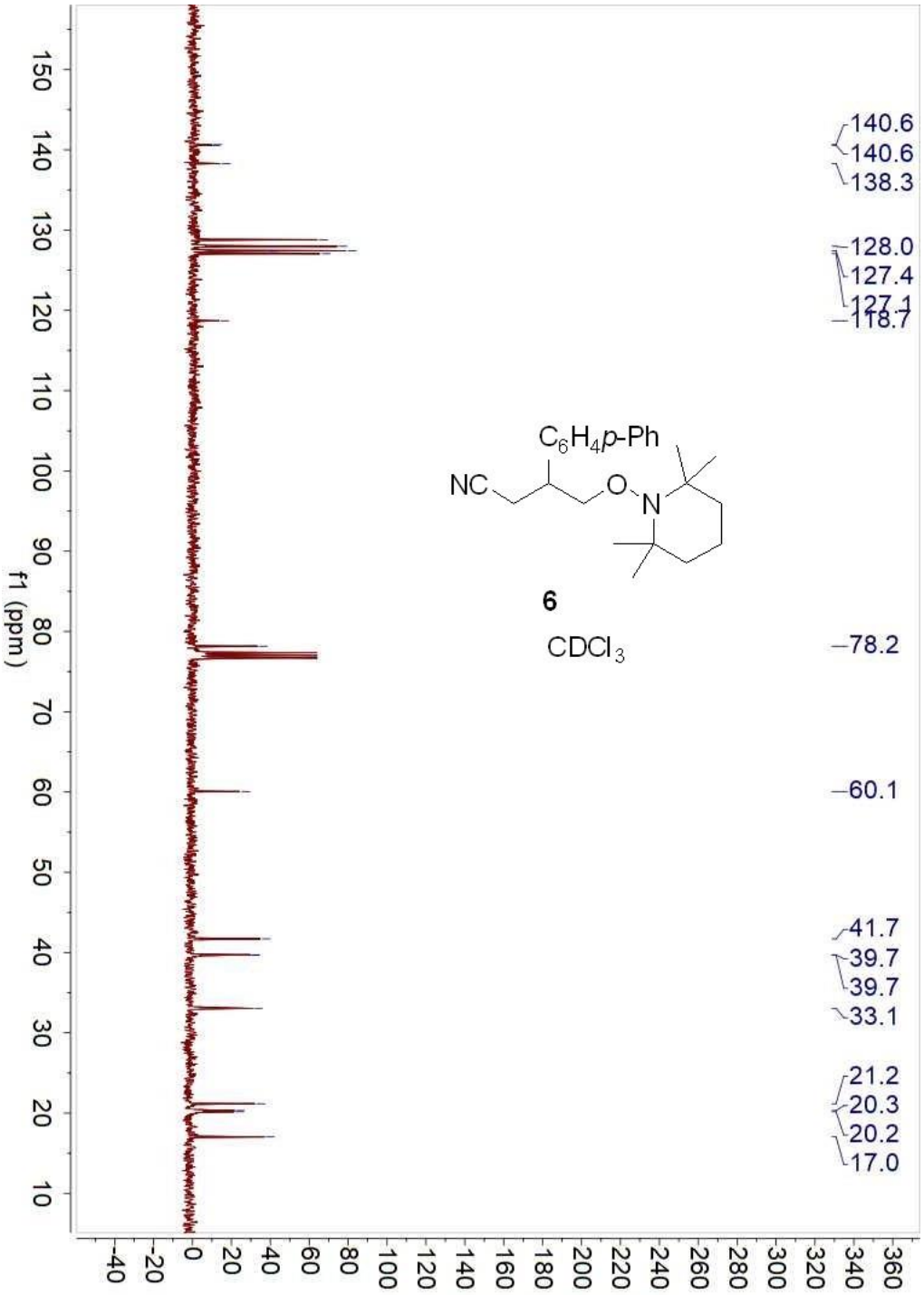
140.6
140.6
138.3
128.0
127.4
127.1
118.7
C6H4p-Ph
NC
O
N
6
CDCl3
78.2
60.1
41.7
39.7
39.7
33.1
21.2
20.3
20.2
17.0
f1 (ppm)

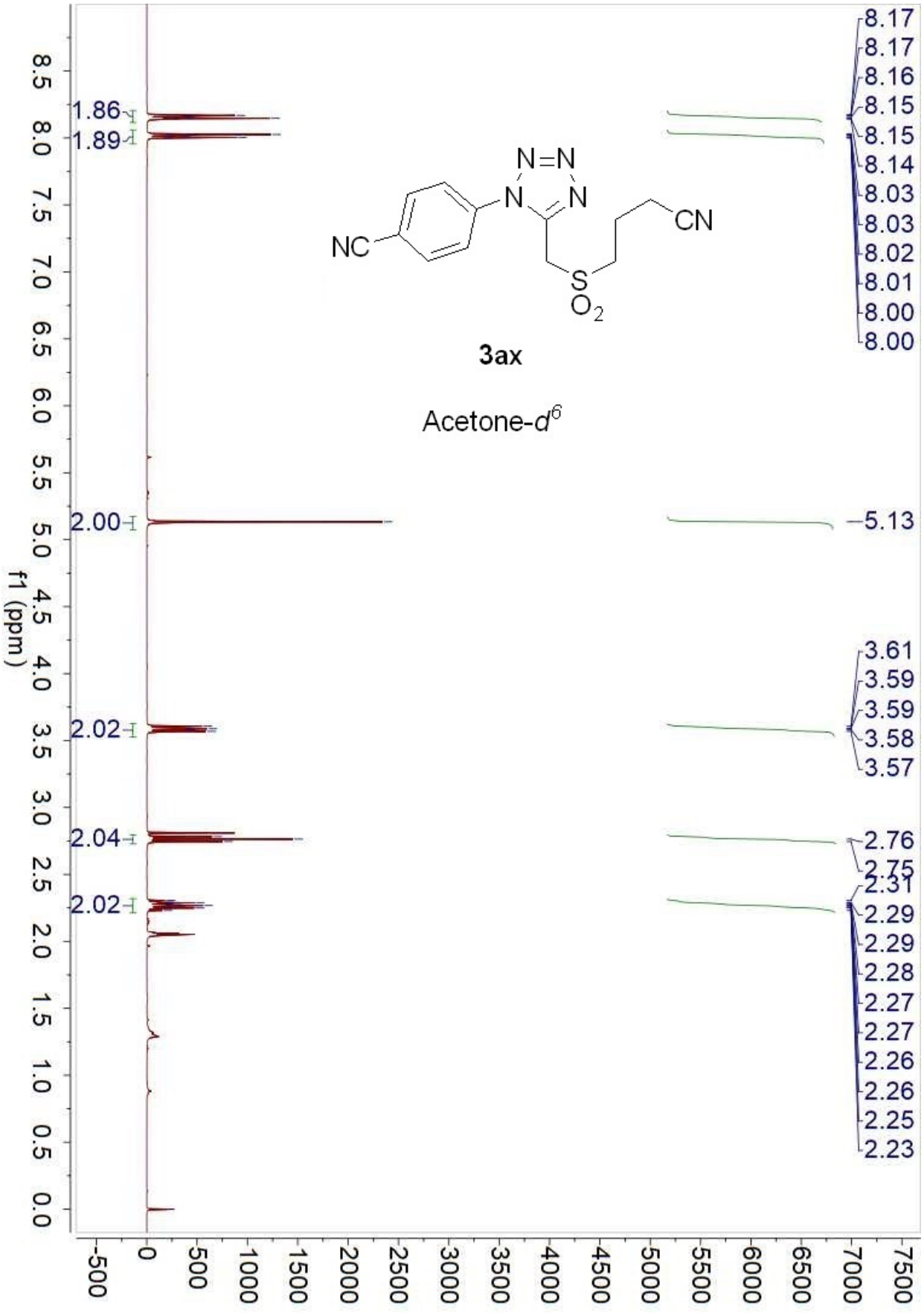
8.17
8.17
8.16
8.15
8.15
8.14
8.03
8.03
8.02
8.01
8.00
8.00
1.86
1.89
N=N
N
N
NC
CN
S
O2
3ax
Acetone-d6
2.00
5.13
3.61
3.59
3.59
3.58
3.57
2.02
2.04
2.76
2.75
2.31
2.02
2.29
2.29
2.28
2.27
2.27
2.26
2.26
2.25
2.23
f1 (ppm)
8.5
8.0
7.5
7.0
6.5
6.0
5.5
5.0
4.5
4.0
3.5
3.0
2.5
2.0
1.5
1.0
0.5
0.0
-500
0
500
1000
1500
2000
2500
3000
3500
4000
4500
5000
5500
6000
6500
7000
7500

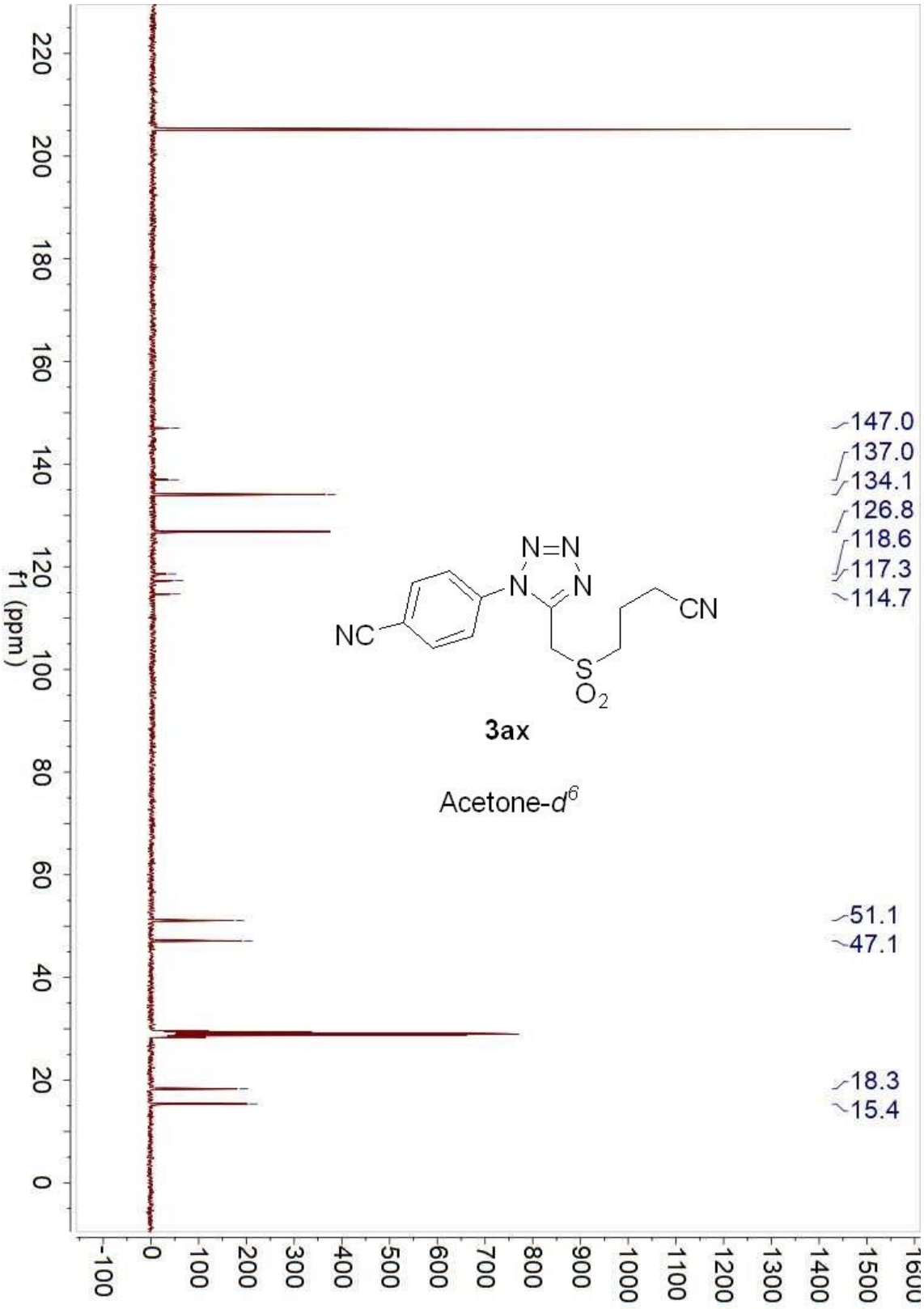
147.0
137.0
134.1
126.8
118.6
117.3
114.7
51.1
47.1
18.3
15.4
N=N
N
N
NC
CN
S
O2
3ax
Acetone-d6
f1 (ppm)

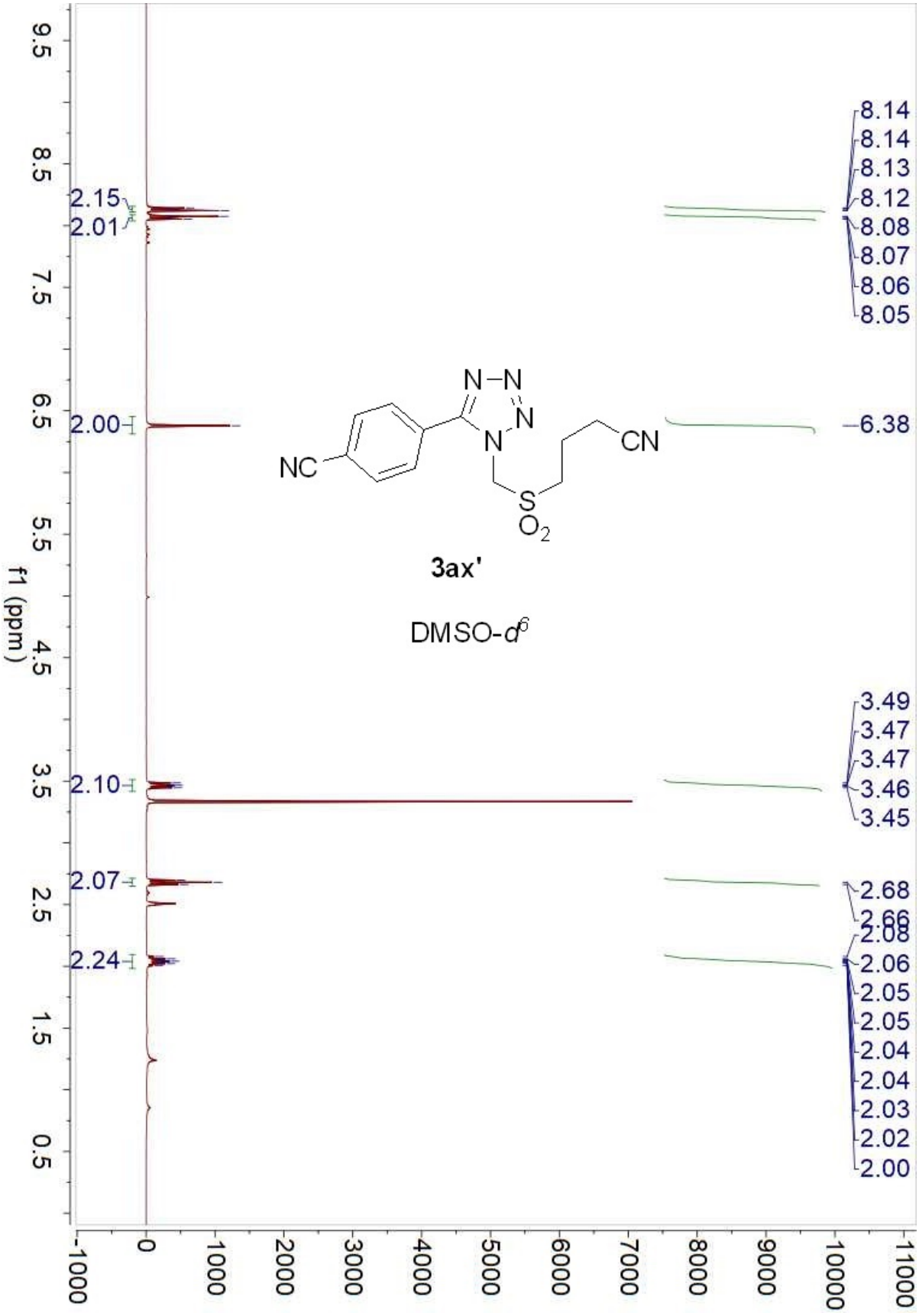
8.14
8.14
8.13
8.12
8.08
8.07
8.06
8.05
6.38
3.49
3.47
3.47
3.46
3.45
2.68
2.66
2.08
2.06
2.05
2.05
2.04
2.04
2.03
2.02
2.00
2.15
2.01
2.00
2.10
2.07
2.24
N–N
N
N
NC
CN
S
O2
3ax'
DMSO-d6
f1 (ppm)
9.5
8.5
7.5
6.5
5.5
4.5
3.5
2.5
1.5
0.5
-1000
0
1000
2000
3000
4000
5000
6000
7000
8000
9000
10000
11000

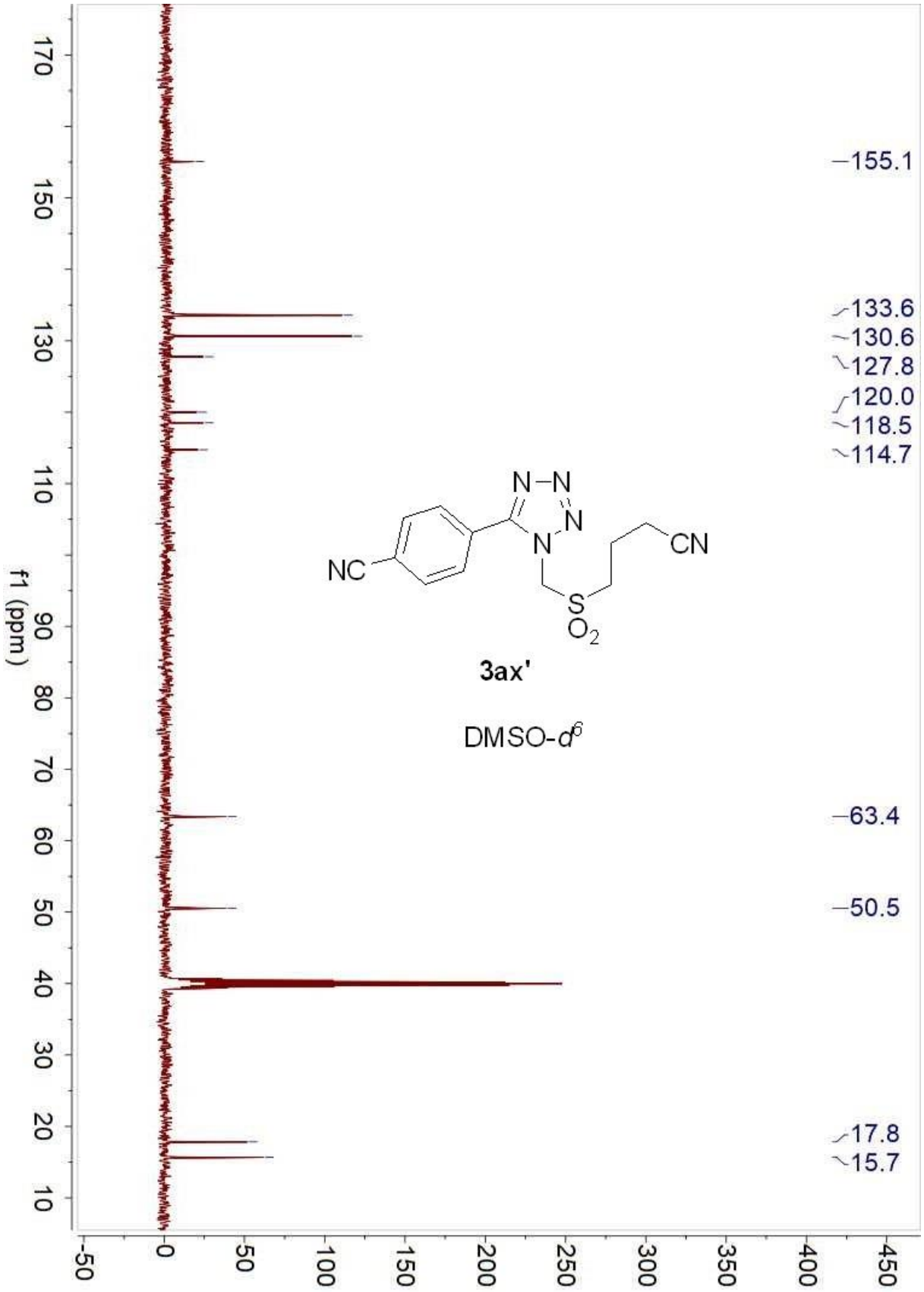

5. Supplemental references

Ai, W., Liu, Y., Wang, Q., Lu, Z. and Liu, Q. (2018). Cu-catalyzed redox-neutral ring cleavage of cycloketone *O*-acyl oximes: chemodivergent access to distal oxygenated nitriles. Org. Lett. *20*, 409-412.

Breed, D.R., Thibault, X., Xie, F., Wang, Q., Hawker, C. J. and Pine, D. J. (2009). Functionalization of polymer microspheres using click chemistry. Langmuir *25*, 4370-4376.

Zhang, Z. and Jiang, X. (2014). Oxidative coupling of terminal clkyne with *α*-hydroxy ketone: an expedient approach toward ynediones. Org. Lett. *16*, 4400-4403.